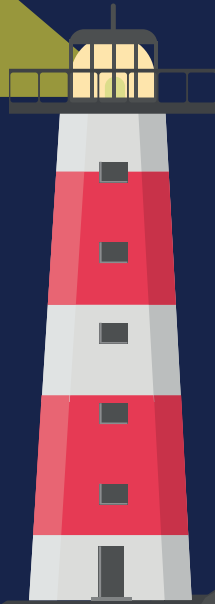


**BRONCHIAL THERMOPLASTY AND OPTICAL COHERENCE
TOMOGRAPHY IN SEVERE ASTHMA:**

USING LIGHT AND HEAT TO TARGET AIRWAY REMODELING



**ANNIKA
GOORSENBERG**

BRONCHIAL THERMOPLASTY AND OPTICAL
COHERENCE TOMOGRAPHY IN SEVERE ASTHMA:
using light and heat to target airway remodeling

Annika Wilhelmina Maria Goorsenberg

Bronchial thermoplasty and optical coherence tomography in severe asthma: using light and heat to target airway remodeling

© Annika W.M. Goorsenberg, 2020

| | |
|--------|---------------------------|
| ISBN | 978-94-6332-689-6 |
| Layout | Loes Kema |
| Print | GVO drukkers & vormgevers |

All rights reserved. No part of this thesis may be reproduced in any form, by print, photocopy, digital file, internet or any other means without permission from the author or the copyright-owning journals for previously published chapters.

This thesis is part of the investigator initiated *Unravelling Targets of Therapy in Bronchial Thermoplasty in Severe Asthma* (TASMA) trial (ClinicalTrials.gov No.NCT02225392). The TASMA trial is an international, multicentre, randomized controlled trial and is funded by the Dutch Lung Foundation (grant number 5.2.13.064JO), the Netherlands Organization for Health Research and Development (ZonMw) (grant number 90713477) and Boston Scientific. St. Jude Medical/ Abbott, Boston Scientific and Olympus provided material support.

BRONCHIAL THERMOPLASTY AND OPTICAL
COHERENCE TOMOGRAPHY IN SEVERE ASTHMA:
using light and heat to target airway remodeling

ACADEMISCH PROEFSCHRIFT

ter verkrijging van de graad van doctor
aan de Universiteit van Amsterdam
op gezag van de Rector Magnificus prof. dr. ir. K.I.J. Maex
ten overstaan van een door het College voor Promoties ingestelde commissie,
in het openbaar te verdedigen in de Agnietenkapel
op donderdag 26 november 2020, te 13.00 uur

door

Annika Wilhelmina Maria Goorsenberg

geboren te Valkenisse

Promotiecommissie

Promotor:

Prof. dr. J.T. Annema

AMC-UvA

Copromotores:

Dr. P.I. Bonta

AMC-UvA

Dr. D.M. de Bruin

AMC-UvA

Overige leden:

Prof. dr. E.H.D. Bel

AMC-UvA

Prof. dr. A.H. Maitland-van der Zee

AMC-UvA

Prof. dr. A.G.J.M. van Leeuwen

AMC-UvA

Prof. dr. D. Stolz

Universitätsspital Basel

Prof. dr. J.K. Burgess

Rijksuniversiteit Groningen

Dr. H.P.A.A. van Veen

Medisch Spectrum Twente

Faculteit der Geneeskunde

Table of contents

Part I Introduction

Chapter 1 General introduction and aims of the thesis

Part II Bronchial thermoplasty in severe asthma

Chapter 2 Airway smooth muscle reduction after Bronchial Thermoplasty correlates with FEV₁
Clinical and Experimental Allergy 2019;49(4):541-544.

Chapter 3 Bronchial Thermoplasty induced airway smooth muscle reduction and clinical response in severe asthma: the TASMA randomized trial
American Journal of Respiratory and Critical Care Medicine 2020; online ahead of print.

Chapter 4 Metabolic differences in bronchial epithelium in asthma patients and healthy individuals: impact of thermoplasty
Submitted for publication

Chapter 5 Resistance of the respiratory system measured with forced oscillation technique (FOT) correlates with Bronchial Thermoplasty response
Respiratory Research 2020; 21(1):52.

Part III Optical coherence tomography for airway wall imaging

Chapter 6 Advances in optical coherence tomography (OCT) and confocal laser endomicroscopy (CLE) in pulmonary diseases
Respiration 2020;99(3):190-205.

Chapter 7 Identification and quantification of airway wall layers with optical coherence tomography: a histology based validation study
PLoS One 2017;12(10):e0184145.

Chapter 8 Optical coherence tomography intensity correlates with extracellular matrix components in the airway wall
American Journal of Respiratory and Critical Care Medicine 2020; online ahead of print.

- Chapter 9 Bronchial Thermoplasty-Induced Acute Airway Effects Assessed with Optical Coherence Tomography in Severe Asthma
Respiration 2018;96(6):564-570.

Part IV Discussion

Chapter 10 Summary and general discussion

Chapter 11 Nederlandse samenvatting

Appendices

Curriculum vitae

PhD portfolio

List of publications

Contributing authors

Dankwoord

Part I.

Introduction

Chapter 1.

General introduction
and aims of the thesis

Severe asthma

Asthma is a highly prevalent disease with over 500.000 patients in the Netherlands [1] and more than 300 million patients worldwide [2]. Asthma is characterized by recurrent wheeze, dyspnea and chest tightness caused by reversible airflow obstruction and airway hyperresponsiveness [3, 4]. The majority of asthma patients have minimal symptoms if they use inhaled corticosteroids (ICS) and bronchodilator therapy. However, a small proportion (approximately 5%) of these patients suffers from severe asthma [5-7]. These patients have uncontrolled disease despite the use of high doses ICS and a second controller and/or a systemic corticosteroid or these patients remain only controlled by using these high doses of medication [8, 9]. Due to frequent exacerbations, hospitalizations and the inability to work, severe asthma has a high impact on health care costs [10, 11].

Treatment of severe asthma

The heterogeneity of severe asthma emphasizes the need for more targeted, personalized treatment options. An emerging field in the treatment of asthma is the development of (anti-interleukin) biological treatments. These treatments are implemented for specific asthma phenotypes: anti-immunoglobulin E (IgE) for allergic asthma [12] and anti-interleukine-5(-receptor) and anti-interleukin-4 receptor treatments for eosinophilic asthma [13, 14]. Not all patients however are eligible for these treatment options and moreover not all patients respond. For this group of patients, bronchial thermoplasty is considered a treatment option [3, 15].

Bronchial thermoplasty

Bronchial thermoplasty (BT) is a bronchoscopic treatment for severe asthma patients using radiofrequency energy to heat up the medium to large airways (2-10 mm) [16]. During three consecutive bronchoscopies with 3 weeks in between, the right lower lobe, left lower lobe and finally both upper lobes are treated. The right middle lobe remains untreated because of the fear of developing a middle lobe syndrome.

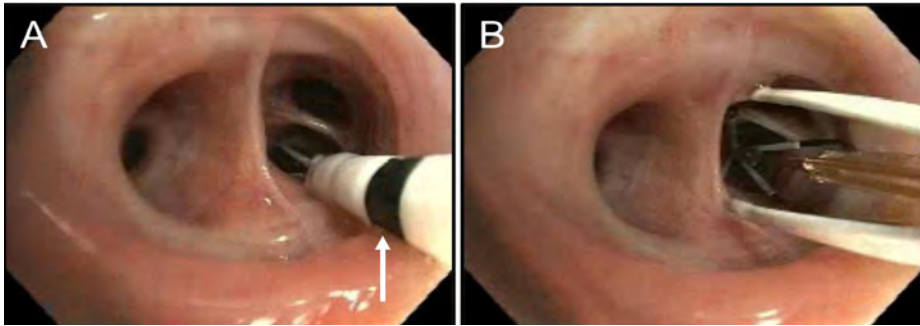


Figure 1. Bronchial thermoplasty procedure with the Alair catheter™ inserted in the airways of a severe asthma patient. A: not expanded catheter in place of the airway of interest; **B:** catheter expanded and electrodes are making contact with the airway wall for activation. Arrow at the 0.5 cm marker of bronchial thermoplasty catheter. (Courtesy of J.T. Annema and P.I. Bonta)

The BT procedures are performed under general anesthesia or moderate to deep sedation. During the procedure, an Alair catheter is inserted through the working channel of a bronchoscope and placed in the target airway of 2-3 mm diameter (**Figure 1A**). Next, the catheter is expanded until at least 3 of the electrodes are in contact with the airway wall and activated with a foot switch to deliver radiofrequency energy for 10 seconds (**Figure 1B**). After this activation, the catheter is closed, and retracted for 0.5 cm, marked by the black stripes on the catheter (**Figure 1B**), and again expanded and activated systematically until all airways in that lobe are treated. Patients are treated with prednisolone (50 mg) 3 days before the treatment, on the day itself and one day after to minimize exacerbation risk.

The U.S. Food and Drug Administration (FDA) approval for BT was obtained in 2010 after several randomized controlled trials had shown the beneficial effects of BT on quality of life and exacerbation rates [16-18]. These effects extend up to 5 years after treatment [19-22]. The hypothesis of BT is that by heating the airways, the airway smooth muscle (ASM) mass decreases, thereby having less ability to contract resulting in a reduction of symptoms and hyperresponsiveness. A reduction in ASM mass after BT has first been described in dogs [23] and ex-vivo human lobectomy specimen [24]. Later, in observational studies in humans, a significant reduction in ASM mass is shown [25-28]. A link with clinical response to BT however has not been reported and the exact mechanism of action of this treatment remains therefore unclear. Potential working mechanisms of BT are illustrated in **Figure 2** such as a reduction of airway nerve fibers, extra cellular matrix components and cytokine and chemokine production in the airways [29, 30]. To further unravel the mechanism of action of BT and as such improve patient selection for BT treatment, the Unravelling Targets of Therapy in Bronchial Thermoplasty in

Severe Asthma (TASMA) study was initiated.

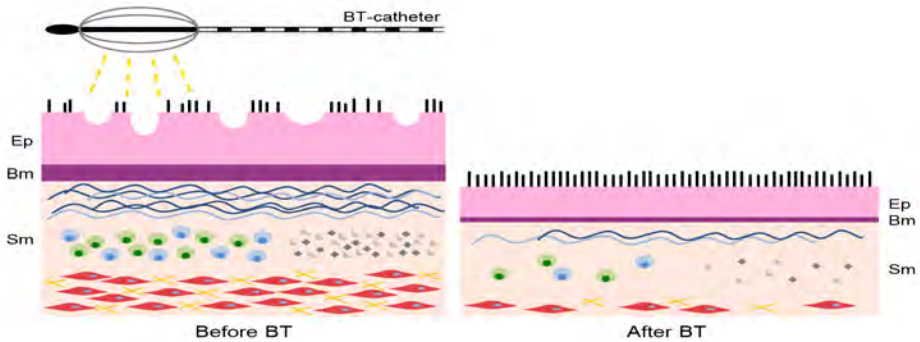







Figure 2. Potential working mechanisms of bronchial thermoplasty (BT) on the airway wall. Before BT typical airway remodeling characteristics are shown: thickened epithelium with reduced epithelial integrity, thickened basement membrane and extracellular matrix components, increased amount of pro-inflammatory cells, chemokines and cytokines and thickened airway smooth muscle layer with innervation. Potential described effects after BT are the regeneration of a thinner layer of epithelium with an increased epithelial integrity [31], reduced thickness of basement membrane and extracellular matrix [27, 28, 32], reduced amount of inflammatory cells, chemokines and cytokines [25, 33] and a reduction of nerve fibers [27, 34] and airway smooth muscle mass [25-28]. Ep: epithelium, Bm: basement membrane, Sm: submucosal layer, BT: bronchial thermoplasty,  extracellular matrix fibers,  inflammatory cells,  pro inflammatory cytokines and chemokines,  airway smooth muscle,  nerve fibers.

TASMA study

The TASMA study is an investigator initiated randomized controlled trial which aims to unravel the mechanism of action of BT (Clinicaltrials.gov number NCT02225392). The study was initiated in 2014 and is sponsored by the Dutch Lung Foundation, the Netherlands Organisation for Health Research and Development (ZonMW) and Boston Scientific. The final goal of this trial is to further understand the working mechanism of BT and to improve patient selection. The TASMA trial is a multicenter international trial: patients were included in two centers in the Netherlands (Amsterdam University Medical Center, location AMC and University Medical Center Groningen) and two centers in the United Kingdom (Royal Brompton Hospital and Imperial College, London).

The study design is shown in **Figure 3**. Before inclusion, the diagnosis of severe asthma was confirmed by a multidisciplinary panel including pulmonologists

and asthma specialists. After diagnosis confirmation, patients signed informed consent and the screening phase started. During screening visits, we collected a set of demographic, clinical, functional (including methacholine provocation tests) and inflammatory variables. The last visit of the screening consisted of a bronchoscopy including bronchoalveolar lavage, endobronchial brushes and biopsies and airway wall imaging with radial endobronchial ultrasound (rEBUS) and OCT. If eligible after these visits, patients were randomized into an immediate treatment group and a delayed control group. The immediate treatment group received BT according to current guidelines. The delayed control group had to wait for 6 months while remaining on standard asthma care with stable medication use. After these 6 months, the same set of data was collected as during the screening visits, including a bronchoscopy with biopsies. Subsequently, patients received BT treatment. Both randomization groups entered a follow-up period of 6 months after BT which ended with collecting again the same data parameters as before BT.

In July 2018 inclusion was completed with a final number per center as follows: 26 patients in the Amsterdam University Medical Center (location AMC), 4 patients in the University Medical Center Groningen and 10 patients in the Royal Brompton Hospital and Imperial College in London.

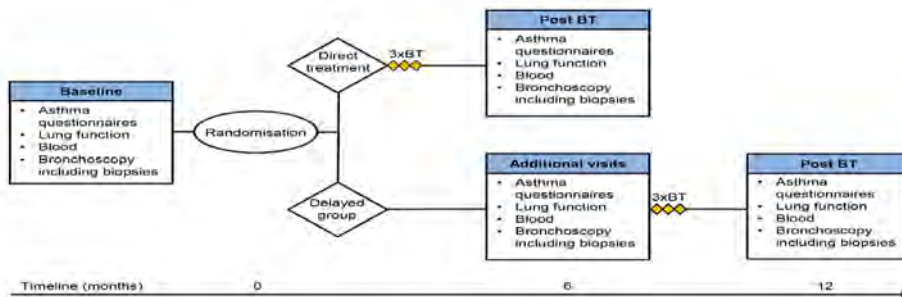


Figure 3. Study design of the TASMA study. BT: Bronchial Thermoplasty.

Airway remodeling

Next to unraveling the mechanism of action of BT, the TASMA study focuses on the use of novel imaging techniques to assess airway remodeling. Airway remodeling is a process of structural alterations in airway tissue and cells which results in a thickened airway wall. Several alterations in the airway wall have been identified such as hypertrophy and hyperplasia of ASM cells, a thickened epithelium and basement membrane layer, neovascularization and hypertrophy of glands [35, 36].

The amount of airway remodeling is related to the severity of asthma [37, 38] and with a lower lung function assessed with forced expiratory volumes in 1 second [39]. Therefore it is important to find methods capable of identifying and quantifying airway remodeling. This might be particularly of interest in patients treated with BT: currently the only asthma treatment available specifically invented to target airway remodeling. A promising imaging technique for this purpose is optical coherence tomography (OCT).

Optical coherence tomography

OCT is an imaging technique that creates high-resolution cross-sectional images with near-infrared light. Tissue structures are imaged up to an imaging depth of 2-3 mm and with a resolution of $\pm 10\text{-}15\ \mu\text{m}$ [40, 41]. The concept is comparable with ultrasound but instead of using sound-waves OCT uses the reflection or scattering of near-infrared light and a transducing medium (such as water in ultrasound) is not required.

OCT has originally been used in ophthalmology to assess the retina [42-44]. Another field in which OCT is used is interventional cardiology to assess stenosis and stent placement in coronary arteries [45]. In pulmonology, OCT imaging has been limited to research settings. It can be applied as an add on to conventional bronchoscopy procedures.

The studies in this thesis have all been performed with a C7 Dragonfly catheter and C7-XR St Jude Medical Inc (Abbott nowadays) system (IL, USA). The OCT probe has a diameter of 0.9 mm and is inserted through the working channel of the bronchoscope and placed in the airway of interest (**Figure 4**). Next, an automated pullback (**Figure 5**) is performed during which the OCT catheter retracts over a length of 5.4 cm thereby generating cross-sectional 2D images that can be reconstructed into an airway segment. The tissue structures in the airway wall partly absorb the 360 degrees circumferential light and scatter it back to the catheter, where the difference in time of backscattering is used to generate images according to optical interferometry principles.

Studies have shown that OCT is able to identify and quantify airway wall layers and structures with a near-histology resolution (**Figure 6**) [46-50]. OCT might therefore qualify as the optimal imaging technique to assess airway remodeling, monitor diseases and potentially evaluate treatment response. An overview of the literature regarding the use of OCT in pulmonary diseases and potential future applications are discussed in chapter 6 of this thesis.

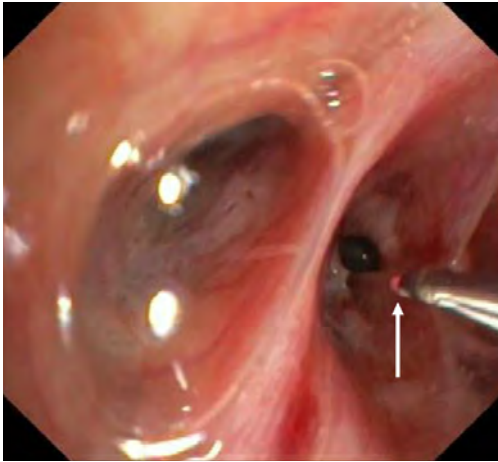


Figure 4. Bronchoscopic view of a C7 Dragonfly OCT catheter (St Jude Medical Inc) inserted through the working channel of a bronchoscope into the airway of interest. This photo is captured during an OCT measurement with the tip of the OCT catheter positioned distally into the airway emitting near infrared light (white arrow) to create cross sectional images.

OCT: optical coherence tomography. (Courtesy of J.T. Annema and P.I. Bonta)

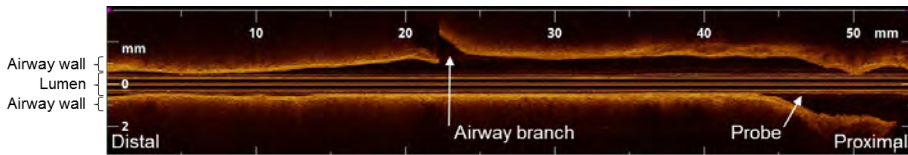


Figure 5. Pullback of an airway segment showing a longitudinal view of the airway wall containing 540 2D images. During a pullback, the OCT probe, positioned in the middle of the lumen (see white arrow), retracts automatically thereby obtaining images over a length of 5.4 cm. OCT: optical coherence tomography. (Courtesy of J.T. Annema and P.I. Bonta)

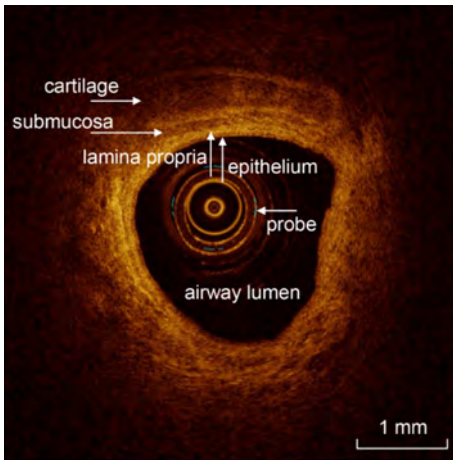


Figure 6. In-vivo optical coherence tomography image of the posterobasal airway showing the probe, airway lumen, epithelium, lamina propria, submucosa and cartilage. (Courtesy of J.T. Annema and P.I. Bonta)

Objectives of this thesis

At the initiation of the TASMA study in 2014, several unanswered questions existed regarding the treatment of severe asthma patients with Bronchial Thermoplasty. We aimed to answer the following research questions in this thesis:

1. What is the influence of bronchial thermoplasty on airway smooth muscle mass? Is the effect on airway smooth muscle mass correlated with response to Bronchial Thermoplasty treatment?
2. What is the response of severe asthma patients after Bronchial Thermoplasty treatment? Can we identify patient characteristics that are associated with a favorable response?
3. What is the influence of Bronchial Thermoplasty on metabolic gene expression profiles of bronchial epithelial cells?
4. What is the impact of Bronchial Thermoplasty on lung function parameters?
5. Can Optical Coherence Tomography be used to identify and measure airway wall layers and characteristics of airway remodeling?
6. What is the acute effect of Bronchial Thermoplasty on the airway wall? And can Optical Coherence Tomography detect these effects?

This thesis consists of four parts:

Part I Introduction

- Background information regarding (severe) asthma, treatment with Bronchial Thermoplasty, the TASMA study and imaging of the airways with Optical Coherence Tomography.

Part II Bronchial thermoplasty treatment in severe asthma

- Reduction of airway smooth muscle after Bronchial Thermoplasty and the correlation with lung function measurements.
- Airway smooth muscle reduction analyzed in a randomized controlled design and exploration of associations between baseline characteristics and response.
- Metabolic gene expression profile of epithelial cells after Bronchial Thermoplasty treatment.
- Forced oscillation technique and conventional lung function measurements to assess treatment effects of Bronchial Thermoplasty.

Part III Airway wall imaging with Optical Coherence Tomography

- Literature review about the use of Optical Coherence Tomography and Confocal Laser Endomicroscopy in pulmonary diseases.
- Airway wall layer identification and quantification with Optical Coherence Tomography and the comparison with histology.
- Using an automated method to identify and quantify the extracellular matrix in the airway wall with Optical Coherence Tomography and correlate this with histology.
- Identify acute effects of Bronchial Thermoplasty on the airway wall with Optical Coherence Tomography.

Part IV Discussion and future implications

- Summary of the studies and a general discussion.

References

1. Volksgezondheidzorg pvaih, 2018, <https://www.volksgezondheidzorg.info/onderwerp/astma/cijfers-context/huidige-situatie>.
2. Global burden of disease due to asthma, 2018, <http://www.globalasthmareport.org/burden/burden.php>.
3. Global Initiative for Asthma. Global Strategy for Asthma Management and Prevention, 2020. Available from: www.ginasthma.org.
4. Reed CE. The natural history of asthma. *The Journal of allergy and clinical immunology*. 2006;118(3):543-8; quiz 9-50.
5. Hekking PP, Wener RR, Amelink M, Zwinderman AH, Bouvy ML, Bel EH. The prevalence of severe refractory asthma. *The Journal of allergy and clinical immunology*. 2015;135(4):896-902.
6. Backman H, Jansson SA, Stridsman C, Eriksson B, Hedman L, Eklund BM, Sandström T, Lindberg A, Lundbäck B, Rönmark E. Severe asthma-A population study perspective. *Clinical and experimental allergy : journal of the British Society for Allergy and Clinical Immunology*. 2019;49(6):819-28.
7. O'Byrne PM, Naji N, Gauvreau GM. Severe asthma: future treatments. *Clinical and experimental allergy : journal of the British Society for Allergy and Clinical Immunology*. 2012;42(5):706-11.
8. Bel EH, Sousa A, Fleming L, Bush A, Chung KF, Versnel J, Wagener AH, Wagers SS, Sterk PJ, Compton CH, Unbiased Biomarkers for the Prediction of Respiratory Disease Outcome Consortium CG. Diagnosis and definition of severe refractory asthma: an international consensus statement from the Innovative Medicine Initiative (IMI). *Thorax*. 2011;66(10):910-7.
9. Chung KF, Wenzel SE, Brozek JL, Bush A, Castro M, Sterk PJ, Adcock IM, Bateman ED, Bel EH, Bleecker ER, Boulet LP, Brightling C, Chanaz P, Dahlen SE, Djukanovic R, Frey U, Gaga M, Gibson P, Hamid Q, Jajour NN, Mauad T, Sorkness RL, Teague WG. International ERS/ATS guidelines on definition, evaluation and treatment of severe asthma. *Eur Respir J*. 2014;43(2):343-73.
10. Serra-Batlles J, Plaza V, Morejon E, Comella A, Bruges J. Costs of asthma according to the degree of severity. *Eur Respir J*. 1998;12(6):1322-6.
11. Settipane RA, Kreindler JL, Chung Y, Tkacz J. Evaluating direct costs and productivity losses of patients with asthma receiving GINA 4/5 therapy in the United States. *Annals of allergy, asthma & immunology : official publication of the American College of Allergy, Asthma, & Immunology*. 2019.
12. Busse W, Corren J, Lanier BQ, McAlary M, Fowler-Taylor A, Cioppa GD, van As A, Gupta N. Omalizumab, anti-IgE recombinant humanized monoclonal antibody, for the treatment of severe allergic asthma. *The Journal of allergy and clinical immunology*. 2001;108(2):184-90.
13. Castro M, Zangrilli J, Wechsler ME, Bateman ED, Brusselle GG, Bardin P, Murphy K, Maspero JF, O'Brien C, Korn S. Reslizumab for inadequately controlled asthma with elevated blood eosinophil counts: results from two multicentre, parallel, double-blind, randomised, placebo-controlled, phase 3 trials. *The Lancet Respiratory medicine*. 2015;3(5):355-66.

14. Pavord ID, Korn S, Howarth P, Bleecker ER, Buhl R, Keene ON, Ortega H, Chanez P. Mepolizumab for severe eosinophilic asthma (DREAM): a multicentre, double-blind, placebo-controlled trial. *Lancet*. 2012;380(9842):651-9.
15. Nederlandse Vereniging van Artsen voor Longziekten en Tuberculose (NVALT). Richtlijn diagnostiek en behandeling van ernstig astma, 2013. Available from: <https://www.nvalt.nl/kwaliteit/richtlijnen/copd-astma-allergie>.
16. Castro M, Rubin AS, Laviolette M, Fiterman J, De Andrade Lima M, Shah PL, Fiss E, Olivenstein R, Thomson NC, Niven RM, Pavord ID, Simoff M, Duhamel DR, McEvoy C, Barbers R, Ten Hacken NH, Wechsler ME, Holmes M, Phillips MJ, Erzurum S, Lunn W, Israel E, Jarjour N, Kraft M, Shargill NS, Quiring J, Berry SM, Cox G, Group AIRTS. Effectiveness and safety of bronchial thermoplasty in the treatment of severe asthma: a multicenter, randomized, double-blind, sham-controlled clinical trial. *American journal of respiratory and critical care medicine*. 2010;181(2):116-24.
17. Cox G, Thomson NC, Rubin AS, Niven RM, Corris PA, Siersted HC, Olivenstein R, Pavord ID, McCormack D, Chaudhuri R, Miller JD, Laviolette M, Group AIRTS. Asthma control during the year after bronchial thermoplasty. *The New England journal of medicine*. 2007;356(13):1327-37.
18. Pavord ID, Cox G, Thomson NC, Rubin AS, Corris PA, Niven RM, Chung KF, Laviolette M, Group RTS. Safety and efficacy of bronchial thermoplasty in symptomatic, severe asthma. *American journal of respiratory and critical care medicine*. 2007;176(12):1185-91.
19. Chupp G, Laviolette M, Cohn L, McEvoy C, Bansal S, Shifren A, Khatri S, Grubb GM, McMullen E, Strauven R, Kline JN. Long-term outcomes of bronchial thermoplasty in subjects with severe asthma: a comparison of 3-year follow-up results from two prospective multicentre studies. *Eur Respir J*. 2017;50(2).
20. Pavord ID, Thomson NC, Niven RM, Corris PA, Chung KF, Cox G, Armstrong B, Shargill NS, Laviolette M, Research in Severe Asthma Trial Study G. Safety of bronchial thermoplasty in patients with severe refractory asthma. *Annals of allergy, asthma & immunology : official publication of the American College of Allergy, Asthma, & Immunology*. 2013;111(5):402-7.
21. Thomson NC, Rubin AS, Niven RM, Corris PA, Siersted HC, Olivenstein R, Pavord ID, McCormack D, Laviolette M, Shargill NS, Cox G, Group AIRTS. Long-term (5 year) safety of bronchial thermoplasty: Asthma Intervention Research (AIR) trial. *BMC pulmonary medicine*. 2011;11:8.
22. Wechsler ME, Laviolette M, Rubin AS, Fiterman J, Lapa e Silva JR, Shah PL, Fiss E, Olivenstein R, Thomson NC, Niven RM, Pavord ID, Simoff M, Hales JB, McEvoy C, Slebos DJ, Holmes M, Phillips MJ, Erzurum SC, Hanania NA, Sumino K, Kraft M, Cox G, Sterman DH, Hogarth K, Kline JN, Mansur AH, Louie BE, Leeds WM, Barbers RG, Austin JH, Shargill NS, Quiring J, Armstrong B, Castro M, Asthma Intervention Research 2 Trial Study G. Bronchial thermoplasty: Long-term safety and effectiveness in patients with severe persistent asthma. *The Journal of allergy and clinical immunology*. 2013;132(6):1295-302.
23. Danek CJ, Lombard CM, Dungworth DL, Cox PG, Miller JD, Biggs MJ, Keast TM, Loomas BE, Wizeman WJ, Hogg JC, Leff AR. Reduction in airway

- hyperresponsiveness to methacholine by the application of RF energy in dogs. *Journal of applied physiology*. 2004;97(5):1946-53.
24. Miller JD, Cox G, Vincic L, Lombard CM, Loomas BE, Danek CJ. A prospective feasibility study of bronchial thermoplasty in the human airway. *Chest*. 2005;127(6):1999-2006.
 25. Denner DR, Doeing DC, Hogarth DK, Dugan K, Naureckas ET, White SR. Airway Inflammation after Bronchial Thermoplasty for Severe Asthma. *Annals of the American Thoracic Society*. 2015;12(9):1302-9.
 26. Pretolani M, Dombret MC, Thabut G, Knap D, Hamidi F, Debray MP, Taille C, Chanez P, Aubier M. Reduction of airway smooth muscle mass by bronchial thermoplasty in patients with severe asthma. *American journal of respiratory and critical care medicine*. 2014;190(12):1452-4.
 27. Pretolani M, Bergqvist A, Thabut G, Dombret MC, Knapp D, Hamidi F, Alavoine L, Taille C, Chanez P, Erjefalt JS, Aubier M. Effectiveness of bronchial thermoplasty in patients with severe refractory asthma: Clinical and histopathologic correlations. *The Journal of allergy and clinical immunology*. 2017;139(4):1176-85.
 28. Chakir J, Haj-Salem I, Gras D, Joubert P, Beaudoin EL, Biardel S, Lampron N, Martel S, Chanez P, Boulet LP, Laviolette M. Effects of Bronchial Thermoplasty on Airway Smooth Muscle and Collagen Deposition in Asthma. *Annals of the American Thoracic Society*. 2015;12(11):1612-8.
 29. d'Hooghe JNS, Ten Hacken NH, Weersink EJM, Sterk PJ, Annema JT, Bonta PI. Emerging understanding of the mechanism of action of Bronchial Thermoplasty in asthma. *Pharmacology & therapeutics*. 2017.
 30. Thomson NC. Recent Developments In Bronchial Thermoplasty For Severe Asthma. *Journal of asthma and allergy*. 2019;12:375-87.
 31. Chernyavsky IL, Russell RJ, Saunders RM, Morris GE, Berair R, Singapuri A, Chachi L, Mansur AH, Howarth PH, Dennison P, Chaudhuri R, Bicknell S, Rose F, Siddiqui S, Brook BS, Brightling CE. In vitro, in silico and in vivo study challenges the impact of bronchial thermoplasty on acute airway smooth muscle mass loss. *Eur Respir J*. 2018;51(5).
 32. Salem IH, Boulet LP, Biardel S, Lampron N, Martel S, Laviolette M, Chakir J. Long-Term Effects of Bronchial Thermoplasty on Airway Smooth Muscle and Reticular Basement Membrane Thickness in Severe Asthma. *Annals of the American Thoracic Society*. 2016;13(8):1426-8.
 33. Ryan DM, Fowler SJ, Niven RM. Reduction in peripheral blood eosinophil counts after bronchial thermoplasty. *The Journal of allergy and clinical immunology*. 2016;138(1):308-10 e2.
 34. Facciolongo N, DiStefano A, Pietrini V, Galeone C, Bellanova F, Menzella F, Scichilone N, Piro R, Bajocchi GL, Balbi B, Agostini L, Salsi PP, Formisano D, Lusuuardi M. Nerve ablation after bronchial thermoplasty and sustained improvement in severe asthma. *BMC pulmonary medicine*. 2018;18(1):29.
 35. Bousquet J, Chanez P, Lacoste JY, White R, Vic P, Godard P, Michel FB. Asthma: a disease remodeling the airways. *Allergy*. 1992;47(1):3-11.
 36. Jeffery PK. Remodeling in asthma and chronic obstructive lung disease. *American journal of respiratory and critical care medicine*. 2001;164(10 Pt 2):S28-38.

37. Pepe C, Foley S, Shannon J, Lemiere C, Olivenstein R, Ernst P, Ludwig MS, Martin JG, Hamid Q. Differences in airway remodeling between subjects with severe and moderate asthma. *The Journal of allergy and clinical immunology*. 2005;116(3):544-9.
38. Awadh N, Müller NL, Park CS, Abboud RT, FitzGerald JM. Airway wall thickness in patients with near fatal asthma and control groups: assessment with high resolution computed tomographic scanning. *Thorax*. 1998;53(4):248-53.
39. Benayoun L, Druilhe A, Dombret MC, Aubier M, Pretolani M. Airway structural alterations selectively associated with severe asthma. *American journal of respiratory and critical care medicine*. 2003;167(10):1360-8.
40. Huang D, Swanson EA, Lin CP, Schuman JS, Stinson WG, Chang W, Hee MR, Flotte T, Gregory K, Puliafito CA, et al. Optical coherence tomography. *Science*. 1991;254(5035):1178-81.
41. Tearney GJ, Brezinski ME, Bouma BE, Boppart SA, Pitris C, Southern JF, Fujimoto JG. In vivo endoscopic optical biopsy with optical coherence tomography. *Science*. 1997;276(5321):2037-9.
42. Fercher AF, Hitzinger CK, Drexler W, Kamp G, Sattmann H. In vivo optical coherence tomography. *American journal of ophthalmology*. 1993;116(1):113-4.
43. Swanson EA, Izatt JA, Hee MR, Huang D, Lin CP, Schuman JS, Puliafito CA, Fujimoto JG. In vivo retinal imaging by optical coherence tomography. *Optics letters*. 1993;18(21):1864-6.
44. Koustenis A, Jr., Harris A, Gross J, Januleviciene I, Shah A, Siesky B. Optical coherence tomography angiography: an overview of the technology and an assessment of applications for clinical research. *The British journal of ophthalmology*. 2017;101(1):16-20.
45. AJJ IJ, Zwaan EM, Oemrawsingh RM, Bom MJ, Dankers F, de Boer MJ, Camaro C, van Geuns RJM, Daemen J, van der Heijden DJ, Jukema JW, Kraaijeveld AO, Meuwissen M, Scholzel BE, Pundziute G, van der Harst P, van Ramshorst J, Dirksen MT, Zivelonghi C, Agostoni P, van der Heyden JAS, Wykrzykowska JJ, Scholte MJ, Nef HM, Kofflard MJM, van Royen N, Alings M, Kedhi E. Appropriate use criteria for optical coherence tomography guidance in percutaneous coronary interventions : Recommendations of the working group of interventional cardiology of the Netherlands Society of Cardiology. *Netherlands heart journal : monthly journal of the Netherlands Society of Cardiology and the Netherlands Heart Foundation*. 2018;26(10):473-83.
46. Hariri LP, Applegate MB, Mino-Kenudson M, Mark EJ, Medoff BD, Luster AD, Bouma BE, Tearney GJ, Suter MJ. Volumetric optical frequency domain imaging of pulmonary pathology with precise correlation to histopathology. *Chest*. 2013;143(1):64-74.
47. Pitris C, Brezinski ME, Bouma BE, Tearney GJ, Southern JF, Fujimoto JG. High resolution imaging of the upper respiratory tract with optical coherence tomography: a feasibility study. *American journal of respiratory and critical care medicine*. 1998;157(5 Pt 1):1640-4.
48. Hariri LP, Applegate MB, Mino-Kenudson M, Mark EJ, Bouma BE, Tearney GJ, Suter MJ. Optical frequency domain imaging of ex vivo pulmonary resection

- specimens: obtaining one to one image to histopathology correlation. *Journal of visualized experiments : JoVE*. 2013(71).
49. Lee AM, Kirby M, Ohtani K, Candido T, Shalansky R, MacAulay C, English J, Finley R, Lam S, Coxson HO, Lane P. Validation of airway wall measurements by optical coherence tomography in porcine airways. *PloS one*. 2014;9(6):e100145.
 50. Chen Y, Ding M, Guan WJ, Wang W, Luo WZ, Zhong CH, Jiang M, Jiang JH, Gu YY, Li SY, Zhong NS. Validation of human small airway measurements using endobronchial optical coherence tomography. *Respiratory medicine*. 2015;109(11):1446-53.

Part II.

Bronchial thermoplasty treatment
in severe asthma

Chapter 2.

Airway smooth muscle reduction after Bronchial Thermoplasty correlates with FEV₁

Goorsenberg AWM
d'Hooghe JNS
Ten Hacken NHT
Weersink EJM
Roelofs JJTH
Mauad T
Shah PL
Annema JT
Bonta PI

Clinical and Experimental Allergy 2019;49(4):541-544.

To the Editor,

Bronchial thermoplasty (BT) is a bronchoscopic treatment for severe asthma patients in whom the airways are treated with radio-frequency energy with the aim to improve asthma symptoms by reducing airway smooth muscle (ASM) [1]. So far, three patient cohorts reported ASM mass reduction after BT by using α -smooth muscle actin staining (α -SMA) [2-4]. However, the exact mechanism of action of BT and its related responder profile is unclear. Elucidating clinical parameters that predict response is a priority. Therefore, the objectives of this study are to: (a) assess the ASM in biopsies with two different staining methods; (b) detect the change in ASM mass after BT and compare this with the untreated right middle lobe (RML); (c) investigate if baseline ASM mass and ASM mass change correlates with baseline FEV₁.

Patients who fulfilled the World Health Organization or modified Innovative Medicines Initiative criteria of severe refractory asthma were included in the TASMA trial (Clin. Trials.gov NCT02225392) [5,6]. Ethical approval was obtained (NL45394.018.13). After informed consent, clinical evaluation was performed and biopsies from (sub)segmental airway carinas obtained during bronchoscopy prior to BT. Bronchoscopy was repeated 6 months post-BT, and airway biopsies were obtained from the BT-treated airways and the non-BT-treated RML.

Patients were treated with BT using the Alair system (Boston Scientific, Natick, MA, USA) [7]. Two desmin-stained (clone-33; biogenex, Fremont, CA, USA) and α -SMA (clone 1A4 DAKO, Santa Clara, CA, USA) sections per biopsy of two biopsies per time-point and one biopsy of the RML were measured, blinded, by automatic digital image analysis (ImageJ; NIH, Bethesda, MD, USA). ASM mass was defined as percentage (%) desmin or α -SMA-positive area of the total biopsy area (**Figure 1A**).

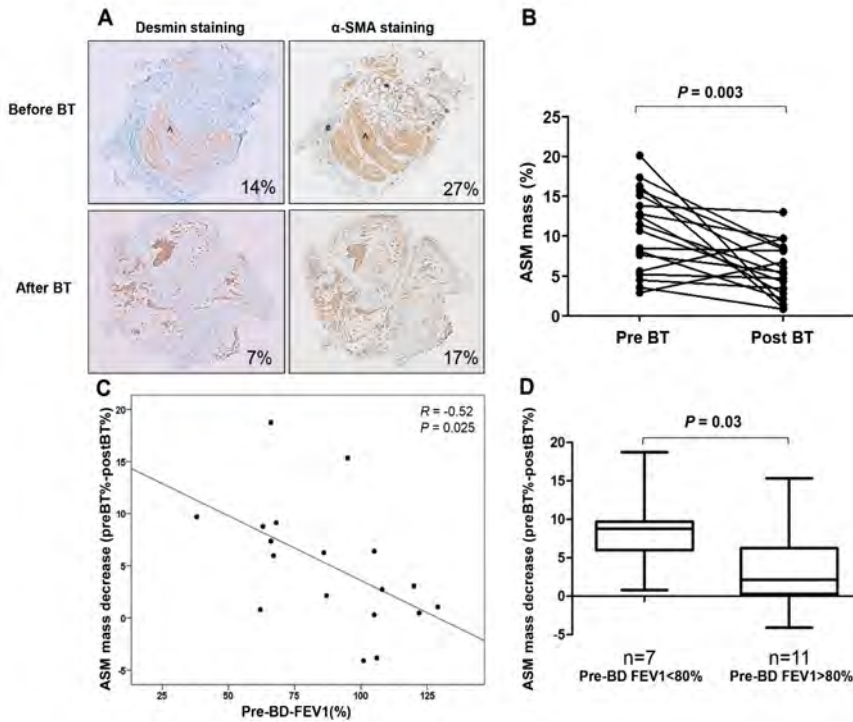


Figure 1

A, Desmin- and α -smooth muscle actin (α -SMA) stained airway biopsy sections before and after bronchial thermoplasty (BT) with the corresponding calculated airway smooth muscle (ASM) mass (%), showing ASM in the ASM layer (^), and for α -SMA the staining of myoepithelial cells in mucus glands (*) and pericytes in capillaries (#). Nuclei stained in blue (haematoxylin); ASM stained in brown (3'-Diaminobenzidine (DAB)). **B**, ASM mass reduction before and 6 months after BT assessed with desmin staining; median ASM mass (%) reduced from 11.1% (5.5; 15.3 IQR) before BT to 5.4% (2.6; 8.4 IQR) after BT (n = 18, P = 0.003). **C**, Negative correlation between pre-BD-FEV₁ (%) and the ASM mass decrease showing that patients with a lower pre-BD-FEV₁ have more reduction of ASM mass 6 months after BT-treatment (n = 18; R = -0.52; P = 0.025). ASM mass decrease defined as pre- minus post-ASM mass (%) assessed with desmin. BD = bronchodilator. **D**, Difference in ASM mass decrease between BT-treated patients with a pre-BD-FEV₁ <80% and pre-BD-FEV₁ >80%. ASM mass decrease defined as pre-BT minus post-BT-ASM mass (%) assessed with desmin. FEV₁ <80% (n = 7): 8.8% (6.0; 9.7 IQR) vs FEV₁ >80% (n = 11): 2.2% (0.3; 6.3 IQR) (P = 0.03)

Mann-Whitney test was performed for between group analysis and paired *t* test or Wilcoxon signed-rank for paired analyses before and after BT (GraphPad Prism 5.01, San Diego, CA, USA). Intraclass correlation coefficient (ICC) was calculated to assess the variability within biopsies and interpreted according

to Landis-Koch: <0.2 poor, 0.21-0.4 fair, 0.41-0.6 moderate, 0.61-0.8 substantial and 0.81-1 excellent.

Eighteen severe asthma patients were evaluated in this ASM mass analysis before and after BT-treatment. Baseline characteristics are presented in **Table 1**.

Table 1. Baseline characteristics

| Characteristics | Baseline |
|-----------------------------------------------------------------|-------------------------|
| No. of patients | 18 |
| Sex (males/females) | 4/14 |
| Age (y) | 45 (±13) |
| Age of asthma onset (y) | 18 (±16) |
| Total serum IgE (kU/L) | 61.6 (17.05; 212.5 IQR) |
| No. of patients with positive blood allergy test | 12 |
| Pre-short-acting BD FEV ₁ (% predicted) ^a | 89 (±25) |
| Post-short-acting BD FEV ₁ (% predicted) | 101 (±21) |
| PC20 methacholine test (mg/mL) (n = 17) ^b | 0.35 (0.03; 1.78 IQR) |
| Blood eosinophil count (10 ⁹ /L) | 0.15 (0.10; 0.29 IQR) |
| ACQ score | 2.6 (±0.7) |
| AQLQ score | 4.5 (±0.95) |
| Dose of LABA (µg/d salmeterol equivalents) | 147 (±62) |
| Dose of ICS (µg/d fluticasone equivalents) | 1208 (±495) |
| No. of patients on maintenance use of OCS | 6 |
| Dose of oral prednisone (mg/d) | 12 (±6) |
| No. of patients on omalizumab | 2 |
| ASM mass (%) assessed with desmin staining | 11.1 (5.5; 15.3 IQR) |
| ASM mass (%) assessed with α-SMA staining | 22.0 (17.6; 29.7 IQR) |

Data are presented as numbers, mean (±SD) or median (IQR). ACQ, Asthma Control Questionnaire; AQLQ, Asthma Quality of Life Questionnaire; ASM, airway smooth muscle; BD, bronchodilator; FEV₁, forced expiratory volume in 1 s; ICS, inhaled corticosteroids; LABA, long-acting beta-2-agonist; OCS, oral corticosteroids; α-SMA, α-smooth muscle actin. ^a Short-acting beta-agonists were stopped at least 6 h before the pulmonary function tests (long-acting beta-agonists and long-acting muscarinic antagonists continued). ^b A single patient fulfilled the reversibility criteria of asthma, but tested negative on PC20 methacholine test and therefore was excluded from this analysis.

Asthma Control Questionnaires (ACQ) and Asthma Quality of Life Questionnaires (AQLQ) significantly improved after BT (ACQ decreased from 2.6 (±0.7) to 1.9 (±1.0) ($P = 0.02$); AQLQ improved from 4.5 (±0.95) to 5.2 (±0.99) ($P = 0.01$)). Additionally, exacerbation rates were significantly lower after 6 months showing a reduction from 1.75 (0.88;3.5 IQR) per 6 months before BT

to 0.00 (0.00;0.25 IQR) per 6 months after BT ($P = 0.0034$). Medication use after BT was not modified in this study because asthma medication needed to be stable during the 6 months of follow-up.

Desmin staining analyses showed >50% reduction of the median ASM mass after BT from 11.1% (5.5; 15.3 IQR) to 5.4% (2.6; 8.4 IQR) ($n = 18$; $P = 0.003$) (**Figure 1B**). The untreated RML remained unchanged at 6 months (median 10.7% (5.4; 14.8 IQR) to 9.2% (3.4; 10.7 IQR) ($n = 17$; $P = 0.45$). Pre- and post-bronchodilator FEV₁ negatively correlated with baseline ASM mass ($R = -0.63$; $P = 0.005$ and $R = -0.63$; $P = 0.005$, respectively). Furthermore, ASM mass decrease after BT negatively correlated with pre- and post-bronchodilator FEV₁ ($R = -0.52$; $P = 0.025$ and $R = -0.49$; $P = 0.04$, respectively) (**Figure 1C**), indicating that patients with a lower FEV₁ had more ASM mass reduction after BT-treatment. Additionally, a significant difference in ASM mass decrease was observed between patients with a FEV₁ below 80% as compared to patients with a FEV₁ larger than 80% (FEV₁<80% ($n = 7$): 8.8% (6.0; 9.7 IQR) vs FEV₁ > 80% ($n = 11$): 2.2% (0.3; 6.3 IQR; $p = 0.03$) (**Figure 1D**).

The same analyses were performed with α -SMA staining which confirmed an ASM mass reduction after BT, although less profound (median 22.0% (17.6; 29.7 IQR) to 13.6% (9.5; 15.1 IQR) ($n = 18$; $P = 0.0005$)). The ASM mass of the RML remained unchanged (baseline median ASM mass of 21.0% (17.5; 28.1 IQR) vs 18.8% (13.7; 25.1 IQR) at 6 months ($n = 17$; $P = 0.09$)). The correlation with FEV₁ and baseline ASM mass or ASM mass decrease was not found with α -SMA staining. A moderate ICC between biopsies of 0.52 for desmin and a fair ICC of 0.33 for α -SMA was found.

This study demonstrates that BT-treatment results in ASM mass decrease by two different staining methods and shows for the first time that baseline FEV₁ is negatively correlated with ASM mass decrease after BT. This might imply that BT is more effective in reducing ASM mass in asthma patients with airway remodelling. Previously, Benayoun et al [8] showed that in asthma patients, an increased ASM mass correlates with a decreased FEV₁. Furthermore, Chakir et al and Pretolani et al have demonstrated ASM reduction following BT using α -SMA but none of these studies have shown a correlation between ASM mass and functional parameters [2,4]. In line with the study of Chakir et al, [2] no correlations were found between clinical improvements and ASM. A larger sample size is needed to explore these correlations. Since ASM is considered a key feature of airway remodelling, the correlations found between FEV₁ and baseline ASM mass and ASM mass decrease after BT using desmin staining, supports the hypothesis that BT has an impact on airway remodelling.

The ASM mass of the RML did not significantly change after BT in this study; however, a trend was seen towards reduction in the α -SMA stained biopsies. One study showed a significant decrease in α -SMA stained ASM mass in the

RML after BT [9], but this decrease was not confirmed in the larger follow-up study [4]. Due to the historical fear of atelectasis and RML syndrome, current recommendations do not advise to treat the RML [10]. A future trial investigating the safety and efficacy of reducing the ASM mass in the RML with BT is indicated. We compared airway biopsies from different predefined (sub) segmental airway carinas which could potentially bias the results. However, comparing ASM biopsies from different areas has been shown feasible with a 7%-12% coefficient of variation for the ASM mass between 10 biopsies taken from the upper lobes, lower lobes and RML within a patient [4]. Furthermore, we compared two different ASM staining methods, desmin and α -SMA. The present data show and confirm that desmin staining specifically identifies the differentiated contractile ASM present in the ASM layer, whereas the α -SMA also stains mucosal myofibroblasts, myoepithelial cells around glands and pericytes in capillaries/myofibroblast in blood vessels (**Figure 1A**) [11,12]. We hypothesize that the correlation between ASM and FEV₁ depends on the fully differentiated contractile ASM located in the airway wall only and is not related to the α -SMA stained glandular myoepithelial cells and vascular pericytes/myofibroblasts. This probably explains the higher pre-BT ASM mass for α -SMA staining when compared to desmin staining, the less profound decrease of ASM mass and the absence of a correlation between ASM mass (change) and FEV₁. In our opinion, desmin is the staining method of choice for analysing BT-treatment effects on ASM.

In conclusion, ASM mass significantly decreased 6 months following BT-treatment. Severe asthma patients with a FEV₁ < 80% have a greater ASM mass at baseline and show the most reduction of ASM mass after BT as shown by ASM layer specific desmin staining. Whether this specific phenotype of severe asthma patients with low FEV₁ responds best to BT, and whether a low FEV₁ should therefore be a pre-requisite for BT, needs to be determined in a larger sample size.

References

1. Chung KF, Wenzel SE, Brozek JL, et al. International ERS/ATS guide-lines on definition, evaluation and treatment of severe asthma. *Eur Respir J.* 2014;43:343-373.
2. Chakir J, Haj-Salem I, Gras D, et al. Effects of bronchial thermo-plasty on airway smooth muscle and collagen deposition in asthma. *Ann Am Thorac Soc.* 2015;12:1612-1618.
3. Denner DR, Doeing DC, Hogarth DK, Dugan K, Naureckas ET, White SR. Airway inflammation after bronchial thermoplasty for severe asthma. *Ann Am Thorac Soc.* 2015;12:1302-1309.
4. Pretolani M, Bergqvist A, Thabut G, et al. Effectiveness of bron-chial thermoplasty in patients with severe refractory asthma: clinical and histopathologic correlations. *J Allergy Clin Immunol.* 2017;139:1176-1185.
5. Bel EH, Sousa A, Fleming L, et al. Diagnosis and definition of severe refractory asthma: an international consensus statement from the Innovative Medicine Initiative (IMI). *Thorax.* 2011;66:910-917.
6. Bousquet J, Mantzouranis E, Cruz AA, et al. Uniform definition of asthma severity, control, and exacerbations: document presentedfor the World Health Organization Consultation on Severe Asthma. *J Allergy Clin Immunol.* 2010;126:926-938.
7. Castro M, Rubin AS, Laviolette M, et al. Effectiveness and safety of bronchial thermoplasty in the treatment of severe asthma: a multi-center, randomized, double-blind, sham- controlled clinical trial. *Am J Respir Crit Care Med.* 2010;181:116-124.
8. Benayoun L, Druilhe A, Dombret MC, Aubier M, Pretolani M. Airway structural alterations selectively associated with severe asthma. *Am J Respir Crit Care Med.* 2003;167:1360-1368.
9. Pretolani M, Dombret MC, Thabut G, et al. Reduction of airway smooth muscle mass by bronchial thermoplasty in patients with se-vere asthma. *Am J Respir Crit Care Med.* 2014;190:1452-1454.
10. Bonta PI, Chanez P, Annema JT, Shah PL, Niven R. Bronchial thermoplasty in severe asthma: best practice recommendations from an expert panel. *Respiration.* 2018;95:289-300.
11. Green FH, Williams DJ, James A, McPhee LJ, Mitchell I, Mauad T. Increased myoepithelial cells of bronchial submucosal glands in fatal asthma. *Thorax.* 2010;65:32-38.
12. Slat AM, Janssen K, van Schadewijk A, et al. Expression of smooth muscle and extracellular matrix proteins in relation to airway func-tion in asthma. *J Allergy Clin Immunol.* 2008;121:1196-1202.

Chapter 3.

Bronchial Thermoplasty induced airway smooth muscle reduction and clinical response in severe asthma: the TASMA randomized trial

Goorsenberg AWM
d'Hooghe JNS
Srikanthan K
Ten Hacken NHT
Weersink EJM
Roelofs JJTH
Kemp SV
Bel EH
Shah PL
Annema JT
Bonta PI

*Accepted for publication in American Journal of Respiratory and Critical
Care Medicine*

Abstract

Rationale Bronchial Thermoplasty (BT) is a bronchoscopic treatment for severe asthma targeting airway smooth muscle (ASM). Observational studies have shown ASM mass reduction after BT but appropriate control groups are lacking. Furthermore, as treatment response is variable, identifying optimal candidates for BT treatment is important.

Aims First, to assess the effect of BT on ASM mass and second, to identify patient characteristics that correlate with BT-response.

Methods Severe asthma patients (n=40) were randomized to immediate (n=20) or delayed (n=20) BT-treatment. Prior to randomization, clinical, functional, blood and airway biopsy data were collected. In the delayed control group, re-assessment, including biopsies, was performed after 6 months of standard clinical care, followed by BT. In both groups, post-BT data including biopsies were obtained after 6 months. ASM mass (% positive desmin or α -smooth muscle actin area in the total biopsy) was calculated with automated digital analysis software. Associations between baseline characteristics and Asthma Control and Asthma Quality of Life Questionnaire (ACQ/ AQLQ) improvement were explored.

Results Median ASM mass decreased by >50% in the immediate BT group (n=17) versus no change in the delayed control group (n=19) (p=0.0004). In the immediate group ACQ scores improved with -0.79 (-1.61;0.02 IQR) compared to 0.09 (-0.25;1.17 IQR) in the delayed group (p=0.006). AQLQ scores improved with 0.83 (-0.15;1.69 IQR) versus -0.02 (-0.77;0.75 IQR) (p=0.04). Treatment response in the total group (n=35) was positively associated with serum IgE and eosinophils, but not with baseline ASM mass.

Conclusion ASM mass significantly decreases after BT when compared to a randomized non-BT treated control group. Treatment response was associated with serum IgE and eosinophil levels but not with ASM mass.

Introduction

Severe asthma is a disease characterized by persistent symptoms and frequent exacerbations despite optimal treatment with high doses of inhaled corticosteroids and long acting bronchodilators [1, 2]. Although only approximately 5% of asthma patients fulfill the criteria for a diagnosis of severe asthma [3], the burden on health care costs is high due to medication use and frequent hospitalizations [4, 5]. Recent advances in treatment options for severe asthma patients are the implementation of biologicals for specific asthma phenotypes such as anti-immunoglobulin E (IgE) treatment for allergic asthma and anti-interleukin-5 (IL-5) treatment for eosinophilic asthma [6-8]. However, not all patients tolerate and/or respond to these treatments and for non-allergic and non-eosinophilic asthma phenotypes no specific biological treatment is available.

Bronchial thermoplasty (BT) is an endoscopic treatment, targeting airway smooth muscle (ASM) by heating the medium to larger sized airways with radio-frequency energy [9]. Observational studies have shown a reduction in ASM mass after BT, however appropriate control groups are lacking and a relationship with treatment response is not clear [10-13]. While clinical studies have shown improvements in asthma control and quality of life and a reduction in exacerbation rate [14-17], not all patients respond equally well to BT. Identification of clinical and physiological characteristics associated with BT response are needed to optimize patient selection and further elucidate the mechanism of action of this treatment.

In this study, we aimed to assess the effect of BT on ASM mass in the airways of severe asthma patients using a randomized controlled design and the untreated right middle lobe. Secondary outcomes included the evaluation of patient characteristics and biomarkers associated with BT response. Some of the results of this study have been previously reported in the form of abstracts [18-22].

Methods

Study design

This study is an investigator initiated, international multicenter randomized controlled trial (Clinical trials.gov NCT02225392). Patients were recruited between 2014 and 2018 in two centers in the Netherlands (Amsterdam University Medical Centers, location Academic Medical Center (AMC) and University Medical Center in Groningen) and two centers in the United Kingdom (Royal Brompton Hospital and the Chelsea & Westminster Hospital, both in London). After informed consent, patients were screened and characterized using demographic data, medical history including exacerbation rate, asthma questionnaires, routine blood analysis including eosinophils and allergy tests,

routine pulmonary function tests, methacholine challenge (PC20) tests and a bronchoscopy for the detection of airway abnormalities and measurement of baseline airway smooth muscle mass in bronchial biopsies. After the bronchoscopy, patients were randomized into an immediate BT treatment group and a 6 months delayed treatment group, the control group. Additional visits, similar to those during screening, were scheduled for the delayed group after 6 months of standard clinical care, including a research bronchoscopy with endobronchial biopsy sampling. In both randomization groups, patients were in follow-up for 6 months after BT treatment after which clinical and functional assessments, blood tests and endobronchial biopsies were collected. Directly after each research bronchoscopy patients were treated with 50 mg of prednisolone for 3 days. Asthma medication remained unchanged during the complete study period. The study design is shown in **Figure 1**.

Randomization and sample size calculation

Patients were randomized into an immediate BT treatment and 6 months delayed BT treatment control group (1:1 ratio, n=20 per group). Stratification factors used in the randomization were forced expiratory volume in 1 sec (FEV₁) lower or higher than 70% of predicted value and eosinophil counts (in sputum < or ≥ 3% or when sputum was not available in blood < or ≥ 0.3×10⁹/L). Power calculation for the primary endpoint was based on an estimated decrease of 20% in ASM mass after treatment and determined as 18 patients per group [23]. Accounting for a 10% dropout rate, we aimed to include 20 patients per group, 40 patients in total.

Subjects

Severe asthma patients between 18 and 65 years old, fulfilling the World Health Organization or modified Innovative Medicines Initiative criteria, were included [1, 24]. See the online supplement for a detailed description of the definition of severe asthma. The diagnosis of asthma needed to be confirmed in the 5 years prior to inclusion by one of the following parameters: reversibility to β₂-agonists in FEV₁ of ≥ 12% predicted and ≥ 200ml, bronchial hyperresponsiveness to methacholine or histamine (PC 20 < 4 mg/ml), peak-flow variability of > 20% over a two weeks period or a fall in FEV₁ of > 12% predicted and > 200 ml after tapering down asthma treatment. Ethical approval was provided by the ethical committees of the 4 centers and informed consent was obtained from all patients. Main exclusion criteria were pre-bronchodilator FEV₁ < 50% predicted or < 1.2L, 5 or more hospitalizations in the year prior to inclusion or more than one intensive care admission for asthma requiring endotracheal intubation, oral corticosteroid maintenance therapy of more than 20 mg/day, asthma exacerbation or a respiratory tract infection in the prior 4 weeks, unable to undergo multiple bronchoscopies due to allergies to the required medications or comorbidities. Additionally patients with BMI ≥ 35, relevant abnormalities on a high-resolution computed tomography scan or current smokers and a pack year history of more than 15 years were excluded from participating in this trial.

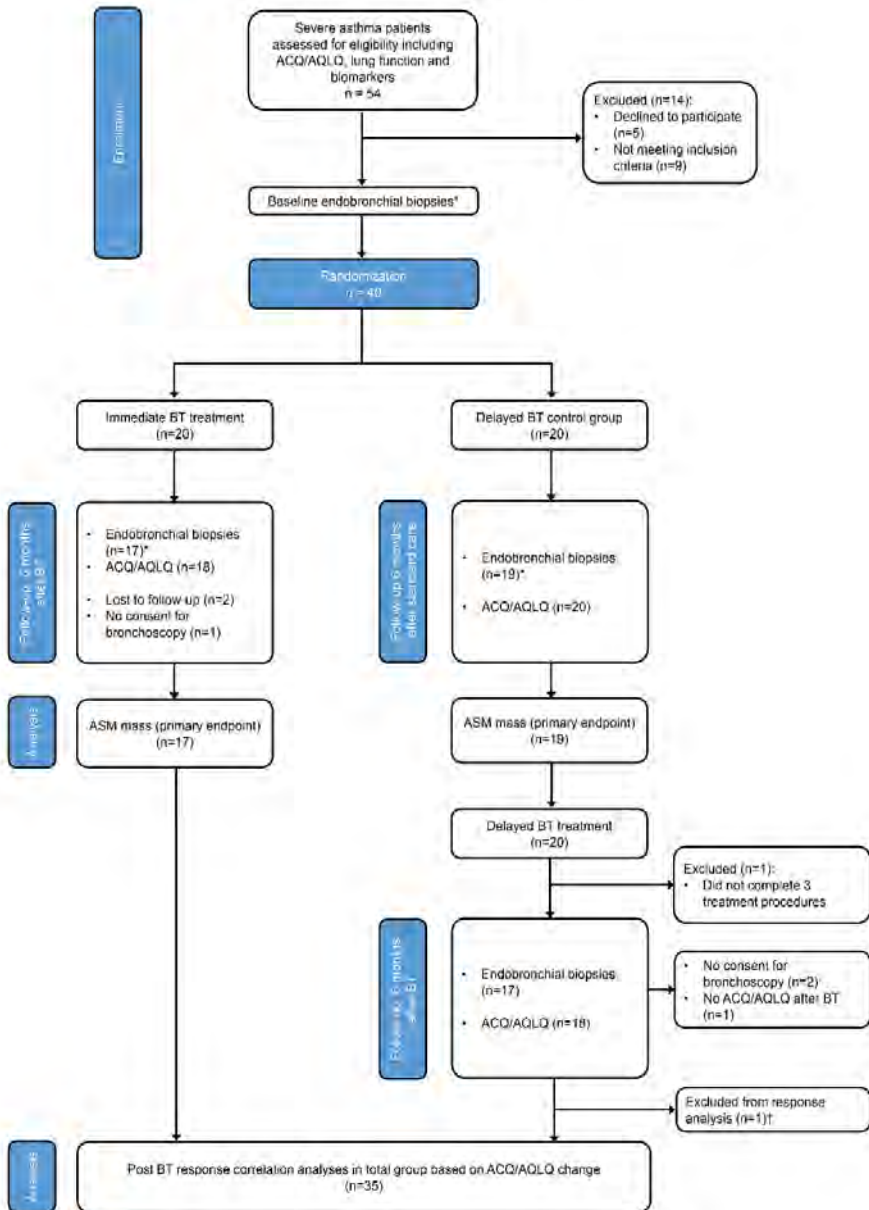


Figure 1. Flowchart of study design and participants (adapted from CONSORT)

The primary endpoint of this study is the comparison between the change in airway smooth muscle (ASM) mass after BT in the immediate BT treatment group and the change in the delayed BT treatment group after 6 months standard clinical care. Time points of primary endpoint data collection are highlighted with an asterisk (*). Response analysis was performed in the total group (n=35) of patients in which ACQ/AQLQ were collected 6 months after BT.

†Excluded from response analysis because this patient started anti IL-5 treatment during follow-up. BT: bronchial thermoplasty, ACQ: asthma control questionnaire, AQLQ: asthma quality of life questionnaire.

Bronchial thermoplasty treatment

Treatment procedures were performed according to current guidelines [25] with the Alair System (Boston Scientific, USA) using general anesthesia or conscious sedation (remifentanyl/propofol) [26]. Treatment sessions of the right lower lobe (RLL), left lower lobe (LLL) and both upper lobes were carried out with at least a 3 weeks interval between procedures. The right middle lobe (RML) remained untreated. Patients were treated with 50 mg of prednisolone 3 days before the treatment, during the procedure and one day thereafter.

Response assessment

Clinical response to BT was measured with asthma control questionnaires (ACQ-6) and asthma quality of life questionnaires (AQLQ) 6 months after BT. In addition, asthma exacerbations, defined as the need to increase the dose of systemic corticosteroids or a doubling dose of inhaled corticosteroids for more than 3 consecutive days, were assessed during the complete study period. Exacerbations after BT treatment were calculated from 6 weeks after the last treatment until the follow-up visit at 6 months and defined as exacerbation rate per 6 months. FEV₁ reversibility (post salbutamol FEV₁ % predicted minus pre salbutamol FEV₁ % predicted) and methacholine challenge tests were also evaluated after treatment.

Histology processing and analysis

Endobronchial biopsies were obtained with large cup forceps of pre-defined (sub)segmental airway carinas. During the research bronchoscopies before treatment, 4 biopsies were obtained. During the bronchoscopy after treatment 6 biopsies were taken, including 2 biopsies (one segmental and one subsegmental) from the untreated right middle lobe. Biopsies were paraffin-embedded, sectioned, attached to glass slides and stained for ASM-specific desmin (clone-33, biogenes, Fremont, USA) and α -smooth muscle actin (α -SMA) (clone 1A4 DAKO, Santa Clara, USA). From each biopsy the two biopsy sections with the highest total surface area were included in the analysis and blindly measured, using automated digital image analysis software (ImageJ, NIH, Bethesda, USA) [27]. Sections without epithelium/mucosal layer or with artefacts were excluded from the analysis. ASM mass was measured as the percentage of positive stained desmin/ α -SMA area as compared to the total biopsy area as previously described [11].

Study endpoints

The primary endpoint of this study was the absolute difference in ASM change between the direct BT treatment group and the delayed control group (post-

BT ASM% minus pre-BT ASM% in the direct group versus delayed group ASM% at control visit minus pre-BT ASM%) (**Figure 1**). Secondary endpoints are the ASM mass change after BT in the total group and in the untreated RML. Additionally, response to BT was evaluated using ACQ-6 and AQLQ scores after BT, exacerbation rates and lung function parameters. Associations between response to BT, as assessed with ACQ-6 and AQLQ questionnaires, and baseline patient characteristics were analyzed. Additional hypothesis generating exploratory endpoints as mentioned on clinicaltrials.gov are not included in this manuscript because these research questions were investigated in one center only and need separate analysis [28].

Statistical analysis

Statistical analyses were performed in GraphPad Prism version 5.01 (GraphPad Software Inc, San Diego, CA, USA) or IBM SPSS Statistics version 25.0 (New York, USA). Demographic parameters were provided as mean with standard deviation or median with interquartile ranges. Mann Whitney U tests were performed to assess the difference in change from baseline between the immediate group, 6 months after BT, and the delayed treatment group, 6 months after standard clinical care. The effect of BT in the total group of patients was calculated with paired t-tests or Wilcoxon signed rank test. The Hodges-Lehman estimator [29] with 95% confidence interval is used to calculate median differences to quantify treatment effects (Rstudio Version 1.2.1335, Boston, USA). Spearman rank correlation was used to explore associations between patient characteristics and ACQ/AQLQ change. An improvement of > 0.5 points on ACQ-6 or AQLQ scores was considered as clinically relevant [30,31]. Two sided p-values were used with a statistical significance at $p < 0.05$.

Results

Subjects

A total of 54 patients were screened for eligibility, 14 patients were excluded. Reasons for exclusion were declining to participate (n=5), negative methacholine challenge tests ($PC_{20} < 4$ mg/ml) (n=6), pre-bronchodilator FEV_1 below 50% of predicted (n=2) and age (n=1). After screening, 40 patients were randomized between immediate and delayed BT treatment (**Figure 1**). Baseline demographic and clinical characteristics between both randomization groups were well matched except for a slightly higher ACQ score in the immediate treatment group (**Table 1**).

Procedural BT information and safety

A mean of 66 (± 29) radiofrequency activations were given in the right lower lobe, 62 (± 17) activations in the left lower lobe and 98 (± 42) activations in both upper lobes. No device related complications occurred. After 43 of the 119 BT procedures (36%) patients experienced an asthma exacerbation.

These exacerbations were all successfully treated with conventional asthma medication such as oral corticosteroids and nebulized bronchodilators. Patients required hospitalization following 9 of these exacerbations with a median length of hospital stay of 4 days (IQR 1;7). Other reported pulmonary adverse events were chest pain or discomfort (12%), dyspnea (15%), (productive) cough (16%), hemoptysis (7%), common cold (1%), bronchitis or sinusitis (3%), fever (1%) and lower respiratory tract infection (3%).

Clinical effectiveness

Changes from baseline in asthma questionnaires were significantly different between the immediate BT group 6 months after treatment and the delayed group 6 months after standard clinical care (**Table 2**). In the immediate BT-treatment group, ACQ scores improved with -0.79 (-1.61; 0.02 IQR) while in the delayed group a difference of 0.09 (-0.25; 1.17 IQR) was found (median difference -1.08 (-1.75; -0.33 95% CI), $p=0.006$). AQLQ improved in the immediate BT-treatment group with 0.83 (-0.15; 1.69 IQR) in comparison with -0.02 (-0.77; 0.75 IQR) in the delayed group (median difference 0.81 (0.06; 1.75 95% CI), $p=0.04$). No significant differences were found in changes in FeNO, pre short acting bronchodilator FEV₁(% predicted) and FEV₁ reversibility. A non-significant change of PC20 values after BT was found in the immediate BT group (0.19 (0.00; 0.85 IQR) as compared to the non-BT treated delayed group (0.0 (-0.03; 0.43 IQR)) (median difference 0.09 (-0.18; 0.64 95% CI), $p=0.08$). Asthma maintenance medication remained unchanged in both groups as requested during the study period.

In the total group of patients that completed the three BT procedures and clinical follow-up (n=35) ACQ scores improved from 2.67 (± 0.64) to 2.00 (± 1.05) ($P=0.0005$) and AQLQ scores improved from 3.99 (± 1.00) to 4.73 (± 1.24) ($P=0.0023$). 21 of the 35 patients (60%) showed a clinical meaningful improvement of more than 0.5 points on ACQ or AQLQ questionnaires [30, 31]. In addition, exacerbation rates per half year declined from 1.5 (1.0; 3.0 IQR) before treatment to 0 (0;1 IQR) after treatment ($P<0.0001$). FEV₁(% predicted) before short actin bronchodilation did not significantly change after BT (83% (± 25) before BT versus 87% (± 24) after BT ($P=0.14$)) while reversibility declined from 10.5 (4;16 IQR) before BT versus 3.5 (2;14 IQR) after BT ($P=0.03$) (n=32). Bronchial hyperresponsiveness, assessed with methacholine challenge tests, did not significantly change (0.25 mg/ml (0.03; 2.42 IQR) before BT versus 0.42 mg/ml (0.04; 4.0 IQR) after BT (n=29) ($P=0.11$)) (**Table 3**). Median differences in these clinical parameters in the total group of patients are shown in Table 3.

Table 1 Baseline characteristics

| Characteristics | Immediate BT group (n=20) | Delayed control group (n=20) |
|----------------------------------------------------------|---------------------------|------------------------------|
| Sex (males/females) | 3/17 | 8/12 |
| Age (years) | 45 ± 14 | 46 ± 10 |
| Age of asthma onset (years) | 20 ± 18 | 21 ± 14 |
| BMI | 29 ± 4 | 27 ± 5 |
| No. of patients with a history of smoking (pack years) | 4 (9 ± 5) | 10 (8 ± 9) |
| Medication | | |
| Dose of LABA (µg/d salmeterol equivalents) | 140 ± 81 | 146 ± 61 |
| Dose of ICS (µg/d fluticasone equivalents) | 1038 ± 609 | 1159 ± 592 |
| No. of patients on maintenance use of OCS (dose in mg/d) | 4 (9.3 ± 1.5) | 6 (15 ± 6.3) |
| No. of patients on omalizumab | 2 | 3 |
| Asthma control | | |
| Exacerbation rate / 6 months | 1.25 (0.5; 4.5) | 2.0 (1.5; 3.0) |
| ACQ-6 score | 2.97 ± 0.62 | 2.53 ± 0.66 |
| AQLQ score | 3.74 ± 0.91 | 4.18 ± 1.01 |
| Total serum IgE (kU/L) | 117 (35; 210) | 43.2 (9.9; 106) |
| Blood eosinophil count (10 ⁹ /L) | 0.15 (0.06; 0.34) | 0.11 (0.06; 0.29) |
| Lung Function | | |
| Pre-BD FEV ₁ (% predicted) | 80.9 ± 20 | 85 ± 27 |
| Post-BD FEV ₁ (% predicted) | 91.7 ± 20 | 100 ± 23 |
| Reversibility FEV ₁ (%) | 8.5 (4.0; 12.8) | 12 (7.0; 23.0) |
| PC20 (mg/ml) | 0.24 (0.03; 2.91) | 0.20 (0.03; 2.83) |
| FeNO | 14.5 (9.5; 59.5) (n=15) | 23.8 (13.5; 45) (n=12) |
| ASM mass (%) assessed with desmin staining | 7.99 (5.6; 11.9 IQR) | 7.14 (5.5; 10.5 IQR) |
| ASM mass (%) assessed with α-SMA staining | 19.69 (15.8; 23.9 IQR) | 18.68 (13.7; 23.3 IQR) |

Data are presented as mean (± SD) or median (IQR)

BMI: body mass index; LABA: long acting beta agonist; ICS: inhaled corticosteroids; OCS: oral corticosteroids; ACQ: asthma control questionnaire; AQLQ: asthma quality of life questionnaire; IgE: total immunoglobulin E; BD: short acting bronchodilation; FEV₁: forced expiratory volume in 1 second; PC20: methacholine provocation test; FeNO: fraction exhaled nitric oxide; ASM: airway smooth muscle; α-SMA: alpha smooth muscle actin.

Table 2 Immediate BT treatment group and delayed control group changes after 6 months

| Characteristics | Immediate treatment group (n=18) | | Delayed BT control group (n=20) | | P-value |
|----------------------------------------------------------------|-------------------------------------|-----------------------------|------------------------------------|---------------------------------|---------------------------------|
| | At inclusion | 6 months after BT | At inclusion | After 6 months standard care | |
| ACQ-6 score | 2.97 ± 0.62 | 2.13 ± 1.13 | 2.53 ± 0.66 | 2.86 ± 0.92 | 0.09 (-0.25; 1.17) |
| AQLQ score | 3.74 ± 0.91 | 4.63 ± 1.05 | 4.18 ± 1.0 | 4.06 ± 0.96 | -0.02 (-0.77; 0.75) |
| Dose of LABA (µg/d salmeterol equivalents) | 127.7 ± 56.0 | 127.7 ± 56.0 | 143.4 ± 57.1 | 140.9 ± 50.6 | 0 (0; 0) |
| Dose of ICS (µg/d fluticasone equivalents) | 1069 ± 629 | 1097 ± 613 | 1209 ± 660 | 1209 ± 660 | - |
| No. of patients on maintenance use of OCS (dose in mg/d) | 3 (9.2 ± 1.4) | 2 (8.8 ± 1.8) | 6 (15.0 ± 6.3) | 7 (14.3 ± 6.1) | 0 (0; 0) |
| Pre-bronchodilator FEV ₁ (%) predicted) | 80.9 ± 20.1 | 82.1 ± 23.4 | 85.5 ± 27 (n=19) | 86.0 ± 26 (n=19) | -1.0 (-7.25; 7.25) (n=19) |
| Reversibility FEV ₁ (%) | 8.5 (4.0;12.8) | 3.0 (2.0;13.5) | 12.0 (7;23) (n=19) | 13.0 (4;21) (n=19) | 1.0 (-5.25; 9.25) (n=19) |
| PC20 (mg/ml)† | 0.24 (0.03;2.91) | 1.33 (0.06;4.0) | 0.20 (0.03;2.83) (n=18) | 0.09 (0.03;2.60) (n=18) | 0.0 (-0.03; 0.43) (n=18) |
| FeNO (ppb) | 14.5 (9.5;59.5) (n=14) | 18.0 (11.3; 40.0) (n=14) | 23.8 (13.5;45.0) (n=12) | 25.0 (15.3;46.5) (n=12) | 1.75 (-5.38; 12.0) (n=12) |

Differences in change from baseline between both groups were analyzed using Mann-Whitney U test. Median changes within groups are shown. *significant difference with p<0.05. ACQ: asthma control questionnaire; AQLQ: asthma quality of life questionnaire; LABA: long acting beta agonist; ICS: inhaled corticosteroids; OCS: oral corticosteroids; FEV₁: forced expiratory volume in 1 sec; PC20: methacholine provocation test; FeNO: fraction exhaled nitric oxide; Medication use needed to be stable during the entire study period including follow-up. †Values were log transformed for statistical analysis.

Table 3. Clinical characteristics before and after bronchial thermoplasty in the total group (n=35)

| Characteristics | Before BT | After BT | Median difference (95% CI) | P-value |
|-----------------------------------------------------------------------------|----------------------|---------------------|----------------------------|----------|
| ACQ-6 score | 2.67 (\pm 0.64) | 2.00 (\pm 1.05) | -0.67 (-0.17; -1.17) | 0.0005* |
| AQLQ score | 3.99 (\pm 1.00) | 4.73 (\pm 1.24) | 0.85 (0.19;1.41) | 0.0023* |
| Exacerbation rate / 6 months | 1.5 (1.0;3.0 IQR) | 0 (0;1 IQR) | -1.0 (-0.50;-1.50) | <0.0001* |
| Pre-short acting bronchodilator FEV ₁ (% predicted) [†] | 83 (\pm 25) | 87 (\pm 24) | 4.00 (-10.00;16.00) | 0.14 |
| Reversibility FEV ₁ (%) [†] | 10.5 (4;16 IQR) | 3.5 (2;14 IQR) | -5.00 (-6.61e-06;-8.00) | 0.03* |
| PC20 (mg/ml) [‡] | 0.25 (0.03;2.42 IQR) | 0.42 (0.04;4.0 IQR) | 0.02 (-0.18; 1.12) | 0.11 |
| ASM mass (%) desmin [§] | 8.6 (5.3;11.6 IQR) | 4.0 (2.7;5.8 IQR) | -4.07 (-2.49;-5.78) | <0.0001* |
| ASM mass (%) α -SMA [§] | 19.5 (15.9;23.9 IQR) | 11.8 (8.9;13.9 IQR) | -7.54 (-5.07;-10.09) | <0.0001* |

Within group analyses performed with paired t-tests or Wilcoxon signed rank test depending on the distribution of the variables. Median differences with 95% confidence intervals (CI) are calculated using the Hodges-Lehmann estimator.

*significant difference with $p < 0.05$. Data are presented as mean (\pm SD) or median (IQR)[†]data available in $n=32$, [‡]Values were log transformed for statistical analysis and not available in 6 patients because of the inability to withhold asthma medications for the methacholine challenge test; [§]data available in $n=34$; ACQ: asthma control questionnaire; AQLQ: asthma quality of life questionnaire; FEV₁: forced expiratory volume in 1 sec; PC20: methacholine provocation test; ASM: airway smooth muscle mass; α -SMA: alfa smooth muscle actin.

Primary endpoint

In the direct treatment group ($n=17$), desmin positive ASM mass decreased by 53% from 8.75% (5.25; 12.0 IQR) to 4.14% (2.73; 6.29 IQR) ($P=0.0015$), while in the delayed group ($n=19$) ASM mass did not change: 7.08% (5.40; 9.98 IQR) at randomization to 7.56% (5.53; 10.44 IQR) after 6 months of standard care ($P=0.43$) (**Figure 2 and 3AB**). The absolute change in desmin positive ASM mass % between both randomization groups was significantly different: -4.44 (-8.3; -1.02 IQR) in the direct treatment group versus 0.62 (-2.30; 3.41 IQR) in the delayed control group (median difference -5.0 (-7.88; -2.56 95% CI), $p=0.0004$) (**Figure 3C**). For α -SMA positive ASM mass, similar results were found (**Figure E1**).

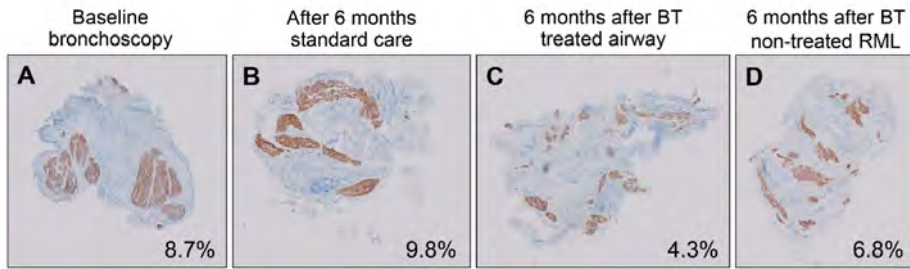


Figure 2. Airway smooth muscle mass percentage in the airways of one patient during the study.

Airway smooth muscle (ASM) mass % assessed with desmin staining **A**) before bronchial thermoplasty (BT) at randomization; **B**) after 6 months standard care; **C**) after BT in treated airways and **D**) after BT in the untreated right middle lobe (RML).

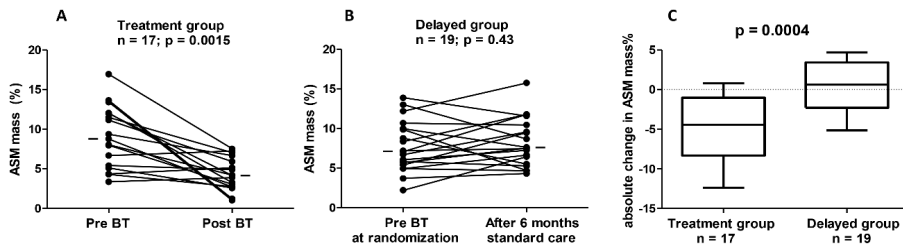


Figure 3. Airway smooth muscle decrease after bronchial thermoplasty as compared with the randomized control group.

A) ASM mass % in the immediate group before and after BT showing a median ASM mass % of 8.75% pre BT versus 4.14% post BT (53% decrease) **B)** ASM mass % in the delayed group before and after 6 months standard care with a median of ASM mass % of 7.08% at randomization versus 7.56% after 6 months standard care (7% increase) **C)** Difference in absolute ASM mass% change between both randomization groups (post BT – pre BT ASM% in the immediate BT-group and for the delayed control group the difference between baseline and 6 months standard care biopsies). ASM mass assessed with desmin staining.

Secondary endpoints

ASM mass in the total group after BT

BT reduced ASM mass in the total group (n=34) from 8.6% (5.3; 11.6 IQR) before BT to 4.02% (2.7; 5.8 IQR) after BT with a median difference of -4.07% (-2.49;-5.78 95% CI), P<0.0001). A difference between pre-BT ASM mass and the untreated post-BT RML (n=33) was also found: ASM mass at baseline was 8.2% (5.5; 11.4 IQR) compared to 5.4% (3.7; 8.2 IQR) in the untreated RML (median difference of -2.31 (-0.63; -4.20 95% CI), P=0.0024). In addition, post-BT ASM mass in

the treated areas (4.14% (2.7; 5.8 IQR)) was different when compared with the untreated RML (5.4% (3.7; 8.2 IQR)) (median difference of 1.35 (0.11; 2.66 95% CI), $P=0.0012$) (**Figure 4A**). When dividing the untreated RML biopsies in subsegmental ($n=29$) and segmental ($n=31$) biopsies, a difference was only found between subsegmental RML biopsies and the treated areas. No difference was found between the segmental RML biopsies and the treated areas (**Figure 4B**).

Associations between clinical response and baseline characteristics ($n=35$)

Associations were explored between ACQ and AQLQ change (post-BT minus pre-BT scores) and baseline patient characteristics in the total group (**Table 4**). ASM mass at baseline, ASM mass after BT and ASM change were not associated with ACQ and/or AQLQ improvement. Associations were found between ACQ improvement and baseline blood eosinophil count and total IgE count ($\rho=-0.46$ $p=0.006$ and $\rho=-0.53$ $p=0.001$ respectively). This association between total IgE level and ACQ improvement remained statistically significant after exclusion of patients who were treated with omalizumab during the study ($\rho=-0.46$ $p=0.009$). For AQLQ change only blood eosinophil counts were associated ($\rho=0.48$ $p=0.004$).

In addition, no associations were found between improvements on asthma questionnaires and changes in lung function such as FEV_1 , reversibility and methacholine challenge tests (PC20) nor with the amount of activations during treatment.

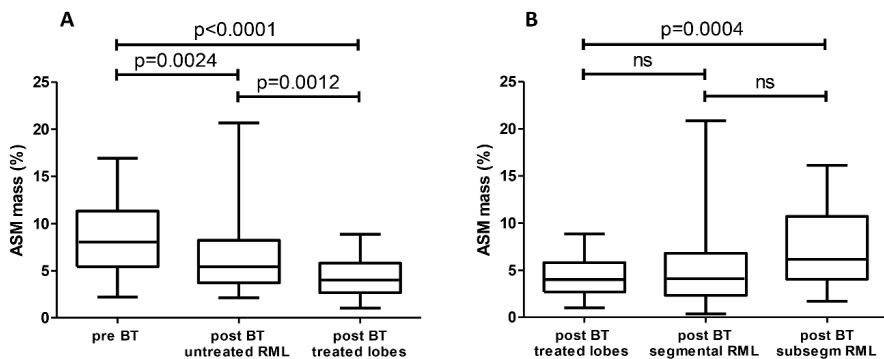


Figure 4. Airway smooth muscle mass reduction in the untreated right middle lobe as compared to BT treated airways.

Paired analyses showed **A**) a significant but less profound reduction in airway smooth muscle mass after bronchial thermoplasty in the untreated right middle lobe and **B**) subsegmental airways of the untreated right middle lobe have significantly more airway smooth muscle mass as compared to the treated airways after bronchial thermoplasty. ASM assessed with desmin staining.

ASM: airway smooth muscle; BT: bronchial thermoplasty; RML: right middle lobe;

Table 4 Associations between ACQ-6 and AQLQ improvement and baseline characteristics (n=35)

| | ACQ-6 change | | AQLQ change | |
|----------------------------------------------------|--------------|---------|-------------|---------|
| | rho | p-value | rho | p-value |
| Asthma age of onset | -0.20 | 0.25 | 0.30 | 0.08 |
| Total IgE [†] | -0.53 | 0.001* | 0.24 | 0.17 |
| Blood eosinophils x10 ⁹ /L [†] | -0.46 | 0.006* | 0.48 | 0.004* |
| Pre-SABA FEV ₁ % predicted [‡] | -0.02 | 0.89 | 0.20 | 0.26 |
| Reversibility FEV ₁ [‡] | -0.13 | 0.48 | 0.21 | 0.25 |
| PC20 (mg/ml) [§] | 0.30 | 0.08 | -0.09 | 0.61 |
| FeNO (ppb) | -0.28 | 0.19 | 0.21 | 0.33 |
| ASM mass (%) desmin | 0.07 | 0.69 | -0.009 | 0.96 |
| ASM mass (%) α -SMA | 0.18 | 0.29 | -0.05 | 0.79 |

Associations analyzed with spearman rho correlation coefficient. *significant correlation with p<0.05; p-value after Bonferroni correction for multiple comparisons p<0.006. [†]data available in n=34. [‡]data available in n=33; [§]Values were log-transformed for statistical analysis. ^{||}data available in n=24; ACQ: asthma control questionnaire; AQLQ: asthma quality of life questionnaire; IgE: immune globuline E; FEV₁: forced expiratory volume in 1 sec; PC20: methacholine provocation test; FeNO: fraction exhaled nitric oxide; ASM: airway smooth muscle mass; α -SMA: alfa smooth muscle actin.

Discussion

This study is the first to show a reduction in ASM mass 6 months after BT when compared to an appropriate non-BT-treated control group. Clinical response analysis could not reveal an association between ASM reduction and response. However, baseline blood eosinophils and total IgE counts were associated with improvements in ACQ and AQLQ scores after BT. These findings suggest that patients with high blood eosinophil counts and /or IgE levels are more likely to respond to BT treatment.

In this study, ASM mass reduction after BT has been investigated in a randomized controlled design using desmin and alpha smooth muscle actin stain. The results showed similar amounts of ASM mass at baseline as found in other severe asthma populations [13, 32] and confirm previously published results in observational studies [10, 12, 13, 32]. The reduction of ASM mass in the untreated RML adds novel information to the discussion about the mechanism of action of BT. While imaging studies using CT [33-35] and OCT [36] showed immediate effects of BT in non-treated parts of the lungs, biopsy studies including the RML were conflicting [12, 13]. The present results suggest that the effect of BT extends to untreated parts of the lungs as well, however not resulting in ASM reduction in the more distal subsegmental parts of these

airways. Several theories have been published regarding the possible extending effect of BT such as a heat shock effect along the bronchial tree, heat extension through (incomplete) fissures or through the distribution of mucus, blood and secretions to the lower lobes as a result of BT treatment in the upper lobes [34]. The decreasing effect of BT on ASM mass in more distal located parts of the RML adds to the hypothesis that indeed a heat-shock effect can be distributed to the distal airways.

A clinically relevant improvement in ACQ/AQLQ scores was found in the majority of patients and exacerbation rates were reduced in almost all patients during 6 months of follow-up after BT. The results in this study confirm the safety profile and clinical benefit of BT that has also been reported by several other research groups [14-17]. The optimal patient responder profile however, remains under debate. One novel and potentially important finding in this study was the correlation between BT response, as assessed by ACQ and AQLQ score changes, and baseline blood eosinophils and total IgE. The correlations found in this study are in line with results from a retrospective multicenter study with 47 patients in which atopic patients showed a better response to BT than non-atopic patients [37]. Currently, BT is mainly provided to patients who are not eligible or not responding to biological treatments [38]. Our results suggest that the same patients who are eligible for biological treatment might also be good candidates for BT. While these results need to be confirmed in larger cohorts, it might be both clinically and health-economically beneficial for some patients to be treated with BT before starting with lifelong biological treatment.

The amount of ASM mass at baseline and the change in ASM after BT did not correlate with BT response. Patient selection for BT based on airway remodeling as assessed in ASM mass analysis is therefore probably not optimal. Consequently, the exact mechanism of action of BT is not yet understood. Other studies have shown decreasing submucosal nerves and neuroendocrine cells in the epithelium after BT [13, 39], possibly correlating with BT-response, indicating that the effect of BT might be more targeted at other components than the ASM layer. We hypothesize that since BT results in denudation of the epithelium [36] and since there is no correlation between ASM reduction and response, the epithelium might be the primary target of BT. As a consequence, the mechanism of action of BT might be comparable to nitrogen cryospray in chronic bronchitis [40]. In this therapy it has been shown that after destroying the epithelium layer, the new regenerated epithelial cells might function as normal cells. Future studies should explore this hypothesis further.

One of the strengths of the present study is the randomized design. By using a control group with patients remaining on their regular asthma medication and management for 6 months, a proper control group was implemented. A sham treatment group was not included in the study design considering the

already high burden of multiple sampling bronchoscopies implemented in the TASMA study and the previously published BT sham randomized controlled trial [14]. In addition, the multicenter international design, with two centers in the Netherlands and two centers in the United Kingdom both including and treating patients, strengthens the generalizability. Also, the relatively large group of 40 severe asthma patients, thorough characterization of the patients and the use of two different staining techniques strengthen the quality of the current findings.

Several limitations need to be addressed. First, biopsies in this study were taken from different predefined (sub)segmental airway carinas. While this could potentially bias the results, variation between different lobes has been shown to be small [12] and by using different sites the risk of analyzing the effect of the previously taken biopsy instead of the BT treatment itself is mitigated. In addition, during each bronchoscopy, biopsies were taken from both the lower and upper lobes thereby limiting bias due to variations between lobes. Second, even though patients were randomized into two groups, the immediate treatment group seemed to have a higher ACQ and lower AQLQ score at baseline compared to the delayed control group. This comparison did not reach the minimally clinically relevant difference of 0.5 points and remained stable in the delayed non-BT control group. Furthermore, by comparing the change from baseline between both groups the statistical test partially corrected for this potential influence. In addition, the questionnaires were not associated with ASM mass and an influence on the primary outcome of this study is therefore not likely. Third, this study was powered for the assessment of ASM mass reduction but not for a response analysis. While the results regarding response add important information to the discussion about the optimal patient for BT, the results need to be confirmed in a larger cohort.

In summary, BT significantly reduces ASM mass in severe asthma patients when compared to non BT-treated controls and seems to affect the proximal parts of the untreated RML as well. No correlation was found between ASM mass and BT response. Importantly, significant correlations were found between blood eosinophil counts and total IgE at baseline and BT response, implicating that patients with higher blood eosinophil counts and/or IgE levels are potentially the most appropriate candidates for BT treatment.

References

1. Bel EH, Sousa A, Fleming L, Bush A, Chung KF, Versnel J, Wagener AH, Wagers SS, Sterk PJ, Compton CH, Unbiased Biomarkers for the Prediction of Respiratory Disease Outcome Consortium CG. Diagnosis and definition of severe refractory asthma: an international consensus statement from the Innovative Medicine Initiative (IMI). *Thorax* 2011; 66: 910-917.
2. Chung KF, Wenzel SE, Brozek JL, Bush A, Castro M, Sterk PJ, Adcock IM, Bateman ED, Bel EH, Bleecker ER, Boulet LP, Brightling C, Chanez P, Dahlen SE, Djukanovic R, Frey U, Gaga M, Gibson P, Hamid Q, Jajour NN, Mauad T, Sorkness RL, Teague WG. International ERS/ATS guidelines on definition, evaluation and treatment of severe asthma. *The European respiratory journal* 2014; 43: 343-373.
3. Hekking PP, Wener RR, Amelink M, Zwinderman AH, Bouvy ML, Bel EH. The prevalence of severe refractory asthma. *The Journal of allergy and clinical immunology* 2015; 135: 896-902.
4. Serra-Batlles J, Plaza V, Morejon E, Comella A, Bruges J. Costs of asthma according to the degree of severity. *The European respiratory journal* 1998; 12: 1322-1326.
5. Settipane RA, Kreindler JL, Chung Y, Tkacz J. Evaluating direct costs and productivity losses of patients with asthma receiving GINA 4/5 therapy in the United States. *Annals of allergy, asthma & immunology : official publication of the American College of Allergy, Asthma, & Immunology* 2019.
6. Busse W, Corren J, Lanier BQ, McAlary M, Fowler-Taylor A, Cioppa GD, van As A, Gupta N. Omalizumab, anti-IgE recombinant humanized monoclonal antibody, for the treatment of severe allergic asthma. *The Journal of allergy and clinical immunology* 2001; 108: 184-190.
7. Castro M, Zangrilli J, Wechsler ME, Bateman ED, Brusselle GG, Bardin P, Murphy K, Maspero JF, O'Brien C, Korn S. Reslizumab for inadequately controlled asthma with elevated blood eosinophil counts: results from two multicentre, parallel, double-blind, randomised, placebo-controlled, phase 3 trials. *The Lancet Respiratory medicine* 2015; 3: 355-366.
8. Pavord ID, Korn S, Howarth P, Bleecker ER, Buhl R, Keene ON, Ortega H, Chanez P. Mepolizumab for severe eosinophilic asthma (DREAM): a multicentre, double-blind, placebo-controlled trial. *Lancet* 2012; 380: 651-659.
9. Castro M, Musani AI, Mayse ML, Shargill NS. Bronchial thermoplasty: a novel technique in the treatment of severe asthma. *Therapeutic advances in respiratory disease* 2010; 4: 101-116.
10. Denner DR, Doeing DC, Hogarth DK, Dugan K, Naureckas ET, White SR. Airway Inflammation after Bronchial Thermoplasty for Severe Asthma. *Annals of the American Thoracic Society* 2015; 12: 1302-1309.
11. d'Hooghe JNS, Goorsenberg AWM, Ten Hacken NHT, Weersink EJM, Roelofs J, Mauad T, Shah PL, Annema JT, Bonta PI. Airway smooth muscle reduction after bronchial thermoplasty in severe asthma correlates with FEV1. *Clinical and experimental allergy : journal of the British Society for Allergy and Clinical Immunology* 2019; 49: 541-544.
12. Pretolani M, Dombret MC, Thabut G, Knap D, Hamidi F, Debray MP, Taille C,

- Chanez P, Aubier M. Reduction of airway smooth muscle mass by bronchial thermoplasty in patients with severe asthma. *American journal of respiratory and critical care medicine* 2014; 190: 1452-1454.
13. Pretolani M, Bergqvist A, Thabut G, Dombret MC, Knapp D, Hamidi F, Alavoine L, Taille C, Chanez P, Erjefalt JS, Aubier M. Effectiveness of bronchial thermoplasty in patients with severe refractory asthma: Clinical and histopathologic correlations. *The Journal of allergy and clinical immunology* 2017; 139: 1176-1185.
 14. Castro M, Rubin AS, Laviolette M, Fiterman J, De Andrade Lima M, Shah PL, Fiss E, Olivenstein R, Thomson NC, Niven RM, Pavord ID, Simoff M, Duhamel DR, McEvoy C, Barbers R, Ten Hacken NH, Wechsler ME, Holmes M, Phillips MJ, Erzurum S, Lunn W, Israel E, Jarjour N, Kraft M, Shargill NS, Quiring J, Berry SM, Cox G, Group AIRTS. Effectiveness and safety of bronchial thermoplasty in the treatment of severe asthma: a multicenter, randomized, double-blind, sham-controlled clinical trial. *American journal of respiratory and critical care medicine* 2010; 181: 116-124.
 15. Chupp G, Laviolette M, Cohn L, McEvoy C, Bansal S, Shifren A, Khatri S, Grubb GM, McMullen E, Strauven R, Kline JN. Long-term outcomes of bronchial thermoplasty in subjects with severe asthma: a comparison of 3-year follow-up results from two prospective multicentre studies. *The European respiratory journal* 2017; 50.
 16. Cox G, Thomson NC, Rubin AS, Niven RM, Corris PA, Siersted HC, Olivenstein R, Pavord ID, McCormack D, Chaudhuri R, Miller JD, Laviolette M, Group AIRTS. Asthma control during the year after bronchial thermoplasty. *The New England journal of medicine* 2007; 356: 1327-1337.
 17. Pavord ID, Cox G, Thomson NC, Rubin AS, Corris PA, Niven RM, Chung KF, Laviolette M, Group RTS. Safety and efficacy of bronchial thermoplasty in symptomatic, severe asthma. *American journal of respiratory and critical care medicine* 2007; 176: 1185-1191.
 18. d'Hooghe JNS, Roelofs JJTH, Annema JT, Bonta PI. Reduction of airway smooth muscle mass in airway biopsies following Bronchial Thermoplasty; the TASMA randomized controlled trial [abstract]. *ERJ* 2016;48:OA3014.
 19. d'Hooghe JNS, ten Hacken NHT, Roelofs JJTH, Annema JT, Bonta PI. Airway smooth muscle mass reduction after Bronchial Thermoplasty; the TASMA randomized controlled trial [abstract]. *ERJ* 2017;50: PA3027.
 20. d'Hooghe JNS, Weersink EJM, ten Hacken NHT, Annema JT, Bonta PI. Clinical response of severe asthma patients following Bronchial Thermoplasty [abstract]. *ERJ* 2017;50:PA3029.
 21. Goorsenberg AWM, d'Hooghe JNS, ten Hacken NHT, Weersink EJM, Bel EH, Shah PL, Annema JT, Bonta PI. Towards optimal patient selection for bronchial thermoplasty treatment in severe asthma: results from the TASMA randomized trial [abstract]. *ERJ* 2019;54: PA2537
 22. Goorsenberg AWM, d'Hooghe JNS, ten Hacken NHT, Weersink EJM, Roelofs JJTH, Srikanthan K, Shah PL, Annema JT, Bonta PI. Bronchial thermoplasty induced reduction of airway smooth muscle: results from the randomized controlled TASMA trial [abstract]. *ERJ* 2019;54:OA1616.
 23. Benayoun L, Druilhe A, Dombret MC, Aubier M, Pretolani M. Airway structural

- alterations selectively associated with severe asthma. *American journal of respiratory and critical care medicine* 2003; 167: 1360-1368.
24. Bousquet J, Mantzouranis E, Cruz AA, Ait-Khaled N, Baena-Cagnani CE, Bleecker ER, Brightling CE, Burney P, Bush A, Busse WW, Casale TB, Chan-Yeung M, Chen R, Chowdhury B, Chung KF, Dahl R, Drazen JM, Fabbri LM, Holgate ST, Kauffmann F, Haahntela T, Khaltaev N, Kiley JP, Masjedi MR, Mohammad Y, O'Byrne P, Partridge MR, Rabe KF, Togias A, van Weel C, Wenzel S, Zhong N, Zuberbier T. Uniform definition of asthma severity, control, and exacerbations: document presented for the World Health Organization Consultation on Severe Asthma. *The Journal of allergy and clinical immunology* 2010; 126: 926-938.
 25. Bonta PI, Chanez P, Annema JT, Shah PL, Niven R. Bronchial Thermoplasty in Severe Asthma: Best Practice Recommendations from an Expert Panel. *Respiration; international review of thoracic diseases* 2018.
 26. d'Hooghe JN, Eberl S, Annema JT, Bonta PI. Propofol and Remifentanyl Sedation for Bronchial Thermoplasty: A Prospective Cohort Trial. *Respiration; international review of thoracic diseases* 2017; 93: 58-64.
 27. Collins TJ. ImageJ for microscopy. *Biotechniques* 2007; 43: 25-30.
 28. Goorsenberg AQM, d'Hooghe JNS, Slat AM, van den Aardweg JG, Annema JT, Bonta PI. Resistance of the respiratory system measured with forced oscillation technique (FOT) correlates with bronchial thermoplasty response. *Respir Res* 2020; 21(1):52.
 29. Hodges JL, Lehmann EL. Estimates of location based on rank tests. *The Annals of Mathematical Statistics* 1963; 34: 598-611.
 30. Juniper EF, Guyatt GH, Willan A, Griffith LE. Determining a minimal important change in a disease-specific Quality of Life Questionnaire. *Journal of clinical epidemiology* 1994; 47: 81-87.
 31. Juniper EF, Svensson K, Mork AC, Stahl E. Measurement properties and interpretation of three shortened versions of the asthma control questionnaire. *Respiratory medicine* 2005; 99: 553-558.
 32. Chakir J, Haj-Salem I, Gras D, Joubert P, Beaudoin EL, Biardel S, Lampron N, Martel S, Chanez P, Boulet LP, Laviolette M. Effects of Bronchial Thermoplasty on Airway Smooth Muscle and Collagen Deposition in Asthma. *Annals of the American Thoracic Society* 2015; 12: 1612-1618.
 33. Debray MP, Dombret MC, Pretolani M, Thabut G, Alavoine L, Brillet PY, Taille C, Khalil A, Chanez P, Aubier M. Early computed tomography modifications following bronchial thermoplasty in patients with severe asthma. *The European respiratory journal* 2017; 49.
 34. d'Hooghe JNS, Bonta PI, van den Berk IAH, Annema JT. Radiological abnormalities following bronchial thermoplasty: is the pathophysiology understood? *The European respiratory journal* 2017; 50.
 35. d'Hooghe JNS, van den Berk IAH, Annema JT, Bonta PI. Acute radiological abnormalities after Bronchial Thermoplasty: a prospective cohort trial. *Respiration; international review of thoracic diseases* 2017; 94: 258-262.
 36. Goorsenberg AWM, d'Hooghe JNS, de Bruin DM, van den Berk IAH, Annema JT, Bonta PI. Bronchial Thermoplasty-Induced Acute Airway Effects Assessed with

- Optical Coherence Tomography in Severe Asthma. *Respiration; international review of thoracic diseases* 2018; 96: 564-570.
37. Melibea Sierra SF-B, Hiren Mehta, Fayez Kheir, Marianne Barry, Michael Jantz, Alex Chee, Mihir Parikh, Adnan Majid. Bronchial Thermoplasty in Severe Uncontrolled Asthma With Different Phenotypes [abstract Annual Meeting Chest]. October 30, 2017, Boston, US.
 38. Global Initiative for Asthma. *Global Strategy for Asthma Management and Prevention*, 2016. Available from: www.ginasthma.org.
 39. Facciolongo N, DiStefano A, Pietrini V, Galeone C, Bellanova F, Menzella F, Scichilone N, Piro R, Bajocchi GL, Balbi B, Agostini L, Salsi PP, Formisano D, Lusuardi M. Nerve ablation after bronchial thermoplasty and sustained improvement in severe asthma. *BMC pulmonary medicine* 2018; 18: 29.
 40. Slebos DJ, Breen D, Coad J, Klooster K, Hartman J, Browning R, Shah PL, McNulty WH, Mohsin MA, Irshad K. Safety and Histological Effect of Liquid Nitrogen Metered Spray Cryotherapy in the Lung. *American journal of respiratory and critical care medicine* 2017; 196: 1351-1352.

Supplementary data and figures

Severe asthma definition:

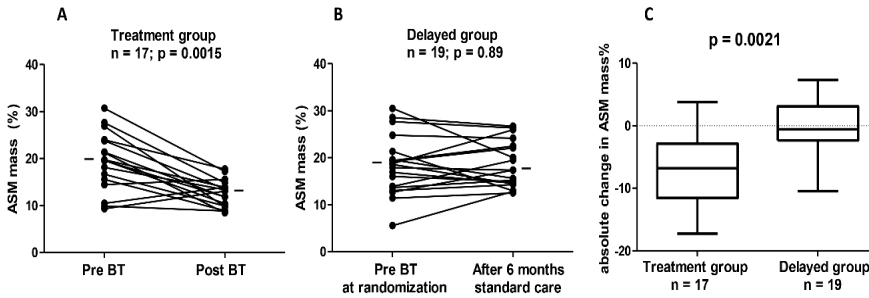
The World Health Organization (WHO) (1) or Innovative Medicines Initiative (IMI) (2) definitions for severe asthma were used. These global definitions are in line with the U-BIOPRED (Unbiased Biomarkers for the Prediction of Respiratory Disease Outcomes) study group. U-BIOPRED is a European-wide project investigating severe asthma. The definition includes the following:

“Patients have asthma for which control is not achieved despite the highest level of recommended treatment (high doses of long acting beta agonists and inhaled corticosteroids and/or systemic corticosteroids) or for which control can be maintained only with the highest level of recommended treatment. Furthermore, patients should have satisfactory adherence to asthma treatment, and co-morbidities should be treated. Lastly, exposure to inhaled asthma triggers should be minimized.”

This definition is similar to the current European Respiratory Society (ERS)/ American Thoracic Society (ATS) guidelines.

References

1. Bousquet J, Mantzouranis E, Cruz AA, Ait-Khaled N, Baena-Cagnani CE, Bleecker ER, Brightling CE, Burney P, Bush A, Busse WW, Casale TB, Chan-Yeung M, Chen R, Chowdhury B, Chung KF, Dahl R, Drazen JM, Fabbri LM, Holgate ST, Kauffmann F, Haahtela T, Khaltaev N, Kiley JP, Masjedi MR, Mohammad Y, O'Byrne P, Partridge MR, Rabe KF, Togias A, van Weel C, Wenzel S, Zhong N, Zuberbier T. Uniform definition of asthma severity, control, and exacerbations: document presented for the World Health Organization Consultation on Severe Asthma. *The Journal of allergy and clinical immunology* 2010; 126: 926-938.
2. Bel EH, Sousa A, Fleming L, Bush A, Chung KF, Versnel J, Wagener AH, Wagers SS, Sterk PJ, Compton CH, Unbiased Biomarkers for the Prediction of Respiratory Disease Outcome Consortium CG. Diagnosis and definition of severe refractory asthma: an international consensus statement from the Innovative Medicine Initiative (IMI). *Thorax* 2011; 66: 910-917.



Supplemental figure E1. Airway smooth muscle decrease after bronchial thermoplasty as compared with the randomized control group assessed with alpha smooth muscle actin staining.

A) ASMI mass % in the immediate group before and after BT showing a median ASMI % of 19.66% pre BT versus 13.06% post BT **B)** ASMI mass % in the delayed group before and after 6 months standard care with a median of ASMI % of 18.60% at randomization versus 17.36% after 6 months of standard care **C)** Difference in absolute ASMI mass% change between both randomization groups (post BT – pre BT ASMI% in the immediate BT-group and for the delayed control group the difference between baseline and 6 months standard care biopsies). ASMI mass assessed with alpha-smooth muscle actin staining. Median values are depicted as -. ASMI: airway smooth muscle; BT: bronchial thermoplasty;

Chapter 4.

Metabolic differences between
bronchial epithelium from healthy
individuals and asthma patients and
the effect of bronchial thermoplasty

Ravi A
Goorsenberg AWM
Dijkhuis A
Dierdorp BS
Dekker T
Sabogal Piñero YS
Shah PL
Ten Hacken NHT
Annema JT
Sterk PJ
Vaz FM
Bonta PI
Lutter R

Submitted for publication

Abstract

Background Asthma is a heterogeneous disease with differences in onset, severity and inflammation. Bronchial epithelial cells (BECs) contribute to asthma pathophysiology. We determined whether the transcriptome of BECs reflects heterogeneity in inflammation and severity in asthma, and whether this was affected in BECs in severe asthma after their regeneration by bronchial thermoplasty.

Methods RNA-sequencing was performed on BECs obtained by bronchoscopy from healthy controls ($n=16$), mild ($n=17$), moderate ($n=5$) and severe ($n=17$) asthma patients and, from the latter, also 6 months after bronchial thermoplasty from treated and untreated airways ($n=23$). Lipidome and metabolome analyses were performed on cultured BECs from healthy controls ($n=7$), severe asthmatics ($n=9$) and, for comparison, COPD patients ($n=7$).

Results Transcriptome analysis of BECs from asthma patients compared to those from healthy controls showed a reduction in oxidative phosphorylation (OXPHOS) genes, most profoundly in severe asthma, but less and more heterogeneous in mild asthma. Genes related to glycolysis were significantly upregulated in BECs from asthma patients. Lipidomics revealed enhanced levels of lipid species (phosphatidylcholines, lysophosphatidyl cholines and bis monoacylglycero) phosphate), whereas OXPHOS metabolites were reduced in BECs from severe asthma patients. BECs from mild asthma patients characterised by hyperresponsive production of mediators implicated in neutrophilic inflammation had decreased OXPHOS genes compared to that from mild patients with normoresponsive production. BECs obtained after thermoplasty had significantly increased expression of OXPHOS genes and decreased expression of glycolysis genes compared to BECs obtained from untreated airways.

Conclusion In asthma, BECs are metabolically different from those of healthy individuals. These differences link with inflammation, asthma severity and can be reversed by bronchial thermoplasty.

Introduction

The airways of patients with obstructive airway diseases such as asthma and COPD are chronically inflamed [1]. Airway epithelial cells together with macrophages constitute the first line of defense to interact and respond to external stimuli, thus driving immune responses. This, together with their abundance, makes airway epithelial cells potential major contributors to the inflammation and pathogenesis of asthma [2] and COPD [3]. Recently, we have identified a defect in translational control in bronchial epithelial cells from asthma patients that correlated well with neutrophilic responses [4]. Several earlier reports have shown that both genetic and acquired defects [5] in airway epithelial cells [6] can lead to impaired mucociliary clearance [7] and barrier function [8]. Apart from genetic defects that may underlie such a defect, airway epithelial cells are continuously exposed to an inflammatory milieu, as a consequence of which epithelial cell biology may change. Even though asthma and COPD are different in etiology and pathophysiology, it is likely that the underlying innate immune mechanisms, especially directed by bronchial epithelium, may at least in part be shared.

Previous studies into differences between epithelial cells from asthma patients in particular have focussed on unbiased stratification of asthma patient cohorts by grouping into different clusters and distinguishing asthma phenotypes using transcriptomics [9] and proteomics [10]. Omics approaches comparing patients and healthy control subjects, however, are virtually lacking. The aim of this study was to compare the transcriptome of bronchial epithelial cells (BECs) from mild to moderate to severe asthma patients and healthy controls, to substantiate major differences and relate these to the earlier described translational defect. To put these findings into further perspective we performed additional analysis in asthma patients subjected to bronchial thermoplasty. Bronchial thermoplasty (BT) is a non-pharmacological bronchoscopic treatment for severe asthma that delivers radiofrequency (RF) energy to heat the airway wall, to target airway smooth muscle cells. Furthermore, the bronchial epithelium is the most superficial airway wall layer that encounters RF heating energy, which has been shown to result in epithelial sloughing as detected by Optical Coherence Tomography directly after BT [11, 12]. Therefore, we postulated that BT may subsequently lead to restoration of bronchial epithelium, which would be reflected in the bronchial epithelial transcriptome.

Methods

Subjects and design

This study comprised a cross-sectional design using bronchial epithelial brushes from three trials and two explorative studies. The RESOLVE (NCT1677) trial [13] involved mild asthma patients and healthy controls. The

MATERIAL (NTR01520051) trial [14] enrolled mild asthma patients, the RILCA study (NL48912.018.14) enrolled moderate asthma patients and severe asthma patients from the TASMA (NCT02225392) trial [15]. The COPD patients were included from the RILCO (NL53354.018.15) study. All study protocols were reviewed and approved by the ethical review committee and were in accordance with the declaration of Helsinki. All study participants provided written informed consent. The collection of BECs in the above-mentioned trials and studies were conducted by one center, the Department of Respiratory Medicine of the Amsterdam University Medical Centre, Amsterdam, The Netherlands. The TASMA trial was also conducted at the Department of Pulmonology, University Medical Center Groningen, Groningen, The Netherlands and Royal Brompton and Imperial College Hospital London, United Kingdom. Baseline characteristics of the asthma patients and healthy controls involved in this study are provided in **Table 1**.

Table 1. Baseline characteristics of mild, moderate and severe asthma patients and healthy controls for transcriptome analyses.

| | Healthy | Mild asthma | Moderate asthma | Severe asthma |
|-------------------------------------------------|---------------|--------------------|-----------------|--------------------|
| Subjects (n) | 16 | 17 | 5 | 17 |
| Age (years) * | 22.42 (19-31) | 22.82 (18-38) | 37 (23-52) | 44.82 (25-66) |
| Sex ratio (male : female) | 0.16 | 0.54 | 0.40 | 0.41 |
| FEV ₁ pre-bronchodilator (L) † | 4.05 (0.72) | 3.94 (0.85) | 3.27 (0.88) | 2.79 (0.76) |
| FEV ₁ post-bronchodilator (L) † | 4.12 (0.72) | 4.23 (0.84) | 3.41 (0.91) | 3.07 (0.76) |
| FEV ₁ pre-bronchodilator (% pred) † | 105.5 (10.92) | 97.43 (6.64) | 93.5 (18.76) | 85.35 (26) |
| FEV ₁ post-bronchodilator (% pred) † | 107.5 (11.15) | 103.83 (8.63) | 97 (18.49) | 100.88 (20.91) |
| FEV ₁ reversibility (%) † | 2 (2.86) | 6.66 (4.36) | 3.5 (2.87) | 15.7 (17.23) |
| PC ₂₀ (mg/ml) ‡ | >16.0 | 1.49 (0.03 - 7.35) | na | 0.28 (0.0075-5.53) |
| FeNO (ppb) † | 21.9 (11.4) | 58.03 (37.14) | 21 (10.04) | 52 (63.97) |

FEV₁, forced expiratory volume in 1 second; PC₂₀, Histamine provocative concentration causing a 20% drop in FEV₁; FeNO, fraction exhaled nitric oxide represented as parts per billion (ppb). *Mean (min-max) † Mean (SD) ‡ Median (min to max)

The inclusion and exclusion criteria for patients with mild asthma (RESOLVE and MATERIAL studies) are described elaborately [16] and in the supplementary data. Patients with severe asthma (TASMA study), fulfilling the World Health Organization or modified innovative medicines initiative criteria of severe

refractory asthma, were included [17, 18]. The RILCA (Role of Innate Lymphoid Cells in Asthma) and RILCO (Role of Innate Lymphoid Cells in COPD) were two explorative studies involving the impact of rhinovirus-16 challenge in moderate asthmatics and COPD patients respectively and exploring mechanisms driven by innate lymphoid cells. The inclusion and exclusion criteria are mentioned in detail in the supplementary data.

Sampling, RNA isolation and sequencing

Bronchoscopy was performed according to a standardized method [14]. Mucosal brushes collected by brushing the left lower lobe, predominantly (>95%) consisted of bronchial epithelial cells. From each participant, two brushes were obtained, pooled and pelleted by centrifugation at 1240 rpm (Rotanta 460S) for 10 minutes at 4°C. The pellet was dissolved in 1 ml of TRIzol™ and stored at -80°C until RNA was isolated. After all samples were obtained, they were thawed at room temperature and, after 200 µl of chloroform was added, shaken vigorously for 30 seconds. The samples were kept at RT for 10 minutes and phases were separated by centrifugation at 16,000g for 15 minutes at 4°C. The aqueous phase was concentrated with protocol 5.3 using the Nucleospin® RNA XS extraction kit (Macherey-Nagel). The quality and concentration of the samples were assessed by fragment analyser (Advanced Analytical Technologies, Inc.). The procedures of cDNA library preparation, sequencing and analysis were performed as described elsewhere [16].

Lipidomics and metabolome analysis

BECs for lipidomics and metabolomics were obtained by brush during bronchoscopy (P0) from healthy individuals, severe asthma and COPD patients. Baseline characteristics for participants subjected to these analyses are provided in **Table 2**.

Table 2. Baseline characteristics of severe asthmatics, COPD patients and healthy controls for lipidomics and metabolomics analyses.

| | Healthy | Severe asthma | COPD |
|-------------------------------------|---------------|---------------|--------------|
| Subjects (n) | 7 | 9 | 6 |
| Age (years) * | 37 (24-56) | 52.8 (40-63) | 63.8 (52-74) |
| Sex ratio (male : female) | 1 | 0.5 | 1.5 |
| FEV1 pre-bronchodilator (L) † | 3.94 (0.98) | 2.66 (0.33) | 2.228 (0.49) |
| FEV1 post-bronchodilator (L) † | 4.15 (1) | 2.61 (0.5) | 2.41 (0.48) |
| FEV1 pre-bronchodilator (% pred) † | 105.75 (0.82) | 84.33 (23.13) | 70.8 (4.95) |
| FEV1 post-bronchodilator (% pred) † | 111.5 (2.17) | 90.66 (21.15) | 77.2 (4.35) |
| FEV ₁ reversibility † | 5.75 (1.63) | 6.5 (4.42) | 6.4 (3) |

For abbreviations please see legends to Table 1. *Mean (min-max) † Mean (SD)

BECs were plated on 6-well plates pre-coated with purecol (Advanced Biomatrix) and grown until confluence in BEBM medium (Lonza) supplemented with growth factors (Lonza) and Ciproxin (Sigma) at 2 µg/ml. The cells were then passaged into T25 flasks (P1) until grown confluent. Subsequently, cells were detached using trypsin/EDTA (Lonza) and after adding trypsin-neutralizing solution were pelleted by centrifugation for 7 minutes at 1240rpm (Rotanta 460S) at 8°C. The pellet was washed twice with PBS and stored at -80°C till all samples were analysed in parallel.

Lipidomics and metabolome analysis was performed on a HPLC system (Ultimate 3000 binary HPLC; Thermo Scientific, Waltham, MA, USA) as described previously (19). The extract of the cell pellet was injected onto a normal phase column (LiChrospher 2x250-mm silica-60 column) and a reverse phase column (Acquity UPLC HSS T3). A Q Exactive plus Orbitrap (Thermo Scientific) mass spectrometer was used in the negative and positive electrospray ionization mode. In both ionization modes, mass spectra of the lipid species were obtained by continuous scanning from m/z 150 to m/z 2000 with a resolution of 280,000 full width at half maximum (FWHM). Detailed analysis of data is provided in the online supplement.

Bronchial Thermoplasty (BT)

The TASMA (Unravelling Targets of Therapy in Bronchial Thermoplasty in Severe Asthma) trial was conducted using a protocol approved by the Medical Ethics Committee (NL45394.018.13) [20]. All subjects provided prior written, informed consent. The design of the TASMA study is elaborately described elsewhere [12, 20]. Twenty-three patients [21] (6 severe asthma patients were included in addition to the severe asthma group mentioned in table 1) were treated with BT by using the Alair System (Boston Scientific, USA) according to the current standard [22] and sedated using remifentanyl/propofol [23] or general anesthesia. Patients were treated with 50 mg of prednisolone 3 days before treatment, on the day of the procedure itself and 1 day thereafter. During the first procedure, the right lower lobe was treated, during the second procedure the left lower lobe, and finally both upper lobes. The right middle lobe remained untreated, therefore this region could be used to compare the treatment effect. Six months after BT, a bronchoscopy was performed in which endobronchial brushes were obtained from the untreated middle lobe and the treated left lower lobe airways. The baseline characteristics of severe asthma patients used to analyze the effects of BT on bronchial epithelium are provided in **Table 3** and are not different from those reported originally for all patients [21].

Table 3. Baseline characteristics of severe asthma patients that underwent BT procedure.

| | Severe asthma |
|-------------------------------------|--------------------|
| Subjects (n) | 23 |
| Age (years) * | 47.69 (25-64) |
| Sex ratio (male : female) | 0.43 |
| FEV1 pre-bronchodilator (L) † | 2.67 (0.57) |
| FEV1 post-bronchodilator (L) † | 3.03 (0.54) |
| FEV1 pre-bronchodilator (% pred) † | 89.3 (19.89) |
| FEV1 post-bronchodilator (% pred) † | 101.13 (18.66) |
| FEV ₁ reversibility † | 12 (11.65) |
| PC ₂₀ (mg/ml) ‡ | 0.41 (0.0075 - 32) |
| ACQ pre bronchial thermoplasty † | 2.62 (0.57) |
| AQLQ pre bronchial thermoplasty † | 3.98 (0.81) |

ACQ, Asthma Common Questionnaire; AQLQ, Asthma Quality of Life Questionnaire. For other abbreviations please see legends to Table 1. *Mean (min-max) † Mean (SD) ‡ Median (min to max)

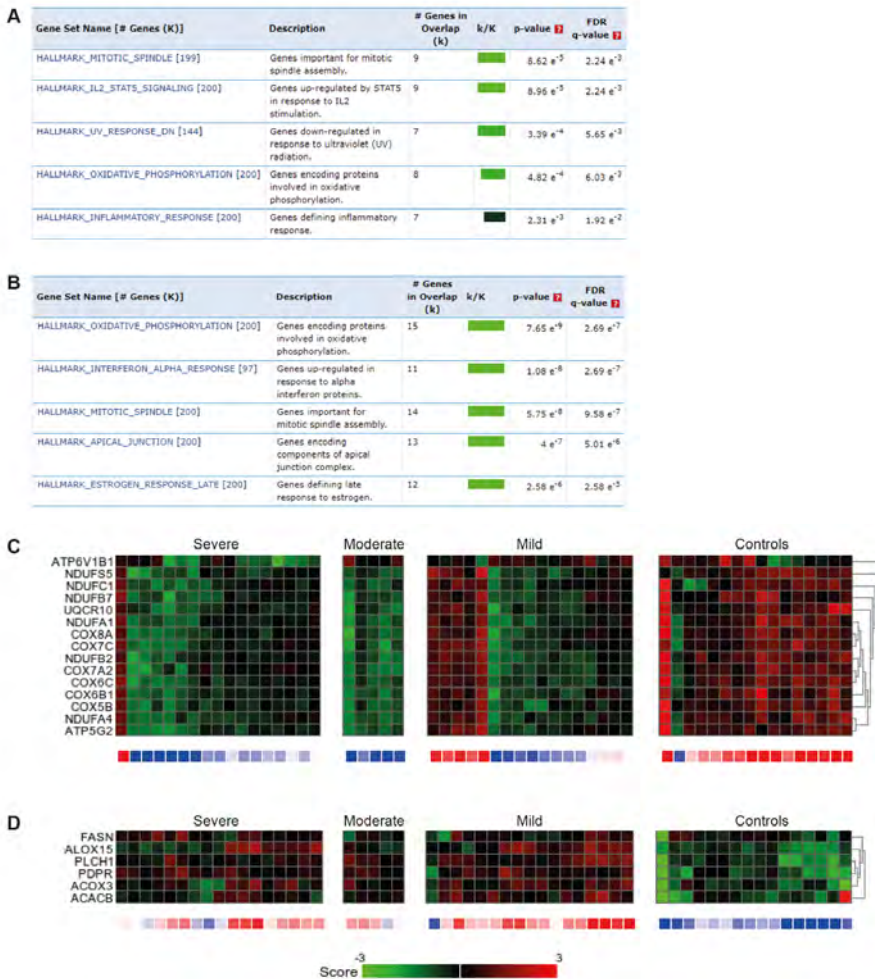
Results

Dysregulation of metabolic genes in bronchial epithelium from severe asthma patients

Despite heterogeneity within each group, there were 472 genes differentially expressed in BECs from mild asthma patients (Table 4) and 640 genes in those from severe asthma patients (Table 5) compared to that from healthy controls (q value <0.05). There were no genes differentially expressed between BECs from mild and severe asthma patients, with q value cut off set below 0.05. Gene set enrichment analysis (GSEA) of differentially expressed genes in BECs from mild asthmatics compared to those from healthy controls showed gene sets belonging to mitotic spindle, IL2-STAT5 signaling, UV response, oxidative phosphorylation (OXPHOS) and inflammatory response (Figure 1A). Similar comparisons for severe asthmatics and healthy controls revealed gene sets belonging to oxidative phosphorylation, interferon- α response, mitotic spindle, apical junction, and late estrogen response (Figure 1B).

Both the mitotic spindle and OXPHOS gene sets stood out in BECs from mild and severe asthma with the mitotic spindle highest in mild asthma and OXPHOS highest in severe asthma. We further investigated the OXPHOS gene set. Heat maps of 15 OXPHOS genes were reduced (green) in BECs from severe and moderate asthma patients in comparison to those from controls (red). In mild asthma patients there was a heterogeneous gene expression pattern, where 5 of 17 patients showed high (red) and the remainder low (green) expression of OXPHOS genes (Figure 1C). Apart from these metabolic OXPHOS genes,

glycolysis-related genes (*FASN*, *ALOX15*, *PLCH1*, *PDPR*, *ACOX3*, *ACACB*) were also analysed by heat maps. Interestingly, in BECs from all asthma patients (mild, moderate and severe) these genes were upregulated (red) compared to those in healthy controls (**Figure 1D**). In addition to GSEA, ingenuity pathway analysis also showed that the OXPHOS pathway was the top dysregulated pathway in BECs from severe asthmatics compared to those from healthy subjects. The downregulated genes were from complex I, III, IV and V of the electron transport chain (**Figure 1E**). Heat maps of 7 mitotic spindle genes displayed significantly enhanced expression particularly in BECs from mild and moderate asthma patients, but not in those from severe asthma patients (**Suppl. Figure 1**).



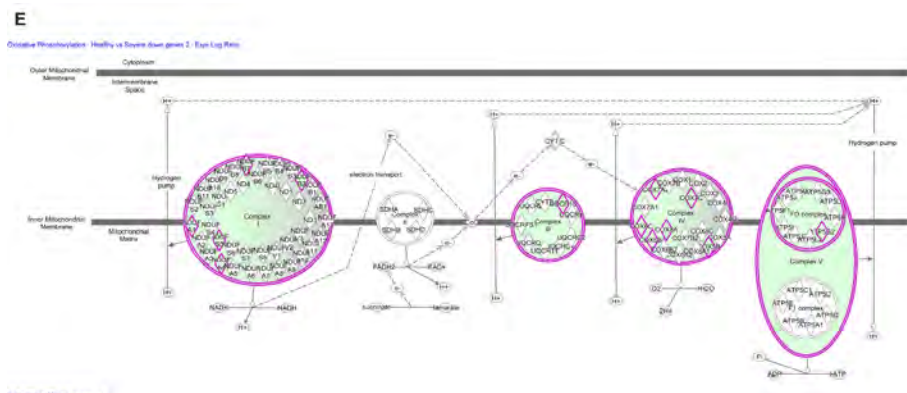
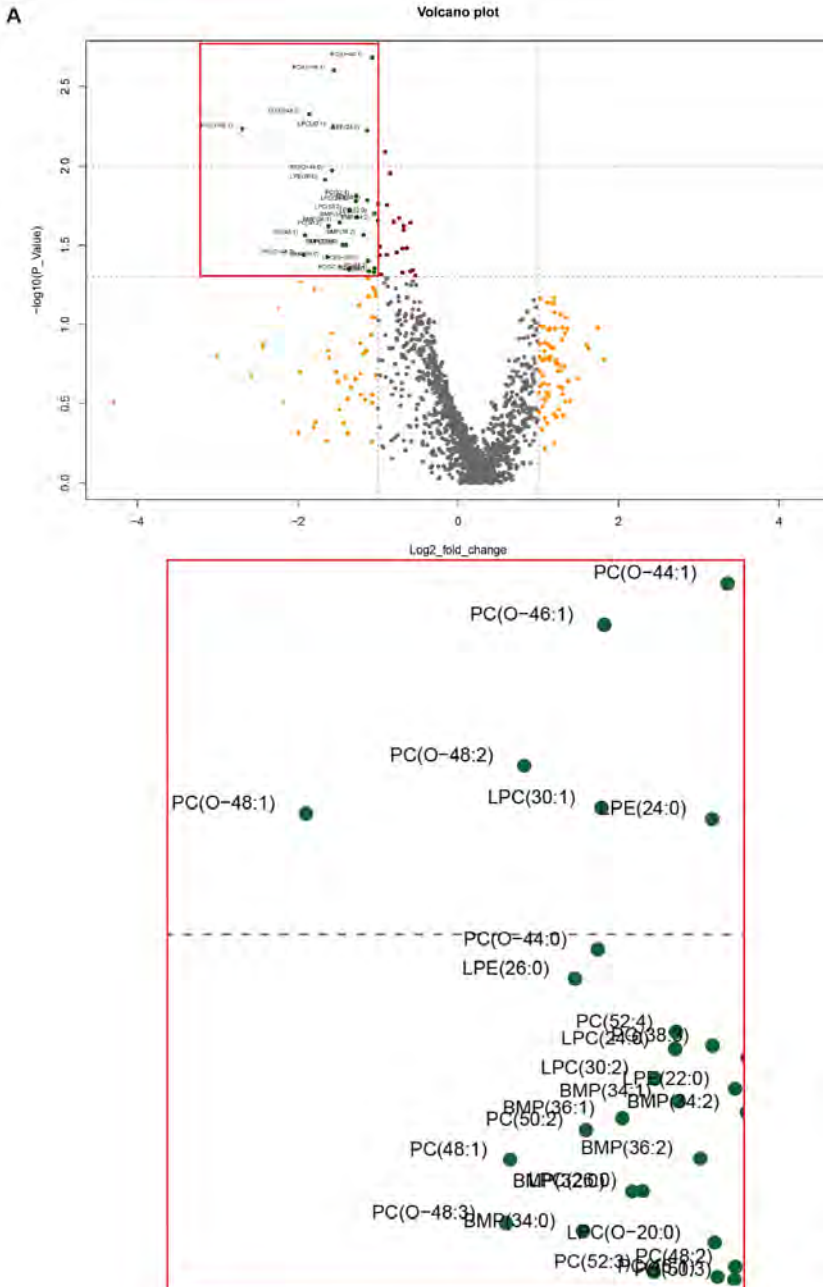


Figure 1. Metabolic genes in BECs from asthma patients compared to those from healthy controls. Gene Set Enrichment Analysis (GSEA) showed differentially expressed gene sets in BECs from mild (A) and severe (B) asthma patients. OXPHOS genes and mitotic spindle genes were predominantly downregulated in BECs from severe ($n=17$) and moderate ($n=5$) asthma patients compared to those from healthy controls ($n=16$). BECs from mild asthma patients ($n=17$) showed a heterogeneous expression of OXPHOS genes (C). Genes related to glycolysis were upregulated in BECs from all asthma patients (mild, moderate and severe) compared to those from controls (D). Colour codes used are red for upregulated and green for downregulated. Ingenuity Pathway Analysis (IPA) of differentially expressed genes in BECs from severe asthma patients compared to those from healthy controls ($n=17$). Oxidative phosphorylation is the top downregulated pathway shown by IPA. The genes highlighted (in pink) are significantly downregulated (p value adjusted of <0.05), the genes not highlighted are present in the pathway, but not significantly different (E).

Elevated lipid profiles in BECs from severe asthma patients when compared to those from controls

To substantiate the findings for metabolic genes, lipid profiles and metabolome were analysed after expanding bronchial epithelium *ex vivo*. As there was a clear and distinct reduction of OXPHOS gene expression in BECs from severe asthma patients compared to those from controls, we compared these cohorts. Volcano plots show all lipid species quantified in BECs and depicted the extent of differences in lipid profiles between the two groups. Phosphatidyl cholines (PC), lyso phosphatidyl cholines (LPC), lyso phosphatidyl ethanolamines (LPE) and bis (monoacylglycero) phosphates (BMP) marked in green were significantly upregulated (p value <0.05 and \log_2 fold change >1) in BECs from severe asthma compared to those from healthy controls (Figure 2A). To visualize the 28 lipids mediators that were significantly upregulated in BECs from severe asthma patients, we plotted these in heat maps. Lipid species (PC, LPC, LPE and BMP) were increased in BECs from severe asthma patients (red) compared to those from healthy controls (blue; Figure 2B). The metabolome

analyses in BECs from severe asthma and healthy controls did not show a clear distinction between these two groups (Figure 2C).



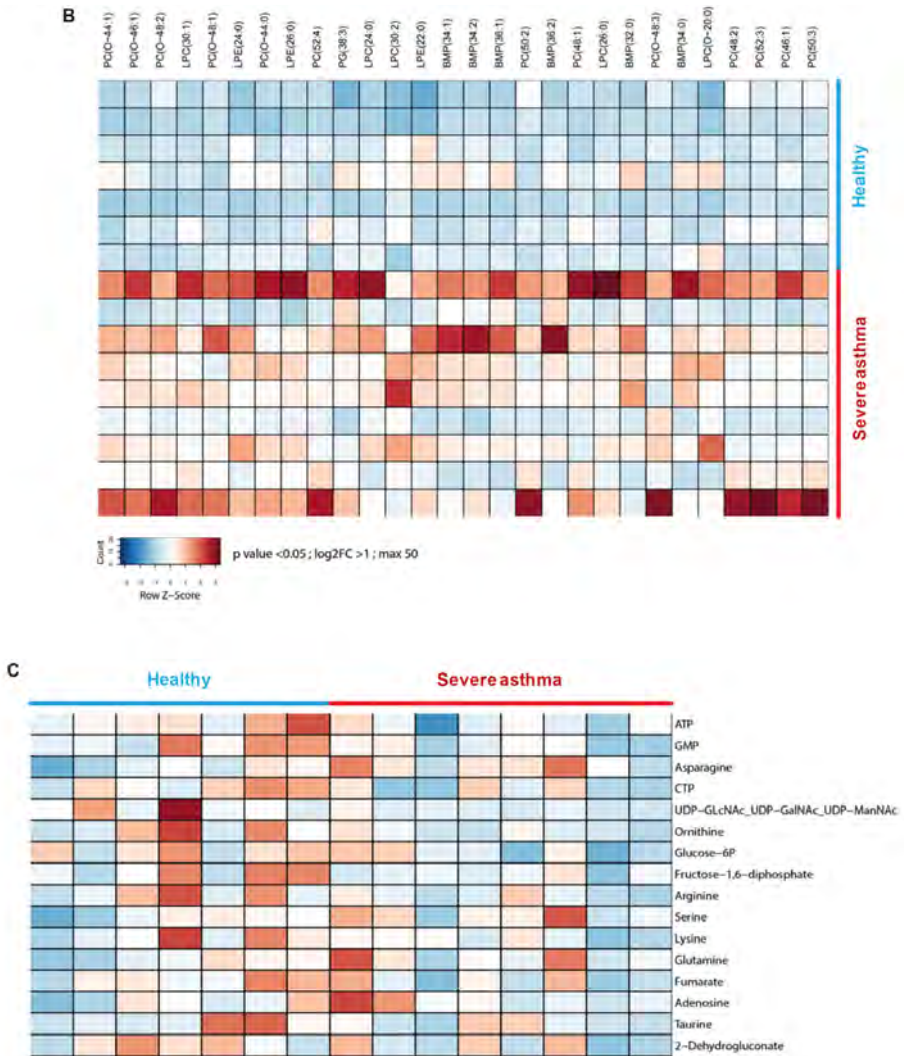


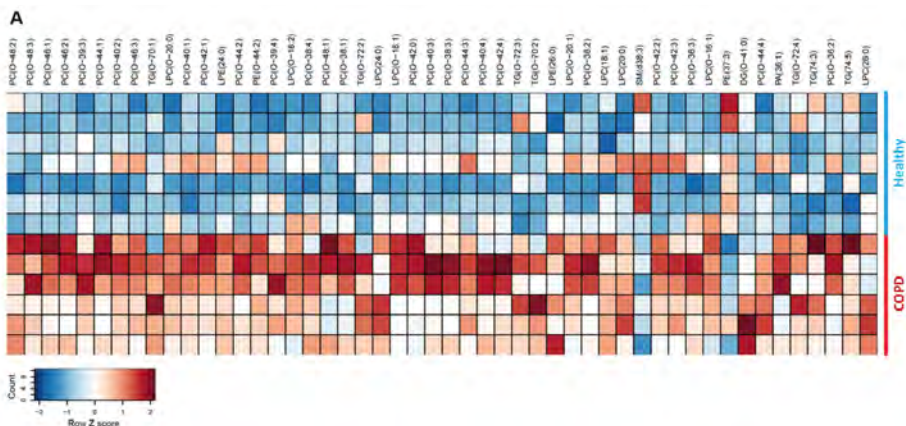
Figure 2. Functional analysis of lipid profiles and metabolites in BECs cultured *ex vivo*. Volcano plots of lipid profiles in BECs from healthy controls ($n=7$) compared to those from severe asthma patients ($n=9$) cultured *ex vivo*. The lipids labelled in green dots are significantly ($p < 0.05$) reduced in control subjects with log-fold change > 1 . Red dots represent lipids that are significantly reduced, but with fold-change of < 1 , while lipids represented by the yellow dots reduced with a fold-change of > 1 , but non-significant. Lipid profiles significantly upregulated in controls were not observed (A). Heat maps of lipid profiles in healthy controls and severe asthma patients in BECs cultured *ex vivo*. (p value < 0.05 with log fold change > 1) (B). Heat maps of metabolome in BECs cultured *ex vivo* from healthy controls ($n=6$) and severe asthma patients ($n=8$). (p value < 0.05 and log fold-change > 1). Colour codes are red for upregulated and blue for downregulated (C).

Distinct lipid species in BECs from COPD patients compared to those from healthy controls and severe asthmatics

Previous reports showed altered metabolites and glycerophospholipids in peripheral blood mononuclear cells (PBMCs) and airway smooth muscle cells [24] from COPD patients [25]. Hence, we analysed whether BECs from COPD patients also displayed a similar difference in metabolic status after *ex vivo* expansion. The heat maps of lipidomics analysis of BECs from COPD patients compared to those from healthy controls showed a prominent upregulation of mainly phosphatidylcholines (PC) lipid species. In addition, triglycerides (TG) and lysophosphatidylcholines (LPC) lipid species were also enhanced in BECs from COPD patients (Figure 3A). Strikingly, when comparing BECs from COPD with those from severe asthma patients, there was also a significant increase in triglycerides in COPD (Figure 3B). With respect to metabolites analysed, UDP-hexose, 2-dehydrogluconate-6P, dAMP, NAD⁺, fructose 1,6 diphosphate, creatine-P, glutamine, alpha-ketoglutarate, NADH, adenine and creatinine were significantly lower levels in BECs from COPD patients compared to those from healthy controls. Heat maps representing these different metabolites in these two groups are provided in Figure 3C.

Bronchial Thermoplasty treatment-induced metabolic shift in BECs

BECs obtained from treated and, as controls, in parallel from untreated airways (i.e. right middle lobe) from severe asthma patients six months after initiation of the treatment were subjected to transcriptomics to analyze differentially expressed genes. Interestingly, heat maps (Figure 4A) and Z scores (Figure 4B) show that BECs obtained from the treated airways had significantly upregulated OXPHOS genes compared to those from untreated airways. In addition, reduced glycolysis gene expression in BECs from treated airways was observed in heat maps (Figure 4C) and Z scores (Figure 4D) when compared to untreated airways. Thus, thermoplasty induced a metabolic shift in bronchial epithelium towards that observed in healthy controls.



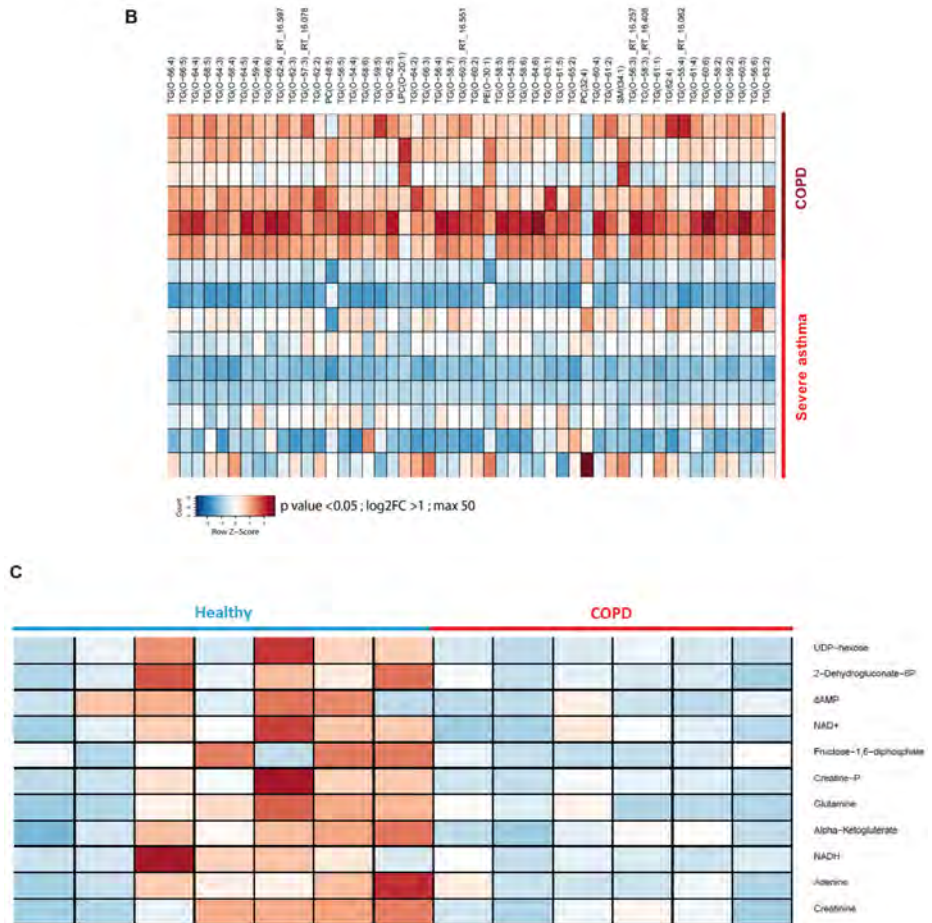


Figure 3. Lipidomics and metabolome analysis of expanded BECs from COPD patients compared to those from controls and severe asthma patients. Heat maps of lipid profiles in cultured *ex vivo* BECs from COPD patients ($n=6$) and healthy controls ($n=7$) (p value < 0.05 with log fold-change > 1). **(A)**. Heat maps of lipid profiles in cultured *ex vivo* BECs from COPD ($n=6$) and severe asthma patients ($n=9$) (p value < 0.05 with log fold-change > 1). **(B)**. Heat maps of metabolome in cultured *ex vivo* BECs from COPD patients ($n=6$) and healthy controls ($n=7$) (p value < 0.05 with log fold-change > 1). **(C)**. Colour codes: red for upregulated and blue for downregulated.

Hyperresponsive BECs have a reduced expression of OXPHOS genes

Earlier we have identified BECs from mild asthma patients with a defective translational control as hyperresponsive (exaggerated and corticosteroid-unresponsive production of CXCL-8 and other cytokines) as opposed to normoresponsive (lower and corticosteroid responsive production of CXCL-8 and other cytokines) [4]. This epithelial hyperresponsiveness correlated

with neutrophilic inflammation. The transcriptome of hyperresponsive BECs from mild asthma patients (subgroup from table 1 and figure 1) displayed a prominent reduced expression of oxidative phosphorylation (OXPHOS) genes compared to that in normoresponsive counterparts (**Figure 4E**).

Figure 4

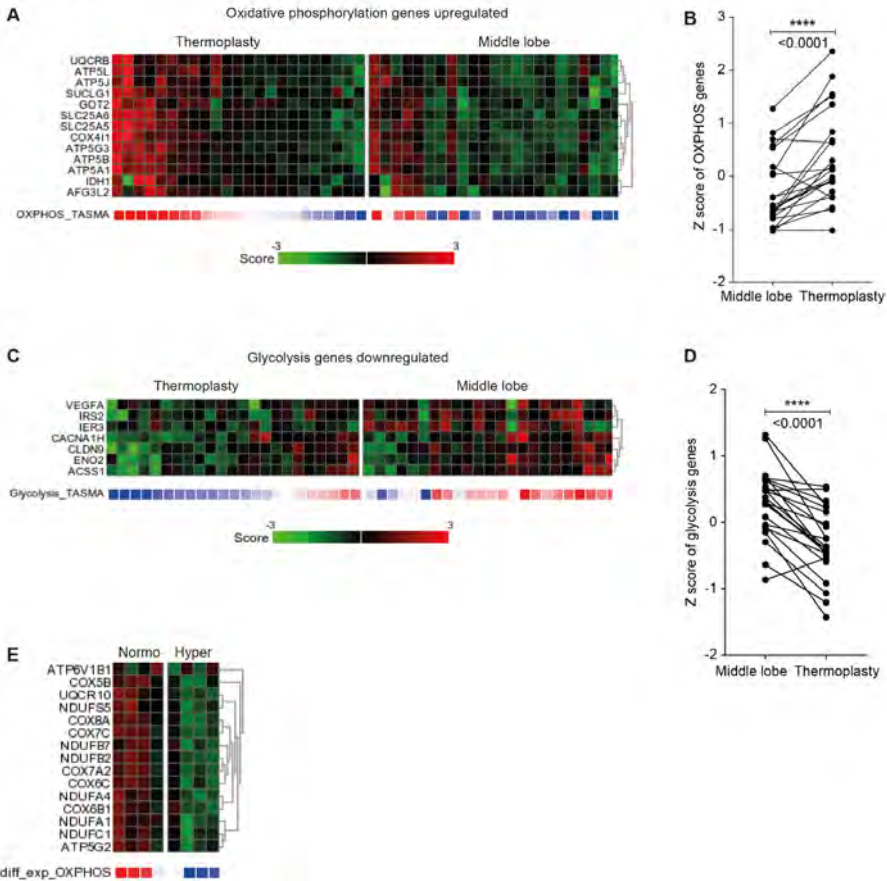


Figure 4. Bronchial Thermoplasty treatment alters metabolic gene expression in BECs from severe asthma patients. Upregulation of oxidative phosphorylation (OXPHOS) genes shown in heat map (**A**) and line graph plotting Z scores (**B**) in a pairwise comparison of BECs obtained 6 months after thermoplasty from the treated (left lower lobe) and untreated region (middle lobe). Also, similar pair-wise analysis in heat maps (**C**) and plotted Z scores (**D**) reduced expression of glycolysis-related genes in BECs from treated *vs.* untreated airways in severe asthma patients ($n=23$). Hyperresponsive (see ref. 4) BECs ($n=4$) from mild asthma patients displayed enhanced expression of OXPHOS genes (same genes mentioned in figure 1A), as compared to that in normoresponsive BECs ($n=4$) (**E**).

Discussion

Unbiased transcriptome analysis of BECs from severe asthma patients compared to those from healthy controls showed a profound reduction in oxidative phosphorylation genes belonging to complexes I, III, IV and V of the electron transport chain, whereas for BECs from mild asthma patients this reduction was heterogeneous. Genes related to glycolysis, however, were significantly upregulated in BECs from all asthma patients, thus differentiating asthmatics from healthy controls. This differential expression in bronchial epithelium was validated by lipidomics with enhanced levels of lipid species (PC, LPC and BMP). The reduction in metabolites in bronchial epithelium of severe asthma was observed trend-wise only, with no clear differences. Most interestingly, in BECs from severe asthma patients subjected to bronchial thermoplasty a metabolic shift towards that of BECs from healthy individuals was observed. In BECs from COPD patients there too was a marked upregulation of lipid profiles compared to that from healthy controls and it was even more pronounced than that from severe asthma patients.

Together these data indicate that bronchial epithelial cells are subject to metabolic adaptations in asthma. Studies have shown a metabolic shift from oxidative phosphorylation to glycolysis, particularly for macrophages [26] and dendritic cells [27], which has been linked to inflammation. Another study showed that enhanced glycolysis in lung epithelium is required for IL-1 α / β -induced pro-inflammatory responses [28]. The reason for the attenuated OXPHOS gene expression could be several. For example, inflammatory mediators like tumor necrosis factor- α (TNF- α), can inhibit COX1 (cytochrome oxidase subunit 1) by tyrosine phosphorylation, thereby switching from aerobic metabolism to glycolysis [29]. Interestingly, we showed here that the attenuated OXPHOS gene expression was observed in BECs that are hyperresponsive, which results in an increased production of pro-inflammatory mediators, prominently the neutrophilic chemoattractant CXCL-8, due to a defective translocation of the translational repressor, T-cell internal antigen-1 related protein (TiAR) [8]. Interestingly, TiAR and the closely related TIA-1 (T-cell internal antigen-1) have also been implicated in mitochondrial biogenesis [30]. In addition, TiAR and TIA-1 knockdown attenuates complex V (ATP synthase) of the oxidative phosphorylation pathway [31]. Therefore, a possible scenario is that a defective TiAR and/or TIA-1 in BECs from asthma patients leads to the observed metabolic shift and the resulting lipid mediators may contribute to activation of the bronchial epithelium [32], which can lead to chronic inflammation in asthma [33]. Alternatively, but not mutually exclusive, enhanced reactive oxygen species (ROS) and mitochondrial damage in bronchial epithelium were found to parallel high CXCL-8, IL-6 and IL-1 β production [34]. Further support for a link between mitochondrial dysfunction and neutrophilic inflammation comes from clustering of genes in sputum from asthma patients, where high neutrophilic inflammation was strongly associated with a significant reduction

in OXPHOS genes in TAC2 (transcriptome-associated cluster; [35]. And, ether lipids from neutrophils [36] downregulate mitochondrial activity [37]. Finally, BECs from patients with COPD, which is associated with neutrophilic inflammation [38], also display a very distinct increase in lipid species even when compared to that from asthma patients. Together, this provides strong evidence for a prominent reduction in mitochondrial activity in BECs that links to neutrophilic inflammation in asthma, and possibly COPD.

Altered mitochondrial metabolism in airway epithelial cells may impact various epithelial functions such as that of the mucociliary escalator. Epithelial cells in healthy lungs require energy for proper hydration of the mucus layer and mucociliary clearance by ciliary beat [39]. Consequently, mitochondrial damage in asthmatic bronchial epithelium leads to ciliary dysfunction resulting in poor mucus clearance [40] and in COPD this has been linked to exacerbations [41]. In the current study, the BECs from some asthma patients from the steroid naïve, mild asthma cohort displayed reduced OXPHOS gene expression. Therefore, at least for this cohort, the reduced expression of OXPHOS genes is independent of corticosteroid usage.

Bronchial thermoplasty (BT) is a treatment option for severe asthma patients who are uncontrolled despite optimal medical therapy including high dose of inhaled bronchodilators and inhaled or oral corticosteroids. Results from biopsy and imaging studies are conflicting as to whether the untreated parts of the airways are also altered by BT [12, 42]. Our results show, however, a significantly increased expression of OXPHOS genes in BECs obtained from treated parts compared to untreated parts (middle lobe). Interestingly, imatinib, a protein tyrosine kinase inhibitor, is shown to improve airway hyperresponsiveness in severe refractory asthma [43], also inhibits platelet derived growth factor that induces airway smooth muscle cell proliferation [44]. In addition, imatinib induces an increase in oxidative phosphorylation gene expression in bronchial epithelium, specifically in the responders to the treatment [45]. This suggests that reversing metabolic defects in asthmatic bronchial epithelium could be beneficial for asthma patients.

For the first time a persistent and altered metabolism in bronchial epithelium was demonstrated *in vivo* in mild asthmatics and more prominently in severe asthmatics. The strengths of our study comprise the inclusion of asthmatics who differ in severity, healthy controls and COPD patients. For severe asthma we also showed that BT affects this altered metabolism in BECs. There has been an earlier report comparing BECs obtained from sequential BT sessions [46], but as samples were collected on different days the analyses may have been biased. In the BT trial we collected and analysed BECs from treated *versus* non-treated airways in parallel. However, there are some potential limitations to the current study. Firstly, the severe asthma patients were on both oral and inhaled corticosteroids which may have influenced the alteration of metabolic

genes in bronchial epithelium. In some mild steroid naïve asthma patients, however, there was a reduced OXPHOS and enhanced glycolysis gene expression. Secondly, functional validation by lipidomics and metabolome analysis was done after culturing and expanding bronchial epithelium. This *ex vivo* expansion of BECs may affect gene expression [47] and we cannot exclude that mitochondrial dysfunction in bronchial epithelium of severe asthmatics is reversible upon culturing BECs *ex vivo*. However, it also has been demonstrated that cultured bronchial epithelial cells maintain their phenotype *ex vivo* [4] and depict asthma severity [48]. This indicates that bronchial epithelium can retain intrinsic features, even after culturing *ex vivo* [4]. Thirdly, due to high variability of lipid mediators measured in lung epithelial lining fluids [49], possibly more patients should have been included for functional validation by metabolome analysis. The transcriptome data, however, were substantiated by lipidomics. Fourthly, oxidative phosphorylation is known to be attenuated by aging [50], and both the severe asthmatics and COPD patients were older compared to the healthy cohort. However, the reduced expression of OXPHOS genes was also observed in younger patients included in the mild asthmatic cohort and thus it is unlikely that aging underlies the observed differences between patients and healthy controls. In addition, BT apparently resets the metabolic changes in BECs, suggesting that the reduced expression of OXPHOS genes is acquired rather than due to aging. With respect to the latter, we cannot exclude that regional differences in the airways underlie the observed different bronchial epithelial transcriptomes after BT.

In summary, we have shown metabolic differences in BECs from asthma and COPD patients compared to those from healthy individuals and the differences worsen with the severity of asthma. As these metabolic defects link to the earlier reported epithelial hyperresponsiveness [4], these metabolic effects appear to underlie airway inflammation. In this context, it is of interest that BT partially normalizes the metabolic differences, thereby resetting the bronchial epithelium which may contribute to BT treatment response.

References

1. Hoogsteden HC, Verhoeven GT, Lambrecht BN, Prins JB. Airway inflammation in asthma and chronic obstructive pulmonary disease with special emphasis on the antigen-presenting dendritic cell: influence of treatment with fluticasone propionate. *Clinical and Experimental Allergy*. 1999;29:116-24.
2. Holgate ST. The airway epithelium is central to the pathogenesis of asthma. *Allergol Int*. 2008;57(1):1-10.
3. Hiemstra PS, McCray PB, Bals R. The innate immune function of airway epithelial cells in inflammatory lung disease. *European Respiratory Journal*. 2015;45(4):1150-62.
4. Ravi A, Chowdhury S, Dijkhuis A, Bonta PI, Sterk PJ, Lutter R. Neutrophilic inflammation in asthma and defective epithelial translational control. *European Respiratory Journal*. 2019;54(2).
5. Moffatt MF, Gut IG, Demenais F, Strachan DP, Bouzigon E, Heath S, et al. A Large-Scale, Consortium-Based Genomewide Association Study of Asthma. *New Engl J Med*. 2010;363(13):1211-21.
6. Moheimani F, Hsu ACY, Reid AT, Williams T, Kicic A, Stick SM, et al. The genetic and epigenetic landscapes of the epithelium in asthma. *Resp Res*. 2016;17.
7. Bonser LR, Zlock L, Finkbeiner W, Erle DJ. Epithelial tethering of MUC5AC-rich mucus impairs mucociliary transport in asthma. *Journal of Clinical Investigation*. 2016;126(6):2367-71.
8. Sweerus K, Lachowicz-Scroggins M, Gordon E, LaFemina M, Huang XZ, Parikh M, et al. Claudin-18 deficiency is associated with airway epithelial barrier dysfunction and asthma. *J Allergy Clin Immunol*. 2017;139(1):72-+.
9. Kuo CS, Pavlidis S, Loza M, Baribaud F, Rowe A, Pandis I, et al. A Transcriptome-driven Analysis of Epithelial Brushings and Bronchial Biopsies to Define Asthma Phenotypes in U-BIOPRED. *Am J Respir Crit Care Med*. 2017;195(4):443-55.
10. Schofield JPR, Burg D, Nicholas B, Strazzeri F, Brandsma J, Staykova D, et al. Stratification of asthma phenotypes by airway proteomic signatures. *J Allergy Clin Immunol*. 2019;144(1):70-82.
11. d'Hooghe JNS, Ten Hacken NHT, Weersink EJM, Sterk PJ, Annema JT, Bonta PI. Emerging understanding of the mechanism of action of Bronchial Thermoplasty in asthma. *Pharmacol Ther*. 2018;181:101-7.
12. Goorsenberg AWM, d'Hooghe JNS, de Bruin DM, van den Berk IAH, Annema JT, Bonta PI. Bronchial Thermoplasty-Induced Acute Airway Effects Assessed with Optical Coherence Tomography in Severe Asthma. *Respiration*. 2018;96(6):564-70.
13. van der Sluijs KF, van de Pol MA, Kulik W, Dijkhuis A, Smids BS, van Eijk HW, et al. Systemic tryptophan and kynurenine catabolite levels relate to severity of rhinovirus-induced asthma exacerbation: a prospective study with a parallel-group design. *Thorax*. 2013;68(12):1122-30.
14. Sabogal Pinos YS, Bal SM, van de Pol MA, Dierdorp BS, Dekker T, Dijkhuis A, et al. Anti-IL-5 in Mild Asthma Alters Rhinovirus-induced Macrophage, B-Cell, and Neutrophil Responses (MATERIAL). A Placebo-controlled, Double-Blind Study. *Am J Respir Crit Care Med*. 2019;199(4):508-17.

15. D'Hooghe JNS, ten Hacken NHT, Roelofs JJTH, Annema JT, Bonta PI. Airway smooth muscle mass reduction after Bronchial Thermoplasty; the TASMA randomized controlled trial. *European Respiratory Journal*. 2017;50.
16. Ravi A, Koster J, Dijkhuis A, Bal SM, Sabogal Pinosos YS, Bonta PI, et al. Interferon-induced epithelial response to rhinovirus 16 in asthma relates to inflammation and FEV1. *J Allergy Clin Immunol*. 2019;143(1):442-7 e10.
17. Bousquet J, Mantzouranis E, Cruz AA, Ait-Khaled N, Baena-Cagnani CE, Bleeker ER, et al. Uniform definition of asthma severity, control, and exacerbations: document presented for the World Health Organization Consultation on Severe Asthma. *J Allergy Clin Immunol*. 2010;126(5):926-38.
18. Bel EH, Sousa A, Fleming L, Bush A, Chung KF, Versnel J, et al. Diagnosis and definition of severe refractory asthma: an international consensus statement from the Innovative Medicine Initiative (IMI). *Thorax*. 2011;66(10):910-7.
19. Herzog K, Pras-Raves ML, Ferdinandusse S, Vervaart MAT, Luyf ACM, van Kampen AHC, et al. Functional characterisation of peroxisomal beta-oxidation disorders in fibroblasts using lipidomics. *J Inherit Metab Dis*. 2018;41(3):479-87.
20. d'Hooghe JNS, Goorsenberg AWM, ten Hacken NHT, Weersink EJM, Roelofs JJTH, Mauad T, et al. Airway smooth muscle reduction after bronchial thermoplasty in severe asthma correlates with FEV1. *Clinical and Experimental Allergy*. 2019;49(4):541-4.
21. Goorsenberg AWM, d'Hooghe JNS, Slats AM, van den Aardweg JG, Annema JT, Bonta PI. Resistance of the respiratory system measured with forced oscillation technique (FOT) correlates with bronchial thermoplasty response. *Respir Res*. 2020;21(1):52.
22. Bonta PI, Chanez P, Annema JT, Shah PL, Niven R. Bronchial Thermoplasty in Severe Asthma: Best Practice Recommendations from an Expert Panel. *Respiration*. 2018;95(5):289-300.
23. d'Hooghe JNS, Eberl S, Annema JT, Bonta PI. Propofol and Remifentanyl Sedation for Bronchial Thermoplasty: A Prospective Cohort Trial. *Respiration*. 2017;93(1):58-64.
24. Wiegman CH, Michaeloudes C, Haji G, Narang P, Clarke CJ, Russell KE, et al. Oxidative stress-induced mitochondrial dysfunction drives inflammation and airway smooth muscle remodeling in patients with chronic obstructive pulmonary disease. *J Allergy Clin Immunol*. 2015;136(3):769-80.
25. Cruickshank-Quinn CI, Jacobson S, Hughes G, Powell RL, Petrache I, Kechris K, et al. Metabolomics and transcriptomics pathway approach reveals outcome-specific perturbations in COPD. *Sci Rep*. 2018;8(1):17132.
26. Jha AK, Huang SCC, Sergushichev A, Lampropoulou V, Ivanova Y, Loginicheva E, et al. Network Integration of Parallel Metabolic and Transcriptional Data Reveals Metabolic Modules that Regulate Macrophage Polarization. *Immunity*. 2015;42(3):419-30.
27. Everts B, Amiel E, van der Windt GJW, Freitas TC, Chott R, Yarasheski KE, et al. Commitment to glycolysis sustains survival of NO-producing inflammatory dendritic cells. *Blood*. 2012;120(7):1422-31.
28. Qian X, Aboushousha R, van de Wetering C, Chia SB, Amiel E, Schneider RW, et

- al. IL-1/inhibitory kappa B kinase epsilon-induced glycolysis augment epithelial effector function and promote allergic airways disease. *J Allergy Clin Immun.* 2018;142(2):435-+.
29. Samavati L, Lee I, Mathes I, Lottspeich F, Huttemann M. Tumor necrosis factor alpha inhibits oxidative phosphorylation through tyrosine phosphorylation at subunit I of cytochrome c oxidase. *J Biol Chem.* 2008;283(30):21134-44.
 30. Carrascoso I, Alcalde J, Sanchez-Jimenez C, Gonzalez-Sanchez P, Izquierdo JM. T-Cell Intracellular Antigens and Hu Antigen R Antagonistically Modulate Mitochondrial Activity and Dynamics by Regulating Optic Atrophy 1 Gene Expression. *Mol Cell Biol.* 2017;37(17).
 31. Isquierdo JM. Control of the ATP synthase beta subunit expression by RNA-binding proteins TIA-1, TIAR, and HuR. *Biochem Bioph Res Co.* 2006;348(2):703-11.
 32. Holtzman MJ. Arachidonic acid metabolism in airway epithelial cells. *Annu Rev Physiol.* 1992;54:303-29.
 33. Wenzel SE. Arachidonic acid metabolites: Mediators of inflammation in asthma. *Pharmacotherapy.* 1997;17(1):S3-S12.
 34. Hoffmann RF, Zarrintan S, Brandenburg SM, Kol A, de Bruin HG, Jafari S, et al. Prolonged cigarette smoke exposure alters mitochondrial structure and function in airway epithelial cells. *Resp Res.* 2013;14.
 35. Kuo CHS, Pavlidis S, Loza M, Baribaud F, Rowe A, Pandis I, et al. T-helper cell type 2 (Th2) and non-Th2 molecular phenotypes of asthma using sputum transcriptomics in U-BIOPRED. *European Respiratory Journal.* 2017;49(2).
 36. Lodhi IJ, Wei XC, Yin L, Feng C, Adak S, Abou-Ezzi G, et al. Peroxisomal Lipid Synthesis Regulates Inflammation by Sustaining Neutrophil Membrane Phospholipid Composition and Viability. *Cell Metab.* 2015;21(1):51-64.
 37. Kuerschner L, Richter D, Hannibal-Bach HK, Gaebler A, Shevchenko A, Ejsing CS, et al. Exogenous Ether Lipids Predominantly Target Mitochondria. *Plos One.* 2012;7(2).
 38. Pilette C, Colinet B, Kiss R, Andre S, Kaltner H, Gabius HJ, et al. Increased galectin-3 expression and intra-epithelial neutrophils in small airways in severe COPD. *European Respiratory Journal.* 2007;29(5):914-22.
 39. Button B, Okada SF, Frederick CB, Thelin WR, Boucher RC. Mechanosensitive ATP Release Maintains Proper Mucus Hydration of Airways. *Sci Signal.* 2013;6(279).
 40. Thomas B, Rutman A, Hirst RA, Haldar P, Wardlaw AJ, Bankart J, et al. Ciliary dysfunction and ultrastructural abnormalities are features of severe asthma. *J Allergy Clin Immun.* 2010;126(4):722-U85.
 41. Lapperre TS, Koh MS, Low SY, Ong TH, Loo CM, Lim WT, et al. Ciliary Dysfunction and Respiratory Epithelial Ultrastructural Abnormalities Are Features of Copd Irrespective of Exacerbator Phenotype. *Respirology.* 2017;22:31-.
 42. Pretolani M, Dombret MC, Thabut G, Knap D, Hamidi F, Debray MP, et al. Reduction of Airway Smooth Muscle Mass by Bronchial Thermoplasty in Patients with Severe Asthma. *Am J Resp Crit Care.* 2014;190(12):1452-4.
 43. Cahill KN, Katz HR, Cui J, Lai J, Kazani S, Crosby-Thompson A, et al. KIT Inhibition by Imatinib in Patients with Severe Refractory Asthma. *N Engl J Med.* 2017;376(20):1911-20.

44. Ingram JL, Bonner JC. EGF and PDGF receptor tyrosine kinases as therapeutic targets for chronic lung diseases. *Curr Mol Med.* 2006;6(4):409-21.
45. Foer D, Baek S, Cahill KN, Israel E, Cui J, Weiss ST, et al. Individual Gene Expression Signatures in Severe Asthmatics Identify Responders and Non-Responders to Imatinib. *Am J Resp Crit Care.* 2019;199.
46. Liao SY, Linderholm AL, Yoneda KY, Kenyon NJ, Harper RW. Airway transcriptomic profiling after bronchial thermoplasty. *ERJ Open Res.* 2019;5(1).
47. Schamberger A, Verhamme F, Lindner M, Behr J, Eickelberg O. Transcriptome analysis of the human airway epithelium during in vitro differentiation. *European Respiratory Journal.* 2016;48.
48. Gras D, Bourdin A, Vachier I, de Senneville L, Bonnans C, Chanez P. An ex vivo model of severe asthma using reconstituted human bronchial epithelium. *J Allergy Clin Immunol.* 2012;129(5):1259-+.
49. Brandsma J, Goss VM, Yang X, Bakke PS, Caruso M, Chanez P, et al. Lipid phenotyping of lung epithelial lining fluid in healthy human volunteers. *Metabolomics.* 2018;14(10).
50. Greco M, Villani G, Mazzucchelli F, Bresolin N, Papa S, Attardi G. Marked aging-related decline in efficiency of oxidative phosphorylation in human skin fibroblasts. *Faseb J.* 2003;17(10):1706-+.

Supplementary data

Methods

Patients with mild allergic asthma (RESOLVE and MATERIAL studies) met the following criteria: a history of episodic chest symptoms, baseline FEV₁ >80% predicted, airway responsiveness to methacholine (provocative concentration causing 20% fall in FEV₁, PC₂₀ < 9.8 mg/mL), and skin prick test positive for at least one of 12 common aeroallergens. Patients were not allowed to use inhaled or systemic corticosteroids or treatment other than inhaled short-acting β_2 -agonists within 2 weeks prior to the start of the study. Healthy individuals from the RESOLVE study had a FEV₁ >80% predicted, PC₂₀ >16 mg/mL and a negative skin prick test for 12 common aeroallergens. All mild asthma patients and healthy controls were non-smoking or had stopped smoking 12 months before their participation with ≤ 5 pack years.

Severe asthma patients from the TASMA study were using inhaled corticosteroid (ICS) at a dosage $\geq 500\mu\text{g}$ fluticasone equivalent per day and long-acting β_2 -agonist (LABA) at a dosage of $\geq 100\mu\text{g}$ per day salmeterol dose aerosol or equivalent for the past 6 months and systemic corticosteroid use ($\leq 20\text{mg/day}$ prednisone equivalent). Furthermore, their ACQ >1,5 for 2 weeks and they were non-smokers for 1 year or more (former smoker ≤ 15 pack years).

The RILCA study involved asthma patients and non-asthmatic healthy controls, between the age of 18 to 50 years at the screening visit. All participants provided informed consent to all study-related procedures. This study included mild to moderate asthma patients using the following criteria. A history of episodic chest tightness and wheezing and controlled asthma according to the criteria by the Global Initiative for Asthma [48]. All these patients were non-smokers or stopped smoking more than 12 months ago and ≤ 5 pack years (PY). They were all clinically stable, no exacerbations within the last 6 weeks prior to the study. The inhaled corticosteroid usage was at a stable dose-equivalent of $\leq 500\text{mcg/day}$ fluticasone propionate for these patients. These asthma patients had baseline FEV₁ 80% of predicted [49] and airway hyperresponsiveness, indicated by a positive acetyl- β -methylcholine bromide (MeBr) challenge with PC₂₀ < 9.8 mg/ml [50]. In addition, they were tested positive for skin prick test (SPT) to one or more of the 12 common aeroallergen extracts (defined as a wheal with an average diameter of 3 mm). They did not have any other clinically significant abnormality on medical history and clinical examination at the screening visit.

The non-asthmatic healthy subjects are recruited using the following inclusion criteria. These individuals were non-smokers or stopped smoking more than 12 months before their participation and ≤ 5 PY. They had a baseline FEV₁ 80% of predicted or above and MeBr challenge with PC₂₀ > 9.8 mg/ml. Steroid-naïve or those participants who were currently not on corticosteroids and have

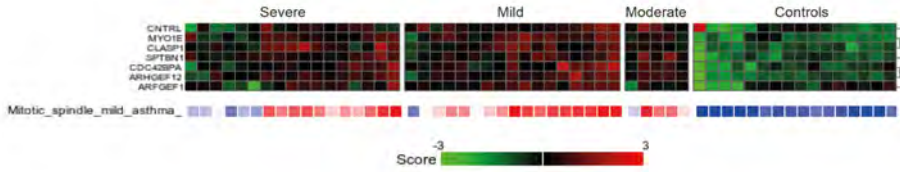
not taken any corticosteroids by any dosing-routes within 8 weeks prior to the study. They had a negative history of pulmonary or any other relevant diseases. The exclusion criteria for this study includes the following. Individuals with any concomitant disease or condition which could interfere with the conduct of the study, or for which the treatment (e.g. immunosuppressive drugs) might interfere with the conduct of the study, or which would, in the opinion of the investigator, pose an unacceptable risk to the patient. Subjects with RV16 titre > 1:6 in serum, measured at visit 1 were excluded. Also, with a history of clinical significant hypotensive episodes or symptoms of fainting, dizziness, or light-headedness. Asthma patients with experience of an asthma exacerbation in the 12 weeks prior to visit 1 requiring management with systemic steroids or has had any acute illness, including a common cold, within 4 weeks prior to visit 1 were excluded. Individuals were excluded when they have donated blood or has had a blood loss of more than 450 mL within 60 days prior to screening visit 1 or plans to donate blood during the study.

All participants from the RILCO study, involving COPD patients and healthy controls, had the following inclusion criteria. None of the subjects had a history of bronchiectasis, lung cancer or other significant respiratory disease and COPD patients were stable on COPD medication, no exacerbation or changes in COPD medication in the past 6 weeks. Also, they were tested negative for skin prick tests for most common aeroallergens. None of the individuals had major comorbidities or had participated in any drug trial in preceding 6 months. COPD patients were 40 to 65 years of age, BMI 17-30 kg.m², non-smoking, or ex-smoking (≥ 2 years before their participation), ≥ 10 pack years; GOLD stage II (post-bronchodilator FEV1 <80% predicted and FEV1/FVC <70%). They were allowed COPD specific medication of LABA and LAMA medication, but no ICS. The healthy controls for this study were age- and smoking history-matched controls.

Metabolomics data analysis

Data processing was done in R, annotation of the peaks were done based on an in-house database containing all possible (phospho)lipid species and metabolites. Each combination of column (normal phase or reverse phase) and scan mode (positive or negative) was processed separately; after normalization, separate peak group lists were combined into three resulting lists, which were used for statistical analysis. Identification was based on exact mass (with 3 ppm tolerance) and retention time including the relation between these two parameters, taking into account the different molecular species of the lipid class. A set of internal standards (ISs), compounds with the same general structure as the lipid classes and metabolites of interest, has been added to each sample in the dataset after sample work-up and before data collection. These ISs have been adequately identified and are used both to locate all other metabolites in the same chemical class and to normalize the intensities for those metabolites. Volcano plots were generated to identify changes in large data sets and plots

significance ($-\log_{10}$ (p-value)) *versus* effect size (\log_2 (fold change)) on the y and x axes, respectively. Heat maps graphically represent data where individual values contained in the sample set are represented as red for high and blue for low respectively (samples in columns and metabolites in rows). The heat maps are represented as Z scores of each individual sample in a row. The Z scores are calculated by: $(X \text{ (value of the individual sample)} - \mu \text{ (average of the row)}) / \sigma$ (standard deviation of the row).



Supplementary Figure 1. Heat map of mitotic spindle genes were upregulated significantly in PBECs from mild ($n=17$) and moderate ($n=5$) asthma patients compared to those from healthy controls ($n=16$). PBECs from severe asthma patients ($n=17$) showed a heterogenous expression of mitotic spindle genes.

Chapter 5.

Resistance of the respiratory system
measured with forced oscillation
technique (FOT) correlates with
Bronchial Thermoplasty response

Goorsenberg AWM
d'Hooghe JNS
Slats AM
van den Aardweg JG
Annema JT
Bonta PI

Respiratory Research 2020; 21(1):52.

Abstract

Background Bronchial Thermoplasty (BT) is an endoscopic treatment for severe asthma using radiofrequency energy to target airway remodeling including smooth muscle. The correlation of pulmonary function tests and BT response are largely unknown. Forced Oscillation Technique (FOT) is an effort-independent technique to assess respiratory resistance (Rrs) by using pressure oscillations including small airways.

Aim To investigate the effect of BT on pulmonary function, assessed by spirometry, bodyplethysmography and FOT and explore associations between pulmonary function parameters and BT treatment response.

Methods Severe asthma patients recruited to the TASMA trial were analyzed in this observational cohort study. Spirometry, bodyplethysmography and FOT measurements were performed before and 6 months after BT. Asthma questionnaires (AQLQ/ACQ-6) were used to assess treatment response.

Results Twenty-four patients were analyzed. AQLQ and ACQ improved significantly 6 months after BT (AQLQ 4.15 (± 0.96) to 4.90 (± 1.14) and ACQ 2.64 (± 0.60) to 2.11 (± 1.04), $p=0.004$ and $p=0.02$ respectively). Pulmonary function parameters remained stable. Improvement in FEV1 correlated with AQLQ change ($r=0.45$ $p=0.03$). Lower respiratory resistance (Rrs) at baseline (both 5 Hz and 19 Hz) significantly correlated to AQLQ improvement ($r=-0.52$ and $r=-0.53$ respectively, $p=0.01$ (both)). Borderline significant correlations with ACQ improvement were found ($r=0.30$ $p=0.16$ for 5 Hz and $r=0.41$ $p=0.05$ for 19 Hz).

Conclusion Pulmonary function remained stable after BT. Improvement in FEV1 correlated with asthma questionnaires improvement including AQLQ. Lower FOT-measured respiratory resistance at baseline was associated with favorable BT response, which might reflect targeting of larger airways with BT.

Abbreviations

ACQ: Asthma control questionnaire
AQLQ: Asthma quality of life questionnaire
ASM: Airway smooth muscle
BT: Bronchial thermoplasty
CT: Computed tomography
FEV1: Forced expiratory volume in 1 s
FOT: Forced oscillation technique
FVC: Forced vital capacity
IMI: Innovative medicine initiative
IQR: Interquartile range
Rrs: Respiratory resistance
WHO: World health organization
Xrs: Reactance

Introduction

Bronchial Thermoplasty (BT) is an endoscopic treatment for patients with severe asthma. It uses radiofrequency energy delivered to the medium and larger airways to reduce airway smooth muscle (ASM) mass [1-5]. Several studies have shown an improvement in asthma quality of life, asthma control, and a reduction in exacerbations after BT [6-8]. The exact mechanism of action however is still incompletely understood and patient responder profile remains under debate.

Pulmonary function measurements before and after BT have shown various results and correlations with treatment response have not been explored comprehensively. The large clinical trials and long term follow up studies thereafter showed a stable one-second forced expiratory volume (FEV1) up to 5 years after BT with only the RISA trial showing an improvement in FEV1 6 months after BT [6-8].

Forced Oscillation Technique (FOT) is an effort-independent technique using various pressure oscillations to assess the relation between flow and pressure in the respiratory system [9]. It has been postulated that FOT is more accurate in detecting small airways disease than conventional tests such as spirometry [10, 11]. Additionally, while with bodyplethysmography the airway resistance is calculated by combining the flow with alveolar pressure, FOT measures the resistance of the entire respiratory system including the surrounding tissue and small airways [12].

This study hypothesized that the BT-induced reduction of ASM in the larger airways influences the mechanical properties of the asthmatic airways. The aims of this trial are (1) to assess the effect of BT on pulmonary function parameters as assessed by spirometry, bodyplethysmography-determined airway resistance and FOT; (2) to evaluate whether pulmonary function parameters are related to BT response.

Methods

Subjects

Patients fulfilling the World Health Organization (WHO) and Innovative Medicine Initiative (IMI) criteria for severe refractory asthma and scheduled for BT and pulmonary function tests including FOT between December 2014 and September 2018 were included (Clinical trials.gov NCT02225392) [13, 14]. Ethical approval was provided by the Medical Ethics Committee of the Academic Medical Center Amsterdam (NL45394.018.13) and written informed consent was obtained. Asthma medication remained stable during the study period.

Bronchial thermoplasty

Patients were treated with BT according to current guidelines using the Alair System (Boston Scientific, USA) [15-17] and under conscious sedation (remifentanyl/propofol) [18] or general anesthesia. Prednisolone 50mg was started 3 days before treatment, on the day itself and 1 day thereafter.

Methods of measurement

All pulmonary function tests were performed in the morning and conducted by experienced staff according to ERS/ATS standards using Jaeger Masterlab software (Erich Jaeger GmbH, Wurtzburg, Germany). The measurements were performed during two visits: one visit before and one visit 6 months after treatment. During the visits, short acting bronchodilators were stopped for at least 6 hours. Long acting beta agonists (LABA) were continued. Spirometry, bodyplethysmography and FOT measurements were performed both before and after administration of 400 µg salbutamol. FOT was performed in an upright position with the Resmon Pro device using a pseudorandom noise signal (Restech, Italy). The subjects received a nose-clip and patients were instructed to support their cheeks with their hands while breathing tidal for 3 min. This measurement was performed twice and the average was used in the analysis.

Outcome parameters

The main outcome parameter of this study was the change in pulmonary function assessed by spirometry, bodyplethysmography and FOT. Other outcome parameters were the correlations between baseline and change in pulmonary function parameters and change in asthma quality of life questionnaires (AQLQ) and asthma control (ACQ-6) [19, 20]. Changes in pulmonary function parameters or asthma questionnaires were defined as post-BT minus pre-BT values. A decrease of 0.5 points on AQLQ and an increase of 0.5 points on ACQ-6 is designated as clinically relevant.

Statistical analysis

GraphPad Prism version 5.01 (GraphPad Software Inc., San Diego, CA, USA) was used for the analysis. Grouped data were reported as mean with standard deviation or median with interquartile ranges, as appropriate. Within group analyses were performed with paired t-tests or Wilcoxon signed rank tests. Correlation analyses were performed with Spearman's rho coefficient. P-values were two sided and a statistical significance was set at $p < 0.05$.

Results

Subjects and clinical outcome

BT and pulmonary function tests including FOT were performed in 26 patients. Two patients were excluded from analyses due to lost to follow up at the 6 months

visit. Baseline characteristics of the included 24 patients are shown in **Table 1**. Due to claustrophobia one patient was excluded from bodyplethysmography analyses. In FOT analysis, one patient was excluded due to extreme coughing and in one other patient only post-bronchodilator measurements were performed. BT significantly improved quality of life and asthma control. AQLQ questionnaires improved from 4.15 (± 0.96) to 4.90 (± 1.14) ($p=0.004$) and ACQ questionnaires improved from 2.64 (± 0.60) to 2.11 (± 1.04) ($p=0.02$).

Pulmonary function measurements

The effect of BT on spirometry and bodyplethysmography parameters are shown in **Table 2**. FEV1 did not significantly change after BT. FVC (% of predicted, pre-bronchodilator) was slightly increased after BT, with a stable FEV1 resulting in a reciprocal decrease in FEV1/FVC. Additionally, a minimal increase in post bronchodilator airway resistance was found (before BT 0.15 (0.14;0.21) kPa*s/L versus after BT 0.23 (0.16;0.24) kPa*s/L ($p<0.05$)).

Total group analyses of FOT measurements did not show a change in respiratory resistance (Rrs) and reactance (Xrs) after BT for both 5 Hz and 19 Hz (**Table 3**).

Correlation analyses

Associations between asthma questionnaires and pulmonary function parameters were explored.

Table 1 Baseline characteristics

| Characteristics | Baseline |
|--------------------------------------------------|-------------------|
| No. of patients | 24 |
| Sex (males/females) | 5/19 |
| Age (y) | 44 \pm 12 |
| BMI | 28.3 \pm 4.9 |
| FeNO (ppb) | 17.8 (12.6; 45.6) |
| Total serum IgE (kU/L) | 67 (14; 219) |
| Blood eosinophil count ($10^9/L$) | 0.15 (0.06; 0.29) |
| ACQ-6 score | 2.64 \pm 0.60 |
| AQLQ score | 4.15 \pm 0.96 |
| Dose of LABA ($\mu g/d$ salmeterol equivalents) | 135 \pm 55 |
| Dose of ICS ($\mu g/d$ fluticasone equivalents) | 1174 \pm 508 |
| No. of patients on maintenance use of OCS | 7 |
| Dose of oral prednisone (mg/d) | 12 \pm 6 |
| No. of patients on omalizumab | 3 |

Data are presented as numbers, mean (\pm SD) or median (IQR)

BMI, body mass index; FeNO, fractional exhaled nitric oxide; ACQ, asthma control questionnaire; AQLQ, asthma quality of life questionnaire; LABA, long acting β -2-agonist; ICS, inhaled corticosteroids; OCS, oral corticosteroids;

Table 2 Pulmonary function parameters before and after Bronchial Thermoplasty treatment

| | Parameter | Before BT | After BT | P-value |
|-------------------------------|--------------------------------------|------------------|------------------|---------|
| Before bronchodilation | FEV₁ (% predicted) | 88 ± 21 | 90 ± 21 | 0.33 |
| | FEF 75 (L/s) | 1.04 ± 0.57 | 0.97 ± 0.70 | 0.44 |
| | FVC (% predicted) | 98 ± 20 | 102 ± 17 | <0.05 |
| | FEV₁/FVC | 0.74 ± 0.11 | 0.73 ± 0.12 | 0.46 |
| | Raw IN (kPa*s/L) | 0.30 (0.20;0.42) | 0.29 (0.19;0.42) | 0.99 |
| | FRC (L) | 2.60 (1.97;3.22) | 2.63 (2.03;3.08) | 0.69 |
| | RV (L) | 1.81 ± 0.74 | 1.80 ± 0.64 | 0.68 |
| After bronchodilation | FEV₁ (% predicted) | 100 ± 18 | 100 ± 15 | 0.72 |
| | FEF 75 (L/s) | 1.28 ± 0.67 | 1.20 ± 0.78 | 0.37 |
| | FVC (% predicted) | 107 ± 15 | 108 ± 13 | 0.33 |
| | FEV₁/FVC | 0.79 ± 0.10 | 0.77 ± 0.10 | <0.05 |
| | FEV₁ reversibility | 11 (3.5;14) | 4 (2;15) | 0.11 |
| | Raw IN (kPa*s/L) | 0.15 (0.14;0.21) | 0.23 (0.16;0.24) | <0.05 |
| | FRC (L) | 2.73 (1.90;3.10) | 2.52 (2.00;2.91) | 0.14 |
| | RV (L) | 1.60 ± 0.55 | 1.65 ± 0.47 | 0.49 |

Data are presented as mean (± SD) or median (IQR); n = 23 for pre-bronchodilator measurements and n = 24 for post-bronchodilator measurements.

FEV₁, forced expiratory volume in 1 second; FEF 75, forced expiratory flow at 75% of the FVC; FVC, forced vital capacity; Raw, airway resistance; FRC, functional residual capacity; RV, residual volume;

Table 3 Forced Oscillation Technique parameters before and after Bronchial Thermoplasty treatment

| | Parameter | Before BT | After BT | P-value |
|-------------------------------|-----------------------------------------|----------------------|----------------------|---------|
| Before bronchodilation | Rrs 5Hz (cm H₂O*s/L) | 3.58 (3.21; 4.24) | 3.70 (2.88; 4.29) | 0.59 |
| | Xrs 5Hz (cm H₂O*s/L) | -1.23 (-1.68; -0.89) | -1.28 (-1.81; -0.95) | 0.21 |
| | Rrs 19Hz (cm H₂O*s/L) | 3.17 (2.85; 3.56) | 3.15 (2.80; 3.67) | 0.95 |
| | Xrs 19Hz (cm H₂O*s/L) | 0.65 (0.09; 0.99) | 0.63 (-0.04; 0.80) | 0.22 |
| After bronchodilation | Rrs 5Hz (cm H₂O*s/L) | 3.06 (2.73; 3.41) | 3.22 (2.78; 3.63) | 0.08 |
| | Xrs 5Hz (cm H₂O*s/L) | -1.00 (-1.15; -0.77) | -0.92 (-1.23; -0.73) | 0.28 |
| | Rrs 19Hz (cm H₂O*s/L) | 2.90 (2.65; 3.09) | 2.97 (2.72; 3.47) | 0.26 |
| | Xrs 19Hz (cm H₂O*s/L) | 0.80 (0.56; 1.07) | 0.87 (0.27; 1.08) | 0.21 |

Data are presented as median (IQR); n = 22 for pre-bronchodilator measurements and n = 23 for post-bronchodilator measurements.

Rrs, respiratory resistance; Xrs, reactance.

Asthma questionnaires and spirometry parameters

No significant correlations were found at baseline before BT between asthma questionnaires and spirometry parameters. After BT, improvements in AQLQ and ACQ showed a correlation with baseline FEV1 reversibility (for AQLQ $r=0.42$ $p=0.05$ and for ACQ $r=-0.45$ $p=0.03$) but not with baseline FEV1. Additionally, after BT improvements in asthma questionnaires were correlated with improvements in pre-bronchodilator FEV1 (% predicted) ($r=0.45$ $p=0.03$ for AQLQ and $r=-0.37$ $p=0.08$ for ACQ) (Fig. 1a and b) but not with post-bronchodilator FEV1.

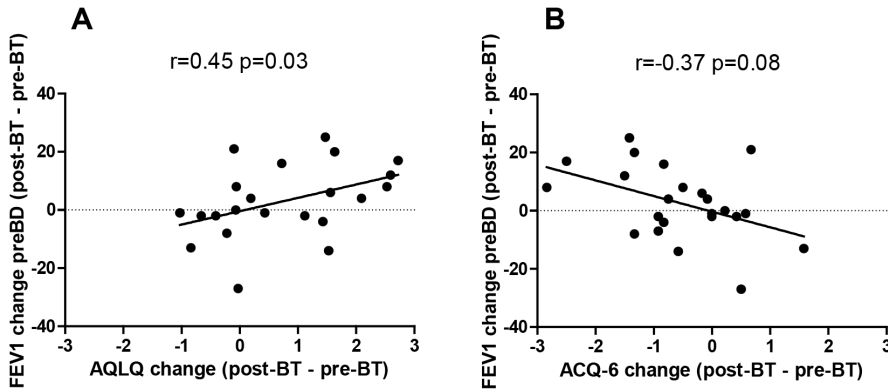


Figure 1 Correlation between asthma questionnaire AQLQ and ACQ-6 changes and pre-BD FEV1(% predicted) change after BT.

An improvement in AQLQ ($n=22$) (1A) and ACQ ($n=23$) (1B) is correlated with post-BT change in FEV1 (%) pre-BD. FEV1, forced expiratory volume in 1 second; BD, bronchodilation; BT, Bronchial Thermoplasty; AQLQ, asthma quality of life questionnaire; ACQ, asthma control questionnaire.

Asthma questionnaires and bodyplethysmography

Regarding bodyplethysmography, a correlation was found between baseline AQLQ and baseline airway resistance (R_{aw}) ($n=23$, $r=0.56$ for both pre-BD and post-BD; $p<0.01$). Baseline measurements of airway resistance were not correlated with baseline ACQ. No correlations were found between changes in AQLQ and ACQ questionnaires and airway resistance measured with bodyplethysmography.

Asthma questionnaires and respiratory resistance

Similar correlations were found for respiratory resistance measured with FOT at both 5Hz and 19Hz. Baseline AQLQ scores showed a significant positive correlation with respiratory resistance at 19Hz ($r=0.67$ $p=0.0005$ for pre-bronchodilator R_{rs} and $r=0.57$ $p=0.005$ for post-bronchodilator R_{rs}) and a trend between baseline AQLQ and pre-bronchodilator respiratory resistance

at 5 Hz ($r=0.36$; $p=0.09$). Baseline ACQ scores were not correlated to baseline FOT measurements.

Next the correlation between changes in asthma questionnaires and baseline respiratory resistance were analyzed. AQLQ improvement was negatively correlated with baseline pre-bronchodilator respiratory resistance (Rrs at 5 Hz $r=-0.52$ $p=0.01$; Rrs at 19 Hz $r=-0.53$ $p=0.01$) (Fig. 2a-b) and baseline post-bronchodilator respiratory resistance (Rrs at 5 Hz $r=-0.43$ $p=0.04$; Rrs at 19 Hz $r=-0.55$ $p=0.01$). A positive trend was found between ACQ improvement and baseline pre-bronchodilator respiratory resistance at both 5 Hz ($r=0.30$ $p=0.16$) and 19 Hz ($r=0.41$ $p=0.05$) (Fig. 2c-d).

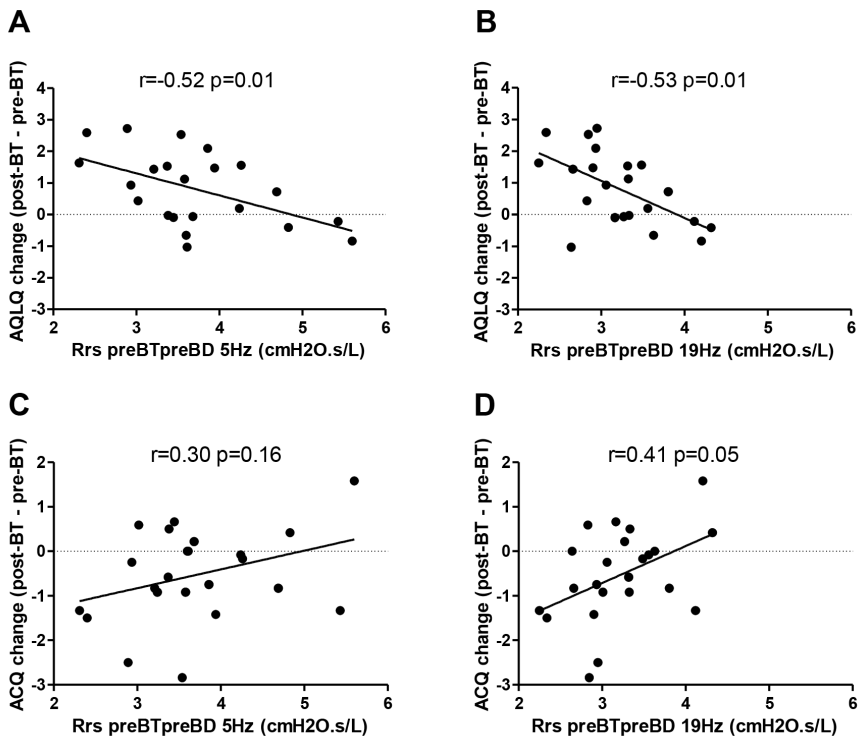


Figure 2 Associations between asthma questionnaire AQLQ and ACQ-6 changes and respiratory resistance measured with FOT at baseline (5Hz and 19Hz).

A negative correlation was found between AQLQ improvement and baseline respiratory resistance at both 5 Hz (2A) and 19 Hz (2B). A positive correlation was seen between ACQ improvement and baseline respiratory resistance at both 5 Hz (2C) and 19 Hz (2D). FOT, forced oscillation technique; AQLQ, asthma quality of life questionnaire; ACQ, asthma control questionnaire; Rrs, respiratory resistance in cmH₂O.s/L; BT, bronchial thermoplasty; BD, bronchodilation.

Asthma questionnaires and airway reactance

Correlations between asthma questionnaires and reactance measurements were only found for AQLQ and reactance at 5 Hz: baseline AQLQ was negatively correlated with airway reactance ($r=-0.42$; $p=0.05$) and improvement of AQLQ was correlated with a higher reactance at baseline ($r=0.48$; $p=0.02$). No significant correlation between baseline / change ACQ and airway reactance was found.

Discussion

This study aimed to investigate the effect of BT on pulmonary function and to explore whether these pulmonary function parameters were associated with BT response. An improvement in asthma control and quality of life was found while overall pulmonary function parameters remained stable. More importantly, this is the first study showing that a low respiratory resistance, measured with FOT, correlated to BT-response. These results can contribute to improved patient selection for BT.

Comparable to previously published larger trials [8, 21], spirometry parameters overall remained stable. A slight increase in pre-bronchodilator FVC (% predicted) and decrease in post-bronchodilator FEV1/FVC after BT were found, although significantly different, the clinical relevance of these small differences is questionable. For the first time however, correlations were found between asthma questionnaire (AQLQ and ACQ) changes and FEV1 change. Although the differences were small, these data suggest that spirometry might improve after BT as previously shown in the RISA trial [7]. In our study, this improvement in FEV1 was only visible in the patients that responded well to BT. This correlation was also explored, but not found in an Australian cohort of severe asthma patients [22]. An explanation can be the difference in baseline characteristics between both cohorts, with a more obstructive asthma phenotype in the Australian cohort compared to the present study (FEV1 (% predicted) of 55% compared to 88%).

When taking all patient data into account a significant increase was found after BT in post-bronchodilator bodyplethysmography airway resistance. This increase is mainly caused by one patient, who gained 7kg during follow-up, which could explain this outcome. Similar to Langton et al. [23] no significant differences in FOT measurements were found after BT in our study. However, a positive correlation was found between airway and respiratory resistance measured with both bodyplethysmography and FOT and AQLQ questionnaires at baseline. For ACQ this correlation was not present. The mechanism underlying this result needs to be further explored.

An important finding of this study is the correlation between improvements on AQLQ and ACQ and respiratory resistance measured with FOT. In this study, patients with a higher respiratory resistance at baseline showed less improvements on both questionnaires after BT compared to patients with a lower resistance. Conventional spirometry and bodyplethysmography-determined airway resistance did not show this correlation. A possible explanation for this difference might be that FOT measures the respiratory resistance of the entire respiratory system, including smaller airways and surrounding tissue. Non-responding patients might be the patients with a higher resistance in surrounding tissue, potentially in the smaller distal airways which are not reached by the BT catheter. Consequently, patients with lower respiratory resistance at baseline might be the patients to select for BT treatment.

An improvement in the respiratory resistance was not observed. Other recently published studies however did show an improvement of ventilation homogeneity after BT [24] and effects of BT on airtrapping parameters with pulmonary function tests [22] and Computed Tomography [25-27] indicating a BT-effect in the peripheral parts of the airways. To measure the resistance in the smaller airways, FOT alone is probably not sufficient. The assessment of small airways disease and/or the effect on the smaller airways of BT might be more accurate when combining multiple techniques together such as CT, FOT and/or impulse oscillometry (IOS) as currently investigated by the Atlantis study group [28].

There are limitations to this study that need to be addressed. The results in this study are part of the TASMA study, a multicenter study, however FOT measurements were only performed in one center. Therefore the present study included patients from one center only. Although single center results, the included group was clinically heterogeneous with allergic, eosinophilic and non-allergic/non-eosinophilic patients included. Additionally, patients were referred to this center from all parts of the Netherlands, thereby decreasing the effect of environmental factors on the outcome. Another limitation is the relatively small number of included patients. Although results need to be confirmed in larger trials, this study does offer important insights that may help to improve patient selection in the future. Strong points of this study are using not only conventional methods to assess lung function parameters but also use FOT, a method known to give a more reliable result on peripheral airway resistance. Also by keeping the medication use stable during follow up, and not start tapering down, which could influence the results, strengthens the observed measurements.

Conclusion

Pulmonary function parameters, including FOT, remained stable after BT. Correlations were found between FEV1 improvement and asthma questionnaires improvement including AQLQ. Additionally, a lower respiratory resistance at baseline, measured with FOT, was associated with a favorable BT-response, which might reflect the main targeting of BT on the larger airways. These results add to understanding the mechanism of action of BT and might contribute to improved patient selection for this treatment.

References

1. Pretolani M, Dombret MC, Thabut G, Knap D, Hamidi F, Debray MP et al. Reduction of airway smooth muscle mass by bronchial thermoplasty in patients with severe asthma. *Am J Respir Crit Care Med.* 2014;190:1452–1454.
2. Denner DR, Doeing DC, Hogarth DK, Dugan K, Naureckas ET, White SR. Airway inflammation after bronchial thermoplasty for severe asthma. *Ann Am Thorac Soc.* 2015;12:1302–1309.
3. Chakir J, Haj-Salem I, Gras D, Joubert P, Beaudoin EL, Biardel S et al. Effects of bronchial thermoplasty on airway smooth muscle and collagen deposition in asthma. *Ann Am Thorac Soc.* 2015;12:1612–1618.
4. Pretolani M, Bergqvist A, Thabut G, Dombret MC, Knapp D, Hamidi F et al. Effectiveness of bronchial thermoplasty in patients with severe refractory asthma: clinical and histopathologic correlations. *J Allergy Clin Immunol.* 2017;139:1176–1185.
5. d’Hooghe JNS, Goorsenberg AWM, ten Hacken NHT, Weersink EJM, Roelofs JJTH, Mauad D et al. Airway smooth muscle reduction after bronchial thermoplasty in severe asthma correlates with FEV₁. *Clin Exp Immunol.* 2019; 49(4):541-544.
6. Cox G, Thomson NC, Rubin AS, Niven RM, Corris PA, Siersted HC et al. Asthma control during the year after bronchial thermoplasty. *N Engl J Med.* 2007;356:1327–1337.
7. Pavord ID, Cox G, Thomson NC, Rubin AS, Corris PA, Niven RM et al. Safety and efficacy of bronchial thermoplasty in symptomatic, severe asthma. *Am J Respir Crit Care Med.* 2007;176:1185–1191.
8. Castro M, Rubin AS, Laviolette M, Fiterman J, De Andrade Lima M, Shah PL et al. Effectiveness and safety of bronchial thermoplasty in the treatment of severe asthma: a multicenter, randomized, double-blind, sham-controlled clinical trial. *Am J Respir Crit Care Med.* 2010;181:116–124.
9. Oostveen E, MacLeod D, Lorino H, Farre R, Hantos Z, Desager K et al. The forced oscillation technique in clinical practice: methodology, recommendations and future developments. *Eur Respir J.* 2003;22:1026-1041.
10. McNulty W, Usmani OS. Techniques of assessing small airways dysfunction. *Eur Clin Respir J.* 2014; <http://dx.doi.org/10.3402/ecrj.v1.25898>.
11. Anderson WJ, Zajda E, Lipworth BJ. Are we overlooking persistent small airways dysfunction in community-managed asthma? *Ann Allergy Asthma Immunol.* 2012;109(3):185-189.
12. Kaminsky DA, Bates JHT. Breathing In and Out: Airway Resistance. In: Kaminsky DA, Irvin CG, eds. *Pulmonary Function Testing. Principles and Practice.* Cham, Switzerland: Humana press; 2018:127-150.
13. Bousquet J, Mantzouranis E, Cruz, Ait-Khaled N, Baena-Cagnani CE, Bleecker ER et al. Uniform definition of asthma severity, control, and exacerbations: document presented for the World Health Organization Consultation on Severe Asthma. *J Allergy Clin Immunol.* 2010;126:926–938.
14. Bel EH, Sousa A, Fleming L, Bush A, Chung KF, Versnel J et al. Diagnosis and definition of severe refractory asthma: an international consensus statement from

- the Innovative Medicine Initiative (IMI). *Thorax*. 2011;66:910–917.
15. Cox G, Miller JD, McWilliams A, Fitzgerald JM, Lam S. Bronchial thermoplasty for asthma. *Am J Respir Crit Care Med*. 2006;173:965–969.
 16. d’Hooghe JNS, Ten Hacken NHT, Weersink EJM, Sterk PJ, Annema JT, Bonta PI. Emerging understanding of the mechanism of action of bronchial thermoplasty in asthma. *Pharmacol Ther*. 2018;181:101–107.
 17. Bonta PI, Chanez P, Annema JT, Shah PL, Niven R. Bronchial thermoplasty in severe asthma: best practice recommendations from an expert panel. *Respiration*. 2018;95(5):289-300
 18. d’Hooghe JN, Eberl S, Annema JT, Bonta PI. Propofol and remifentanyl sedation for bronchial thermoplasty: a prospective cohort trial. *Respiration*. 2017;93:58–64.
 19. Juniper EF, O’Byrne PM, Guyatt GH, Ferrie PJ, King DR. Development and validation of a questionnaire to measure asthma control. *Eur Respir J*. 1999;14(4):902–907.
 20. Juniper EF, Buist AS, Cox FM, Ferrie PJ, King DR. Validation of a standardized version of the asthma quality of life questionnaire. *Chest* 1999;115:1265–70.
 21. Chupp G, Laviolette M, Cohn L, McEvoy C, Bansal S, Shifren A et al. Long-term outcomes of bronchial thermoplasty in subjects with severe asthma: a comparison of 3-year follow-up results from two prospective multicentre studies. *Eur Respir J*. 2017;50(2).
 22. Langton D, Ing A, Bennetts K, Wang W, Farah C, Peters M et al. Bronchial thermoplasty reduces gas trapping in severe asthma. *BMC Pulmonary Medicine*. 2018; 18:155.
 23. Langton D, Ing A, Sha J, Bennetts K, Hersch N, Kwok M et al. Measuring the effects of bronchial thermoplasty using oscillometry. *Respirology*. 2018;24(5):431-436.
 24. Donovan GM, Elliot JG, Green FHY, James AL, Noble PB. Unravelling a clinical paradox – why does bronchial thermoplasty work in asthma? *Am. J. Respir. Cell Mol. Biol*. 2018;59:355–62
 25. Zanon M, Strieder DL, Rubin AS, Watte G, Marchiori E, Cardoso PFG et al. Use of MDCT to Assess the Results of Bronchial Thermoplasty. *Am J Roentgen*. 2017; 209(4):752-756.
 26. Konietzke P, Weinheimer O, Wielputz MO, Wagner WL, Kaukel P, Eberhardt R et al. Quantitative CT detects changes in airway dimensions and air-trapping after bronchial thermoplasty for severe asthma. *Eur J Radiol*. 2018; 107:33-38.
 27. Ishii S, Iikura M, Shimoda Y, Izumi S, Hojo M, Sugiyama H. Evaluation of expiratory capacity with severe asthma following bronchial thermoplasty. *Respirol Case Rep*. 2018;7(1).
 28. Postma DS, Brightling C, Baldi S, Van den Berge M, Fabbri LM, Gagnatelli A et al. Exploring the relevance and extent of small airways dysfunction in asthma (ATLANTIS): baseline data from a prospective cohort study. *Lancet Respiratory Medicine*. 2019;7(5):402-416.

Part III.

Airway wall imaging with optical coherence tomography

Chapter 6.

Advances in optical coherence tomography (OCT) and confocal laser endomicroscopy (CLE) in pulmonary diseases

Goorsenberg AWM
Kalverda K
Annema JT
Bonta PI

Respiration 2020;99(3):190-205.

Abstract

Diagnosing and monitoring pulmonary diseases is highly dependent on imaging, physiological function tests and tissue sampling. Optical coherence tomography (OCT) and confocal laser endomicroscopy (CLE) are novel imaging techniques with near-microscopic resolution that can be easily and safely combined with conventional bronchoscopy. Disease-related pulmonary anatomical compartments can be visualized, real time, using these techniques. In obstructive lung diseases, airway wall layers and related structural remodelling can be identified and quantified. In malignant lung disease, normal and malignant areas of the central airways, lung parenchyma, lymph nodes and pleura can be discriminated. A growing number of interstitial lung diseases (ILDs) have been visualized using OCT or CLE. Several ILD-associated structural changes can be imaged: fibrosis, cellular infiltration, bronchi(ol) ectasis, cysts and microscopic honeycombing. Although not yet implemented in clinical practice, OCT and CLE have the potential to improve detection and monitoring pulmonary diseases and can contribute in unravelling the pathophysiology of disease and mechanism of action of novel treatments. Indeed, assessment of the airway wall layers with OCT might be helpful when evaluating treatments targeting airway remodelling. By visualizing individual malignant cells, CLE has the potential as a real-time lung cancer detection tool. In the future, both techniques could be combined with laser-enhanced fluorescent-labelled tracer detection. This review discusses the value of OCT and CLE in pulmonary medicine by summarizing the current evidence and elaborating on future perspectives.

Introduction

Diagnosing pulmonary diseases is highly dependent on imaging techniques such as high-resolution computed tomography of the chest (HRCT) or minimal invasive procedures like bronchoscopy for tissue sampling. HRCT imaging contributes to the diagnosis of many pulmonary diseases; however, spatial resolution is limited and patients are subjected to ionizing radiation. Endobronchial sampling, such as mucosal and parenchymal biopsies and needle aspiration, is associated with a complication risk, subject to sampling error and provides only information on one specific sampling site.

To diagnose and understand the pathophysiology of pulmonary diseases and monitor treatments, higher imaging resolution beyond HRCT on a histological/cellular level might be helpful. Optical coherence tomography (OCT) and confocal laser endomicroscopy (CLE) are 2 novel imaging techniques that can fill this gap between invasive and selective tissue sampling and the limited resolution of HRCT. All these techniques are complementary: from a large overview of the lung (HRCT) to near-microscopic imaging (CLE; **Fig. 1**). In this review, we discuss the value of bronchoscopic OCT and CLE in pulmonary diseases by summarizing OCT and CLE-based imaging studies using the anatomical compartments related to obstructive lung diseases, pulmonary malignancies and interstitial lung diseases (ILD; **Fig. 2, Table 1**). Furthermore, potential future clinical applications of these imaging techniques in pulmonary disease management are discussed (**Table 1**). The applicability of OCT in pulmonary vascular diseases has been described in a previously published review and is discussed less extensively [1].

Table 1: Imaging studies in humans using OCT and CLE in respiratory medicine

| Pulmonary diseases | Anatomical compartment | Optical Coherence Tomography (OCT) | Confocal Laser Endomicroscopy (CLE) | Potential future clinical implications |
|----------------------------------|-------------------------|---------------------------------------------------------------------------------------------------------------------------------------------------------------------------------------------------------------------------------------------------------------------------------------------------------------------------------------|-----------------------------------------------------------------------------------------------------------------------------------------------------------------------------------------------|-----------------------------------------------------------------------------------------------------------------------------------------------------------------------------------------------------------------------------------------------------|
| Obstructive lung diseases | Airway wall | Asthma <ul style="list-style-type: none"> · ASM detection⁴¹ and airway wall thickness³⁹ · Assess airway compliance by measuring airway lumen at different pressures³⁸ · (Acute) BT effects: sloughing of epithelium⁴⁰, airway wall edema^{39,40} | Asthma <ul style="list-style-type: none"> · Visualization of elastin fibre pattern in airway wall¹⁷ | <ul style="list-style-type: none"> · Evaluate airway remodelling including structural airway components as part of extensive phenotyping in obstructive airways disease |
| | | COPD <ul style="list-style-type: none"> · Evaluate airway lumen and wall thickness in different COPD stages³⁵⁻³⁷ · Assess airway compliance by measuring airway lumen at different pressures³⁸ | COPD <ul style="list-style-type: none"> · Visualization of elastin fibre pattern in airway wall⁴⁶ · Detection and quantification of emphysema⁴⁷ | <ul style="list-style-type: none"> · Evaluate effect of treatments targeting airway remodelling (e.g. Bronchial Thermoplasty, immunotherapy) · OCT combined with laser for the detection of fluorescently labelled tracers. |
| Malignancies | Airway wall | Lung cancer <ul style="list-style-type: none"> · Detection of endobronchial neoplastic and non-neoplastic lesions⁴⁹⁻⁵⁴ | Lung cancer <ul style="list-style-type: none"> · Detection of endobronchial neoplastic and non-neoplastic lesions^{16,57,59,60} | <ul style="list-style-type: none"> · Improvement of the (early) detection of lung cancer · Improvement of diagnostic yield of lung cancer diagnostic bronchoscopic procedures |
| | Mediastinal lymph nodes | Lung cancer <ul style="list-style-type: none"> · Identification of malignancies in lymph nodes (ex vivo)⁵⁶ | Lung cancer <ul style="list-style-type: none"> · Identification of malignant cells in lymph nodes^{25,26} | <ul style="list-style-type: none"> · Improvement of diagnostic yield for endosonographic staging in lung cancer · Differentiate malignant (subtypes), granulomatous and reactive lymph nodes |

table continues

| Pulmonary diseases | Anatomical compartment | Optical Coherence Tomography (OCT) | Confocal Laser Endomicroscopy (CLE) | Potential future clinical implications |
|------------------------------------|------------------------|-----------------------------------------------------------------------------------------------------------------------------------------------------------------------------------------------------------------------------------------------------------------------------------------------------------------------------------------------------------------------------------------------------------|---------------------------------------------------------------------------------------------------------------------------------------------------------------------------------------------------------------------------------------------------------------------------------------------------|------------------------------------------------------------------------------------------------------------------------------------------------------------------------------------------------------------|
| | Pleura | - | <ul style="list-style-type: none"> Pleural lesions Differentiation between pleural fibrosis and mesothelioma¹¹ Visualization malignant lesions during thoracoscopy⁶⁵ | <ul style="list-style-type: none"> Guidance towards (malignant) lesion Differentiate benign versus malignant lesions |
| | Lung parenchyma | <ul style="list-style-type: none"> Lung cancer Identification of malignant nodules (ex-vivo)³⁵ | <ul style="list-style-type: none"> Pleural effusion Identification of malignant cells in pleural effusion⁶⁶ Lung cancer Identification of malignant nodules: ex-vivo⁶² and in-vivo^{22,58,61} | <ul style="list-style-type: none"> Improvement of diagnostic yield of needle aspiration Guidance tool for transbronchial and transthoracic biopsies |
| Interstitial lung diseases | Lung parenchyma | <ul style="list-style-type: none"> ILD OCT characteristics: thickening/loss of alveolar network structure (fibrosis), honeycombing, cysts and bronchiectasis^{53,70,72} | <ul style="list-style-type: none"> ILD CLE characteristics of ILD^{82,83} Fibrosis detection⁸²⁻⁸⁴ Identification of acute lung transplant rejection^{80,81} | <ul style="list-style-type: none"> Discrimination of fibrotic versus cellular ILD Guidance towards optimal biopsy location in ILD Early detection of transplant rejection |
| Pulmonary vascular diseases | Pulmonary vasculature | <ul style="list-style-type: none"> Pulmonary artery hypertension Pulmonary artery structure: thickened media⁹⁵ and intima (fibrosis)^{96,97} <p>Chronic thromboembolic pulmonary hypertension</p> <ul style="list-style-type: none"> Thrombotic occlusion, luminal bands/webs^{95,97} Visualize the effect of BPA⁹⁸ | <ul style="list-style-type: none"> Differentiation between different forms of PH e.g. PAH and CTEPH Determine the location of pulmonary artery remodelling within the pulmonary artery system Evaluate effects of PAH treatments on pulmonary artery remodelling | |

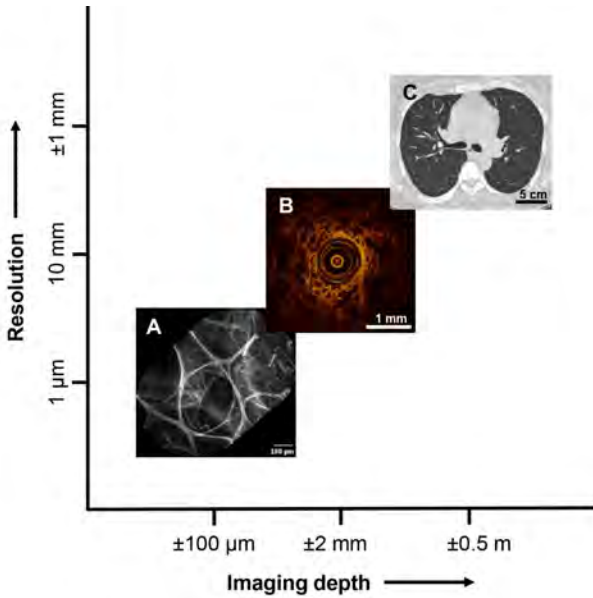


Figure 1 Imaging techniques applied to the alveolar compartment with their corresponding resolution and imaging depth. **a** CLE. **b** OCT. **c** HRCT of the chest.

Technical Background

Optical Coherence Tomography

OCT is an imaging technique using near-infrared light to generate high-resolution images of tissue structures with a resolution of $\pm 10\text{--}15 \mu\text{m}$ and depth of 2–3 mm (**Fig. 1**) [2, 3]. The conceptual idea of OCT is comparable to ultrasound, but instead of using the reflection of acoustic waves, OCT uses the scattering of near-infrared light to generate images. An advantage of OCT over (radial) endobronchial ultrasound is that light waves do not need a transducing medium or direct contact with the tissue and therefore has excellent properties to be used in air filled anatomical compartments such as the airways. In short, in OCT, an optical beam generates near-infrared light and focuses on the tissue. The difference in time of light backscattering in structures is measured and compared with a reference beam by using principles of optical interferometry. This enables the OCT system to generate 2D cross-sectional images (**Fig. 2, 3**). Subsequently, consecutive 2D images generated by pullbacks can be reconstructed to 3D structures. Although many applications in medicine are explored, at first, OCT was clinically implemented in ophthalmology to image the retina [4–6]. Furthermore, OCT is nowadays applied to assess stenosis and stent apposition in coronary arteries in interventional cardiology [7–10]. For pulmonary purposes, OCT has not yet been clinically implemented. However in the last decade, studies have shown that OCT is feasible, safe and has added

value in pulmonary medicine for a broad field of indications (Table 1). The studies in this review investigating the use of OCT in pulmonary medicine have used either company build OCT probes (St. Jude Medical Inc., Abbott, IL, USA; Pentax Corp., Tokyo, Japan; light-CTTM scanner, LLTech, France; LightLab Imaging Inc., Westford, USA; Niris Imaging System, Imalux Corp., Cleveland, OH, USA) or custom build devices. OCT images of the airways and/or alveolar compartment are captured during bronchoscopy (Fig. 3a-c). The OCT catheter is inserted through the working channel of a bronchoscope and advanced until the region of interest is reached. Subsequently by manual or automated pullback, the OCT catheter generates sequential cross-sectional images of segments of the anatomical compartment of interest including the airways, lung parenchyma and pulmonary arteries (Fig. 3, Table 1). This review summarizes the advances that OCT made in improving diagnosis and management of obstructive lung diseases, malignancies and ILDs.

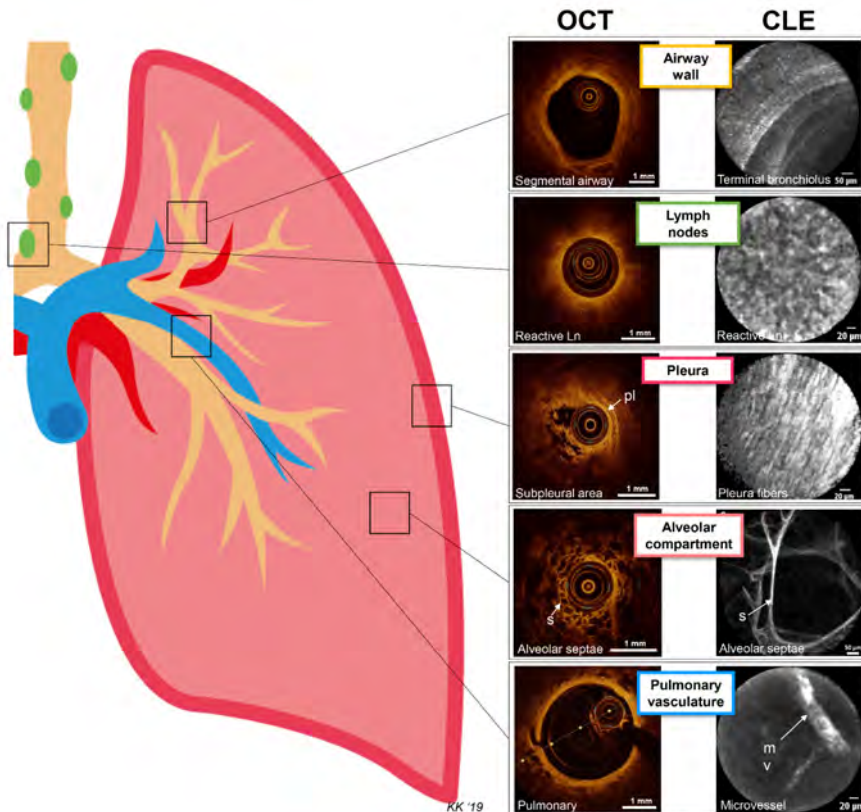


Figure 2. Overview of the pulmonary anatomical compartments with corresponding OCT and CLE images. Airway wall: OCT, cross-sectional view of airway wall in segmental airway; CLE, pCLE image showing a typical helical ring-like pattern of terminal bronchiolus. Lymph nodes: OCT, image in a reactive lymph node; CLE, nCLE

image showing abundant lymphocytes in a reactive lymph node. Pleura: OCT, image of subpleural area, pl is indicated by the white arrow; CLE, lamellar organized elastin fibres in the pl as seen with pCLE. Alveolar compartment: OCT, cross-sectional view of alveolar compartment with network of alveolar s; CLE, pCLE image of alveolar compartment showing alveolar septae with rectangular airspaces. Pulmonary vasculature: OCT, cross-sectional view from pulmonary artery; CLE, nCLE image of an mv in a lymph node. OCT, optical coherence tomography; CLE, confocal laser endomicroscopy; Ln, lymph node; pl, pleura; s, septa; mv, microvessel.

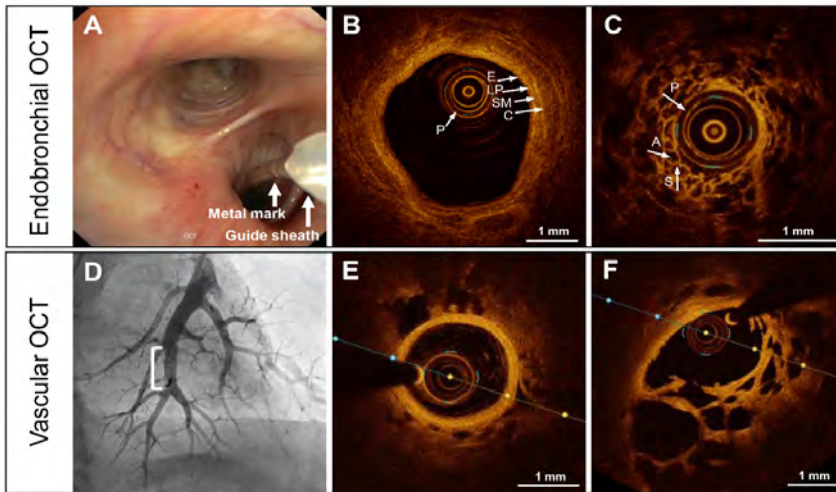


Fig. 3. OCT imaging procedures of the airway wall and alveolar compartment (endobronchial OCT; a–c) and pulmonary artery (vascular OCT, d–f). **a** Bronchoscopic view of an OCT imaging procedure showing the guide sheath and the OCT catheter positioned in the right lower lobe. The metal mark guides the distance of 5.4 cm to the distal tip of the OCT catheter. **b** OCT image of a normal segmental airway wall showing the airway wall layer identification. **c** OCT image of the alveolar compartment showing normal alveoli and septae. **d** Angiography of the left lower lobe pulmonary artery with a stenosis in a chronic thromboembolic pulmonary hypertension (CTEPH) patient (white bracket). **e** OCT image of a normal proximal pulmonary artery. **f** OCT image of a pulmonary artery with webs/bands in a CTEPH patient. (Images provided by H.J. Bogaard, MD, PhD; N. van Royen, MD, PhD and M. Beijk, MD, PhD). OCT, optical coherence tomography; P, probe; A, alveolar space; S, septae; E, epithelium; LP, lamina propria; SM, submucosa; C, cartilage.

Confocal Laser Endomicroscopy

CLE is an imaging technique compatible with bronchoscopy, thoracoscopy and transthoracic needle-based interventions [11], which provides real-time images of the airways, alveoli, lung tumours, pleura and lymph nodes with a resolution

up to $3.5\ \mu\text{m}$, with a maximum depth of $70\ \mu\text{m}$ and a maximum field of view of $600\ \mu\text{m}$ (Fig. 1, 2). A fibre-optic probe is advanced through the working channel of a bronchoscope, thoracoscope or needle and directed to the area of interest where it illuminates tissue with laser light (most commonly used $488\ \text{nm}$). Reflected light is redirected back through a pinhole. Only light that is exactly in focus will pass through the pinhole, resulting in high-resolution images. Moving the laser beam vertically or horizontally enables reconstruction of 3D images by special software. In literature, CLE is also referred to as fibred confocal fluorescence microscopy, confocal microendoscopy or alveolscopy. In this paper, we use the term CLE for this imaging technique. When the CLE probe is combined with a needle (CLE probe advanced through a hollow needle), the term “needle-based CLE” (nCLE) is used. “Probe-based CLE” (pCLE) refers to the technique where the CLE probe is advanced to the tissue, thereby directly omitting the need of a needle (Fig. 4).

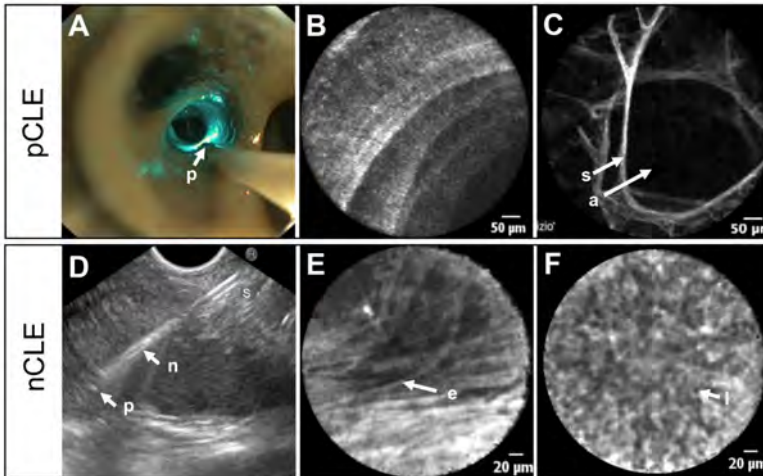


Fig. 4. pCLE imaging procedures in vivo with corresponding images of the normal alveolar and airway wall compartment (a–c); nCLE imaging in vivo with corresponding images of reactive lymph node capsula and cortex (d–f). **a** pCLE with the probe (p) positioned in the central airways of the right lower lobe on its way to be advanced to the alveolar compartment. $488\ \text{nm}$ laser light reflecting at the airway wall (blue). **b** pCLE image of the distal airway wall showing a helical ring-like pattern of the terminal bronchiole. **c** pCLE image of the alveolar compartment showing air-filled alveoli (a) and alveolar septae (s). **d** nCLE during an EUS procedure for staging of lung cancer, with the probe (p) extending $2\ \text{mm}$ distal to the tip of the needle (n). **e** nCLE image showing elastin fibres (e) of the capsula of a lymph node. **f** nCLE image showing lymphocytes (l) in a reactive lymph node Wijmans et al. [85]. pCLE, probe based confocal laser endomicroscopy; S, septae; A, alveolar space; nCLE, needle based confocal laser endomicroscopy.

Most evidence for the application of CLE in clinical practice is available in gastro-intestinal diseases, for instance, in the detection of neoplasia in the oesophagus [12, 13] and pancreatic cysts [14]. In non-malignant diseases like ulcerative colitis, CLE has been shown to be superior to any other imaging modality to assess mucosal healing [15].

First in vivo, in humans, reports on pCLE in the respiratory tract date back to 2007. Earliest studies showed feasibility of imaging of the airway wall and demonstrated that the images obtained by pCLE rely on the presence of elastin fibres, which is auto-fluorescent at 488 nm laser light [16, 17]. As elastin forms the backbone of structural components in the alveolar compartment including alveolar septae and microvessels [18-20] and the pleura, these can be visualized, real time and in vivo, using pCLE. Additionally, cellular components including inflammatory cells such as alveolar macrophages can be imaged based on auto-fluorescence as well [21].

Currently, in pulmonary diseases, one CLE system is commercially available (Cellvizio Endomicroscopy System, Mauna Kea Technologies, Paris, France). For pCLE, a miniprobe compatible with 1.9 mm working channel (AlveoflexTM) can be used to visualize all segments of the bronchial tree and lung parenchyma (**Fig. 2**). However, when reaching for the upper lobes (apical and posterior segments) a thinner, more flexible, probe (CholangioflexTM) might be advisable [22].

Imaging the bronchi and alveolar compartment with pCLE does not require additional staining. Studies have shown no advantage using fluorescein to visualize epithelial cells. Indeed, it has been reported that the visualization of alveoli is reduced using fluorescein because of a foam-like substance that appears [23, 24].

For imaging of lung masses and/or mediastinal lymph nodes, the needle-based CLE technique can be used. For this purpose, the thinnest confocal probe (AQ-flexTM) is advanced through a 19-Gauge needle. Unlike using pCLE in the respiratory tract, intravenous fluorescein-dinatrium should be administered. Fluorescein enables the visualization of individual cells by enhancing fluorescence of the stromal background. Single cells are not stained by fluorescein, which results in a negative-like image where the individual cells are seen as dark dots on a bright background (**Fig. 4f**). With nCLE, different anatomical structures in lymph nodes can be identified. The capsula with auto fluorescent elastin fibres can be distinguished from the cortex in which the lymphoid cells can be identified (**Fig. 4**), as well as the lymphoid follicles, which appear as large dark discs [25, 26].

Obstructive Lung Diseases

Optical Coherence Tomography

Obstructive lung diseases such as asthma and chronic obstructive pulmonary disease (COPD) are characterized by airway remodelling, which includes structural changes and thickening of the airway wall [27-29]. Next to inflammation, airway remodelling is a key pathophysiological characteristic in asthma, which is associated with disease severity. Therefore, it is of importance to develop accurate tools to assess airway wall remodelling [30]. By showing a high correlation with histology for both identification (Fig. 3c) and quantification of airway wall layers in both animal studies [31] and human airways [32-34], OCT is considered a promising technique to assess airway remodelling in obstructive lung diseases.

The value of OCT is further substantiated by several studies that have correlated OCT imaging of the airway wall to HRCT and pulmonary function parameters. Coxson et al. [35] have compared HRCT with OCT imaging in a cohort of 44 current and former smokers and showed a strong correlation for airway wall thickness. In addition, in this study, forced expiratory volume in 1 second (FEV1) was measured and correlated to airway wall thickness of fifth-generation airways measured by both HRCT and OCT, with OCT showing the strongest correlation. This correlation between FEV1 and airways was confirmed in another study in which several stages of COPD patients were included and a high correlation between OCT measured airway wall dimensions and FEV1-based staging was found [36]. In allergic asthma patients, FEV1/FVC correlated with OCT measured epithelial thickness and mucosal buckling, a potential method to assess bronchoconstriction [37]. Also with impulse oscillometry, a lung function test that uses sound waves to assess the respiratory resistance found that a correlation existed between the airway wall areas of small airways (seventh to ninth generation) assessed with OCT and respiratory resistance in heavy smokers and COPD patients [38]. Additionally, OCT can be used to assess elastic properties of the airway wall when combined with airway pressure increasing methods [39].

Next to assessing airway remodelling in patients with obstructive lung diseases, OCT might contribute in unravelling the mechanism of action of new treatment techniques and the evaluation of treatment response. In severe asthma, OCT was used in a pilot study of 2 severe asthma patients to assess the effect of bronchial thermoplasty (BT) on the airway wall up to 2 years after treatment [40]. Although the 2 included patients in this study showed similar clinical asthma symptoms and spirometry measurements, only 1 patient responded to BT. OCT was used to explore differences between these 2 patients and revealed a thickened, probably inflamed, epithelium in the non-responder patient, while the responder had a thickened airway wall without signs of inflammation. Also, after BT a difference was described: in the responder the total airway

wall thickness declined, while in the non-responder, the thickness remained the same. These results suggested that OCT might have a potential role in identifying characteristics at baseline for optimal patient selection for BT.

In severe asthma, OCT has also been used to assess the acute effects of BT on the airway wall and identified acute patterns within the airway wall including epithelial sloughing and oedema (Fig. 5). Interestingly, acute BT effects extended to the distal smaller non-BT-treated airways and this suggested that BT treatment might also impact the smaller airways in severe asthmatic patients [41].

Although different airway wall layers are detectable with OCT, measuring the layers manually is time consuming and it remains difficult to identify the different structures and components within these layers such as extracellular matrix (ECM) proteins (e.g., collagen) or airway smooth muscle (ASM). By adding a birefringent platform to the OCT system, Adams et al. [42] automatically identified and quantified ASM fibres in 3 asthma patients and 3 healthy controls showing a significant difference in the thickness of ASM fibres between these 2 groups.

Confocal Laser Endomicroscopy

Visualization of the airway wall using pCLE relies on elastin fibres in subepithelial ECM. In the bronchi, 5 different patterns can be identified, depending on the depth of the probe in the bronchial tree [16]. Ranging from dense unidirectional elastin fibres, with an occasional bronchial gland opening in proximal main bronchi, to cross-sectional fibres and loose, web-like fibres in distal, smaller airways, the distal terminal bronchiole shows a typical ring like helical pattern (Fig. 4).

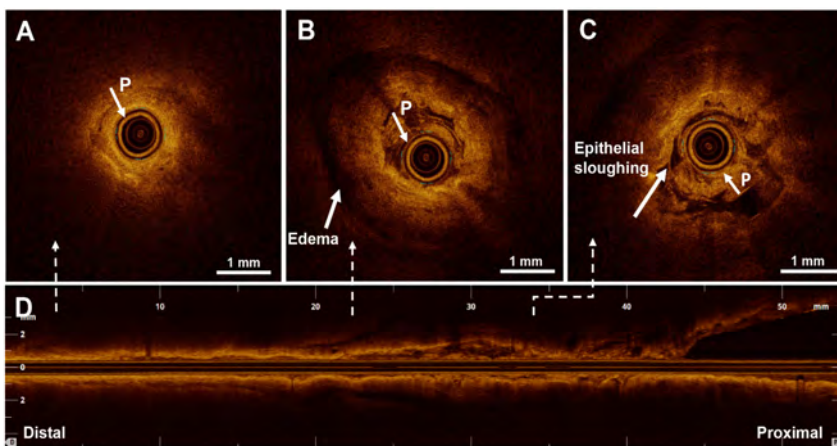


Fig. 5. OCT images of the anterior segment (LB3) of the left upper lobe directly after bronchial thermoplasty (BT) treatment. **a** Normal, non-directly-BT-treated

distal airway area. **b** BT-treated airway area with peribronchial edema. **c** BT-treated airway area showing epithelial sloughing. **d** Corresponding reconstructed pullback of the airway (540 2D images, total length of 5.4 cm; Goorsenberg et al. [41]). P, probe.

In patients with asthma, elastin fibres have been described to be decreased or fragmented [43]. However, in a study that focused on pCLE imaging in asthma patients and healthy controls, it was described that a dense lamellar pattern was associated with lower FEV1 [17]. In COPD, to our knowledge, only a single study imaged the airway walls with CLE. Of the different subepithelial elastin patterns, COPD patients were described to have more loose arrangements of elastin fibres, instead of a lamellar or mixed pattern of fibres, as compared to non-COPD smokers and healthy volunteers. Possibly indicating destruction of elastin fibres in the ECM of the airway wall of COPD patients, which is in line with a previous histological study by Black et al. [44].

In the alveolar compartment, animal studies have shown a correlation between pulmonary emphysema and enlarged airspaces with thinner capillaries and a loss of capillary density [45, 46]. This correlation was reproduced using pCLE in COPD patients *in vivo*, thus without the need for biopsy. Furthermore, COPD patients were shown to have decreased auto fluorescence intensity of alveolar septae when compared to healthy volunteers, potentially indicating destruction of these, elastin containing, alveolar septae [24, 47, 48]. Although pCLE shows specific findings in patients with COPD, the additional value of pCLE over standard chest CT and pulmonary function tests is yet to be established.

Malignancies

Optical Coherence Tomography

The detection of lung cancer tissue for diagnosis and staging purposes, but also for margin assessment in lung cancer surgery, is highly important in the management of pulmonary oncology. Several groups have investigated the use of OCT in other oncology specialties, mainly in dermatology, urology and gastroenterology [49].

The involvement of pulmonary malignancies in different anatomical compartments can be imaged with OCT including central airway endobronchial malignancies, lung parenchymal pulmonary masses or nodules and metastases in lymph nodes.

For the identification of endobronchial tumours, promising results have been published both *in vivo* [50-52] and *ex vivo* [52-55]. In these endobronchial tumours, one study identified different characteristics for 3 subtypes of cancer: squamous cell carcinomas, adenocarcinomas and poorly differentiated

carcinomas [55]. Three reviewers were trained to identify these criteria in a cohort of 82 ex vivo tumour samples that showed an average accuracy of 82.6% (range 73.7–94.7%). To the best of our knowledge, there are no studies published investigating the value of OCT in assessing the margin of the tumour-resected tissue.

In pulmonary masses, nodules and lymph node metastases, a potential use of OCT is needle-based OCT imaging in the setting of trans-bronchial needle aspiration. One research group conducted a study in pulmonary nodules showing high sensitivity and specificity (both >95%) for ex vivo differentiation between pulmonary nodules and healthy parenchymal tissue [56]. The same research group investigated the use of OCT for the identification of pulmonary lymph node metastases. Needle-based OCT was performed in 26 ex vivo lymph nodes, both healthy and metastatic disease [57]. The characteristics of metastatic disease were distinct from those of the lymph nodes without cancer and even had features connected with the subtype of the tumour. Both applications of needle-based OCT in pulmonary nodules and lymph nodes have not been validated in vivo yet.

Confocal Laser Endomicroscopy

Several studies have shown that pCLE has the ability to identify the abnormal area in endobronchial [16, 58-61] and parenchymal-located malignancies (both primary lung cancer and metastatic) [58, 62, 63]. Using pCLE to image endobronchial lesions, Filner et al. [61] showed the ability to differentiate between normal versus neoplastic lesions and normal versus non-neoplastic lesions. In a study performed in 112 patients with a peripheral pulmonary nodule, pCLE was able to detect the abnormal area in 92% [64]. Additionally, Sorokina et al. [63] showed the presence of a specific pattern of alveolar dystelectasis, oedema and influx of macrophages to be present in malignant nodules in 18 lobectomy specimens. Additionally, pCLE histopathology confirmed distinctive features of adenocarcinoma, squamous cell carcinoma and small cell carcinoma. However, in a study performed by Seth et al. [64], 91 patients with peripheral lung nodule were imaged with pCLE, and although in 92% the abnormal area was identified, pCLE was not able to discriminate benign from malignant lesions. It is thought that this is due to the difficulty of staining epithelial cells of the bronchial mucosa [16, 59, 63, 64]. Unlike the mucosa of the gastrointestinal tract, fluorescein does not penetrate into the epithelial layer of the bronchi [23, 24]. Topical administrated acriflavine has shown high sensitivity and specificity to visualize malignant cells in endobronchial located tumours; however, its use is under discussion because of its potential carcinogenic properties [60].

An approach where the nodule is punctured by a needle combined with the CLE probe might resolve the problem of bronchial epithelial staining. In 2016, Wijmans et al. [65] presented a case of non-small cell lung cancer in which the

primary tumour was imaged with nCLE in combination with intravenous fluorescein. Where all the previous mentioned studies for peripheral pulmonary nodules have used pCLE, Wijmans et al. [65] demonstrated in this study a case in which the primary tumour was visualized with nCLE combined with endosonography. Dark, large aggregates of cells imaged with nCLE were compatible with the malignant cells of adenocarcinoma. Thereafter, a study was performed using nCLE in both centrally located primary pulmonary tumours ($n = 6$) and metastasis suspected lymph nodes ($n = 21$). Three characteristics were developed to predict malignancy: enlarged pleomorphic cells, dark clumps and directional streaming. These criteria were prospectively validated to determine malignancy of the tumours or lymph nodes with high diagnostic accuracy of 90% [26] (Fig. 6).

In pleural lesions, both pCLE and nCLE have been used to detect malignant cells. Bonhomme et al. [66] reported 3 cases with pleura imaging using pCLE. Three different images of the pleura were presented: normal pleura, pleural metastasized non-small cell lung cancer and a case of mesothelioma. pCLE of the pleura showed clear capability to differentiate normal pleura from malignant pleura in these cases. Shortly thereafter, a larger study was undertaken using both pCLE and nCLE to distinguish malignant mesothelioma from areas of pleural fibrosis. Characteristics of different pleural lesions were identified and prospectively validated in 105 pleural biopsies from 15 patients with moderate inter-observer agreement [11]. When it comes to malignant pleural effusion, one ex vivo study found high sensitivity and specificity for pleural malignancy using pCLE in pleural effusion [67].

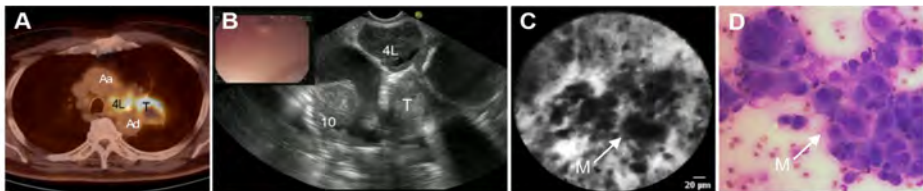


Fig. 6. Endosonography guided nCLE of a mediastinal lymph node metastasis of a tumour in the left upper lobe. a PET-CT scan showing fludeoxyglucose-avid lymph node station 4 L, and the primary lung tumour (T). **b** EUS image showing an enlarged lymph nodes at station 4 L. **c** Real-time nCLE image of lymph node station 4 L showing large pleomorphic cells and dark clumps recognized as malignant cells (M). **d** Fine needle aspirate showing malignant cells of squamous cell carcinoma (Wijmans et al. [26]). 10, lymph node station 10 L (left); Aa, ascending aorta; Ad, descending aorta.

ILDs and Other Parenchymal Lung Diseases

Optical Coherence Tomography

OCT has predominantly been used to assess abnormalities in the airway due to both obstructive airway diseases and (endobronchial) malignancies. However, recently, the use of OCT for the assessment of the alveolar compartment has been investigated [68-70]. Especially in ILDs the added value of high-resolution, near-microscopic imaging next to HRCT can be envisioned. In 2013, Hariri et al. [54] compared the histology of human lung specimens with optical frequency domain imaging in 4 patients ex vivo. Characteristics of fibrosis were identified in these OCT images. More recently, the first in vivo in human results of OCT in diagnosis of idiopathic pulmonary fibrosis has been published [71-73]. These results showed that OCT was able to identify microscopic honeycombing with alveolar OCT, while radiological honeycombing was not visible on HRCT [71]. Furthermore, characteristics for fibrotic ILDs such as thickening of alveolar septae and loss of alveolar structure, microscopic honeycombing, cysts and bronchi(ol)ectasis were identified with OCT [71-73].

Confocal Laser Endomicroscopy

Since ILD is a disease located in the alveolar compartment, CLE has been used to visualize ILD in vivo. Normal alveolar compartment images show thin alveolar septae in a round, helical or looped shape depending on the angle of penetration of the alveolar unit (**Fig. 2, 4**). Microvessels can be visualized and are typically thicker than the alveolar septae, and may have branches. In smoking individuals, highly fluorescent macrophages are visible throughout the alveoli, which has a positive correlation with the number of cigarettes used [21]. Also, the fluorescent intensity of alveolar structures varies: older individuals tend to have stronger fluorescent signals of alveolar elastin fibres [21, 24].

The first report of CLE in ILD was a case of pulmonary alveolar proteinosis, in which highly fluorescent globular structures were identified in vivo, compatible with globular lipoproteinaceous material in broncho-alveolar lavage. Similar findings were described in a case series of 6 patients with pulmonary alveolar proteinosis [74]. Later, case reports of amiodarone induced ILD, pulmonary alveolar microlithiasis, invasive aspergillosis, pneumocystis jiroveci pneumonia, lymphangioliomyomatosis and metastatic pulmonary calcification were published [75-80].

In addition to the above, CLE has also been studied for the surveillance of acute cellular rejection (ACR) in lung transplant recipients. Two studies have focused on the use of pCLE in these patients and found that specific characteristics are associated with ACR. Yserbyt et al. [81] showed in 2014 the correlation between ACR and an increase in auto fluorescent alveolar cells. This finding was confirmed by Keller et al. [82] in 2019, with the addition of the perivascular distribution of the cells. Perivascular cellularity was significantly correlated with ACR.

Several studies have been performed to identify specific characteristics of pCLE images in ILD. Meng et al. [83] identified 6 different patterns to discriminate chronic fibrosing ILD from other ILDs. Salaün et al. [84] identified 9 specific CLE characteristics using data from 80 individuals (59 ILD patients, 21 healthy individuals). Based on these characteristics they were able to discriminate normal from diseased lung, and found that certain ILDs were associated with a cellular CLE pattern (presence of fluorescent bronchial and alveolar cells), while others were associated with a fibrotic CLE pattern (small alveolar mouths, disorganized dense elastin fibre network with thickened septae). They showed good reproducibility of inter-observer interpretation. In another observational study in 14 ILD patients pCLE was able to detect normal and abnormal parenchymal areas, and to discriminate mild from severe fibrosis (Fig. 7). Additionally the pleura and the adjacent subpleural alveolar space could be identified [85].

Based on the studies reviewed above, it seems plausible that pCLE can differentiate cellular ILDs from fibrotic ILDs; however, whether CLE can differentiate between specific subsets of ILDs remains to be established. The potential of CLE to identify these different compartments, along with an added value to characterize ILD, paves the way to use CLE as a guidance tool for endoscopic (cryo-)lung biopsies.

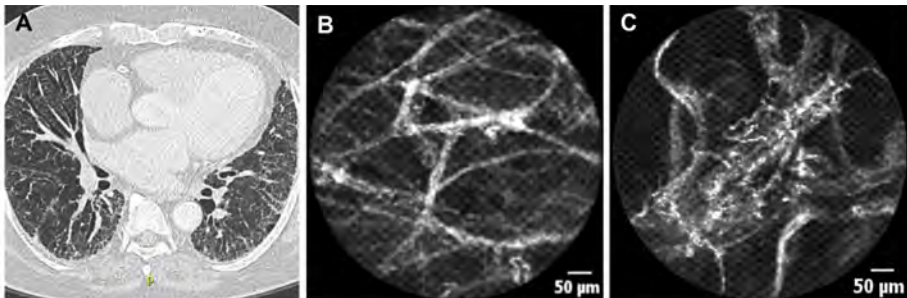


Fig. 7. pCLE images of the alveolar compartment in a patient with a fibrotic non specific interstitial pneumonia (NSIP). **a** HRCT image showing diffuse reticulation and bronchi(ol)ectasis. **b** pCLE image showing an increased density of alveolar elastin fibre intact network. **c** pCLE image showing an increased density of thickened alveolar elastin fibre network with loss of normal architecture Wijmans et al. [85]. P, posterior.

Pulmonary Vascular Diseases

Optical Coherence Tomography

The use of OCT in pulmonary vascular diseases has been described thoroughly in previously published reviews by our group and others [1, 86]. In short, OCT has been investigated in characterizing pulmonary artery wall remodelling

in pulmonary arterial hypertension [87-89]. Pulmonary artery wall thickness has been reported to correlate to hemodynamic parameters [90, 91]. In chronic thromboembolic pulmonary hypertension, OCT was able to assess thrombotic occlusion and luminal webs and/or bands [87, 89] (Fig. 3f) and has been reported to guide balloon sizing and to evaluate the effect of balloon pulmonary angioplasty treatment [92, 93]. Additionally, one study investigated the use of OCT in diagnosing peripheral pulmonary artery thrombus as compared to selective pulmonary angiography in 12 patients [94]. In this study, OCT found significantly more thrombi in the distal segments of peripheral pulmonary arteries than selective pulmonary angiography. Moreover, OCT was able to differentiate between acute “red” and chronic “white” thrombi.

Confocal Laser Endomicroscopy

To the best of our knowledge, no studies have been published regarding the use of CLE in pulmonary vascular diseases.

Future Perspectives

In summary, in pulmonary medicine, OCT and CLE are promising high-resolution, real-time, in vivo imaging techniques to visualize important disease associated anatomical compartments of the respiratory tract. However, unlike in ophthalmology and cardiology, OCT and CLE have not found their implementation into standard clinical care yet.

In our opinion, the use of both CLE and OCT techniques has high potential to add to guidance and/or improvement in diagnostic yield driven by its near-microscopic resolution and real-time properties. For instance, the development of a CLE or OCT integrated cytological needle (so called smart needle) to guide the biopsy site and provide real-time feedback for the detection of lung cancer and pleura mesothelioma [11].

In addition, since advanced OCT and CLE have shown the potential of in situ cytological analysis in malignancy-suspected lymph nodes, it seems reasonable that these techniques also have the capability of detecting granulomas in, for instance, sarcoidosis. The scope of novel imaging techniques in endoscopy may be broadened in the near future by implementing the use of fluorescently labelled tracers. In this field of imaging, optical techniques are combined with laser to detect fluorescently labelled components. In oncology, fluorescently labelled antibody detection can further boost tumour identification for cancer diagnosis, staging and assessment of tumour margins. For instance, fluorescently labelled anti-CD47 was used to detect bladder cancer [95]. Both fluorescently labelled labetuzumab and erlotinib have been used to assess colorectal cancer and EGFR-mutated lung tumours, respectively, in xenografted mouse models [96, 97]. Furthermore, to evaluate the effect of novel treatments,

pCLE might be of value as was demonstrated by a study in which apoptotic cells were visualized after the administration of erlotinib in EGFR-mutated tumours in animal models [98]. In severe asthma patients, it can be envisioned that molecular labelling of monoclonal antibodies used for immunotherapy can help to visualize cellular targets and biodistribution of these antibodies with the ultimate goal to improve patient selection for these expensive therapies.

In the field of infectious diseases, efforts are made to directly visualize the presence of pathogens. So far, both in- and ex vivo studies have been published to visualize aspergillus [99-101] and staphylococcus aureus [102] in animal models using CLE.

Currently, analyzing OCT and CLE images is elaborative and this makes it a time-consuming process. The development of automated software is essential for the implementation of these techniques. Automated segmentation based on intensity analyses or deep learning techniques might prove very helpful in image analyses and will be a necessity for broader clinical application. Improvements are being made, such as automated quantification [42] and automated mucus segmentation [37, 103]. Also, research is focused on improving the techniques, for instance, by using polarization sensitive OCT, which shows not only the structural layers of the airway wall but also the arrangement of the tissue [104].

This makes it possible to distinguish several structures in the airways such as structural airway components (e.g., ECM/ASM). Additionally, the resolution of OCT imaging might be improved by using a nano-optic endoscope: a conventional OCT system with a metalens integrated in the design [105]. Potentially these techniques can be used to assess treatment effects on airway wall structures involved in airway wall remodelling, without the need for taking a biopsy. Other factors limiting the implementation of these techniques in clinical practice are the lack of larger validation trials, costs and availability of OCT and CLE systems. Currently, pulmonary OCT and CLE have been used only in research trials in expert centres with expertise in interventional bronchoscopy with relatively small amounts of patients included.

Conclusion

Both OCT and CLE are complementary, high-resolution imaging techniques that have shown to be feasible and safe to use in a variety of pulmonary diseases. Both techniques have considerable potential to improve diagnostics and monitoring of pulmonary diseases and their treatments; however, larger in vivo validation studies and automated software are needed before these techniques can be implemented in clinical practice.

Acknowledgements

We would like to thank H.J. Bogaard, MD, PhD, N. van Rooijen, MD, PhD, and M. Beijk, MD, PhD for providing OCT images of the pulmonary vasculature and L. Wijmans for providing CLE images.

References

1. Wijmans L, d'Hooghe JN, Bonta PI, Annema JT. Optical coherence tomography and confocal laser endomicroscopy in pulmonary diseases. *Curr Opin Pulm Med*. 2017 May;23(3): 275–83.
2. Huang D, Swanson EA, Lin CP, Schuman JS, Stinson WG, Chang W, et al. Optical coherence tomography. *Science*. 1991 Nov; 254(5035):1178–81.
3. Tearney GJ, Brezinski ME, Bouma BE, Boppart SA, Pitris C, Southern JF, et al. In vivo endoscopic optical biopsy with optical coherence tomography. *Science*. 1997 Jun; 276(5321):2037–9.
4. Fercher AF, Hitzinger CK, Drexler W, Kamp G, Sattmann H. In vivo optical coherence tomography. *Am J Ophthalmol*. 1993 Jul;116(1):113–4.
5. Swanson EA, Izatt JA, Hee MR, Huang D, Lin CP, Schuman JS, et al. In vivo retinal imaging by optical coherence tomography. *Opt Lett*. 1993 Nov;18(21):1864–6.
6. Koustenis AJr, Harris A, Gross J, Januleviciene I, Shah A, Siesky B. Optical coherence tomography angiography: an overview of the technology and an assessment of applications for clinical research. *Br J Ophthalmol*. 2017 Jan;101(1):16–20.
7. IJsselmuiden AJ, Zwaan EM, Oemrawsingh RM, Bom MJ, Dankers FJ, de Boer MJ, et al. Appropriate use criteria for optical coherence tomography guidance in percutaneous coronary interventions : recommendations of the working group of interventional cardiology of the Netherlands Society of Cardiology. *Neth Heart J*. 2018 Oct;26(10):473–83.
8. Sotomi Y, Tateishi H, Suwannasom P, Dijkstra J, Eggermont J, Liu S, et al. Quantitative assessment of the stent/scaffold strut embedment analysis by optical coherence tomography. *Int J Cardiovasc Imaging*. 2016 Jun; 32(6):871–83.
9. Bezerra HG, Costa MA, Guagliumi G, Rollins AM, Simon DI. Intracoronary optical coherence tomography: a comprehensive review clinical and research applications. *JACC Cardiovasc Interv*. 2009 Nov;2(11):1035–46.
10. Brezinski ME, Tearney GJ, Boppart SA, Swanson EA, Southern JF, Fujimoto JG. Optical biopsy with optical coherence tomography: feasibility for surgical diagnostics. *J Surg Res*. 1997 Jul;71(1):32–40.
11. Wijmans L, Baas P, Sieburgh TE, de Bruin DM, Ghuijs PM, van de Vijver MJ, et al. Confocal Laser Endomicroscopy as a Guidance Tool for Pleural Biopsies in Malignant Pleural Mesothelioma. *Chest*. 2019, Epub ahead of print.
12. Sharma P, Meining AR, Coron E, Lightdale CJ, Wolfsen HC, Bansal A, et al. Real-time increased detection of neoplastic tissue in Barrett's esophagus with probe-based confocal laser endomicroscopy: final results of an international multicenter, prospective, randomized, controlled trial. *Gastrointest Endosc*. 2011 Sep;74(3):465–72.
13. Shah T, Lippman R, Kohli D, Mutha P, Solomon S, Zfass A. Accuracy of probe-based confocal laser endomicroscopy (pCLE) compared to random biopsies during endoscopic surveillance of Barrett's esophagus. *Endosc Int Open*. 2018 Apr;6(4):E414–20.
14. Napoleon B, Palazzo M, Lemaistre AI, Caillol F, Palazzo L, Aubert A, et al. Needlebased confocal laser endomicroscopy of pancreatic cystic lesions: a

- prospective multicenter validation study in patients with definite diagnosis. *Endoscopy*. 2019 Sep; 51(9):825–35.
15. Macé V, Ahluwalia A, Coron E, Le Rhun M, Boureille A, Bossard C, et al. Confocal laser endomicroscopy: a new gold standard for the assessment of mucosal healing in ulcerative colitis. *J Gastroenterol Hepatol*. 2015 Mar;30 Suppl 1:85–92.
 16. Thiberville L, Moreno-Swirc S, Vercauteren T, Peltier E, Cavé C, Bourg Heckly G. In vivo imaging of the bronchial wall microstructure using fibered confocal fluorescence microscopy. *Am J Respir Crit Care Med*. 2007 Jan; 175(1):22–31.
 17. Yick CY, von der Thüsen JH, Bel EH, Sterk PJ, Kunst PW. In vivo imaging of the airway wall in asthma: fibered confocal fluorescence microscopy in relation to histology and lung function. *Respir Res*. 2011 Jun; 12(1):85.
 18. Mercer RR, Crapo JD. Spatial distribution of collagen and elastin fibers in the lungs. *J Appl Physiol* (1985). 1990 Aug;69(2):756–65.
 19. Gonçalves CA, Figueiredo MH, Bairos VA. Three-dimensional organization of the elastic fibres in the rat lung. *Anat Rec*. 1995 Sep; 243(1):63–70.
 20. Toshima M, Ohtani Y, Ohtani O. Three-dimensional architecture of elastin and collagen fiber networks in the human and rat lung. *Arch Histol Cytol*. 2004 Mar;67(1):31–40.
 21. Thiberville L, Salaün M, Lachkar S, Dominique S, Moreno-Swirc S, Vever-Bizet C, et al. Human in vivo fluorescence microimaging of the alveolar ducts and sacs during bronchoscopy. *Eur Respir J*. 2009 May;33(5): 974–85.
 22. Hassan T, Thiberville L, Hermant C, Lachkar S, Piton N, Guisier F, et al. Assessing the feasibility of confocal laser endomicroscopy in solitary pulmonary nodules for different part of the lungs, using either 0.6 or 1.4 mm probes. *PLoS One*. 2017 Dec;12(12):e0189846.
 23. Fuchs FS, Zirlik S, Hildner K, Frieser M, Ganslmayer M, Schwarz S et al. Fluorescein-aided confocal laser endomicroscopy of the lung. *Respiration*. 2011;81(1):32–8.
 24. Newton RC, Kemp SV, Yang GZ, Elson DS, Darzi A, Shah PL. Imaging parenchymal lung diseases with confocal endomicroscopy. *Respir Med*. 2012 Jan;106(1):127–37.
 25. Benias PC, D’Souza LS, Papafragkakis H, Kim J, Harshan M, Theise ND, et al. Needle-based confocal endomicroscopy for evaluation of malignant lymph nodes - a feasibility study. *Endoscopy*. 2016 Oct;48(10):923–8.
 26. Wijmans L, Yared J, de Bruin DM, Meijer SL, Baas P, Bonta PI, et al. Needle-based confocal laser endomicroscopy for real-time diagnosing and staging of lung cancer. *Eur Respir J*. 2019 Jun;53(6):1–9.
 27. Jeffery PK. Remodeling in asthma and chronic obstructive lung disease. *Am J Respir Crit Care Med*. 2001 Nov; 164(10 Pt 2 supplement_2):S28–38.
 28. James AL, Wenzel S. Clinical relevance of airway remodelling in airway diseases. *Eur Respir J*. 2007 Jul;30(1):134–55.
 29. Patel BD, Coxson HO, Pillai SG, Agustí AG, Calverley PM, Donner CF, et al.; International COPD Genetics Network. Airway wall thickening and emphysema show independent familial aggregation in chronic obstructive pulmonary disease. *Am J Respir Crit Care Med*. 2008 Sep;178(5):500–5.
 30. Benayoun L, Druilhe A, Dombret MC, Aubier M, Pretolani M. Airway structural

- alterations selectively associated with severe asthma. *Am J Respir Crit Care Med.* 2003 May;167(10): 1360–8.
31. Lee AM, Kirby M, Ohtani K, Candido T, Shalansky R, MacAulay C, et al. Validation of airway wall measurements by optical coherence tomography in porcine airways. *PLoS One.* 2014 Jun;9(6):e100145.
 32. Chen Y, Ding M, Guan WJ, Wang W, Luo WZ, Zhong CH, et al. Validation of human small airway measurements using endobronchial optical coherence tomography. *Respir Med.* 2015 Nov;109(11):1446–53.
 33. d’Hooghe JN, Goorsenberg AW, de Bruin DM, Roelofs JJ, Annema JT, Bonta PI. Optical coherence tomography for identification and quantification of human airway wall layers. *PLoS One.* 2017 Oct;12(10):e0184145.
 34. Kirby M, Ohtani K, Nickens T, Lisbona RM, Lee AM, Shaipanich T, et al. Reproducibility of optical coherence tomography airway imaging. *Biomed Opt Express.* 2015 Oct;6(11): 4365–77.
 35. Coxson HO, Quiney B, Sin DD, Xing L, McWilliams AM, Mayo JR, et al. Airway wall thickness assessed using computed tomography and optical coherence tomography. *Am J Respir Crit Care Med.* 2008 Jun;177(11):1201–6.
 36. Ding M, Chen Y, Guan WJ, Zhong CH, Jiang M, Luo WZ, et al. Measuring Airway Remodeling in Patients With Different COPD Staging Using Endobronchial Optical Coherence Tomography. *Chest.* 2016 Dec;150(6): 1281–90.
 37. Adams DC, Miller AJ, Applegate MB, Cho JL, Hamilos DL, Chee A, et al. Quantitative assessment of airway remodelling and response to allergen in asthma. *Respirology.* 2019, Epub ahead of print.
 38. Su ZQ, Guan WJ, Li SY, Ding M, Chen Y, Jiang M, et al. Significances of spirometry and impulse oscillometry for detecting small airway disorders assessed with endobronchial optical coherence tomography in COPD. *Int J Chron Obstruct Pulmon Dis.* 2018 Oct;13: 3031–44.
 39. Williamson JP, McLaughlin RA, Noffsinger WJ, James AL, Baker VA, Curatolo A, et al. Elastic properties of the central airways in obstructive lung diseases measured using anatomical optical coherence tomography. *Am J Respir Crit Care Med.* 2011 Mar;183(5):612–9.
 40. Kirby M, Ohtani K, Lopez Lisbona RM, Lee AM, Zhang W, Lane P, et al. Bronchial thermoplasty in asthma: 2-year follow-up using optical coherence tomography. *Eur Respir J.* 2015 Sep;46(3):859–62.
 41. Goorsenberg AWM, d’Hooghe JNS, de Bruin DM, van den Berk IAH, Annema JT, Bonta PI. Bronchial Thermoplasty-Induced Acute Airway Effects Assessed with Optical Coherence Tomography in Severe Asthma. *Respiration.* 2018;96(6):564–70.
 42. Adams DC, Hariri LP, Miller AJ, Wang Y, Cho JL, Villiger M, et al. Birefringence microscopy platform for assessing airway smooth muscle structure and function in vivo. *Sci Transl Med.* 2016 Oct;8(359): 359ra131.
 43. Bousquet J, Lacoste JY, Chanez P, Vic P, Godard P, Michel FB. Bronchial elastic fibers in normal subjects and asthmatic patients. *Am J Respir Crit Care Med.* 1996 May;153(5): 1648–54.
 44. Black PN, Ching PS, Beaumont B, Ranasinghe S, Taylor G, Merrilees MJ. Changes in elastic fibres in the small airways and alveoli in COPD. *Eur Respir J.* 2008

- May;31(5):998–1004.
45. Yamato H, Sun JP, Churg A, Wright JL. Cigarette smoke-induced emphysema in guinea pigs is associated with diffusely decreased capillary density and capillary narrowing. *Lab Invest*. 1996 Aug;75(2):211–9.
 46. Schraufnagel DE, Schmid A. Capillary structure in elastase-induced emphysema. *Am J Pathol*. 1988 Jan;130(1):126–35.
 47. Cosío BG, Shafiek H, Fiorentino F, Gómez C, López M, Rios A, et al. Structure-function relationship in COPD revisited: an in vivo microscopy view. *Thorax*. 2014 Aug;69(8):724–30.
 48. Yserbyt J, Doms C, Janssens W, Verleden GM. Endoscopic advanced imaging of the respiratory tract: exploring probe-based confocal laser endomicroscopy in emphysema. *Thorax*. 2018 Feb;73(2):188–90.
 49. van Manen L, Dijkstra J, Boccaro C, Benoit E, Vahrmeijer AL, Gora MJ, et al. The clinical usefulness of optical coherence tomography during cancer interventions. *J Cancer Res Clin Oncol*. 2018 Oct;144(10):1967–90.
 50. Lam S, Standish B, Baldwin C, McWilliams A, leRiche J, Gazdar A et al. In vivo optical coherence tomography imaging of preinvasive bronchial lesions. *Clin Cancer Res*. 2008 Apr; 14(7):2006–11.
 51. Michel RG, Kinasewitz GT, Fung KM, Keddissi JI. Optical coherence tomography as an adjunct to flexible bronchoscopy in the diagnosis of lung cancer: a pilot study. *Chest*. 2010 Oct;138(4):984–8.
 52. Tsuboi M, Hayashi A, Ikeda N, Honda H, Kato Y, Ichinose S, et al. Optical coherence tomography in the diagnosis of bronchial lesions. *Lung Cancer*. 2005 Sep;49(3):387–94.
 53. Jain M, Narula N, Salamoan B, Shevchuk MM, Aggarwal A, Altorki N, et al. Full-field optical coherence tomography for the analysis of fresh unstained human lobectomy specimens. *J Pathol Inform*. 2013 Sep;4(1): 26.
 54. Hariri LP, Applegate MB, Mino-Kenudson M, Mark EJ, Medoff BD, Luster AD, et al. Volumetric optical frequency domain imaging of pulmonary pathology with precise correlation to histopathology. *Chest*. 2013 Jan; 143(1):64–74.
 55. Hariri LP, Mino-Kenudson M, Lanuti M, Miller AJ, Mark EJ, Suter MJ. Diagnosing lung carcinomas with optical coherence tomography. *Ann Am Thorac Soc*. 2015 Feb;12(2): 193–201.
 56. Hariri LP, Mino-Kenudson M, Applegate MB, Mark EJ, Tearney GJ, Lanuti M, et al. Toward the guidance of transbronchial biopsy: identifying pulmonary nodules with optical coherence tomography. *Chest*. 2013 Oct; 144(4):1261–8.
 57. Shostak E, Hariri LP, Cheng GZ, Adams DC, Suter MJ. Needle-based Optical Coherence Tomography to Guide Transbronchial Lymph Node Biopsy. *J Bronchology Interv Pulmonol*. 2018 Jul;25(3):189–97.
 58. Wellikoff AS, Holladay RC, Downie GH, Chaudoir CS, Brandi L, Turbat-Herrera EA. Comparison of in vivo probe-based confocal laser endomicroscopy with histopathology in lung cancer: A move toward optical biopsy. *Respirology*. 2015 Aug;20(6):967–74.
 59. Shah PL, Kemp SV, Newton RC, Elson DS, Nicholson AG, Yang GZ. Clinical Correlation between Real-Time Endocytoscopy, Confocal Endomicroscopy, and

- Histopathology in the Central Airways. *Respiration*. 2017;93(1):51–7.
60. Fuchs FS, Zirlik S, Hildner K, Schubert J, Vieth M, Neurath MF. Confocal laser endomicroscopy for diagnosing lung cancer in vivo. *Eur Respir J*. 2013 Jun;41(6):1401–8.
 61. Filner JJ, Bonura EJ, Lau ST, Abounasr KK, Naidich D, Morice RC, et al. Bronchoscopic fibered confocal fluorescence microscopy image characteristics and pathologic correlations. *J Bronchology Interv Pulmonol*. 2011 Jan;18(1):23–30.
 62. Hassan T, Piton N, Lachkar S, Salaün M, Thiberville L. A Novel Method for In Vivo Imaging of Solitary Lung Nodules Using Navigational Bronchoscopy and Confocal Laser Microendoscopy. *Lung*. 2015 Oct; 193(5):773–8.
 63. Sorokina A, Danilevskaya O, Averyanov A, Zabozaev F, Sazonov D, Yarmus L, et al. Comparative study of ex vivo probe-based confocal laser endomicroscopy and light microscopy in lung cancer diagnostics. *Respirology*. 2014 Aug;19(6):907–13.
 64. Seth S, Akram AR, McCool P, Westerfeld J, Wilson D, McLaughlin S, et al. Assessing the utility of autofluorescence-based pulmonary optical endomicroscopy to predict the malignant potential of solitary pulmonary nodules in humans. *Sci Rep*. 2016 Aug;6(1): 31372.
 65. Wijmans L, de Bruin DM, Meijer SL, Annema JT. Real-Time Optical Biopsy of Lung Cancer. *Am J Respir Crit Care Med*. 2016 Oct; 194(8):e10–1.
 66. Bonhomme O, Duysinx B, Heinen V, Detrembleur N, Corhay JL, Louis R. First report of probe based confocal laser endomicroscopy during medical thoracoscopy. *Respir Med*. 2019 Feb;147:72–5.
 67. Zirlik S, Hildner K, Rieker RJ, Vieth M, Neurath MF, Fuchs FS. Confocal Laser Endomicroscopy for Diagnosing Malignant Pleural Effusions. *Med Sci Monit*. 2018 Aug;24:5437–47.
 68. Quirk BC, McLaughlin RA, Curatolo A, Kirk RW, Noble PB, Sampson DD. In situ imaging of lung alveoli with an optical coherence tomography needle probe. *J Biomed Opt*. 2011 Mar;16(3):036009.
 69. McLaughlin RA, Yang X, Quirk BC, Lorensen D, Kirk RW, Noble PB, et al. Static and dynamic imaging of alveoli using optical coherence tomography needle probes. *J Appl Physiol* (1985). 2012 Sep;113(6):967–74.
 70. Meissner S, Knels L, Krueger A, Koch T, Koch E. Simultaneous three-dimensional optical coherence tomography and intravital microscopy for imaging subpleural pulmonary alveoli in isolated rabbit lungs. *J Biomed Opt*. 2009 Sep-Oct;14(5):054020.
 71. Hariri LP, Adams DC, Wain JC, Lanuti M, Muniappan A, Sharma A, et al. Endobronchial Optical Coherence Tomography for LowRisk Microscopic Assessment and Diagnosis of Idiopathic Pulmonary Fibrosis In Vivo. *Am J Respir Crit Care Med*. 2018 Apr;197(7): 949–52.
 72. Wijmans L, de Bruin DM, Bonta PI, Jonkers RE, Poletti V, Annema JT. OCT, a Valuable Novel Tool for Assessing the Alveolar Compartment in ILD? *Am J Respir Crit Care Med*. 2017;197(9):1231–2.
 73. Wijmans L dBD, Jonkers R, Roelofs J, van den Berk I, Bonta P, Annema J. Visualizing the alveolar compartment in ILD patients by optical coherence tomography [abstract]. Presented at the European Respiratory Society Congress. September 10, 2017, Milan, Italy. Abstract 5061.

74. Danilevskaya O, Averyanov A, Lesnyak V, Chernyaev A, Sorokina A. Confocal laser endomicroscopy for diagnosis and monitoring of pulmonary alveolar proteinosis. *J Bronchology Interv Pulmonol*. 2015 Jan;22(1):33–40.
75. Salaün M, Roussel F, Bourg-Heckly G, VeverBizet C, Dominique S, Genevois A, et al. In vivo probe-based confocal laser endomicroscopy in amiodarone-related pneumonia. *Eur Respir J*. 2013 Dec;42(6):1646–58.
76. Yserbyt J, Alamé T, Dooms C, Ninane V. Pulmonary alveolar microlithiasis and probebased confocal laser endomicroscopy. *J Bronchology Interv Pulmonol*. 2013 Apr;20(2): 159–63.
77. Yserbyt J, Dooms C, Ninane V, Decramer M, Verleden G. Perspectives using probe-based confocal laser endomicroscopy of the respiratory tract. *Swiss Med Wkly*. 2013 Mar; 143:w13764.
78. Danilevskaya O, Averyanov A, Klimko N, Lesnyak V, Sorokina A, Sazonov D, et al. The case of diagnostics of invasive pulmonary aspergillosis by in vivo probe-based confocal laser endomicroscopy of central and distal airways. *Med Mycol Case Rep*. 2014 Jul;5:35–9.
79. Shafiek H, Fiorentino F, Cosio BG, Kersul A, Thiberville L, Gomez C et al. Usefulness of Bronchoscopic Probe-Based Confocal Laser Endomicroscopy in the Diagnosis of Pneumocystis jirovecii Pneumonia. *Respiration*. 2016;92(1):40–7.
80. Vasilev I, Mamenko I, Tabanakova I, Vikulova I, Shevel V, Ushkov A, et al. Probe-based Confocal Laser Endomicroscopy in Metastatic Pulmonary Calcification. *J Bronchology Interv Pulmonol*. 2018 Jan;25(1):60–2.
81. Yserbyt J, Dooms C, Decramer M, Verleden GM. Acute lung allograft rejection: diagnostic role of probe-based confocal laser endomicroscopy of the respiratory tract. *J Heart Lung Transplant*. 2014 May;33(5):492–8.
82. Keller CA, Khor A, Arenberg DA, Smith MA, Islam SU. Diagnosis of Acute Cellular Rejection Using Probe-based Confocal Laser Endomicroscopy in Lung Transplant Recipients: A Prospective, Multicenter Trial. *Transplantation*. 2019 Feb;103(2):428–34.
83. Meng P, Tan GL, Low SY, Takano A, Ng YL, Anantham D. Fibred confocal fluorescence microscopy in the diagnosis of interstitial lung diseases. *J Thorac Dis*. 2016 Dec;8(12): 3505–14.
84. Salaün M, Guisier F, Dominique S, Genevois A, Jounieaux V, Bergot E, et al. In vivo probebased confocal laser endomicroscopy in chronic interstitial lung diseases: specific descriptors and correlation with chest CT. *Respirology*. 2019 Aug;24(8):783–91.
85. Wijmans L, Bonta PI, Rocha-Pinto R, de Bruin DM, Brinkman P, Jonkers RE, et al. Confocal Laser Endomicroscopy as a Guidance Tool for Transbronchial Lung Cryobiopsies in Interstitial Lung Disorder. *Respiration*. 2019; 97(3):259–63.
86. Jorge E, Baptista R, Calisto J, Faria H, Monteiro P, Pan M, et al. Optical coherence tomography of the pulmonary arteries: A systematic review. *J Cardiol*. 2016 Jan;67(1):6–14.
87. Tatebe S, Fukumoto Y, Sugimura K, Nakano M, Miyamichi S, Satoh K et al. Optical coherence tomography as a novel diagnostic tool for distal type chronic thromboembolic pulmonary hypertension. *Circ J*. 2010 Aug;74(8): 1742–4.

88. Domingo E, Grignola JC, Aguilar R, Montero MA, Arredondo C, Vázquez M, et al. In vivo assessment of pulmonary arterial wall fibrosis by intravascular optical coherence tomography in pulmonary arterial hypertension: a new prognostic marker of adverse clinical follow-up. *Open Respir Med J*. 2013 Apr;7(1): 26–32.
89. Jiang X, Peng FH, Liu QQ, Zhao QH, He J, Jiang R, et al. Optical coherence tomography for hypertensive pulmonary vasculature. *Int J Cardiol*. 2016 Nov;222:494–8.
90. Homma Y, Hayabuchi Y, Ono A, Kagami S. Pulmonary Artery Wall Thickness Assessed by Optical Coherence Tomography Correlates With Pulmonary Hemodynamics in Children With Congenital Heart Disease. *Circ J*. 2018 Aug 24;82(9):2350–7.
91. Dai Z, Fukumoto Y, Tatebe S, Sugimura K, Miura Y, Nochioka K, et al. OCT imaging for the management of pulmonary hypertension. *JACC Cardiovasc Imaging*. 2014 Aug;7(8):843–5.
92. Sugimura K, Fukumoto Y, Satoh K, Nochioka K, Miura Y, Aoki T et al. Percutaneous transluminal pulmonary angioplasty markedly improves pulmonary hemodynamics and longterm prognosis in patients with chronic thromboembolic pulmonary hypertension. *Circ J*. 2012;76(2):485–8.
93. Roik M, Wretowski D, Łabyk A, Kostrubiec M, Rowiński O, Pruszczyk P. Optical coherence tomography of inoperable chronic thromboembolic pulmonary hypertension treated with refined balloon pulmonary angioplasty. *Pol Arch Med Wewn*. 2014;124(12):742–3.
94. Hong C, Luo FQ, Liu CL, Zhong NS, Li JY, Wang W. Clinical study of optical coherence tomography in the diagnosis of peripheral pulmonary artery thrombus. *Thromb Res*. 2018 Jan;161:52–9.
95. Pan Y, Volkmer JP, Mach KE, Rouse RV, Liu JJ, Sahoo D, et al. Endoscopic molecular imaging of human bladder cancer using a CD47 antibody. *Sci Transl Med*. 2014 Oct; 6(260):260ra148.
96. Feroldi F, Verlaan M, Knaus H, Davidoiu V, Vugts DJ, van Dongen GA, et al. High resolution combined molecular and structural optical imaging of colorectal cancer in a xenograft mouse model. *Biomed Opt Express*. 2018 Nov;9(12):6186–204.
97. Patout M, Guisier F, Brune X, Bohn P, Romieu A, Sarafan-Vasseur N, et al. Real-time molecular optical micro-imaging of EGFR mutations using a fluorescent erlotinib based tracer. *BMC Pulm Med*. 2019 Jan; 19(1):3.
98. Guisier F, Bohn P, Patout M, Piton N, Farah I, Vera P, et al. In- and ex-vivo molecular imaging of apoptosis to assess sensitivity of non-small cell lung cancer to EGFR inhibitors using probe-based confocal laser endomicroscopy. *PLoS One*. 2017 Jul; 12(7):e0180576.
99. Morisse H, Heyman L, Salaün M, Favennec L, Picquenot JM, Bohn P, et al. In vivo and in situ imaging of experimental invasive pulmonary aspergillosis using fibered confocal fluorescence microscopy. *Med Mycol*. 2012 May;50(4):386–95.
100. Morisse H, Heyman L, Salaün M, Favennec L, Picquenot JM, Bohn P, et al. In vivo molecular microimaging of pulmonary aspergillosis. *Med Mycol*. 2013 May;51(4):352– 60.
101. Vanherp L, Poelmans J, Hillen A, Govaerts K, Belderbos S, Buelens T, et al.

- Bronchoscopic fibered confocal fluorescence microscopy for longitudinal in vivo assessment of pulmonary fungal infections in free-breathing mice. *Sci Rep*. 2018 Feb;8(1): 3009.
102. Mills B, Akram AR, Scholefield E, Bradley M, Dhaliwal K. Optical Screening of Novel Bacteria-specific Probes on Ex Vivo Human Lung Tissue by Confocal Laser Endomicroscopy. *J Vis Exp*. 2017 Nov;129.
 103. Adams DC, Pahlevaninezhad H, Szabari MV, Cho JL, Hamilos DL, Kesimer M, et al. Automated segmentation and quantification of airway mucus with endobronchial optical coherence tomography. *Biomed Opt Express*. 2017 Sep;8(10):4729–41.
 104. Feroldi F, Willemsse J, Davidoiu V, Gräfe MG, van Iperen DJ, Goorsenberg AW, et al. In vivo multifunctional optical coherence tomography at the periphery of the lungs. *Biomed Opt Express*. 2019 May;10(6):3070– 91.
 105. Pahlevaninezhad H, Khorasaninejad M, Huang YW, Shi Z, Hariri LP, Adams DC, et al. Nano-optic endoscope for high-resolution optical coherence tomography in vivo. *Nat Photonics*. 2018 Sep;12(9):540– 7.

Chapter 7.

Identification and quantification of airway wall layers with optical coherence tomography: a histology based validation study

Goorsenberg AWM
d'Hooghe JNS
de Bruin DM
Roelofs J
Annema JT
Bonta PI

Abstract

Background High-resolution computed tomography has limitations in the assessment of airway wall layers and related remodeling in obstructive lung diseases. Near infrared-based Optical Coherence Tomography (OCT) is a novel imaging technique that combined with bronchoscopy generates highly detailed images of the airway wall. The aim of this study is to identify and quantify human airway wall layers both *ex-vivo* and *in-vivo* by OCT and correlate these to histology.

Methods Patients with lung cancer, prior to lobectomy, underwent bronchoscopy including *in-vivo* OCT imaging. *Ex-vivo* OCT imaging was performed in the resected lung lobe after needle insertion for matching with histology. Airway wall layer perimeters and their corresponding areas were assessed by two independent observers. Airway wall layer areas (total wall area, mucosal layer area and submucosal muscular layer area) were calculated.

Results 13 airways of 5 patients were imaged by OCT. Histology was matched with 51 *ex-vivo* OCT images and 39 *in-vivo* OCT images. A significant correlation was found between *ex-vivo* OCT imaging and histology, *in-vivo* OCT imaging and histology and *ex-vivo* OCT imaging and *in-vivo* OCT imaging for all measurements ($p < 0.0001$ all comparisons). A minimal bias was seen in Bland-Altman analysis. High inter-observer reproducibility with intra-class correlation coefficients all above 0.90 were detected.

Conclusions OCT is an accurate and reproducible imaging technique for identification and quantification of airway wall layers and can be considered as a promising minimal-invasive imaging technique to identify and quantify airway remodeling in obstructive lung diseases.

Abbreviations list

| | |
|--------|--------------------------------------------------|
| AMC | academic Medical Center |
| ASM | airway smooth muscle |
| BT | bronchial thermoplasty |
| COPD | chronic pulmonary obstructive disease |
| H&E | hematoxylin and eosin |
| HRCT | high resolution computed tomography |
| ICC | intra-class correlation |
| NSCLC | non-small cell lung cancer |
| OCT | optical coherence tomography |
| PET-CT | positron emission tomography-computed tomography |

Introduction

Airway remodeling is defined by structural changes and thickening of the airway wall, which is seen in several pulmonary diseases, such as asthma and chronic obstructive pulmonary disease (COPD) [1-3]. The identification and severity of airway remodeling is important as it relates to disease severity [4]. Currently, airway remodeling can be assessed by high resolution computed tomography (HRCT)-scan of the chest. However this imaging technique requires patient exposition to ionizing radiation and has limited resolution that hampers visualization and quantification of the different airway wall layers. Bronchial mucosal biopsies taken during bronchoscopy, can visualize the different airway wall layers very precisely but are invasive. Furthermore these biopsies, provide only information of a small selected site of the airways and the processing of biopsies is time consuming and often causes artefacts [5].

Optical Coherence Tomography (OCT) is a promising real-time high-resolution imaging technique to assess airway remodeling [6, 7]. Using near-infrared light cross-sectional images are created by the backscattering of light by the tissue [8]. For example, in ophthalmology, OCT is used in clinical practice for retina assessment [9] and in cardiology for stent positioning during percutaneous coronary interventions [10]. Former studies have shown that OCT is able to visualize the different airway wall layers including mucosa (epithelium and lamina propria), submucosa (including airway smooth muscle, glands) and cartilage [11-15]. Only limited data are available on the quantification of total airway wall area and the correlation with histology [5, 16] and CT [5, 6]. The feasibility of OCT to quantify separate airway wall layers, including the mucosa and submucosa, and the correlation with histology in human airways is unknown. Furthermore correlating *ex-vivo* and *in-vivo* OCT images has never been done before. The aim of this study is to identify and quantify airway wall layers in *ex-vivo* and *in-vivo* OCT images and correlate these to histology, and assess the inter-observer reproducibility. We hypothesize that: 1) airway wall layer areas assessed on *ex-vivo* OCT images correlate well with matched histology sections, 2) airway wall layer areas assessed on *in-vivo* OCT images correlate well with both *ex-vivo* OCT images and histology sections, and, 3) there is a good inter-observer reproducibility for manually traced OCT airway wall layer perimeters and their corresponding areas.

Methods

Study design

This is a prospective observational cohort study, performed in the Academic Medical Center (AMC) in Amsterdam, the Netherlands. Ethical approval was obtained from the Medical Ethics Committee of the AMC (NL51605.018.14). **Fig 1** shows the flow of study conduct.

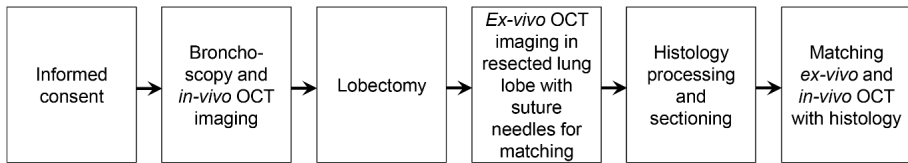


Figure 1. Flow chart of study conduct. OCT: optical coherence tomography.

Study subjects

Patients with a strong suspicion or tissue proven peripheral non-small cell lung cancer (NSCLC) staged cT1-3N0-1M0 based on a positron emission tomography-computed tomography (PET-CT) and in need of a standard diagnostic bronchoscopic work-up and lobectomy were eligible for the study. Signed informed consent was obtained prior to the procedure.

In-vivo OCT imaging

OCT images of *in-vivo* airways were acquired using a C7-XR St. Jude Medical Inc. system interfaced with a C7 Dragonfly catheter (\varnothing 0.9 mm diameter) (St. Jude Medical Inc., St. Paul, MN, USA). After standard diagnostic bronchoscopy, the OCT catheter was inserted through a guide sheath into the working channel of the bronchoscope into the airways of interest where an automated pullback of 5.4 cm was performed (**S1A Fig**). All airways in the lobe candidate for surgical resection were imaged from subsegmental to segmental airways. Each pullback was repeated at least two times.

Ex-vivo OCT imaging

Following surgical resection, the lobectomy specimen was subjected to OCT imaging within three hours after removal. In preparation for *ex-vivo* OCT imaging the airways were partially exposed and instilled with phosphate buffered saline. In order to correlate the *ex-vivo* OCT imaging with histology, two to four curved suture needles were inserted in the *in-vivo* OCT imaged airways (**S1B Fig**). These needles were clearly visible on *ex-vivo* OCT imaging (**S1C Fig**) and guided matching of *ex-vivo* OCT images with histology sections. *Ex-vivo* OCT imaging was performed similarly to *in-vivo* OCT imaging as described above.

Histological preparation

After performing *ex-vivo* OCT imaging of the airways, the lobectomy sample was fixed in phosphate buffered formalin overnight. Measured airways were dissected and sectioned according to the sutures needles. Subsequently the tissue samples were dehydrated with increasing concentrations of ethanol for ~4 hours, cleared in xylene and impregnated in paraffin, using a standard tissue processor (A82300001 Excelsior AS Tissue Processor, ThermoFisher Scientific, Waltham, MA, USA). Next, tissues were manually embedded in paraffin. Sections of 4 μ m thickness were stained with hematoxylin and eosin (H&E) to visualize the airway wall structures (**Figs 2A and 2B**). Immunostaining with

desmin was used to identify the airway smooth muscle layer (Figs 2C and 2D). We used Philips Digital Pathology Solution 2.3.1.1 to digitalize the histology slides (Philips Electronics, the Netherlands).

OCT measurements protocol and training

Before analyzing the *ex-vivo* and *in-vivo* OCT images, a protocol was written that defined how to identify and quantify the airway wall layers in OCT images. For training purposes, according to this protocol a test series of OCT images were analyzed by two independent OCT image experts (JH and AG). The test OCT imaging set contained 51 randomly selected OCT images which were obtained from another study. Luminal perimeter (P_L), outer perimeter of the mucosa (P_{muc}) and outer perimeter of the submucosal muscular layer ($P_{submusc}$) were traced.

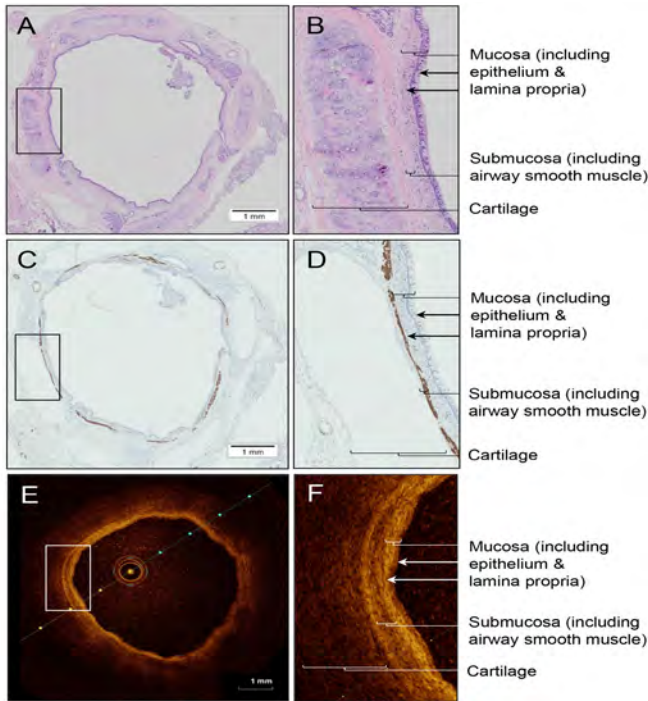


Figure 2 Ex-vivo OCT cross-sectional image visualizing the different layers of the human airway wall and corresponding histology image.

(A) Histology cross section, stained with H&E. (B) Higher magnification view of the square of histology image A, visualizing the different layers of the airway wall of the segmental LLL. (C) Histology cross section, stained with desmin. (D) Higher magnification view of the square of histology image C, visualizing the submucosal muscular layer of the airway wall. (E) Corresponding cross section of OCT of *ex-vivo* airway to histology airway image A and C. (F) Higher magnification view of the square of OCT image E, visualizing the corresponding layers of the airway wall.

OCT – histology matching

Ex-vivo OCT images and histology sections were matched by one observer (JH) based on the needles which were clearly visible in OCT. *In-vivo* OCT images were linked with *ex-vivo* OCT images and histology by matching luminal perimeters and corresponding areas in mm² combined with the distance from reference points and segmentations in corresponding airways.

OCT and histology measurements

We used ImageJ software for Windows (National Institutes of Health, Bethesda, MD, USA) to manually trace the luminal perimeter (P_L), mucosal perimeter (P_{muc}) and submucosal muscular perimeter ($P_{submusc}$) in the desmin stained histology images of our study population (Figs 3A and 3B). The same perimeters were traced in *in-vivo* and *ex-vivo* OCT images using St. Jude Medical Inc. software (Figs 3C and 3D). The criteria for tracing the airway wall layer perimeters in OCT images were based on the differences in light intensity as shown in S2 Fig. From the inside of the airway lumen to the outer wall, the first thin low intensity layer identified is the epithelial layer. The second, high intensity, layer matches the lamina propria layer (the mucosal layer includes the epithelial layer and lamina propria layer). The third, lower intensity, layer is the submucosa layer which includes the airway smooth muscle. The next, very low intensity, layer is the cartilage layer identified by a surrounded thin high intensity layer, the perichondrium. Subsequently, the luminal areas A_L (in mm²), mucosal areas A_{muc} (in mm²) and submucosal muscular areas $A_{submusc}$ (in mm²) corresponding to the traced perimeters P_L , P_{muc} , $P_{submusc}$ were automatically calculated. These areas were used to calculate the surface areas of the different layers; total airway wall area ($WA_t = A_{submusc} - A_L$), mucosal wall layer area ($WA_{muc} = A_{muc} - A_L$) and submucosal muscular wall layer area ($WA_{submusc} = A_{submusc} - A_{muc}$) in mm². Both JH and AG analysed the blinded histology, OCT *ex-vivo* and OCT *in-vivo* images independently in order to assess the inter-observer reproducibility.

Primary endpoint

The primary endpoint was the correlation between *ex-vivo* OCT and histology for the above described parameters (A_L , A_{muc} , $A_{submusc}$, WA_t , WA_{muc} and $WA_{submusc}$ in mm²).

Secondary endpoints

Secondary endpoints were the correlation between *in-vivo* OCT and *ex-vivo* OCT and between *in-vivo* OCT and histology for the above described parameters (A_L , A_{muc} , $A_{submusc}$, WA_t , WA_{muc} and $WA_{submusc}$ and in mm²). Furthermore the inter-observer reproducibility of the manually traced perimeters and corresponding areas between two observers was analyzed (A_L , A_{muc} , $A_{submusc}$ in mm²).

Statistical analysis

Data were tested for normality using a D'Agostino and Pearson omnibus normality test and histograms. The relationship between histology and

OCT images (*ex-vivo* and *in-vivo*) and the inter-observer reproducibility was determined by using a Pearson correlation coefficient (r) for normally distributed data and the Spearman's rank correlation coefficient (r) for non-normally distributed data with its least squares linear regression models. The agreement between measurements is shown in Bland-Altman plots. Both analysis were performed in GraphPad Prism version 5.01 (GraphPad Software Inc, San Diego, CA, USA). To analyze if both observers indeed measured the same values we calculated the intra-class correlation coefficient (ICC) using SPSS statistics for Windows version 23.0. The used P values in our analysis were all two sided and sat at a level of statistical significance of $P < 0.05$.

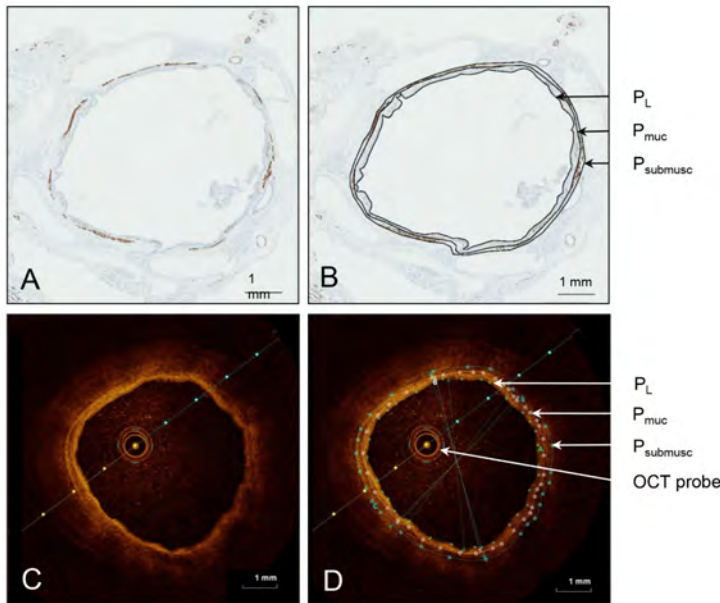


Figure 3 Ex-vivo OCT cross-sectional image and corresponding histology image of human airway. (A) Clean histology cross section of human airway of the segmental LLL, stained with desmin. (B) cross section images of histology, stained with desmin, with manually traced perimeters; P_L : lumen perimeter, P_{muc} : mucosal perimeter, $P_{submusc}$: submucosal muscular perimeter. (C) Corresponding cross section of OCT of *ex-vivo* airway to histology airway image A. (D) cross section images of OCT and with manually traced perimeters; P_L : lumen perimeter, P_{muc} : mucosal perimeter, $P_{submusc}$: submucosal muscular perimeter and OCT probe in situ.

Results

From April 2015 until November 2015 5 patients with NSCLC who underwent an lobectomy were included in this study. Patient characteristics are shown in **Table 1**.

Primary endpoint

In total 13 *ex-vivo* airways in 5 patients were imaged with OCT, resulting in 51 matching cross sectional OCT images and histology sections. Airway wall layers could be identified as shown in **Figs 2** and **3**. Linear regression analysis showed a significant correlation between *ex-vivo* OCT imaging and histology for all parameters (A_L $r=0.96$, $p<0.0001$, A_{muc} $r=0.92$, $p<0.0001$, A_{sub} $r=0.87$, $p<0.0001$, WA_t $r=0.79$, $p<0.0001$, WA_{muc} $r=0.78$, $p<0.0001$ and $WA_{submusc}$ $r=0.62$, $p=0.0001$) (**Table 2**, **Fig 4 A-F** left graphs). Bland-Altman analysis showed a minimal bias for (all measurements of) these parameters (**Fig 4 A-F** right graphs). A proportional error was found for mucosal wall area (WA_{muc} in mm^2) and submucosal muscular wall area ($WA_{submusc}$ in mm^2).

Secondary endpoints

Ex-vivo OCT and *in-vivo* OCT images

A total of 39 *in-vivo* OCT cross sectional images could be compared with their corresponding *ex-vivo* OCT images. Images were matched according to luminal perimeters for the same airways. High correspondence between *in-vivo* and *ex-vivo* OCT imaging for the luminal area was shown (A_L $r=0.99$, $p<0.0001$). Linear regression analysis showed a significant correlation for all other parameters (A_{muc} $r=0.97$, $p<0.0001$, $A_{submusc}$ $r=0.88$, $p<0.0001$, WA_t $r=0.54$, $p<0.0001$, WA_{muc} $r=0.68$, $p<0.0001$ and $WA_{submusc}$ $r=0.40$, $p=0.0001$). Bland-Altman analysis showed a negligible bias between OCT *ex-vivo* and OCT *in-vivo* images (**S3 Fig**). Similar results were found when *in-vivo* OCT was compared with histology (**S4 Fig**).

Table 1. Patient characteristics undergoing OCT and lobectomy

| | Patient 1 | Patient 2 | Patient 3 | Patient 4 | Patient 5 |
|------------------------------|-----------|-----------|-----------|-----------|-----------|
| Age (years) | 57 | 69 | 71 | 60 | 64 |
| Sex | Male | Male | Female | Male | Male |
| FEV ₁ % predicted | 97 | 94 | 90 | 36 | 48 |
| COPD GOLD status | n.a. | n.a. | n.a. | GOLD III | GOLD III |
| Resected lung lobe | RUL | LLL | LLL | LLL | RUL |

FEV₁: forced expiratory volume in one second. COPD: chronic obstructive pulmonary disease. n.a.: not applicable. RUL: right upper lobe. LLL: left lower lobe

Table 2. Correlation between ex-vivo OCT and histology for airway wall area measurements

| Parameter | r | P-value |
|----------------|------|---------|
| A_L | 0.96 | <0.0001 |
| A_{muc} | 0.92 | <0.0001 |
| $A_{submusc}$ | 0.87 | <0.0001 |
| WA_t | 0.79 | <0.0001 |
| WA_{muc} | 0.78 | <0.0001 |
| $WA_{submusc}$ | 0.62 | <0.0001 |

A_L : luminal area. A_{muc} : mucosal area. $A_{submusc}$: submucosal muscular area, WA_t : total airway wall area. WA_{muc} : mucosal wall layer area. $WA_{submusc}$: submucosal muscular wall layer area

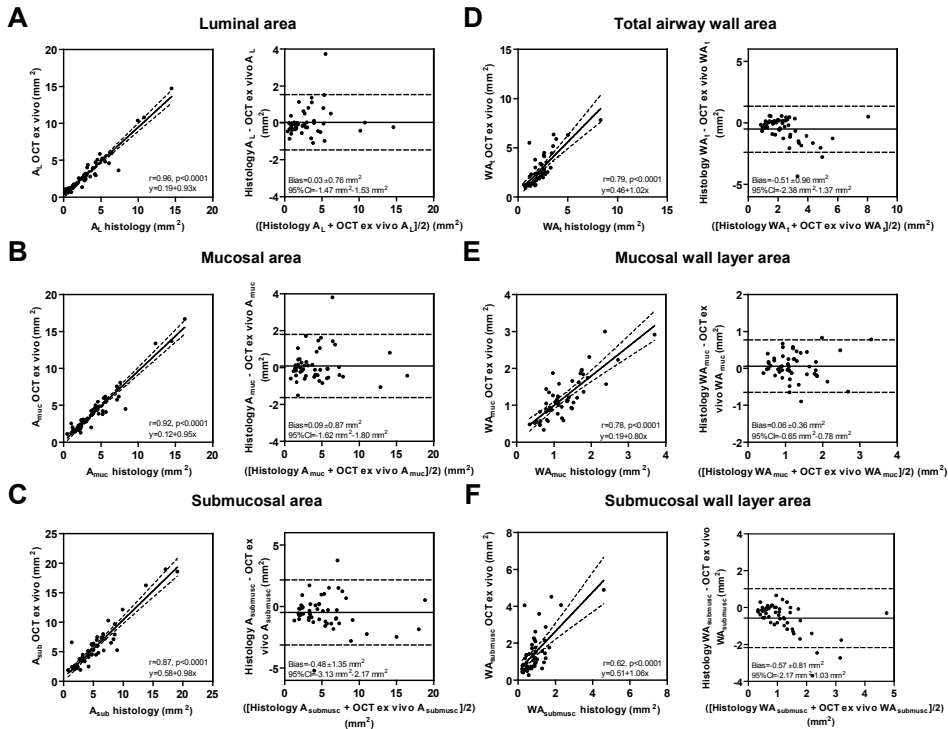


Figure 4 Linear regression analysis and Bland-Altman plots for histology and OCT ex-vivo airway wall area measurements (n=51).

(A) A_L lumen area in mm^2 . (B) A_{muc} mucosal area in mm^2 . (C) $A_{submusc}$ submucosal muscular area in mm^2 . (D) WA_t total airway wall area in mm^2 . (E) WA_{muc} mucosal wall area in mm^2 . (F) $WA_{submusc}$ submucosal muscular wall area in mm^2 .

Inter-observer reproducibility

All 51 *ex-vivo* OCT images and 39 *in-vivo* OCT images were analyzed independently by the two observers. The intra-class correlation coefficients to assess the accuracy of *ex-vivo* and *in-vivo* OCT measurements by the two observers were high for all parameters (**S1 Table**). Linear regression analysis of the *ex-vivo* OCT measurements between the two observers showed a significant correlation ($r \geq 0.98$, $p < 0.0001$ for all measurements) (**S5 Fig**). Bland-Altman plots showed a minimal bias for all three parameters (A_L -0.02 (95% CI = -0.22-0.19), A_{muc} -0.06 (95% CI = -0.52-0.41) and $A_{submusc}$ 0.02 (95% CI = -0.99-1.04) (**S5 Fig**). Comparable results were found for the *in-vivo* OCT measurements between the two observers (**S6 Fig**).

Discussion

To the best of our knowledge, this is the first study to show the feasibility of OCT to identify and subsequently quantify separate human airway wall layers showing a strong and significant correlation with histology for both *ex-vivo* and *in-vivo* OCT images. Besides, this is the first report comparing *ex-vivo* and *in-vivo* OCT imaging and showing its significant correlation. Importantly, a high inter-observer reproducibility was detected between two independent observers.

The correlations for separate airway wall areas measured by OCT and histology were less strong when compared to the previous animal study performed in porcine lungs, which are known to have more widespread airway cartilage than human airways [16]. This makes it easier to distinguish the different perimeters in OCT images of porcine airways [17]. The proportional error in Bland-Altman analysis of $WA_{submusc}$ (mm²) and WA_l (mm²) for *ex-vivo* OCT imaging versus histology, suggests that a small systematic difference between histology and OCT, is present. Probably, this is the result of formalin fixation, alcohol dehydration and paraffin embedding, which are known to cause tissue shrinkage, however without disturbing the intrinsic proportions of the various tissue layers. The high correlation we found for the lumen and total airway wall quantification is comparable to the *in-vivo* OCT study performed by Chen et al [5].

Since we could not use suture needles as landmarks for matching the OCT *in-vivo* images with histology, we used a corresponding inner luminal area from the same airway instead. A decrease of the airway lumen after resection and especially after histological processing can be expected. This can contribute to the observed differences between the *in-vivo* OCT and *ex-vivo* OCT measurements and *in-vivo* OCT and histological measurements. However, the correlation for A_{muc} and $A_{submusc}$ remained strong and significant for *in-vivo* OCT imaging compared to histology and suggests that an exact match is not

necessary when you measure the same airway with a corresponding lumen. A previous study assessing insertion-reinsertion reproducibility of the total airway wall area in OCT found similar results and stated that heterogeneity in airway wall structure seemed to be relatively small [18].

This study has multiple strengths. First, all measurements were independently assessed by two observers, making it possible to analyze the inter-observer reproducibility. By using an anonymized test series of different patients, we avoided creating bias by already seeing the OCT images from our own cohort. Based on histology and the OCT test series both observers with knowledge of the histology of airway walls were able to analyze OCT images of the airway wall. With high intra-class correlation coefficients and a negligible bias for all measurements between two independent observers this study shows that OCT imaging has a strong inter-observer reproducibility. The strong inter-observer reproducibility in both *ex-vivo* and *in-vivo* OCT imaging, confirms data from previous studies [16, 18]. Second, a large sample size of 51 matched cross sectional OCT and histology images were analyzed. Third, the unique study method, where human airways were measured with OCT both *in-vivo* and *ex-vivo* and subsequently compared with each other and with histology, ensured a reliable comparison. Finally, we believe that the method of airway wall layer quantification as executed in this study is of interest. Since subtracting airway wall area measurements from one another results in areas of the airway wall layer that are independent of the shape of the airway.

There are several limitations to this study. First, not all *ex-vivo* airways were also measured with OCT *in-vivo*, therefore 39 of the 52 *ex-vivo* OCT images had a corresponding *in-vivo* OCT image. Since it was not possible to use sutures during OCT *in-vivo* imaging, the luminal area and distance to reference points and segmentations was used to match with histology. In addition, matching was done by a single person. Second, our cohort contained a heterogeneous population with both subjects with a non-obstructive lung function and subjects with COPD. However, in these 5 patients several airways were imaged, creating 51 histology–OCT *ex-vivo* matches. Since the aim of this study was to correlate histology to OCT images independent of the health status of the airway wall, the heterogeneity of the study population does not interfere with the study aim. Another possible limitation is generated by artefacts after processing histology tissue. A well-known artefact is shrinkage of histology tissue caused by fixation [19]. This could potentially have caused the small proportional error seen in the Bland-Altman analysis. In addition, OCT imaging artifacts can contribute to the found differences between OCT and histological measurements. As shown in **Figs 2** and **3** the sensitivity decreases with the distance between the probe and the airway wall. Furthermore minimal artefacts are expected from the angle of the airway wall surface relative to the light beam, the refractive index radial calibration and refractive effects.

One major advantage of OCT over histology is that OCT is able to measure airway segments real-time in their natural state *in-vivo*. With OCT being significantly correlated to histology and easy to learn with high reproducibility, it could be an ideal instrument to assess airway wall remodeling, understand airway disease pathogenesis and eventually monitor and evaluate treatment results over time in patients with airway diseases such as asthma [20]. For instance, there is evidence that Bronchial Thermoplasty (BT) induces a reduction in airway smooth muscle (ASM) mass in severe asthma [21]. As OCT is able to visualize and quantify the different airway wall layers in a specific airway segment, it could potentially detect changes in the submucosal muscular layer, containing the ASM after BT. As such OCT may serve as an ideal BT treatment evaluation instrument and might be used for identification of patients that have a large ASM mass. In the future, combining OCT with technical advancements such as polarisation will make it possible to visualize and quantify the ASM itself, which could be of added value in these patients [22]. For this purpose, although the high inter-observer reproducibility of OCT measurements are reassured, automated software for airway wall measurements is highly needed. In conclusion, OCT is an accurate and reproducible imaging technique for identification and quantification of the airway wall areas in total and in sublayers. OCT can be considered a promising non-invasive imaging technique to identify and quantify airway remodeling in patients with obstructive lung diseases.

Acknowledgments

The authors would like to acknowledge and thank O. de Boer and T. Dirksen for their committed and professional work.

References

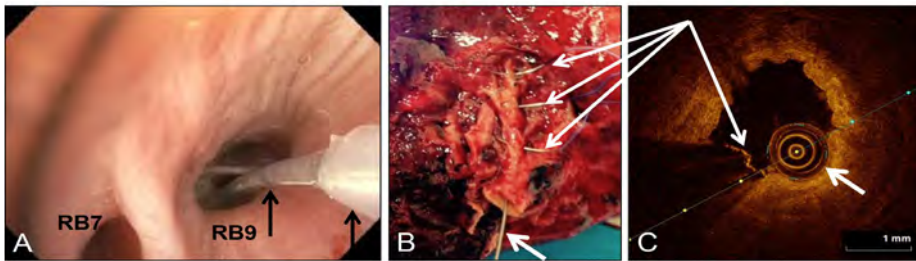
1. Jeffery PK. Remodeling in asthma and chronic obstructive lung disease. *American journal of respiratory and critical care medicine*. 2001;164(10 Pt 2):S28-38. doi: 10.1164/ajrcm.164.supplement_2.2106061. PubMed PMID: 11734464.
2. James AL, Wenzel S. Clinical relevance of airway remodelling in airway diseases. *The European respiratory journal*. 2007;30(1):134-55. doi: 10.1183/09031936.00146905. PubMed PMID: 17601971.
3. Patel BD, Coxson HO, Pillai SG, Agusti AG, Calverley PM, Donner CF, et al. Airway wall thickening and emphysema show independent familial aggregation in chronic obstructive pulmonary disease. *American journal of respiratory and critical care medicine*. 2008;178(5):500-5. doi: 10.1164/rccm.200801-059OC. PubMed PMID: 18565956.
4. Benayoun L, Druilhe A, Dombret MC, Aubier M, Pretolani M. Airway structural alterations selectively associated with severe asthma. *American journal of respiratory and critical care medicine*. 2003;167(10):1360-8. doi: 10.1164/rccm.200209-1030OC. PubMed PMID: 12531777.
5. Chen Y, Ding M, Guan WJ, Wang W, Luo WZ, Zhong CH, et al. Validation of human small airway measurements using endobronchial optical coherence tomography. *Respiratory medicine*. 2015;109(11):1446-53. doi: 10.1016/j.rmed.2015.09.006. PubMed PMID: 26427628.
6. Coxson HO, Quiney B, Sin DD, Xing L, McWilliams AM, Mayo JR, et al. Airway wall thickness assessed using computed tomography and optical coherence tomography. *American journal of respiratory and critical care medicine*. 2008;177(11):1201-6. doi: 10.1164/rccm.200712-1776OC. PubMed PMID: 18310475; PubMed Central PMCID: PMC2408438.
7. Ding M, Chen Y, Guan WJ, Zhong CH, Jiang M, Luo WZ, et al. Measuring Airway Remodeling in Patients With Different COPD Staging Using Endobronchial Optical Coherence Tomography. *Chest*. 2016;150(6):1281-90. Epub 2016/08/16. doi: 10.1016/j.chest.2016.07.033. PubMed PMID: 27522957.
8. Huang D, Swanson EA, Lin CP, Schuman JS, Stinson WG, Chang W, et al. Optical coherence tomography. *Science*. 1991;254(5035):1178-81. PubMed PMID: 1957169; PubMed Central PMCID: PMCPMC4638169.
9. Koustenis A, Jr., Harris A, Gross J, Januleviciene I, Shah A, Siesky B. Optical coherence tomography angiography: an overview of the technology and an assessment of applications for clinical research. *The British journal of ophthalmology*. 2017;101(1):16-20. doi: 10.1136/bjophthalmol-2016-309389. PubMed PMID: 27707691.
10. Sotomi Y, Tateishi H, Suwannasom P, Dijkstra J, Eggermont J, Liu S, et al. Quantitative assessment of the stent/scaffold strut embedment analysis by optical coherence tomography. *The international journal of cardiovascular imaging*. 2016. Epub 2016/02/24. doi: 10.1007/s10554-016-0856-6. PubMed PMID: 26898315.
11. Hariri LP, Applegate MB, Mino-Kenudson M, Mark EJ, Medoff BD, Luster AD, et al. Volumetric optical frequency domain imaging of pulmonary pathology with precise correlation to histopathology. *Chest*. 2013;143(1):64-74. doi: 10.1378/

- chest.11-2797. PubMed PMID: 22459781; PubMed Central PMCID: PMC3537541.
12. Tsuboi M, Hayashi A, Ikeda N, Honda H, Kato Y, Ichinose S, et al. Optical coherence tomography in the diagnosis of bronchial lesions. *Lung cancer*. 2005;49(3):387-94. Epub 2005/06/01. doi: 10.1016/j.lungcan.2005.04.007. PubMed PMID: 15922488.
 13. Yang Y, Whiteman S, Gey van Pittius D, He Y, Wang RK, Spiteri MA. Use of optical coherence tomography in delineating airways microstructure: comparison of OCT images to histopathological sections. *Phys Med Biol*. 2004;49(7):1247-55. Epub 2004/05/07. PubMed PMID: 15128202.
 14. Hariri LP, Applegate MB, Mino-Kenudson M, Mark EJ, Bouma BE, Tearney GJ, et al. Optical frequency domain imaging of ex vivo pulmonary resection specimens: obtaining one to one image to histopathology correlation. *Journal of visualized experiments : JoVE*. 2013;(71). doi: 10.3791/3855. PubMed PMID: 23381470; PubMed Central PMCID: PMC3582683.
 15. Pitris C, Brezinski ME, Bouma BE, Tearney GJ, Southern JF, Fujimoto JG. High resolution imaging of the upper respiratory tract with optical coherence tomography: a feasibility study. *American journal of respiratory and critical care medicine*. 1998;157(5 Pt 1):1640-4. doi: 10.1164/ajrccm.157.5.9707075. PubMed PMID: 9603149.
 16. Lee AM, Kirby M, Ohtani K, Candido T, Shalansky R, MacAulay C, et al. Validation of airway wall measurements by optical coherence tomography in porcine airways. *PloS one*. 2014;9(6):e100145. doi: 10.1371/journal.pone.0100145. PubMed PMID: 24949633; PubMed Central PMCID: PMC4064993.
 17. Rogers CS, Abraham WM, Brogden KA, Engelhardt JF, Fisher JT, McCray PB, Jr., et al. The porcine lung as a potential model for cystic fibrosis. *Am J Physiol Lung Cell Mol Physiol*. 2008;295(2):L240-63. doi: 10.1152/ajplung.90203.2008. PubMed PMID: 18487356; PubMed Central PMCID: PMC2519845.
 18. Kirby M, Ohtani K, Nickens T, Lisbona RM, Lee AM, Shaipanich T, et al. Reproducibility of optical coherence tomography airway imaging. *Biomedical optics express*. 2015;6(11):4365-77. doi: 10.1364/BOE.6.004365. PubMed PMID: 26601002; PubMed Central PMCID: PMC4646546.
 19. Chatterjee S. Artefacts in histopathology. *J Oral Maxillofac Pathol*. 2014;18(Suppl 1):S111-6. doi: 10.4103/0973-029X.141346. PubMed PMID: 25364159; PubMed Central PMCID: PMC4211218.
 20. Kirby M, Ohtani K, Lopez Lisbona RM, Lee AM, Zhang W, Lane P, et al. Bronchial thermoplasty in asthma: 2-year follow-up using optical coherence tomography. *The European respiratory journal*. 2015;46(3):859-62. doi: 10.1183/09031936.00016815. PubMed PMID: 26022958.
 21. Pretolani M, Dombret MC, Thabut G, Knap D, Hamidi F, Debray MP, et al. Reduction of airway smooth muscle mass by bronchial thermoplasty in patients with severe asthma. *American journal of respiratory and critical care medicine*. 2014;190(12):1452-4. Epub 2014/12/17. doi: 10.1164/rccm.201407-1374LE. PubMed PMID: 25496106.
 22. Adams DC, Hariri LP, Miller AJ, Wang Y, Cho JL, Villiger M, et al. Birefringence microscopy platform for assessing airway smooth muscle structure and function in vivo. *Science translational medicine*. 2016;8(359):359ra131. doi: 10.1126/scitranslmed.aag1424. PubMed PMID: 27708064.

S1 Table. Inter-observer reproducibility of OCT measurements between two independent observers.

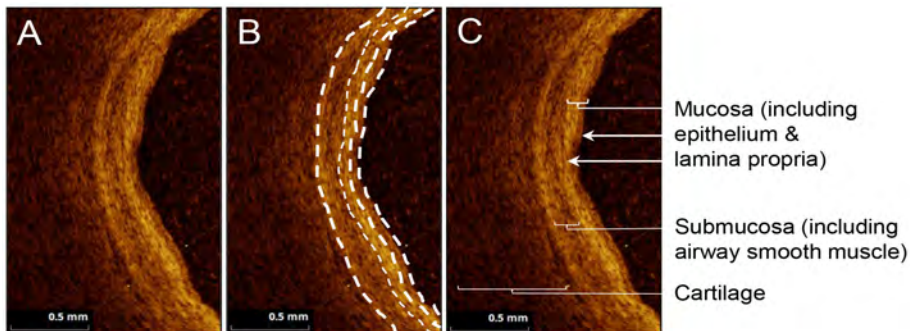
| Parameter | <i>Ex-vivo</i> OCT imaging (n = 51) | | | <i>In-vivo</i> OCT imaging (n = 39) | | |
|-----------------------------------------|-------------------------------------|-------------|---------|-------------------------------------|-------------|---------|
| | ICC | 95% CI | P-value | ICC | 95% CI | P-value |
| A _L (mm ²) | 0.999 | 0.999-1.000 | <0.0001 | 0.999 | 0.999-1.000 | <0.0001 |
| A _{muc} (mm ²) | 0.997 | 0.995-0.998 | <0.0001 | 0.997 | 0.993-0.999 | <0.0001 |
| A _{submusc} (mm ²) | 0.991 | 0.985-0.995 | <0.0001 | 0.983 | 0.959-0.992 | <0.0001 |

ICC: intraclass correlation. A_L: luminal area. A_{muc}: mucosal area. A_{submusc}: submucosal muscular area.



S1 Figure Bronchoscopic OCT imaging technique.

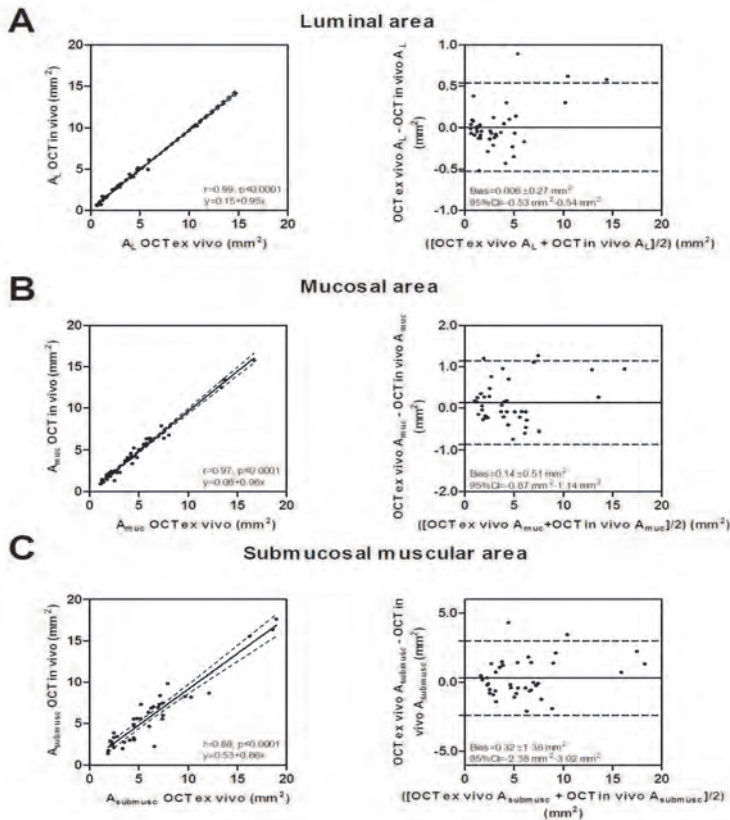
(A) Bronchoscopic view: *In-vivo* OCT imaging with OCT catheter (left arrow) outside the sheet (right arrow) in the posterior segment (RB9) of the right lower lobe. The medial-basal segment (RB7) is used as reference point for the end of the pullback track of 5.4 cm marked by a metal part (left arrow). (B) Resected lung lobe with 3 suture needle marks (long arrows) through the lumen of the airway. OCT catheter placed in airway with needle marks (short arrow). (C) OCT cross-section of an *ex-vivo* imaged airway with a needle mark visible (long arrow). OCT probe visible in the center of the airway (short arrow).



S2 Figure OCT criteria for identification of airway wall structures and layers.

(A) OCT image of the airway wall of a segmental airway of the left lower lobe. (B) Manual tracing of perimeters based on differences in light intensities of the airway wall layers. From right to left the dotted lines represent; luminal perimeter, epithelial

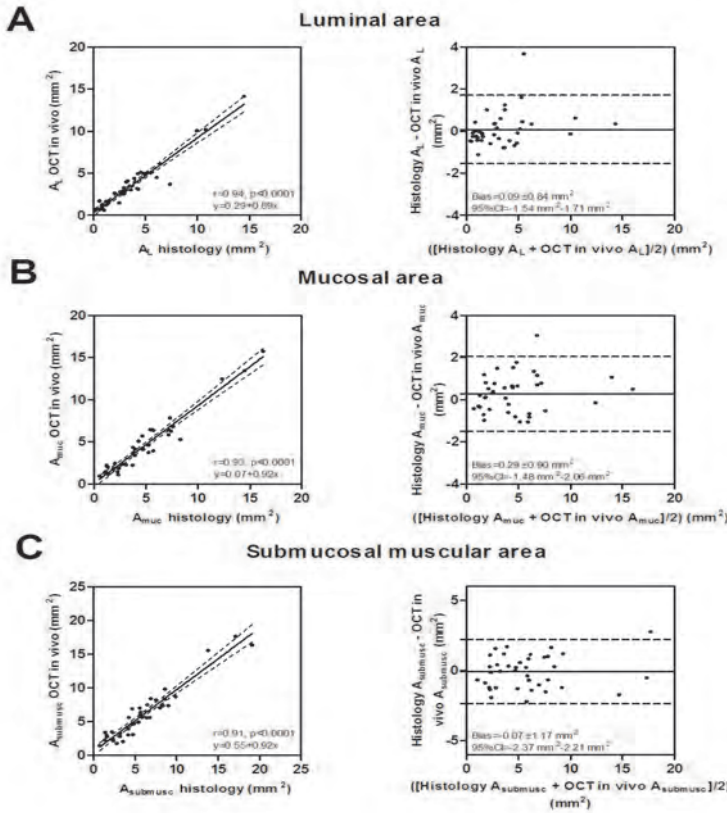
perimeter, mucosal perimeter, submucosal perimeter. **(C)** Corresponding annotated airway wall layers based on differences in light intensities. From right to left: first, low intensity, layer is the epithelial layer. The second, high intensity, layer matches the lamina propria layer. The third, low intensity, layer the submucosa including the airway smooth muscle. The next, very low intensity, layer is the cartilage layer which is identified by a surrounded thin high intensity layer, the perichondrium.



S3 Figure Linear regression analysis and Bland-Altman plots for OCT *ex-vivo* and OCT *in-vivo* airway wall area measurements ($n=39$).

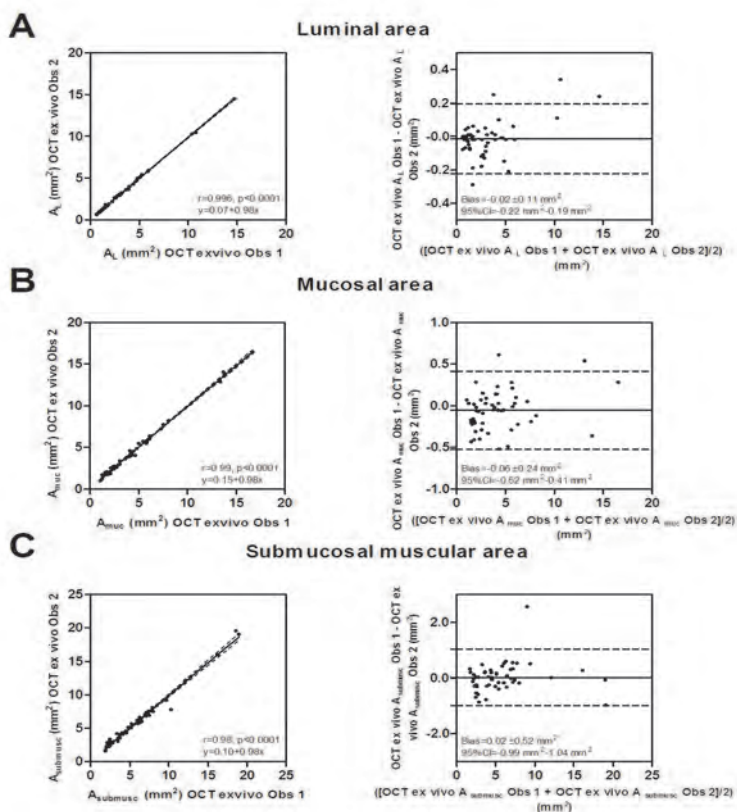
(A) A_L lumen area in mm^2 . **(B)** A_{muc} mucosal area in mm^2 . **(C)** A_{submusc} submucosal muscular area in mm^2 .

7



S4 Figure Linear regression analysis and Bland-Altman plots for histology and OCT *in-vivo* airway wall area measurements (n = 39).

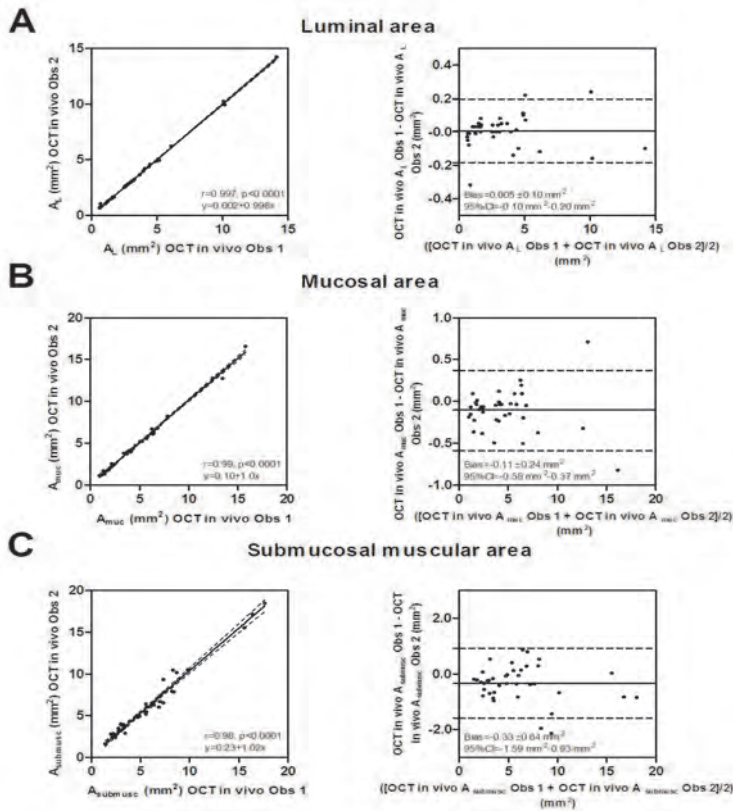
(A) A_L lumen area in mm^2 . (B) A_{muc} mucosal area in mm^2 . (C) A_{submuc} submucosal muscular area in mm^2 .



S5 Figure Linear regression analysis and Bland-Altman plots for *ex-vivo* OCT airway wall measurements between two observers (n = 51).

(A) A_L lumen area in mm². **(B)** A_{muc} mucosal area in mm². **(C)** $A_{submusc}$ submucosal muscular area in mm².

7



S6 Figure Linear regression analysis and Bland-Altman plots for *in-vivo* OCT airway wall measurements between two observers (n = 39).

(A) A_L lumen area in mm². (B) A_{muc} mucosal area in mm². (C) $A_{submusc}$ submucosal muscular area in mm².

Chapter 8.

Optical coherence tomography intensity correlates with extracellular matrix components in the airway wall

Goorsenberg AWM
Carpaij OA
d'Hooghe JNS
de Bruin DM
van den Elzen RM
Nawijn MC
Annema JT
van den Berge M
Bonta PI
Burgess JK

*Accepted for publication in American Journal of Respiratory and Critical
Care Medicine*

To the editor,

Obstructive pulmonary diseases are characterised by structural airway remodeling, including alterations in extracellular matrix (ECM) [1]. The ECM profile differs between asthmatic and non-asthmatic airways, with less elastin, and higher abundance of collagen I and fibronectin in asthma [2]. Additionally, increased airway wall collagen deposition is associated with more severe disease in asthma [3]. In COPD, alterations in collagen and elastin affect the mechanical properties of the lung, subsequently decreasing lung elasticity and contributing to emphysema [1]. Currently, two diagnostic tools are available to assess airway remodeling: thorax computed tomography and endobronchial biopsies. While bronchial wall thickness and lumen area can be assessed by computed tomography, the resolution is insufficient to assess separate airway wall layers and ECM components, leaving the pathophysiology of airway wall remodeling unclear. Biopsies are the gold standard for determining airway remodeling; however, the applicability is limited due to its invasiveness, small sample area and elaborative histology processing.

Optical coherence tomography (OCT) generates high resolution, real-time, near-infrared-based crosssectional images of the airway wall [4,5], with potential for visualizing airway remodeling and enabling 3D reconstructions. Several studies found an increased airway wall thickness and decreased lumen area in asthma and COPD patients using OCT [5,6]. Furthermore, OCT imaging was able to identify and quantify mucosal and submucosal airway layers [4]. To the best of our knowledge, no study has linked OCT imaging to ECM protein deposition in the airway wall. We hypothesized that the ECM deposition within the airway wall can be detected using OCT. The aim of this study was to relate the OCT scattering characteristics with ECM deposition in the airway wall.

Data were acquired as previously described [4]. The medical ethics committee of the AMC approved the protocol (NL51605.018.14) and informed consent was obtained. In brief, five patients scheduled for a lobectomy were included. From these five lobectomies, thirteen airways were dissected and marked with needles to match ex-vivo OCT images with histological sections. Ex-vivo OCT imaging was performed immediately after resection, using a C7 Dragonfly from St Jude Medical (St Paul, MN, USA). The OCT images were analysed using Matlab software (Natick MA, USA), which enabled the use of roll-off correction and the point spread function as previously described [7]. Three sequential frames were combined to minimize noise. Sheath and lumen segmentation were applied according to Adams et al. to minimize the influence of scattering intense components in the lumen [8]. OCT areas were calculated using a threshold in light scattering intensity, illustrated in **Figure 1**. To correct for probe optics and the imperfect sampling of the OCT system in depth, the fixed threshold was adjusted for the probe's distance to the airway wall in each axial line: a lower threshold was used in longer distances and vice versa.

Within each calculated OCT area, the median OCT intensity was measured. The histological sections were stained with Picosirius Red (TC; total collagen), Masson's Trichrome blue (MT blue; total collagen, bone), anti-collagen A1 antibody (CA1; collagen type 1 A1), Verhoeff's (EL; elastin) and anti-fibronectin antibody (FN; fibronectin). The region of interest (ROI) was defined as the area of the airway wall between the epithelium and the outer border of the desmin-positive smooth muscle. Sections without distortions within the ROI were included. The stained sections for each airway were aligned and colour deconvoluted using ImageJ [9]. Thereafter, the positive area and mean grayscale of the stained airway wall were calculated (threshold of >150 and mean of 0 – 255 grayscale intensity respectively). Associations were tested using linear mixed effects model with intercept per subject.

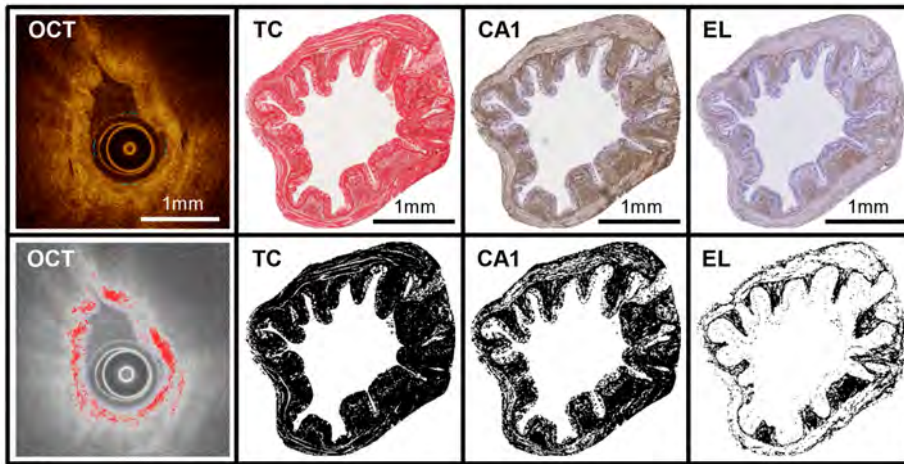


Figure 1. Three airway wall ECM staining sections aligned to the paired OCT-image. The upper panel shows the OCT image and matched histology sections, the lower panel shows the corresponding OCT threshold image and histology sections after color deconvolution. OCT: optical coherence tomography image after sheath and lumen segmentation (blue line), showing the area above the threshold (threshold adjusted per axial line for the distance between the lumen and the airway wall) in red, TC: total collagen, CA1: collagen A1, EL: elastin, all three stained sections with the area above the threshold (i.e. >150 of 255 grayscale) in black.

For in vitro experiments, 1x1x3cm plastic containers were printed with a 3D printer, then filled with 0,5ml 5% Gelatin methacrylamide (GelMA) and 0,5% Lithium acylphosphinate (LAP) photo-initiator, containing 1x10⁶ primary lung fibroblasts/ml. The gels were polymerized by UV light (405nm, 2x2 minutes). On one side of the container a droplet of 50µl containing 4,7mg Bovine Serum Albumin (BSA, Sigma Aldrich, the Netherlands), 4,7mg Elastin peptides (Biorbyt, UK), or 4,7mg/ml CA1 (Rat-tail Collagen I, Germany) was

applied. These droplets were mixed with 5% GelMA and polymerized, covered by 0,5ml 5% GelMA cell-mixture, and polymerized again. The container was subsequently perforated in order to insert the OCT probe. OCT images were captured, starting at the position where the proteins were added, followed by GelMA without proteins, and ending outside the container.

A total of 36 from the 51 OCT-histology pairs from the right upper lobe and left lower lobe were analysed. Reasons for exclusion were damaged histology sections (7 pairs), unavailability for additional staining (6 pairs), and OCT images of airway bifurcations (2 pairs). The mean lumen area of the included sections was 2.38 (± 2.06) mm². ECM component stained areas showed a similar spatial pattern as the OCT threshold measured area (**Figure 1**). Quantification of ECM component stained areas were positively correlated with the OCT area, while MT blue mean grayscale also correlated with OCT intensity (**Table 1**). In the in vitro studies, CA1 and elastin were detected using OCT, while BSA was not detected. (**Figure 2**). In the absence of exogenous protein no OCT signal was observed in the hydrogel.

Table 1 Regression coefficients paired OCT-histology areas and intensities

| | Optical Coherence Tomography area (mm ²) | | Optical Coherence Tomography intensity (arbitrary unit) | |
|-------------------------------------------------|------------------------------------------------------|------------------------------|---------------------------------------------------------|------------------------------|
| | B-value (95% CI) | P-value | B-value (95% CI) | P-value |
| Total collagen area (mm ²) | 0.39 (0.22-0.57) | 7.3 x 10⁻⁵ | - | - |
| Total collagen mean grayscale | - | - | 0.97 (-0.14-2.08) | 8.2 x 10 ⁻² |
| Masson's Trichrome blue area (mm ²) | 0.42 (0.23-0.62) | 1.4 x 10⁻⁴ | - | - |
| Masson's Trichrome blue mean grayscale | - | - | 0.58 (0.09-1.08) | 2.3 x 10⁻² |
| Collagen A1 area (mm ²) | 0.28 (0.09-0.48) | 5.8 x 10⁻³ | - | - |
| Collagen A1 mean grayscale | - | - | 0.19 (-0.89 - 1.26) | 7.0 x 10 ⁻² |
| Elastin area (mm ²) | 0.70 (0.39-1.01) | 2.8 x 10⁻⁴ | - | - |
| Elastin mean grayscale | - | - | 0.48 (-0.68-1.63) | 4.1 x 10 ⁻¹ |
| Fibronectin area (mm ²) | 0.49 (0.12-0.86) | 1.1 x 10⁻² | - | - |
| Fibronectin mean grayscale | - | - | 0.32 (-0.53-1.16) | 4.5 x 10 ⁻¹ |

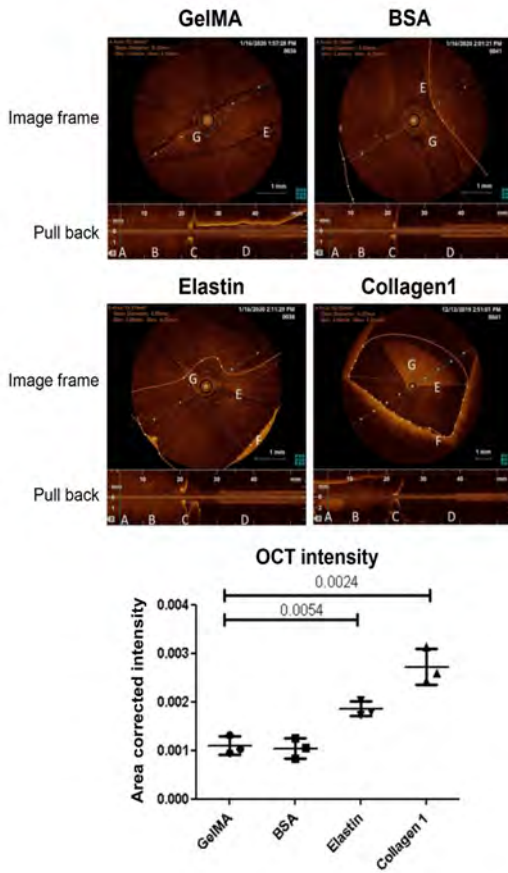


Figure 2. OCT images of plastic containers filled with cells (0,5ml 5% GelMA, 0,5% LAP), BSA (including a droplet of 50 μ l of 4,7mg BSA), Elastin (including 50 μ l of 4,7mg elastin peptides), and Collagen I (including 50 μ l of 4,7mg Rat-tail collagen). A: protein containing area, B: GelMA without protein, C: OCT probe leaving the container, D: OCT probe outside the container, E: boundary between different layers, F: plastic container reflection, G: measured OCT signal.

This study shows for the first time that OCT is able to detect and quantify ECM protein deposition in the airway wall. In other research areas focusing on skin and ovarian tissue, an association has been made between collagen deposition and OCT imaging [10,11]. In the airways however, OCT imaging studies have mainly focused on the identification and quantification of the airway wall structure. Intriguingly, elastin and fibronectin area correlated the strongest with OCT area, yet no significant difference was found between intensity parameters. Our findings that OCT may directly reflect ECM deposition, without the need of extracting biopsies is of interest in obstructive lung

diseases in which airway remodeling plays an important role. Furthermore, by assessing not only thickness but also ECM content of the airway wall, it might be possible to monitor treatments targeting airway remodeling in more detail, such as bronchial thermoplasty and liquid nitrogen spray.

An achievement of this study is the development of an automated analysis of the OCT image and light scattering intensity areas by threshold and segmentation technique. While in previous studies OCT areas were drawn manually, this study shows that a light scattering-based intensity threshold can be used to automatically identify and quantify ECM structures. Additionally, by combining this method with innovative polarization sensitive - OCT systems, it may be possible to analyse individual structural components of the airway wall with even greater accuracy [12].

A limitation needs to be addressed: in order to make a comparison between OCT and histology we used ex-vivo material. However, by using this approach we were able to assess ECM structures of the entire airway wall in a cross sectional manner, which would not be possible in-vivo. Despite this, a strong correlation between OCT light scattering areas and ECM stained components within the airways was found, which was validated in our in vitro studies.

In conclusion, our data shows that increased OCT intensity areas correspond to and correlate with higher ECM abundance in the airway wall. This suggests that it is possible to directly measure airway remodeling in vivo, in a minimally invasive, real-time manner.

References

- 1 Ito JT, Lourenço JD, Righetti RF, et al. Extracellular Matrix Component Remodeling in Respiratory Diseases: What Has Been Found in Clinical and Experimental Studies? *Cells* 2019;8:342.
- 2 Vignola AM, Kips J, Bousquet J. Tissue remodeling as a feature of persistent asthma. *J Allergy Clin Immunol* 2000;105:1041–53.
- 3 Benayoun L, Druilhe A, Dombret M-C, et al. Airway structural alterations selectively associated with severe asthma. *Am J Respir Crit Care Med* 2003;167:1360–8.
- 4 D’Hooghe JNS, Goorsenberg AWM, De Bruin DM, et al. Optical coherence tomography for identification and quantification of human airway wall layers. *PLoS One* 2017;12:1–13.
- 5 Ding M, Chen Y, Guan WJ, et al. Measuring Airway Remodeling in Patients With Different COPD Staging Using Endobronchial Optical Coherence Tomography. *Chest* 2016;150:1281–90.
- 6 Hariri LP, Adams DC, Applegate MB, et al. Distinguishing tumor from associated fibrosis to increase diagnostic biopsy yield with polarization-sensitive optical coherence tomography. *Clin Cancer Res* 2019;:clincanres.0566.2019.
- 7 Freund JE, Faber DJ, Bus MT, et al. Grading upper tract urothelial carcinoma with the attenuation coefficient of in-vivo optical coherence tomography. *Lasers Surg Med* 2019;51:399–406.
- 8 Adams DC, Pahlevaninezhad H, Szabari M V, et al. Automated segmentation and quantification of airway mucus with endobronchial optical coherence tomography. *Biomed Opt Express* 2017;8:4729–41.
- 9 Schneider CA, Rasband WS, Eliceiri KW. NIH Image to ImageJ: 25 years of image analysis. *Nat Methods* 2012;9:671–5. d
- 10 Ud-Din S, Foden P, Stocking K, et al. Objective assessment of dermal fibrosis in cutaneous scarring: using optical coherence tomography, high frequency ultrasound and immuno-histo-morphometry of human skin. *Br J Dermatol* 2019;:0–2.
- 11 Yang Y, Wang T, Biswal NC, et al. Optical scattering coefficient estimated by optical coherence tomography correlates with collagen content in ovarian tissue. *J Biomed Opt* 2011;16:090504.
- 12 Feroldi F, Davidoui V, Gräfe M, et al. In vivo multifunctional optical coherence tomography at the periphery of the lungs. *Biomed Opt Express* 2019;10(6):3070-3091

Chapter 9.

Bronchial Thermoplasty-Induced Acute Airway Effects Assessed with Optical Coherence Tomography in Severe Asthma

Goorsenberg AWM
d'Hooghe JNS
de Bruin DM
van den Berk IAH
Annema JT
Bonta PI

Respiration 2018;96(6):564-70

Abstract

Background Bronchial thermoplasty (BT) is an endoscopic treatment for severe asthma targeting airway smooth muscle (ASM) with radiofrequent energy. Although implemented worldwide, the effect of BT treatment on the airways is unclear. Optical coherence tomography (OCT) is a novel imaging technique, based on near-infrared light, that generates high-resolution cross-sectional airway wall images.

Objective To assess the safety and feasibility of OCT in severe asthma patients and determine acute airway effects of BT by OCT and compare these to the untreated right middle lobe (RML).

Methods Severe asthma patients were treated with BT (TASMA trial). During the third BT procedure, OCT imaging was performed immediately following BT in the airways of the upper lobes, the right lower lobe treated 6 weeks prior, and the untreated RML.

Results 57 airways were imaged in 15 patients. No adverse events occurred. Three distinct OCT patterns were discriminated: low-intensity scattering pattern of (1) bronchial and (2) peribronchial edema and (3) high-intensity scattering pattern of epithelial sloughing. (Peri)bronchial edema was seen in all BT-treated airways, and less pronounced in only 1/3 of the RML airways. These effects extended beyond the ASM layer and more distal than the directly BT-treated areas and were reduced, but not resolved, after 6 weeks. Epithelial sloughing occurred in 11/14 of the BT-treated airways and was absent in untreated RML airways.

Conclusions Acute BT effects can be safely assessed with OCT and 3 distinct patterns were identified. The acute effects extended beyond the targeted ASM layer and distal of directly BT-treated airway areas, suggesting that BT might also target smaller distal airways.

Introduction

Bronchial thermoplasty (BT) is a relatively new non-pharmacological treatment for severe asthma patients based on the delivery of radiofrequent energy to the airways [1]. BT was designed to target airway remodeling of the larger airways by reducing the airway smooth muscle (ASM) mass by thermal ablation. Besides preclinical studies, in recent years a reduction of the ASM mass has been reported in airway biopsies after BT treatment [2–5]. Randomized trials have shown that BT is safe and effective in reducing exacerbation rates in asthmatic patients and improving asthma-related quality of life [6–8]. However, these trials were not able to define a specific asthma phenotype that responds best to BT. Studies including the TASMA trial (ClinicalTrials.gov No.: NCT02225392) are underway to unravel the mechanism of action of BT to further define which phenotype of severe asthma patients might benefit most.

There is limited data available on the acute effects of BT on the airway wall. Two recent studies described radiological patterns including peribronchial consolidations after BT detected on computed tomography (CT) [9, 10]. However, the limitation in resolution makes it difficult to assess the exact nature and extent of acute effects in the airway wall. Optical coherence tomography (OCT) is a novel imaging technique in which near-infrared light is used to obtain cross-sectional, high-resolution images of the airway wall over a length of 5.4 cm [11–13]. Previous studies have shown a high correlation between histology and OCT for assessing and quantifying the airway wall [14, 15]. So far, in severe asthma, OCT has only been reported in 2 patients [16].

The aim of this study was to: (1) assess the safety and feasibility of OCT in a severe asthmatic patient cohort; (2) identify the acute effects of BT on the airway wall by OCT, and (3) compare these effects to the untreated right middle lobe (RML). We hypothesized that OCT is able to distinguish acute effects in BT-treated airways from non-BT-treated airways and that these effects resolve with time.

Methods

Design and Subjects

This observational study, conducted between July 2014 and February 2017, is part of the TASMA “Unravelling Targets of Therapy in Bronchial Thermoplasty in Severe Asthma” trial. The Medical Ethics Committee of the AMC provided ethical approval (NL45394.018.13). The study design is shown in **Figure 1**. Patients with severe refractory asthma according to the World Health Organization (WHO) guidelines and the Innovative Medicine Initiative (IMI) criteria were included in the TASMA trial [17, 18]. Written informed consent was provided.

Bronchial Thermoplasty

15 patients were treated with BT by using the Alair System (Boston Scientific, USA) according to the current standard [19–21] and sedated using remifentanyl/propofol [22]. Patients were treated with 50 mg of prednisolone 3 days before treatment, on the day of the procedure itself and 1 day thereafter. During the first procedure, the right lower lobe (RLL) was treated, during the second procedure the left lower lobe, and finally both upper lobes. The RML remained untreated.

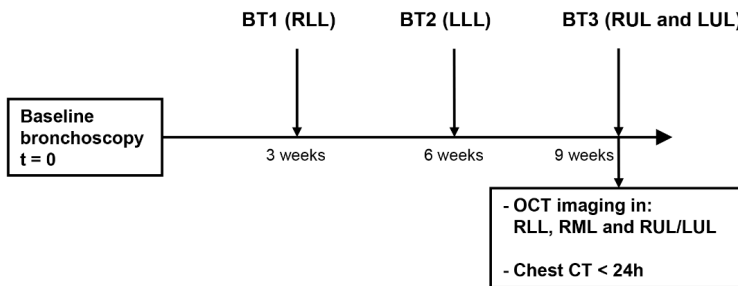


Figure 1. Flowchart of the study design. BT1, bronchial thermoplasty session 1, treatment of the right lower lobe (RLL); BT2, bronchial thermoplasty session 2, treatment of the left lower lobe (LLL); BT3, bronchial thermoplasty session 3, treatment of the right upper lobe (RUL) and left upper lobe (LUL); OCT, optical coherence tomography; RML, right middle lobe; CT, computed tomography.

Imaging

During the third BT procedure, OCT imaging was performed using a C7-XR St. Jude Medical Inc. system interfaced with a C7 Dragonfly catheter (diameter 0.9 mm; St. Jude Medical Inc., St. Paul, MN, USA). Directly after the BT procedure, the OCT catheter was inserted through the working channel of the bronchoscope using a guide sheath in the following (sub)segmental airways: first, 2 airways of the 6 weeks earlier treated RLL; subsequently, the untreated RML; and finally, 1 airway of the BT-treated left or right upper lobe. The proximal marker of the catheter, situated 5.4 cm from the distal tip, was inserted until the level of the segmental carina and was used as reference point. In each airway, an automated pullback, during which the OCT system automatically images the airway segment over a length of 5.4 cm, was performed twice. Low-dose chest CT was routinely performed directly or 1 day after the last procedure and airway reconstructions were made by an experienced chest radiologist using Impax Volume Viewing software (Agfa HealthCare, Mortsel, Belgium).

OCT Image Analysis

All OCT images and pullbacks were evaluated by one experienced OCT observer and confirmed by a second blinded observer and compared to normal

[15]. A set of OCT patterns detected directly after BT in the airway wall were identified. The presence or absence of these patterns was assessed for all imaged airways. Low-intensity scattering, depicted as black areas, within the airways corresponds to air, while within the airway wall itself the black areas correspond to fluid (i.e., edema or blood vessels). The first high-intensity scattering yellow layer of the airway wall corresponds to the mucosa and contains the epithelium and lamina propria as described by d'Hooghe et al. [15].

Statistical Analysis

GraphPad Prism version 5.01 (GraphPad Software Inc, San Diego, CA, USA) was used to calculate descriptive statistics. For normal distributed variables, a mean and standard deviation (SD) were given. Categorical characteristics were shown as a number and percentage.

Results

A total of 57 airways were imaged in 15 patients. Baseline characteristics are shown in **Table 1**. There were no adverse events reported related to OCT imaging and the added bronchoscopy time was 9.51 (± 1.17) min.

Three distinctive patterns were identified by OCT (**Fig. 2**; online suppl. video 1): a low-intensity scattering pattern within the (sub)mucosal layer of the airway wall, corresponding to bronchial wall edema (**Fig. 2c**); a broader pattern of low-intensity scattering beyond the cartilage of the airway wall corresponding to peribronchial edema (**Fig. 2c**); and a third high-intensity scattering pattern of epithelium sloughing in which the epithelium is (partly) disconnected from the airway wall (**Fig. 2d**).

The first pattern, bronchial wall edema, was seen in almost all airways imaged directly after BT (13/14; 93%). Both peribronchial edema and epithelial sloughing were detected in 11/14 (79%) airways (**Fig. 2**; **Table 2**). Both patterns of edema (peribronchial and bronchial) extended more distal than the directly BT-treated parts of the airways, which is limited to ~2–3 mm or larger diameter airways (**Fig. 2a**), indicating an acute BT effect more distal than the directly BT-treated areas. Furthermore, peri-bronchial edema extended beyond the cartilage rings of the airway wall, indicating an effect deeper than the BT-targeted ASM layer (**Fig. 2c**). Epithelial sloughing and edema (both peribronchial and bronchial) coincided directly after BT in almost all BT-treated airways, although epithelial sloughing occurred mainly in the proximal part of the airway, where the BT electrodes made contact with the airway wall, while edema was also shown in distal parts.

Table 1. Baseline characteristics

| | |
|----------------------------------------------|-----------|
| Subjects, <i>n</i> | 15 |
| Age, years | 38.1±13.6 |
| Male/female gender | 1/14 |
| FEV1 before BD, % | 91.3±23.0 |
| FEV1 after BD, % | 103.9±19 |
| LABA dose, µg/day salmeterol equivalents | 153±90.5 |
| ICS dose, µg/day fluticasone equivalents | 1167±497 |
| Patients on maintenance use of OCS, <i>n</i> | 6 |
| Oral prednisone dose, mg/day | 12.5±6.1 |
| Added bronchoscopy time for OCT imaging, min | 9.51±1.17 |
| Airways imaged, <i>n</i> | |
| Left upper lobe or right upper lobe | 14 |
| Right lower lobe | 29 |
| Middle lobe | 14 |

Presented data are shown as *n* or mean ± SD. FEV1, forced expiratory volume in 1 second before and after bronchodilation (BD) expressed in % of predicted; LABA, long-acting beta-2-agonist; ICS, inhaled corticosteroids; OCS, oral corticosteroids; OCT, optical coherence tomography.

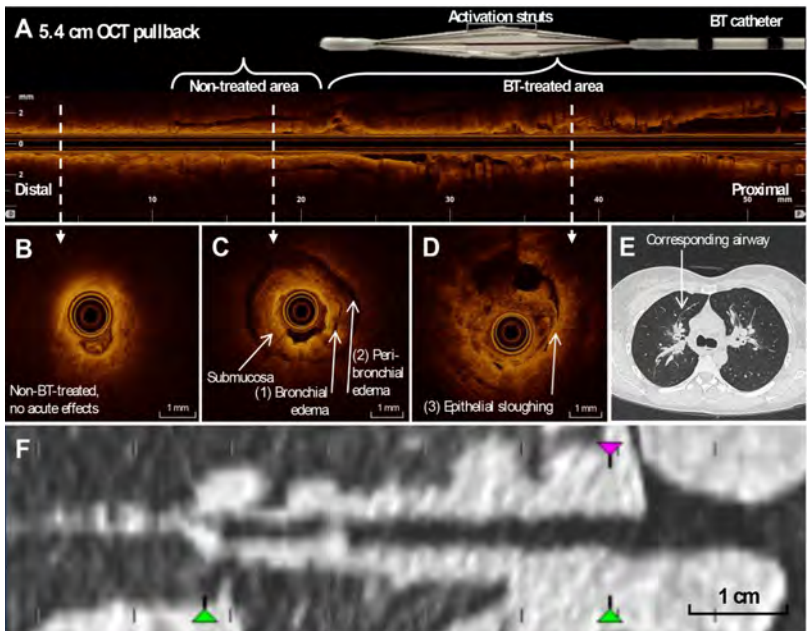


Figure 2. Optical coherence tomography (OCT) characteristics in comparison to computed tomography (CT) in the anterior segment of the right upper lobe (RB3) after bronchial thermoplasty (BT). a Pullback of 5.4 cm with an airway

diameter of ~1 to 3.5 mm. **b** A non-BT-treated airway area without acute effects of BT. **c** A distal non-BT-treated airway area with (1) bronchial and (2) peribronchial edema. **d** Epithelial sloughing in a directly BT-treated area. **e** CT image directly after BT showing peribronchial consolidations in RB3 corresponding to the OCT pullback. **f** Reconstructed CT image showing the same airway segment as in a–d.

Next, we compared the acute OCT effects in directly BT-treated airways with the 6 weeks earlier BT-treated airways of the RLL and the non-BT-treated RML (as control). All 3 patterns of acute effects were identified in a lower proportion of the RLL airways 6 weeks after treatment: 9 of 29 (31%) airways showed bronchial wall edema, 18 of 29 (62%) showed peribronchial edema, and 1/29 (3%) showed signs of epithelial sloughing (**Table 2**). For bronchial wall edema, the low-intensity scattering pattern of edema was less pronounced (dark grey instead of black) (**Fig. 3b**), compared to OCT-imaged airways immediately after treatment (**Fig. 3a**). In the untreated airways of the RML, bronchial edema was present in only 1/3 of patients and in these 1/3 less pronounced as compared to the peribronchial edema seen in upper lobe airways directly after BT treatment. Epithelial sloughing did not occur in untreated airways (**Table 2**).

The OCT-detected BT effects in the different bronchial wall layers could not be distinguished on corresponding reconstructed CT images (**Fig. 2f**). Consistent with previous published reports by this group and others [9, 10], on CT peribronchial consolidations were seen directly after BT and this CT pattern in these airway segments corresponded with the (peri)bronchial edema pattern seen on OCT imaging. Due to the limited resolution of reconstructed CT and/or CT analysis software, no direct correlation with the OCT pattern of epithelial sloughing and any pattern in the smaller airways could be made.

Table 2. OCT patterns after BT

| OCT patterns | Acute airways (RUL or LUL) 14 airways | 6 weeks after BT (RLL) 29 airways | Untreated (RML) 14 airways |
|-----------------------------------------------------------------|---------------------------------------------|-----------------------------------------|----------------------------------|
| Low-intensity scattering pattern of bronchial edema | 13 (93) | 9 (31) | 5 (36) |
| Low-intensity scattering pattern of peribronchial edema | 11 (79) | 18 (62) | 2 (14) |
| High-intensity scattering pattern of epithelial sloughing | 11 (79) | 1 (3) | 0 (0) |

Findings presented as n (%). BT, bronchial thermoplasty; OCT, optical coherence tomography; RUL, right upper lobe; LUL, left upper lobe; RLL, right lower lobe; RML, right middle lobe.

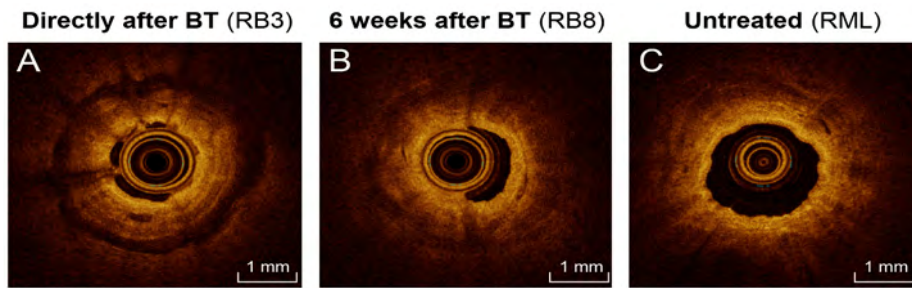


Fig. 3. Optical coherence tomography (OCT) imaging immediately and 6 weeks after bronchial thermoplasty (BT) of BT-treated airways and of the untreated RML. OCT images captured in 1 procedure, in 1 patient, of the anterior segment of the right upper lobe (RB3) immediately after BT (a); the anterior basal segment (RB8) of the right lower lobe 6 weeks after treatment (b); and the BT-untreated right middle lobe (RML) (c).

Discussion

This OCT imaging study is the first study showing that OCT is safe and feasible in a cohort of severe asthmatic patients. Three distinct OCT patterns directly after BT treatment were identified: 2 low-intensity scattering patterns corresponding to bronchial and peribronchial edema and 1 high-intensity scattering pattern of epithelial sloughing. These patterns extended beyond the BT-targeted ASM layer and diminished over time. Interestingly, OCT-imaged acute BT treatment effects were detected distal to the directly BT-treated airway areas extending to the smaller airways.

Almost all airways directly after BT showed a pattern of edema and epithelial sloughing. In the untreated RML, edema was also present in a substantial but reduced proportion, less pronounced, and without signs of epithelial damage. None of these effects were seen in earlier published OCT data in asthmatic [16, 23] and non-asthmatic airways [12, 15], indicating that the identified effects were most likely related to BT treatment. The identified acute OCT effects in airways directly treated with BT are in line with previously published CT imaging studies in severe asthma patients in which CT was performed immediately after BT and peribronchial consolidations with ground glass opacities were described in almost all treated lobes [9, 10]. This study shows acute effects of BT not only in directly BT-treated airway areas but also in more distal non-BT-treated airway areas.

OCT imaging showed abnormalities in non-BT-treated airways, a phenomenon which also has been observed on CT imaging after BT [9, 10]. There are several hypotheses formulated explaining non-BT-treated acute effects detected on CT: a heat shock effect along the bronchial tree, heat extension through (incomplete)

fissures or distribution of mucus, blood, and secretions to the lower lobes as a result of BT treatment in the upper lobes [10, 24]. In the absence of histology directly after BT, it is uncertain which mechanism is correct. Moreover, it is unclear whether the described effects contribute to treatment response or should be considered a side effect of treatment. One study has shown a decrease of ASM after BT in the untreated RML, suggesting that the effect seen in the RML might contribute to treatment response [5]. These results, however, could not be confirmed in a subsequent larger study [4]. Histology studies are needed to assess whether untreated distal airway areas are affected by BT as well.

The described OCT patterns were less pronounced in the airways imaged 6 weeks after BT. This corresponds to the results of a previous study in which, based on histology of lobectomy samples, epithelial sloughing was found in 3 out of 8 non-asthmatic patients 3 weeks after BT [25], while another study showed no signs of epithelial damage 3 months after BT [4]. It is therefore plausible that epithelial damage is a direct effect of BT and resolves within 3–6 weeks. The repair or regeneration of the airway wall epithelium after being disrupted by BT could potentially contribute to the increased epithelial integrity 6 weeks after BT, found in a recent published study [26].

While the mechanism of action of BT is incompletely understood, several elements of the airway wall have been postulated to influence treatment response to BT [27]. By demonstrating a BT effect with OCT imaging in the mucosa, submucosa, and peribronchial area of the airway wall, it is well possible that the structures within these layers, such as the epithelium, ASM, and nerves, are modulated by BT. Additionally, small airway dysfunction is of importance in the pathophysiology of asthma [28]. By showing a BT treatment effect in the distal parts of the BT-treated airways, the OCT findings suggest that BT treatment might also have an impact on the smaller airways.

A limitation of this study is that the untreated RML was originally designed as the control but unexpectedly showed effects of treatment as well. One could argue whether the shown effects were a result of BT treatment alone or if they could also appear after manipulation of asthmatic airways with a bronchoscope, although the RML was not manipulated during BT itself. Indeed, the majority of airways of the RML did not show OCT patterns of edema, making it more plausible that the observed effects are a result of being adjacent to the treated upper lobes as described in previous CT studies. This could also explain the earlier reported less prominent decrease of ASM in the untreated RML [4]. Strong points of the current data are the large sample size and detailed high-resolution airway wall imaging in various stages after BT treatment during 1 session. Additionally, by performing both CT and OCT imaging after BT, it was possible to compare, in several airways, both techniques, thereby showing the additional value of more detailed real-time imaging of the airway wall by OCT when compared to CT.

In conclusion, this study showed that OCT is feasible and safe in severe asthmatic patients. Three patterns of acute BT effects were identified corresponding to a low-intensity scattering pattern of (peri)bronchial edema and a high-intensity scattering pattern of epithelial sloughing. OCT was able to assess the acute effects of BT on the airways in more detail than CT and showed an effect in distal non-BT-treated airway areas and to a lesser extent in the non-BT-treated RML as well. Whether these effects contribute to treatment response remains to be investigated.

References

1. Chung KF, Wenzel SE, Brozek JL, Bush A, Castro M, Sterk PJ, Adcock IM, Bateman ED, Bel EH, Bleecker ER, Boulet LP, Brightling C, Chanez P, Dahlen SE, Djukanovic R, Frey U, Gaga M, Gibson P, Hamid Q, Jajour NN, Mauad T, Sorkness RL, Teague WG: International ERS/ATS guidelines on definition, evaluation and treatment of severe asthma. *Eur Respir J* 2014;43:343–373.
2. Chakir J, Haj-Salem I, Gras D, Joubert P, Beaudoin EL, Biardel S, Lampron N, Martel S, Chanez P, Boulet LP, Laviolette M: Effects of bronchial thermoplasty on airway smooth muscle and collagen deposition in asthma *Ann Am Thorac Soc* 2015;12:1612–1618.
3. Denner DR, Doeing DC, Hogarth DK, Dugan K, Naureckas ET, White SR: Airway inflammation after bronchial thermoplasty for severe asthma. *Ann Am Thorac Soc* 2015;12: 1302–1309.
4. Pretolani M, Bergqvist A, Thabut G, Dombret MC, Knapp D, Hamidi F, Alavoine L, Taille C, Chanez P, Erjefalt JS, Aubier M: Effectiveness of bronchial thermoplasty in patients with severe refractory asthma: clinical and histopathologic correlations. *J Allergy Clin Immunol* 2017;139:1176–1185.
5. Pretolani M, Dombret MC, Thabut G, Knap D, Hamidi F, Debray MP, Taille C, Chanez P, Aubier M: Reduction of airway smooth muscle mass by bronchial thermoplasty in patients with severe asthma. *Am J Respir Crit Care Med* 2014;190:1452–1454.
6. Castro M, Rubin AS, Laviolette M, Fiterman J, De Andrade Lima M, Shah PL, Fiss E, Olivenstein R, Thomson NC, Niven RM, Pavord ID, Simoff M, Duhamel DR, McEvoy C, Barbers R, Ten Hacken NH, Wechsler ME, Holmes M, Phillips MJ, Erzurum S, Lunn W, Israel E, Jarjour N, Kraft M, Shargill NS, Quiring J, Berry SM, Cox G; AIR2 Trial Study Group: Effectiveness and safety of bronchial thermoplasty in the treatment of severe asthma: a multicenter, randomized, double-blind, sham-controlled clinical trial. *Am J Respir Crit Care Med* 2010;181: 116–124.
7. Cox G, Thomson NC, Rubin AS, Niven RM, Corris PA, Siersted HC, Olivenstein R, Pavord ID, McCormack D, Chaudhuri R, Miller JD, Laviolette M; AIR2 Trial Study Group: Asthma control during the year after bronchial thermoplasty. *N Engl J Med* 2007;356: 1327–1337.
8. Pavord ID, Cox G, Thomson NC, Rubin AS, Corris PA, Niven RM, Chung KF, Laviolette M; RISA Trial Study Group: Safety and efficacy of bronchial thermoplasty in symptomatic, severe asthma. *Am J Respir Crit Care Med* 2007;176:1185–1191.
9. d’Hooghe JNS, van den Berk IAH, Annema JT, Bonta PI: Acute radiological abnormalities after bronchial thermoplasty: a prospective cohort trial. *Respiration* 2017;94:258–262.
10. Debray MP, Dombret MC, Pretolani M, Thabut G, Alavoine L, Brillet PY, Taille C, Khalil A, Chanez P, Aubier M: Early computed tomography modifications following bronchial thermoplasty in patients with severe asthma. *Eur Respir J* 2017;49:1601565.
11. Coxson HO, Quiney B, Sin DD, Xing L, Mc-Williams AM, Mayo JR, Lam S: Airway wall thickness assessed using computed tomography and optical coherence tomography. *Am J Respir Crit Care Med* 2008;177:1201–126.

12. Ding M, Chen Y, Guan WJ, Zhong CH, Jiang M, Luo WZ, Chen XB, Tang CL, Tang Y, Jian QM, Wang W, Li SY, Zhong NS: measuring airway remodeling in patients with different COPD staging using endobronchial optical coherence tomography. *Chest* 2016; 150: 1281–1290.
13. Huang D, Swanson EA, Lin CP, Schuman JS, Stinson WG, Chang W, Hee MR, Flotte T, Gregory K, Puliafito CA, et al: Optical coherence tomography. *Science* 1991;254:1178– 1181.
14. Chen Y, Ding M, Guan WJ, Wang W, Luo WZ, Zhong CH, Jiang M, Jiang JH, Gu YY, Li SY, Zhong NS: Validation of human small airway measurements using endobronchial optical coherence tomography. *Respir Med* 2015; 109:1446–1453.
15. d’Hooghe JNS, Goorsenberg AWM, de Bruin DM, Roelofs J, Annema JT, Bonta PI: Optical coherence tomography for identification and quantification of human airway wall layers. *PLoS One* 2017;12:e0184145.
16. Kirby M, Ohtani K, Lopez Lisbona RM, Lee AM, Zhang W, Lane P, Varfolomeva N, Hui L, Ionescu D, Coxson HO, MacAulay C, FitzGerald JM, Lam S: Bronchial thermoplasty in asthma: 2-year follow-up using optical coherence tomography. *Eur Respir J* 2015;46: 859–862.
17. Bousquet J, Mantzouranis E, Cruz AA, Ait- Khaled N, Baena-Cagnani CE, Bleecker ER, Brightling CE, Burney P, Bush A, Busse WW, Casale TB, Chan-Yeung M, Chen R, Chowdhury B, Chung KF, Dahl R, Drazen JM, Fabbri LM, Holgate ST, Kauffmann F, Haahtela T, Khaltaev N, Kiley JP, Masjedi MR, Moham- mad Y, O’Byrne P, Partridge MR, Rabe KF, Togias A, van Weel C, Wenzel S, Zhong N, Zuberbier T: Uniform definition of asthma severity, control, and exacerbations: document presented for the World Health Organi- zation Consultation on Severe Asthma. *J Allergy Clin Immunol* 2010;126:926–938.
18. Bel EH, Sousa A, Fleming L, Bush A, Chung KF, Versnel J, Wagener AH, Wagers SS, Sterk PJ, Compton CH; Unbiased Biomarkers for the Prediction of Respiratory Disease Out- come (U-BIOPRED) Consortium, Consensus Generation: Diagnosis and definition of severe refractory asthma: an international consensus statement from the Innovative Medicine Initiative (IMI). *Thorax* 2011;66:910– 917.
19. d’Hooghe JNS, Ten Hacken NHT, Weersink EJM, Sterk PJ, Annema JT, Bonta PI: Emerging understanding of the mechanism of action of bronchial thermoplasty in asthma. *Pharmacol Ther* 2018;181:101–107.
20. Cox G, Miller JD, McWilliams A, Fitzgerald JM, Lam S: Bronchial thermoplasty for asth- ma. *Am J Respir Crit Care Med* 2006;173: 965–969.
21. Bonta PI, Chanez P, Annema JT, Shah PL, Niven R: Bronchial thermoplasty in severe asthma: best practice recommendations from an expert panel. *Respiration* 2018, DOI 10.1159/000488291.
22. d’Hooghe JN, Eberl S, Annema JT, Bonta PI: Propofol and remifentanyl sedation for bronchial thermoplasty: a prospective cohort trial. *Respiration* 2017;93:58–64.
23. Adams DC, Hariri LP, Miller AJ, Wang Y, Cho JL, Viliger M, Holz JA, Szabari MV, Hamilos DL, Scott Harris R, Griffith JW, Bou- ma BE, Luster AD, Medoff BD, Suter MJ: Birefringence microscopy platform for assess- ing airway smooth muscle structure and function in vivo. *Sci Transl Med* 2016;8:359ra131.
24. d’Hooghe JNS, Bonta PI, van den Berk IAH, Annema JT: Radiological abnormalities

- following bronchial thermoplasty: is the pathophysiology understood? *Eur Respir J* 2017;50: 1701537.
- 25 Miller JD, Cox G, Vincic L, Lombard CM, Loomas BE, Danek CJ: A prospective feasibility study of bronchial thermoplasty in the human airway. *Chest* 2005;127:1999–2006.
 - 26 Chernyavsky IL, Russell RJ, Saunders RM, Morris GE, Berair R, Singapuri A, Chachi L, Mansur AH, Howarth PH, Dennison P, Chaudhuri R, Bicknell S, Rose FRAJ, Siddiqui S, Brook BS, Brightling CE: In vitro, in silico and in vivo study challenges the impact of bronchial thermoplasty on acute airway smooth muscle mass loss. *Eur Respir J* 2018; 51:1701680.
 - 27 d’Hooghe JNS, Ten Hacken NHT, Weersink EJM, Sterk PJ, Annema JT, Bonta PI: Emerging understanding of the mechanism of action of bronchial thermoplasty in asthma. *J Pharmacol Ther* 2017;181:101–107.
 - 28 van der Wiel E, ten Hacken NH, Postma DS, van den Berge M: Small-airways dysfunction associates with respiratory symptoms and clinical features of asthma: a systematic review. *J Allergy Clin Immunol* 2013;131:646– 657.

Part IV.

Discussion

Chapter 10.

Summary and general discussion

Background

Asthma is a chronic inflammatory airways disease with over 300 million people diagnosed worldwide [1]. Although most people suffer from mild disease, around 5% of the asthmatic population is suffering from severe asthma [2-5]. In these patients, asthma remains uncontrolled despite optimal treatment including treatment of co-morbidities, evaluating compliance and using high dose inhaled and / or systemic corticosteroids [6, 7]. The socio-economic burden and health care costs of the total asthma population but in particular severe asthma patients is huge and novel treatments are necessary [8-11].

Novel pharmacological treatment options for severe asthma have been developed in the last decade such as anti-immunoglobuline E (IgE) [12] for allergic asthma and anti-interleukin-5 (IL-5), anti-interleukin-4 (IL-4) and anti-interleukin-13 (IL-13) receptor [13-16] for eosinophilic asthma. A non-pharmacological, endoscopic treatment option for severe asthma is bronchial thermoplasty (BT). BT uses radiofrequency energy to target airway remodeling of the medium to larger sized airways [17]. While the clinical effectiveness of this treatment has been shown by several trials [18-20], treatment response varies and a clear responder phenotype has not yet been established. Treatment guidelines currently suggest BT as treatment option for severe asthma patients who remain uncontrolled despite optimal therapy or for patients who were not eligible for biological treatments [8, 21].

In order to optimally incorporate BT in asthma guidelines it is highly important to define the patient phenotype or characteristics associated with a treatment response. When BT received FDA approval in 2010, the general hypothesis was that it would improve asthma symptoms by reducing airway smooth muscle (ASM) mass. The effect of BT on ASM mass was however not yet established. In addition, it was not clear whether patients should be selected based on a higher amount of ASM mass. These are both questions that the *Unravelling Targets of Therapy in Bronchial Thermoplasty in Severe Asthma* TASMA trial aimed to answer (ClinicalTrials.gov, NCT02225392). The international multicenter TASMA trial is an investigator initiated randomized controlled trial in which 40 severe asthma patients were extensively phenotyped and randomized into a direct BT treatment group or a 6 months delayed, control group. Next to the effect of BT on ASM mass, this trial also intends to investigate the effect of BT on other airway wall structures such as the extra cellular matrix (ECM) and inflammation. In addition, novel imaging techniques to assess the airway wall and airway remodeling, such as optical coherence tomography (OCT), are investigated. The inclusion of the TASMA study was completed in July 2018. In this thesis several research questions are answered based on the available data.

This thesis consists of four parts. **Part I** consists of the general introduction and aims of this thesis (chapter 1). In **Part II** the effect of BT on clinical parameters,

ASM mass and bronchial epithelial cells is investigated with an emphasis on clinical characteristics associated with a favorable BT-response (chapters 2-5). **Part III** focuses on airway wall imaging with OCT in order to assess airway remodeling and immediate effects of BT on the airway structure (chapters 6-9). The final part of this thesis, **Part IV**, contains the summary and general discussion (chapters 10-11). In this last part of the thesis, the research questions are discussed and key findings and future perspectives are provided.

Research question 1 (Chapter 2 and 3): What is the influence of bronchial thermoplasty (BT) on airway smooth muscle (ASM) mass? Is the effect on ASM mass correlated with response to BT?

A reduction of ASM mass after BT was first shown in dogs by Danek et al. [22], and shortly thereafter in ex-vivo lung specimens of lung cancer patients [23]. This effect however was not yet investigated in severe asthma patients when the TASMA study started in 2014 and encouraged the need for a randomized controlled design to obtain high-level evidence.

Since the first two biopsy studies, several research groups published observational study results which reported a reduction of ASM mass after BT. The first study that reports on this in severe asthma patients was performed by Pretolani et al. [24]. In a preliminary report of 10 severe asthma patients a reduction of ASM mass between 48.7% and 78.5% was found 3 months after BT. In 2017, the results in all patients (n=15) were published confirming a reduction in ASM as result of BT [25]. Two other studies found similar results in respectively 11 patients 6 weeks after BT [26] and 17 patients 3 weeks after BT [27]. While Pretolani et al. and Denner et al. used alpha smooth muscle actin stain (α -SMA) to measure ASM mass in endobronchial biopsies, Chakir et al. used Masson Trichrome. None of these studies involved a control group, which hampered a correlation with clinical outcome.

In **Chapter 2** we show initial results of ASM mass decrease in 18 severe asthma patients from the TASMA study. Biopsies were analyzed at inclusion and 6 months after BT treatment. We used both desmin and α -SMA staining to assess ASM mass as this would strengthen the results and also enables comparison with previous studies. Our results showed >50% reduction of desmin positive ASM mass and approximately 40% reduction of α -SMA positive ASM mass. At present α -SMA is the most commonly used technique to measure ASM mass. In our experience automated analysis techniques are difficult to interpret with α -SMA as this not only stains the ASM but also pericytes in capillaries, myoepithelial cells surrounding glands and myofibroblasts in the mucosa and perivascular areas. Desmin on the other hand seems to only stain the contractile ASM areas. It is therefore not surprising that ASM mass percentages of α -SMA stained biopsies are higher than desmin stained biopsies. In our opinion, desmin

is the most appropriate technique to use to evaluate treatment effects of BT.

While all above mentioned studies showed a decrease of ASM mass after BT, appropriate control groups were lacking. In **Chapter 3** we report for the first time a reduction of ASM mass after BT in a randomized controlled design. After a screening period including endobronchial biopsy sampling, 40 patients were randomized into a direct BT group and a delayed treatment group. The direct BT group received BT treatment and was sampled again 6 months after BT. The delayed group served as control group, these patients waited for 6 months while on standard clinical care and stable medication use. After these 6 months endobronchial biopsies were sampled and patients received BT treatment. In addition, patients were seen 6 months after BT and biopsies were taken again. The effect of BT in the immediate group was compared with the delayed group at 6 months after baseline: in the immediate group a reduction of ASM mass was seen of > 50% while in the delayed control group no change was observed. An important difference in our study compared to previous published biopsy studies is the location of biopsies. All previous studies sampled the same location or airway before and after BT for comparison [24-27]. In the TASMA study we sampled pre-defined carinas which were not sampled before in order to avoid analyzing the effect of sampling instead of the treatment. A potential limitation of this method might be variation of ASM mass between airways, however a previous study showed no significant variation in ASM mass between different lobes [24].

A possible effect of BT on ASM mass in the untreated RML remains an interesting question. While preliminary results of Pretolani et al. showed a reduction of ASM in the untreated RML as well [24], these results were not confirmed in the larger population of 15 severe asthma patients [25]. In **Chapter 3** we report results of the entire patient cohort before and after BT. Biopsies in the RML were taken only during the 6 months post BT timepoint to avoid sampling the same location twice. Biopsies of the RML were available in 33 patients and showed significantly lower ASM mass in the RML in comparison with the treated parts of the airways. Although the data had a large spread, it is interesting to see that the reduction in the ASM mass of the RML was more pronounced in the segmental biopsies compared to the subsegmental biopsies. In combination with the pattern of BT induced abnormalities seen on radiology [28, 29] and OCT imaging (**Chapter 9**) it seems plausible that also non treated parts of the airways, such as the RML, are influenced by BT. With only two studies investigating the RML and both using a different sampling method, it remains unclear whether the difference is indeed caused by BT or whether these airways had a lower ASM mass at baseline already.

The combination of several observational studies and our randomized controlled trial has given sufficient evidence to conclude that BT indeed reduces ASM mass in severe asthma patients. The significant lower ASM mass in the untreated RML in our patient cohort needs to be interpreted with care.

Although there is compelling evidence that ASM mass reduces after BT, the question remains whether the amount of ASM mass predicts response. In our severe asthma patients from the TASMA study we did not find associations between ASM mass at baseline, ASM mass change or ASM mass after BT and improvements in ACQ-6 or AQLQ scores. An association between ASM mass and decline in exacerbation rate after BT needs to be further investigated. Although the study was not powered to predict response, finding no trend of an association does raise the concern that ASM at least by itself is not the most important driver of response.

Research question 2 (Chapter 2, 3, 5): What is the response of severe asthma patients after BT treatment? Can we identify patient characteristics that are associated with a favorable response?

The efficacy of BT treatment has been subject of debate since the AIR-2 multicenter sham controlled randomized trial was published in 2010 [19]. In this study almost 300 severe asthma patients were randomized into a BT group and a sham group in a 2:1 ratio. The primary endpoint was the difference in asthma related quality of life (AQLQ) scores from baseline to 6, 9 and 12 months after BT or sham procedures. When comparing both groups, AQLQ was significantly more improved in the BT group versus the sham group. This difference however did not reach a difference of more than 0.5 points which is the minimal clinically important difference on AQLQ scores [30]. Although significantly more patients in the BT group showed improvements in AQLQ scores and exacerbation rates, the large placebo effect observed in the sham treatment group in combination with uncertainty on the responder profile and mechanism of action of BT has led to challenges in the implementation of this treatment. In addition, the implementation of several new biologics for severe asthma and the lack of comparative BT versus biologic therapy trials, further complicated its position in severe asthma treatment guidelines.

In **Chapter 3** we report significant and clinically important improvements in both ACQ-6 and AQLQ scores in the BT-treatment group compared with the delayed control group. In the total group of 35 patients, 60% showed a clinically relevant improvement in asthma questionnaires while almost all patients had a decline in exacerbation rate. Although the TASMA study has no sham treatment group, the difference between the changes in the immediate BT treatment group compared to the delayed BT group is significant and comparable to other studies.

As currently several biological treatment options are available for specific asthma phenotypes it is of importance to define the asthma phenotype for BT treatment as well. In **Chapter 2** we investigated this by correlating FEV₁ with ASM mass at baseline and/or change after BT. One other study by Chakir et

al. reported previously about the higher reduction of ASM mass in patients with higher ASM mass at baseline [27]. The preliminary results of **Chapter 2** showed that patients with lower FEV₁ values have more ASM mass at baseline and that these more obstructive patients have more ASM mass reduction after BT. As a consequence, one could argue that these more obstructive patients are the optimal patients for BT treatment. However, response analysis in 35 patients from **Chapter 3** did not confirm this hypothesis. We explored associations between ACQ-6 and AQLQ improvements after BT and patient characteristics at baseline. Next to ASM mass, we explored associations with age of onset, total IgE, blood eosinophils, lung function parameters and bronchial hyperresponsiveness as assessed with methacholine challenge tests. Statistically significant associations were found between improvements in asthma questionnaires and higher levels of total IgE and eosinophils at baseline. In addition, data in a smaller cohort of patients from **Chapter 5** reported that patients with a lower respiratory resistance measured with FOT showed more improvement on asthma questionnaires when compared to patients with a high respiratory resistance. A hypothesis for this effect might be that BT directly targets the larger airways while respiratory resistance is also influenced by the smaller airways.

One other research group investigated the prediction of BT response in severe asthma patients in a cohort of 77 patients [31]. In this Australian study, no associations were found between response, assessed with ACQ scores, and blood IgE or eosinophils. The only potential predictor for response in this study was a higher ACQ score at baseline. This association was not studied in the TASMA population however it is not surprising that a higher ACQ score at baseline is associated with more improvement after treatment. Reason for discrepancies between the TASMA results and this Australian study might be the difference in study population: the Australian patients were more obstructive (mean FEV₁ of $55.8 \pm 19.8\%$), more patients used maintenance oral corticosteroids (50% compared to 25% in the TASMA study) and a larger proportion of patients was treated with monoclonal antibodies (43% compared to 12.5% in the TASMA population).

Another potential predictor of response is the amount of activations [32]. In our analysis we did not find this association. Differences in the amount of activations between patients were however small and maybe therefore not associated with response.

To summarize, several potential response predictors have been identified but validation in larger patient cohorts are missing. As the exact mechanism of action of BT is still unclear and the optimal patient candidate not yet established, implementation of BT treatment in current asthma guidelines remains hampered.

Research question 3 (Chapter 4): What is the influence of BT on metabolic gene expression profiles of bronchial epithelial cells?

One of the hypotheses on the working mechanism of BT is that BT might influence the epithelium layer by inducing regeneration. In **Chapter 9** we reported epithelial sloughing on OCT images as a direct result of BT-treatment suggesting a potential effect on the epithelium layer by BT. Histology studies have shown conflicting results regarding epithelium regeneration and integrity after BT [25, 33]. One study used immunohistochemistry on endobronchial biopsies before and after BT and found that MUC5AC and IL-13 expression, associated with mucus hypersecretion, was reduced after 3 weeks and up to 12 months after BT [34]. It is suggested in this study that after BT, the epithelium regenerates to a state with increased airway epithelium integrity.

To further investigate the effect of BT on the epithelium layer we conducted the study in **Chapter 4**. First we compared the metabolic gene expression profile of severe asthma patients with healthy controls. We found a downregulation of metabolic phosphorylation genes and an upregulation of glycolysis-related genes in severe asthma compared to healthy participants. In addition, we sampled primary bronchial epithelium cells 6 months after BT treatment and we compared differentially expressed genes in treated airways with the untreated right middle lobe. Genes associated with oxidative phosphorylation were significantly upregulated in the treated airways as compared to the untreated right middle lobe while glycolysis genes were downregulated in the treated airways. These results suggest that BT induces a change in the epithelium cells towards a more healthy state.

This ‘reprogramming’ of bronchial epithelium cells has also been reported by another study. In 23 severe asthma patients, transcriptome analyses were performed on isolated bronchial epithelial cells both before and after BT treatment [35]. In addition, broncho-alveolar lavage fluid was collected to perform proteome analysis. Results from this study suggested that before BT mitochondrial and fibroblast proliferation were stimulated by the expression of protein arginine methyltransferase-1 (PRMT1) which in its turn is regulated by heat shock protein-60 (HSP60). After BT, a reduction of HSP60 was found and subsequently less expression of PRMT1. According to the authors, reducing the function of epithelial cells and thereby decreasing the amount of remodeling caused by fibroblasts be the mechanism explaining the sustained reduction of airway remodeling after BT.

The benefit of using these expensive omics technologies is to better understand the mechanisms involved in severe asthma patients and BT treatment but moreover to link these (molecular) findings to clinical parameters and treatment response.

Research question 4 (Chapter 5): What is the impact of BT on lung function parameters?

The first large clinical trials of severe asthma patients treated with BT showed favorable effects of BT on asthma symptom scores, quality of life, exacerbation rates, emergency department visits and use of rescue medication [18-20]. Results in lung function measurements however are conflicting with only the RISA trial showing a benefit in FEV₁ [20]. Long-term follow-up studies and registries confirm these results with stable FEV₁ values between 3 to 5 years after BT [36-39]. In summary, on the long-term BT does not seem to have harmful effects on lung function parameters.

As conventional lung function measurements such as spirometry and bodyplethysmography have limitations in distinguishing larger and smaller airway involvement, we investigated the effect of BT on lung function in **Chapter 5** with an additional technique, forced oscillation (FOT). FOT uses pressure oscillations to measure the resistance of the entire respiratory system in an effort independent manner [40]. Oscillation techniques such as FOT and impulse oscillometry (IOS) are believed to be more accurate than conventional lung function tests in evaluating small airways disease [41, 42].

The results of **Chapter 5** showed that in a group of more than 20 severe asthma patients, no significant changes in spirometry, bodyplethysmography and FOT measurements occurred 6 months after BT. This is similar to an Australian cohort in which impulse oscillometry (IOS) was used to investigate changes after BT and no difference was observed as well [43]. Difficulties in the interpretation of these results have to be acknowledged. FOT is not used in standard clinical care and therefore clear normal values are not yet established. In addition, the evidence regarding the use of different oscillation frequencies to differentiate between small and large airways disease is mainly limited to animal studies [44, 45].

In contrast to our findings, one recently published study reported a significant reduction of plethysmography measured airway resistance after BT [46]. A possible explanation for the difference in findings is that airway resistance in the other study was already three times higher at baseline than the airway resistance in the TASMA study. In addition, in the study of Langton et al. an influence of high doses of oral corticosteroids (given before and after the BT-procedures) on the plethysmography measurements cannot be excluded as airway resistance was measured only 6 weeks post BT as opposed to 6 months after BT in the TASMA trial.

An interesting finding in our study was that while FEV₁ did not significantly change in the whole group, it did seem to improve in the patients that responded well to BT. The patient cohort is only small with 22 (ACQ) and 23 (AQLQ) patients but it might be important for other research groups to look into this association

as well. One other Australian study in BT treated severe asthmatic patients did not find this improvement in FEV₁ [47], however comparison between both studies is difficult as patients in the Australian cohort had much lower FEV₁ values (55% predicted) at baseline when compared to our cohort (88% predicted).

A clear influence of BT on lung function parameters is therefore still not shown. Other studies used imaging techniques to assess effects of BT and found significant improvements in CT-measured airtrapping [48, 49] and improved ventilation defects assessed with helium magnetic resonance imaging [50]. Perhaps these imaging techniques are more useful in the BT-setting. In addition, pooling data from different countries to enlarge patient cohorts might help in further understanding the physiological effect of BT. Promising initiatives are the Bronchial Thermoplasty Global Registry including follow-up data from 157 patients from the Netherlands, Italy, Spain, Germany, the United Kingdom, the Czech Republic, Australia and South Africa (clinicaltrials.gov NCT02104856) and an initiative from Russell et al. to combine biopsy data from 99 patients from seven different countries [51]. Different asthma phenotypes and differences per country need to be taken into account to accurately interpret the results from these global initiatives.

Research question 5 (Chapters 6-8). Can optical coherence tomography (OCT) be used to identify and measure airway wall layers and characteristics of airway remodeling?

Airway remodeling is currently measured with high-resolution computed tomography (HR-CT) scans and endobronchial biopsies but both techniques have their limitations. HR-CT scans provide information of the entire bronchial tree, however the resolution is too low to assess the airways in detail and patients are subjected to radiation. Endobronchial biopsies are currently the golden standard. Taking a biopsy however is invasive and gives only detailed information of one specific spot of the airways.

Optical coherence tomography is a probe based imaging technique using near-infrared light to obtain high-resolution images of the airway wall in a real-time matter [52-54]. By using (automated) pullbacks, OCT is able to image large areas of an airway instead of only one point. **Chapter 6** of this thesis provides additional background information about the technique and reviews the currently available literature regarding the use of OCT in pulmonary diseases. The ability of OCT to identify airway wall layers [55-57] and quantify the total airway wall [58, 59] encouraged the study in **Chapter 7**. By comparing cross-sectional histology sections of resected airways from lobectomy specimens with corresponding OCT images we showed that OCT is not only able to identify different airway wall layers but also able to quantify these separate layers. In addition, a high inter-observer reproducibility was shown.

Although the results are promising, one of the most important pitfalls of the OCT technique is the lack of automated analysis methods. Images are provided in a real-time matter but the analysis of the large amount of data is time-consuming and algorithms are still in a developmental phase. Before OCT can be implemented in practice it is necessary to further improve these automatic analyses methods. In **Chapter 8** we have shown within the same dataset of chapter 3, that by using the intensity of the OCT images it is possible to identify components of the extracellular matrix (ECM) in the airway wall. We developed an analysis method in Matlab (Natick MA, USA) using a threshold algorithm to segment and measure the scattering layer in the OCT images and correlated these areas with the ECM deposition in the corresponding histology sections. In-vitro experiments with cultured primary lung fibroblasts and ECM components confirmed our results. Although the analysis is not fully computerized, it does show that by using OCT properties such as the scattering intensity it is possible to measure characteristics of airway remodeling in a minimally invasive and less-time consuming matter.

Another OCT property currently used in research settings to identify and segment airway wall structures is the arrangement of airway wall fibers measured with polarization sensitive OCT (PS-OCT) systems [60, 61]. With this novel imaging technique, it might be possible to automatically segment the ASM and / or ECM fibers in the airway wall [28, 62], which makes it especially interesting to use in BT patients to evaluate treatment effects on airway remodeling in a minimally invasive matter. In addition, it might also be interesting to investigate whether OCT is able to differentiate between airway wall inflammation and airway remodeling in relation to response to BT treatment but also to other severe asthma treatments such as biologics.

Other interesting research questions in which this promising imaging technique might be able to play a role is distinguishing severe asthma from mild asthma or healthy subjects. One study by Adams et al. compared OCT characteristics of allergic asthma patients with allergic non-asthmatic patients before and after allergen challenge [63]. Significant differences were found in epithelial and mucosal thickness, airway buckling and mucus between both groups. In addition, the epithelial thickness and mucosal buckling were significantly related to airway obstruction measured with lung function. Another study in current and former smokers showed correlations between OCT measured airway wall thickness and FEV₁ [64]. These studies confirm the importance of airway remodeling and the potential of OCT imaging to measure and evaluate this process in obstructive lung diseases. In regard to this thesis it might be specifically of interest to investigate whether there are OCT characteristics in severe asthma patients that might help predict the response to BT treatment. OCT might therefore become a tool to predict the effect of asthma treatment but moreover it might help in evaluating the effect of asthma treatment over time.

Research question 6 (Chapter 9): What is the acute effect of BT on the airway wall? And can OCT detect these effects?

Previous published studies showed that immediately after BT, patients have a decline in their FEV₁ [65] and various radiological abnormalities were reported such as peribronchial consolidations with surrounding ground glass, atelectasis, partial bronchial occlusions and bronchial dilatations [28, 62]. The extent of these imaging abnormalities and in which part of the airways this effect of BT was present was difficult to assess with conventional HR-CT images and/or chest X-rays. To better understand what happens during the BT procedure and directly thereafter, a subgroup of included TASMA study patients were imaged with OCT (**Chapter 9**). This is the first study showing that OCT imaging is safe to use in a severe asthma patients cohort. By imaging directly after the third treatment in the right lower lobe, right middle lobe (RML) and upper lobes we were able to investigate the BT effects in three different time frames after BT: 6 weeks after treatment (right lower lobe), untreated airways (RML) and directly after treatment (upper lobes). We showed epithelial sloughing and (peri) bronchial edema effects in areas that were directly targeted with the BT-catheter. The edema however was also present in more distal non-treated parts of the airways suggesting that the effect extends further than the directly treated parts. As some studies, including our own data in chapter 8, showed effects of BT on the ASM mass in the untreated RML it is plausible that indeed an effect extends to untreated parts of the airways, potentially even reaching the smaller airways.

One other study investigated OCT images in two severe asthmatic patients prior to BT-treatment and up to 2 years after the procedures [66]. In this small study one patient was defined as responder and the other patient as non-responder. When comparing these two patients at baseline, the authors reported that the responder had less characteristics of inflammation in the thickened epithelium layer compared to the non-responder. In addition airway wall thickness decreased after BT in the responder compared to the non-responder. Although these results in only two patients need to be interpreted with care, it confirms the potential of OCT imaging in predicting and understanding treatment response. Also in the TASMA study patients are entering an extensive follow-up period of 5 years after BT with an optional bronchoscopy including OCT imaging after 2 years.

Although OCT has the ability to create high-resolution images, knowing what happens on cellular level in the airways is not (yet) possible. It is therefore uncertain whether the seen effects indeed contribute to the favorable effect of BT or if we are looking at side effects of the treatment. Although not certain, the results found in chapter 5 do help further unravel the mechanism of action of BT. By seeing the epithelial layer sloughed from the airway wall directly after BT, one might raise the question whether the favorable effect of BT should be found in the ASM layer or perhaps in the epithelial layer? It might be interesting to see whether the regrown epithelium, as we have shown in the 6 weeks after

BT regions, functions similar as before BT or whether it acts more like normal healthy epithelium. To fully understand the consequences of BT treatment on the airway wall, it is probably necessary to link more detailed analysis methods such as cellular effects in bronchoalveolar lavage or omics technology to these novel imaging techniques.

Key findings of this thesis

Bronchial thermoplasty (BT) is a safe treatment option for severe asthma and improves asthma quality of life and asthma control questionnaires in approximately 60% of the patients. Exacerbation rates decline in almost all patients after BT however, lung function measurements, including forced oscillation technique (FOT), do not show important changes. BT reduces airway smooth muscle (ASM) mass, especially in patients with a lower FEV₁ at baseline. The amount of ASM mass at baseline nor the change of ASM mass after BT correlate with BT-response. Higher total IgE levels, blood eosinophils and lower FOT measured respiratory resistance are associated with improvements in asthma questionnaires. These findings need to be confirmed in future larger trials. In addition, BT seems to induce a metabolic shift of bronchial epithelium gene expression profiles towards a more healthy state but the relationship with response needs to be further investigated.

In addition results of this thesis showed that high-resolution optical coherence tomography (OCT) images can be used to assess airway remodeling. OCT can identify and quantify airway wall layers with a high inter-observer reproducibility. Furthermore, the intensity of OCT images might be linked to extra cellular matrix components in the airway wall. OCT is safe to use in severe asthma patients and shows direct BT effects in both treated and non-treated areas of the airways.

Future perspectives

Bronchial Thermoplasty treatment

Even though the clinical effectiveness of BT has been shown by several large and smaller trials, the treatment remains subject of debate. An important reason for this debate is the lack of understanding the mechanism of action of BT and as a consequence, patient selection is not optimized. Current guidelines implement BT as treatment for patients that are not eligible for or remain uncontrolled during treatment with biologics. In this thesis, we found especially good responses to BT in the patients that might have been eligible for biologics as well. While the optimal patient candidate for BT is not clear, the position of this treatment in guidelines will remain under discussion. In addition, cost effectiveness studies are needed to compare the expensive

treatments for severe asthma, including BT and biologics. One study in moderate to severe allergic asthma patients used a Markov decision model to compare BT with omalizumab and standard inhalation medication. Results of his study suggested that there is a 60% chance of BT to become cost-effective as compared to omalizumab and standard inhalation treatment [67]. Long term follow-up of BT treated patients is necessary to obtain more data regarding the cost-effectiveness. A trial comparing the effectiveness and costs of BT with biologics should be considered, especially in the allergic and eosinophilic asthma phenotype. Therefore the position of BT in the treatment guidelines of severe asthma might change in the future.

The effect of BT on ASM mass is well investigated but this effect does not seem to fully explain the mechanism by which BT induces its improvements in asthma symptoms. Investigating severe asthma and the effect of BT in more detail with different techniques (e.g. omics technology and novel imaging) and linking these techniques to (less invasive) clinical parameters is needed to further understand and better monitor severe asthma.

In addition, the physiological consequence of reducing ASM mass needs to be further investigated. An important measurement might be bronchial hyperresponsiveness. Improvements in bronchial hyperresponsiveness after BT are only shown in dogs [22] and mild asthmatics [68], but reports of investigating the effect of BT on PC20 are scarce in severe asthma patients. For instance, the AIR-2 trial did not report measuring PC20 post BT [19] while the RISA trial only compared 6 BT treated patients with 9 controls without seeing an effect. In our study in chapter 3 we reported a trend-wise improvement of PC20 in the BT-treated group (n=18) compared to the non treated control group (n=18) (p=0.08). This might explain why several patients in the TASMA trial have reported a different response from their lungs to strong perfumes after BT and the observed reduction in exacerbations. Long term follow-up in the TASMA extension study might provide an answer to this question.

An interesting question that might come up in the future is whether patients can be retreated with BT. Although the initial clinical effect seems to sustain over several years, asthma control can deteriorate in some patients after initially a good response. Currently there is no evidence available that these patients might benefit from a re-BT treatment, however if a re-BT is considered it is highly recommended to do this in a research setting [69].

To further evaluate the clinical effect of BT and evaluate the long-term safety profile it is important to monitor BT-treated patients for a longer period of time. Studies have shown a sustained effect of BT on AQLQ and exacerbation rates up to five to ten years after BT [36-39, 70]. The long-term effect on ASM mass after BT is less clear. Therefore we initiated the TASMA extension study (clinicaltrials.gov No: NCT02975284). In this study, BT-treated patients from the

TASMA study are entering a 5 year follow-up period including yearly visits to fill in asthma questionnaires, evaluate health care utilization and exacerbation rates, lung function and bronchial hyperresponsiveness measurements and after two years optionally bronchial biopsy sampling and OCT for the assessment of ASM mass.

Airway wall imaging

OCT is a technique widely used in the fields of ophthalmology and to a lesser extent in cardiology. The last decade several research groups started investigating the use of OCT in the airways, but the implementation of OCT in clinical practice is challenging. Currently, the analysis of OCT images is time-consuming as it is for a large part done manually. In order to implement OCT in clinical practice, it is important to automate and validate the analysis. Working together with other researchers from other fields might speed up this process and should be encouraged.

Next to the analysis methods, improvements to the OCT probe and/or technique itself might change the position of OCT in the clinic as well. Polarization sensitive OCT probes are recently developed and [60, 61] show promising results to assess ASM layers with greater accuracy. This technique might be especially interesting to use in obstructive lung diseases such as severe asthma in which ASM mass is increased. Also in the evaluation of treatments targeting ASM mass, like BT, OCT might fulfil an important role.

Another interesting development is the combination of OCT with immunofluorescence. By labeling antibodies with a fluorescent molecule it is possible to study the distribution of antibodies in high detail [71]. As the safety of endobronchial OCT in severe asthma patients has been shown in this thesis, it would be interesting to use this labeling technique to visualize the distribution of antibodies targeted with other treatments for severe asthma such as anti-IgE, anti-IL-5 or anti-IL-13 treatments. Improving the understanding of these expensive treatment options with imaging techniques might also help further improve patient selection.

Summary

Chapter 1 is the introduction of this thesis and focuses on background information regarding (severe) asthma, bronchial thermoplasty treatment, the TASMA study, airway remodeling, optical coherence tomography (OCT) as novel imaging technique of the airways and the research questions of this thesis.

Chapter 2 shows preliminary results of the TASMA study with airway smooth muscle (ASM) mass reduction after bronchial thermoplasty treatment and the correlation between change in ASM and FEV₁.

The primary endpoint of the TASMA study is reported in **Chapter 3**. The study shows that ASM mass significantly reduces after BT when a treatment group is compared with a delayed control group. This decrease in ASM mass is not associated with the response to BT. Other patient characteristics are also investigated and higher immunoglobulin E (IgE) and higher blood eosinophils are found to be correlated with BT response.

Chapter 4 reports on the hypothesis that BT influences the airway epithelium layer in severe asthma patients. By using endobronchial brushes in patients treated with BT, the data shows that the metabolic gene expression profile of treated parts of the airways seems to shift towards a healthier state. An association with response to BT needs further investigation.

In **Chapter 5** the effect of BT on lung function is reported. In this chapter forced oscillation technique (FOT) is used to measure changes in respiratory resistance after BT. The study shows that BT has no effect on conventional lung function parameters measured with spirometry and bodyplethysmography and also FOT measured respiratory resistance is not influenced by BT. The data does show that a lower respiratory resistance at baseline is associated with a higher improvement on asthma questionnaires after BT.

In **Chapter 6** a detailed overview of the current literature regarding the use of two novel imaging techniques in respiratory medicine is provided: OCT and confocal laser endomicroscopy. This chapter includes background information about both techniques, the clinical use in several anatomical compartments of the respiratory system and potential future implications.

The use of OCT to assess airway wall structures and remodeling is investigated in **Chapter 7** and **8**. In **Chapter 7** the feasibility of OCT to identify and quantify different airway wall layers is shown by comparing airway wall histology sections with matching ex-vivo and in-vivo OCT images. In addition a high inter-observer reproducibility for the assessment of OCT images was found. **Chapter 8** further investigates the same dataset by automatically segment the high scattering layer of the OCT image and correlate this area with extra cellular matrix components in the airway wall as stained in histology sections. To better understand the acute effect of bronchial thermoplasty on the airway wall, **Chapter 9** reports characteristics seen when imaging the airways with OCT immediately after bronchial thermoplasty treatment. This chapter shows that the acute effect of bronchial thermoplasty seems to extend deeper than the cartilage layer in the airway wall and further than the activation sites.

Chapter 10 contains the general discussion, key findings and summary of this thesis. This chapter also focuses on future perspectives.

The last chapter of this thesis is **Chapter 11** and contains the Dutch summary.

References

1. Global burden of disease due to asthma, 2018, <http://www.globalasthmareport.org/burden/burden.php>.
2. O'Byrne PM, Naji N, Gauvreau GM. Severe asthma: future treatments. *Clinical and experimental allergy : journal of the British Society for Allergy and Clinical Immunology*. 2012;42(5):706-11.
3. Barnes PJ, Woolcock AJ. Difficult asthma. *Eur Respir J*. 1998;12(5):1209-18.
4. Busse WW, Banks-Schlegel S, Wenzel SE. Pathophysiology of severe asthma. *The Journal of allergy and clinical immunology*. 2000;106(6):1033-42.
5. Hekking PP, Wener RR, Amelink M, Zwinderman AH, Bouvy ML, Bel EH. The prevalence of severe refractory asthma. *The Journal of allergy and clinical immunology*. 2015;135(4):896-902.
6. Bel EH, Sousa A, Fleming L, Bush A, Chung KF, Versnel J, Wagener AH, Wagers SS, Sterk PJ, Compton CH, Unbiased Biomarkers for the Prediction of Respiratory Disease Outcome Consortium CG. Diagnosis and definition of severe refractory asthma: an international consensus statement from the Innovative Medicine Initiative (IMI). *Thorax*. 2011;66(10):910-7.
7. Chung KF, Wenzel SE, Brozek JL, Bush A, Castro M, Sterk PJ, Adcock IM, Bateman ED, Bel EH, Bleecker ER, Boulet LP, Brightling C, Chanez P, Dahlen SE, Djukanovic R, Frey U, Gaga M, Gibson P, Hamid Q, Jajour NN, Mauad T, Sorkness RL, Teague WG. International ERS/ATS guidelines on definition, evaluation and treatment of severe asthma. *Eur Respir J*. 2014;43(2):343-73.
8. Global Initiative for Asthma. Global Strategy for Asthma Management and Prevention, 2020. Available from: www.ginasthma.org.
9. Accordini S, Corsico A, Cerveri I, Gislason D, Gulsvik A, Janson C, Jarvis D, Marcon A, Pin I, Vermeire P, Almar E, Bugiani M, Cazzoletti L, Duran-Tauleria E, Jogi R, Marinoni A, Martinez-Moratalla J, Leynaert B, de Marco R. The socio-economic burden of asthma is substantial in Europe. *Allergy*. 2008;63(1):116-24.
10. Serra-Batlles J, Plaza V, Morejon E, Comella A, Bruges J. Costs of asthma according to the degree of severity. *Eur Respir J*. 1998;12(6):1322-6.
11. Settupane RA, Kreindler JL, Chung Y, Tkacz J. Evaluating direct costs and productivity losses of patients with asthma receiving GINA 4/5 therapy in the United States. *Annals of allergy, asthma & immunology : official publication of the American College of Allergy, Asthma, & Immunology*. 2019.
12. Busse W, Corren J, Lanier BQ, McAlary M, Fowler-Taylor A, Cioppa GD, van As A, Gupta N. Omalizumab, anti-IgE recombinant humanized monoclonal antibody, for the treatment of severe allergic asthma. *The Journal of allergy and clinical immunology*. 2001;108(2):184-90.
13. Busse WW, Bleecker ER, FitzGerald JM, Ferguson GT, Barker P, Sproule S, Olsson RF, Martin UJ, Goldman M. Long-term safety and efficacy of benralizumab in patients with severe, uncontrolled asthma: 1-year results from the BORA phase 3 extension trial. *The Lancet Respiratory medicine*. 2019;7(1):46-59.
14. Castro M, Corren J, Pavord ID, Maspero J, Wenzel S, Rabe KF, Busse WW, Ford L, Sher L, FitzGerald JM, Katelaris C, Tohda Y, Zhang B, Staudinger H, Pirozzi G,

- Amin N, Ruddy M, Akinlade B, Khan A, Chao J, Martincova R, Graham NMH, Hamilton JD, Swanson BN, Stahl N, Yancopoulos GD, Teper A. Dupilumab Efficacy and Safety in Moderate-to-Severe Uncontrolled Asthma. *The New England journal of medicine*. 2018;378(26):2486-96.
15. Castro M, Zangrilli J, Wechsler ME, Bateman ED, Brusselle GG, Bardin P, Murphy K, Maspero JF, O'Brien C, Korn S. Reslizumab for inadequately controlled asthma with elevated blood eosinophil counts: results from two multicentre, parallel, double-blind, randomised, placebo-controlled, phase 3 trials. *The Lancet Respiratory medicine*. 2015;3(5):355-66.
 16. Pavord ID, Korn S, Howarth P, Bleecker ER, Buhl R, Keene ON, Ortega H, Chanez P. Mepolizumab for severe eosinophilic asthma (DREAM): a multicentre, double-blind, placebo-controlled trial. *Lancet*. 2012;380(9842):651-9.
 17. Castro M, Musani AI, Mayse ML, Shargill NS. Bronchial thermoplasty: a novel technique in the treatment of severe asthma. *Therapeutic advances in respiratory disease*. 2010;4(2):101-16.
 18. Cox G, Thomson NC, Rubin AS, Niven RM, Corris PA, Siersted HC, Olivenstein R, Pavord ID, McCormack D, Chaudhuri R, Miller JD, Laviolette M, Group AIRTS. Asthma control during the year after bronchial thermoplasty. *The New England journal of medicine*. 2007;356(13):1327-37.
 19. Castro M, Rubin AS, Laviolette M, Fiterman J, De Andrade Lima M, Shah PL, Fiss E, Olivenstein R, Thomson NC, Niven RM, Pavord ID, Simoff M, Duhamel DR, McEvoy C, Barbers R, Ten Hacken NH, Wechsler ME, Holmes M, Phillips MJ, Erzurum S, Lunn W, Israel E, Jarjour N, Kraft M, Shargill NS, Quiring J, Berry SM, Cox G, Group AIRTS. Effectiveness and safety of bronchial thermoplasty in the treatment of severe asthma: a multicenter, randomized, double-blind, sham-controlled clinical trial. *American journal of respiratory and critical care medicine*. 2010;181(2):116-24.
 20. Pavord ID, Cox G, Thomson NC, Rubin AS, Corris PA, Niven RM, Chung KF, Laviolette M, Group RTS. Safety and efficacy of bronchial thermoplasty in symptomatic, severe asthma. *American journal of respiratory and critical care medicine*. 2007;176(12):1185-91.
 21. Nederlandse Vereniging van Artsen voor Longziekten en Tuberculose (NVALT). Richtlijn diagnostiek en behandeling van ernstig astma, 2013. Available from: <https://www.nvalt.nl/kwaliteit/richtlijnen/copd-astma-allergie>.
 22. Danek CJ, Lombard CM, Dungworth DL, Cox PG, Miller JD, Biggs MJ, Keast TM, Loomas BE, Wizeman WJ, Hogg JC, Leff AR. Reduction in airway hyperresponsiveness to methacholine by the application of RF energy in dogs. *Journal of applied physiology*. 2004;97(5):1946-53.
 23. Miller JD, Cox G, Vincic L, Lombard CM, Loomas BE, Danek CJ. A prospective feasibility study of bronchial thermoplasty in the human airway. *Chest*. 2005;127(6):1999-2006.
 24. Pretolani M, Dombret MC, Thabut G, Knap D, Hamidi F, Debray MP, Taille C, Chanez P, Aubier M. Reduction of airway smooth muscle mass by bronchial thermoplasty in patients with severe asthma. *American journal of respiratory and critical care medicine*. 2014;190(12):1452-4.

25. Pretolani M, Bergqvist A, Thabut G, Dombret MC, Knapp D, Hamidi F, Alavoine L, Taille C, Chanez P, Erjefalt JS, Aubier M. Effectiveness of bronchial thermoplasty in patients with severe refractory asthma: Clinical and histopathologic correlations. *The Journal of allergy and clinical immunology*. 2017;139(4):1176-85.
26. Denner DR, Doeng DC, Hogarth DK, Dugan K, Naureckas ET, White SR. Airway Inflammation after Bronchial Thermoplasty for Severe Asthma. *Annals of the American Thoracic Society*. 2015;12(9):1302-9.
27. Chakir J, Haj-Salem I, Gras D, Joubert P, Beaudoin EL, Biardel S, Lampron N, Martel S, Chanez P, Boulet LP, Laviolette M. Effects of Bronchial Thermoplasty on Airway Smooth Muscle and Collagen Deposition in Asthma. *Annals of the American Thoracic Society*. 2015;12(11):1612-8.
28. d'Hooghe JNS, van den Berk IAH, Annema JT, Bonta PI. Acute Radiological Abnormalities after Bronchial Thermoplasty: A Prospective Cohort Trial. *Respiration; international review of thoracic diseases*. 2017;94(3):258-62.
29. Debray MP, Dombret MC, Pretolani M, Thabut G, Alavoine L, Brilllet PY, Taille C, Khalil A, Chanez P, Aubier M. Early computed tomography modifications following bronchial thermoplasty in patients with severe asthma. *Eur Respir J*. 2017;49(3).
30. Juniper EF, Guyatt GH, Willan A, Griffith LE. Determining a minimal important change in a disease-specific Quality of Life Questionnaire. *Journal of clinical epidemiology*. 1994;47(1):81-7.
31. Langton D, Wang W, Sha J, Ing A, Fielding D, Hersch N, Plummer V, Thien F. Predicting the Response to Bronchial Thermoplasty. *The journal of allergy and clinical immunology In practice*. 2019.
32. Langton D, Sha J, Ing A, Fielding D, Thien F, Plummer V. Bronchial thermoplasty: activations predict response. *Respiratory research*. 2017;18(1):134.
33. Chernyavsky IL, Russell RJ, Saunders RM, Morris GE, Berair R, Singapuri A, Chachi L, Mansur AH, Howarth PH, Dennison P, Chaudhuri R, Bicknell S, Rose F, Siddiqui S, Brook BS, Brightling CE. In vitro, in silico and in vivo study challenges the impact of bronchial thermoplasty on acute airway smooth muscle mass loss. *Eur Respir J*. 2018;51(5).
34. Haj Salem I, Gras D, Joubert P, Boulet LP, Lampron N, Martel S, Godbout K, Chanez P, Laviolette M, Chakir J. Persistent Reduction of Mucin Production after Bronchial Thermoplasty in Severe Asthma. *American journal of respiratory and critical care medicine*. 2019;199(4):536-8.
35. Sun Q, Fang L, Roth M, Tang X, Papakonstantinou E, Zhai W, Louis R, Heinen V, Schleich FN, Lu S, Savic S, Tamm M, Stolz D. Bronchial thermoplasty decreases airway remodelling by blocking epithelium-derived heat shock protein-60 secretion and protein arginine methyltransferase-1 in fibroblasts. *Eur Respir J*. 2019;54(6).
36. Chupp G, Laviolette M, Cohn L, McEvoy C, Bansal S, Shifren A, Khatri S, Grubb GM, McMullen E, Strauven R, Kline JN. Long-term outcomes of bronchial thermoplasty in subjects with severe asthma: a comparison of 3-year follow-up results from two prospective multicentre studies. *Eur Respir J*. 2017;50(2).
37. Pavord ID, Thomson NC, Niven RM, Corris PA, Chung KF, Cox G, Armstrong B, Shargill NS, Laviolette M, Research in Severe Asthma Trial Study G. Safety

- of bronchial thermoplasty in patients with severe refractory asthma. *Annals of allergy, asthma & immunology : official publication of the American College of Allergy, Asthma, & Immunology*. 2013;111(5):402-7.
38. Thomson NC, Rubin AS, Niven RM, Corris PA, Siersted HC, Olivenstein R, Pavord ID, McCormack D, Laviolette M, Shargill NS, Cox G, Group AIRTS. Long-term (5 year) safety of bronchial thermoplasty: Asthma Intervention Research (AIR) trial. *BMC pulmonary medicine*. 2011;11:8.
 39. Wechsler ME, Laviolette M, Rubin AS, Fiterman J, Lapa e Silva JR, Shah PL, Fiss E, Olivenstein R, Thomson NC, Niven RM, Pavord ID, Simoff M, Hales JB, McEvoy C, Slebos DJ, Holmes M, Phillips MJ, Erzurum SC, Hanania NA, Sumino K, Kraft M, Cox G, Sterman DH, Hogarth K, Kline JN, Mansur AH, Louie BE, Leeds WM, Barbers RG, Austin JH, Shargill NS, Quiring J, Armstrong B, Castro M, Asthma Intervention Research 2 Trial Study G. Bronchial thermoplasty: Long-term safety and effectiveness in patients with severe persistent asthma. *The Journal of allergy and clinical immunology*. 2013;132(6):1295-302.
 40. Oostveen E, MacLeod D, Lorino H, Farre R, Hantos Z, Desager K, Marchal F. The forced oscillation technique in clinical practice: methodology, recommendations and future developments. *Eur Respir J*. 2003;22(6):1026-41.
 41. Anderson WJ, Zajda E, Lipworth BJ. Are we overlooking persistent small airways dysfunction in community-managed asthma? *Annals of allergy, asthma & immunology : official publication of the American College of Allergy, Asthma, & Immunology*. 2012;109(3):185-9.e2.
 42. McNulty W, Usmani OS. Techniques of assessing small airways dysfunction. *Eur Clin Respir J*. 2014;1.
 43. Langton D, Ing A, Sha J, Bennetts K, Hersch N, Kwok M, Plummer V, Thien F, Farah C. Measuring the effects of bronchial thermoplasty using oscillometry. *Respirology*. 2018.
 44. Frantz ID, 3rd, Close RH. Alveolar pressure swings during high frequency ventilation in rabbits. *Pediatric research*. 1985;19(2):162-6.
 45. Fullton JM, Hayes DA, Pimmel RL. Pulmonary impedance in dogs measured by forced random noise with a retrograde catheter. *Journal of applied physiology: respiratory, environmental and exercise physiology*. 1982;52(3):725-33.
 46. Langton D, Bennetts K, Noble P, Plummer V, Thien F. Bronchial thermoplasty reduces airway resistance. *Respiratory research*. 2020;21(1):76.
 47. Langton D, Ing A, Bennetts K, Wang W, Farah C, Peters M, Plummer V, Thien F. Bronchial thermoplasty reduces gas trapping in severe asthma. *BMC pulmonary medicine*. 2018;18(1):155.
 48. Konietzke P, Weinheimer O, Wielputz MO, Wagner WL, Kaukel P, Eberhardt R, Heussel CP, Kauczor HU, Herth FJ, Schuhmann M. Quantitative CT detects changes in airway dimensions and air-trapping after bronchial thermoplasty for severe asthma. *European journal of radiology*. 2018;107:33-8.
 49. Zanon M, Strieder DL, Rubin AS, Watta G, Marchiori E, Cardoso PFG, Hochegger B. Use of MDCT to Assess the Results of Bronchial Thermoplasty. *AJR American journal of roentgenology*. 2017;209(4):752-6.
 50. Thomen RP, Sheshadri A, Quirk JD, Kozlowski J, Ellison HD, Szczesniak RD,

- Castro M, Woods JC. Regional ventilation changes in severe asthma after bronchial thermoplasty with (3)He MR imaging and CT. *Radiology*. 2015;274(1):250-9.
51. Russell R AM, Pretolani M, Laviolette M, Chakir J, Bonta P, Annema J, Howarth P, Chanez P, Chaudhuri R, Singapuri A, Chachi L, Stolz D, Schumann D, Castro M, Brightling C. Bronchial Thermoplasty leads to rapid and persistent improvements in airway remodeling. *European Respiratory Journal* 2019; 54: Suppl. 63, PA3718 [Abstract]. .
 52. Huang D, Swanson EA, Lin CP, Schuman JS, Stinson WG, Chang W, Hee MR, Flotte T, Gregory K, Puliafito CA, et al. Optical coherence tomography. *Science*. 1991;254(5035):1178-81.
 53. Pitris C, Brezinski ME, Bouma BE, Tearney GJ, Southern JF, Fujimoto JG. High resolution imaging of the upper respiratory tract with optical coherence tomography: a feasibility study. *American journal of respiratory and critical care medicine*. 1998;157(5 Pt 1):1640-4.
 54. Tearney GJ, Brezinski ME, Bouma BE, Boppart SA, Pitris C, Southern JF, Fujimoto JG. In vivo endoscopic optical biopsy with optical coherence tomography. *Science*. 1997;276(5321):2037-9.
 55. Hariri LP, Applegate MB, Mino-Kenudson M, Mark EJ, Medoff BD, Luster AD, Bouma BE, Tearney GJ, Suter MJ. Volumetric optical frequency domain imaging of pulmonary pathology with precise correlation to histopathology. *Chest*. 2013;143(1):64-74.
 56. Tsuboi M, Hayashi A, Ikeda N, Honda H, Kato Y, Ichinose S, Kato H. Optical coherence tomography in the diagnosis of bronchial lesions. *Lung cancer*. 2005;49(3):387-94.
 57. Yang Y, Whiteman S, Gey van Pittius D, He Y, Wang RK, Spiteri MA. Use of optical coherence tomography in delineating airways microstructure: comparison of OCT images to histopathological sections. *Phys Med Biol*. 2004;49(7):1247-55.
 58. Chen Y, Ding M, Guan WJ, Wang W, Luo WZ, Zhong CH, Jiang M, Jiang JH, Gu YY, Li SY, Zhong NS. Validation of human small airway measurements using endobronchial optical coherence tomography. *Respiratory medicine*. 2015;109(11):1446-53.
 59. Lee AM, Kirby M, Ohtani K, Candido T, Shalansky R, MacAulay C, English J, Finley R, Lam S, Coxson HO, Lane P. Validation of airway wall measurements by optical coherence tomography in porcine airways. *PloS one*. 2014;9(6):e100145.
 60. Adams DC, Hariri LP, Miller AJ, Wang Y, Cho JL, Villiger M, Holz JA, Szabari MV, Hamilos DL, Scott Harris R, Griffith JW, Bouma BE, Luster AD, Medoff BD, Suter MJ. Birefringence microscopy platform for assessing airway smooth muscle structure and function in vivo. *Science translational medicine*. 2016;8(359):359ra131.
 61. Feroldi F, Willemse J, Davidoiu V, Gräfe MGO, van Iperen DJ, Goorsenberg AWM, Annema JT, Daniels JMA, Bonta PI, de Boer JF. In vivo multifunctional optical coherence tomography at the periphery of the lungs. *Biomedical optics express*. 2019;10(6):3070-91.
 62. Debray MP, Dombret MC, Pretolani M, Thabut G, Alavoine L, Brillet PY, Taille C, Khalil A, Chanez P, Aubier M. Radiological abnormalities following bronchial thermoplasty: is the pathophysiology understood? *Eur Respir J*. 2017;50(6).

63. Adams DC, Miller AJ, Applegate MB, Cho JL, Hamilos DL, Chee A, Holz JA, Szabari MV, Hariri LP, Harris RS, Griffith JW, Luster AD, Medoff BD, Suter MJ. Quantitative assessment of airway remodelling and response to allergen in asthma. *Respirology*. 2019.
64. Coxson HO, Quiney B, Sin DD, Xing L, McWilliams AM, Mayo JR, Lam S. Airway wall thickness assessed using computed tomography and optical coherence tomography. *American journal of respiratory and critical care medicine*. 2008;177(11):1201-6.
65. Langton D, Wang W, Thien F, Plummer V. The acute effects of bronchial thermoplasty on FEV1. *Respiratory medicine*. 2018;137:147-51.
66. Kirby M, Ohtani K, Lopez Lisbona RM, Lee AM, Zhang W, Lane P, Varfolomeva N, Hui L, Ionescu D, Coxson HO, MacAulay C, FitzGerald JM, Lam S. Bronchial thermoplasty in asthma: 2-year follow-up using optical coherence tomography. *Eur Respir J*. 2015.
67. Zafari Z, Sadatsafavi M, Marra CA, Chen W, FitzGerald JM. Cost-Effectiveness of Bronchial Thermoplasty, Omalizumab, and Standard Therapy for Moderate-to-Severe Allergic Asthma. *PloS one*. 2016;11(1):e0146003.
68. Cox G, Miller JD, McWilliams A, Fitzgerald JM, Lam S. Bronchial thermoplasty for asthma. *American journal of respiratory and critical care medicine*. 2006;173(9):965-9.
69. Bonta PI, Chanez P, Annema JT, Shah PL, Niven R. Bronchial Thermoplasty in Severe Asthma: Best Practice Recommendations from an Expert Panel. *Respiration; international review of thoracic diseases*. 2018.
70. Chaudhuri R RA, Da Costa Fiterman J, Sumino K, Lapa E Silva JR, Niven R, Siddiqui S, Olivenstein R, Klooster K, Mcevoy C, Shah P, Simoff M, Duhamel D, Khatri S, Barbers R, Nolan F, Laviolette M. Ten-year follow-up of subjects who received bronchial thermoplasty (BT) in 3 randomized controlled studies (BT10+) [abstract]. *European Respiratory Journal* 2019 54: RCT3782;.
71. Feroldi F, Verlaan M, Knaus H, Davidoiu V, Vugts DJ, van Dongen G, Molthoff CFM, de Boer JF. High resolution combined molecular and structural optical imaging of colorectal cancer in a xenograft mouse model. *Biomedical optics express*. 2018;9(12):6186-204.

Chapter 11.

Nederlandse samenvatting

Algemene inleiding

Astma is een veelvoorkomende chronische ziekte die wereldwijd bij meer dan 300 miljoen mensen is vastgesteld. De luchtwegen van patiënten met astma zijn ontstoken en vaak vernauwd. Hierdoor hebben patiënten last van een piepende ademhaling, hoesten en een drukkend gevoel op de borst. De meeste patiënten hebben last van milde ziekte. Deze patiënten gebruiken inhalatiemedicatie om de luchtwegen beter open te zetten en de ontsteking te onderdrukken. Ongeveer 5% van de astmapatiënten heeft echter ernstig astma. Dit zijn patiënten die ondanks maximale doseringen van inhalatiemedicatie, therapietrouw en behandeling van co-morbiditeiten veel klachten ervaren. Deze relatief kleine groep patiënten heeft een groot aandeel in de totale (zorg) kosten vanwege dure medicijnen, ziekenhuisopnames en ziekteverzuim. Het is daarom van groot belang dat er nieuwe behandelingen worden ontwikkeld voor deze patiëntengroep.

Eén van de kenmerken van ernstig astma is *airway remodeling*. Dit is een verzamelwoord voor structurele veranderingen van de luchtwegwand zoals het dikker worden van de luchtwegwand door een toename van glad spierweefsel. De mate van *airway remodeling* is geassocieerd met de ernst van de luchtwegziekte. Het is daarom belangrijk om een betrouwbare methode te vinden om de mate van *remodeling* te kunnen meten. Een voor longziekten nieuwe beeldvormende techniek die hier mogelijk geschikt voor zou kunnen zijn is Optische Coherentie Tomografie (OCT). Dit is een op *near-infrared* licht gebaseerde techniek waarmee cross-sectionele beelden van de luchtweg worden gegenereerd. Door de endoscopische probe handmatig danwel automatisch terug te trekken kunnen er hoge resolutie beelden worden gemaakt over de gehele lengte van een luchtweg.

Een behandeling die speciaal is ontwikkeld om *airway remodeling* te verminderen is Bronchiale Thermoplastiek (BT). BT is een endoscopische behandeling waarbij radiofrequente energie wordt gebruikt om de middelgrote tot grote luchtwegen te verhitten. De behandeling wordt verricht tijdens drie procedures met 3 weken hersteltijd tussen elke behandeling; tijdens de eerste procedure wordt de rechter onderkwab behandeld, tijdens de tweede procedure de linker onderkwab en tijdens de laatste procedure beide bovenkwabben. De hypothese over het werkingsmechanisme van BT is dat het spierweefsel in de luchtwegwand zou afnemen door de radiofrequente energie waardoor de luchtwegen minder kunnen samentrekken en patiënten minder klachten ervaren. Deze hypothese is echter nog niet bewezen. Bovendien is het onduidelijk in welke patiënt BT het beste helpt. Zijn er bepaalde patiëntkenmerken die kunnen voorspellen of iemand gaat reageren op de behandeling? Reageert iemand met veel spierweefsel in de luchtwegwand bijvoorbeeld beter dan iemand met weinig spierweefsel?

Om deze vragen te beantwoorden is in 2014 de TASMA studie gestart. Dit is een door het Academisch Medisch Centrum (AMC) geïnitieerde, gerandomiseerde, internationale studie waarin patiënten met ernstig astma worden behandeld met BT. Drie verschillende centra doen mee: het AMC in Amsterdam, het Universitair Medisch Centrum in Groningen en de Royal Brompton/Imperial College in Londen (clinicaltrials.gov NCT02225392). In deze studie worden 40 ernstig astma patiënten geïnccludeerd en gerandomiseerd in twee groepen: een groep die direct de behandeling ondergaat en een groep die een half jaar moet wachten voordat de behandeling wordt aangeboden. De groep die een half jaar moet wachten blijft op de standaard astmamedicatie ingesteld en fungeert op deze manier als controlegroep voor de directe BT-groep.

In dit proefschrift proberen we dichter bij een antwoord te komen over hoe BT werkt in ernstig astma patiënten. Daarnaast wordt het gebruik van OCT in de luchtwegen onderzocht.

Resultaten

Bronchiale Thermoplastiek behandeling voor ernstig astma

Hoofdstuk 2 bevat de eerste resultaten van het effect van BT op het spierweefsel in de luchtwegwand. Het gladde spierweefsel in de luchtwegwand van een deel van de TASMA patiënten is geanalyseerd met twee kleuringstechnieken voor en 6 maanden na de BT-behandeling. Met beide kleuringstechnieken werd een afname van meer dan 50% gevonden in glad spierweefsel na de behandeling. Daarnaast vonden we dat patiënten met een ernstigere luchtwegobstructie (FEV_1) meer glad spierweefsel in de luchtwegwand hadden voor de behandeling. Deze patiënten hadden ook meer afname van glad spierweefsel na de BT. Of dit ook samen hangt met de klinische respons moet in een grotere groep patiënten worden onderzocht.

Het primaire eindpunt van de TASMA studie wordt beschreven in **Hoofdstuk 3**. In dit hoofdstuk laten we middels gerandomiseerde studieresultaten zien dat het gladde spierweefsel in de luchtwegen is afgenomen 6 maanden na BT terwijl dit in de controle groep na 6 maanden stabiele astmamedicatie en zorg niet is veranderd. Tevens laten we zien dat de astma controle (ACQ) en astma kwaliteit van leven (AQLQ) vragenlijsten significant zijn verbeterd in de direct behandelende groep vergeleken met de controle groep. In de totale groep van patiënten (n=35) wordt een klinisch relevante verbetering op de vragenlijsten gezien in ongeveer 60% van de patiënten. Deze verbetering is niet gecorreleerd met de hoeveelheid glad spierweefsel op voorhand of met de afname hiervan. Wel lijkt er een associatie te bestaan tussen hogere totaal immunoglobuline E (IgE) en bloed eosinofielen en verbetering op astma vragenlijsten.

In **Hoofdstuk 4** onderzoeken we het effect van BT op genexpressie van bronchiale epitheelcellen in ernstig astma patiënten. Allereerst worden ernstig astma patiënten vergeleken met gezonde controles waarbij een *downregulation* van oxidatieve fosforylering wordt gevonden en een *upregulation* van glycolyse. Vervolgens vergelijken we genexpressie van epitheelcellen in behandelde luchtwegen met onbehandelde luchtwegen, 6 maanden na BT. Hierin worden significante verschillen gevonden waarbij de epitheelcellen van de behandelde luchtwegen lijken te veranderen richting de gezonde luchtwegen. Dit suggereert een reset van epitheelcellen na BT echter moet de associatie met klinische respons nog onderzocht worden.

In **Hoofdstuk 5** rapporteren we het effect van BT op de longfunctie van ernstig astma patiënten. We gebruiken hiervoor de conventionele longfunctietechnieken zoals spirometrie en lichaamsplethysmografie maar ook de minder bekende geforceerde oscillatietechniek (FOT) die de respiratoire weerstand kan meten. De resultaten laten geen effect zien van BT op de parameters die met deze drie technieken zijn onderzocht. Er wordt echter wel een associatie gevonden tussen een lagere respiratoire weerstand vóór de behandeling (gemeten met FOT) en verbeteringen op astma vragenlijsten ná BT. Daarnaast zien we in een deel van de patiënten wel verbetering optreden van de mate van obstructie (FEV₁) en deze verbetering is geassocieerd met verbetering in astma vragenlijsten.

Optische coherentie tomografie in de luchtwegen

In **Hoofdstuk 6** wordt de techniek achter OCT en *Confocal Laser Endomicroscopy* (CLE) toegelicht en een uitgebreid literatuuroverzicht gegeven van toepassingsgebieden van beide endoscopische beeldvormende technieken in de longziekten.

Hoofdstuk 7 laat zien dat het mogelijk is om met OCT verschillende lagen in de luchtwegwand te identificeren en kwantificeren. Dit is onderzocht in zowel in-vivo als ex-vivo luchtwegen van patiënten die een lobectomie ondergingen in verband met een maligniteit. Er werd een hoge correlatie gevonden tussen de histologie meting en de OCT-meting voor zowel in-vivo als ex-vivo beelden. Bovendien werd er een hoge *inter-observer* reproduceerbaarheid gevonden van de OCT-metingen.

In **Hoofdstuk 8** wordt gebruik gemaakt van hetzelfde onderzoeksmateriaal van luchtwegen als hoofdstuk 3. We rapporteren hier een semi-automatische methode om de OCT-beelden te analyseren aan de hand van de lichtintensiteit. Door gebruik te maken van vooraf vastgestelde *thresholds* kan de laag met een hoge lichtintensiteit geselecteerd worden uit de OCT-beelden. Deze laag laat een correlatie zien met extracellulaire matrix componenten in de bijpassende histologie coupes.

In **Hoofdstuk 9** wordt OCT gebruikt om de acute effecten van BT op de luchtwegwand te onderzoeken. We laten zien dat er direct na BT-afwijkingen te zien zijn van epitheel destructie en oedeem. De afwijkingen zijn ook distaal van het geactiveerde gebied zichtbaar, zowel peri-bronchiaal als bronchiaal en zijn ook te vinden in niet behandelde luchtwegen. Na 6 weken zijn de meeste luchtwegen grotendeels hersteld.

Hoofdstuk 10 bevat de discussie, belangrijkste bevindingen en samenvatting van dit proefschrift.

Appendices.

Curriculum Vitae

Annika Wilhelmina Maria Goorsenberg werd geboren op 7 juli 1991 te Koudekerke. Na het behalen van haar vwo-diploma aan de Stedelijke Scholengemeenschap Nehalennia in Middelburg verhuisde zij naar Amsterdam. In 2010 behaalde ze haar propedeuse Pedagogische Wetenschappen en Onderwijskunde aan de Universiteit van Amsterdam. Het jaar daarna ging ze Geneeskunde studeren in het Academisch Medisch Centrum (AMC). Gedurende de master fase deed ze onder andere haar wetenschappelijke stage in het AMC met als onderwerp optische coherentie tomografie in de luchtwegen en behaalde ze haar semi-arts stage op de longafdeling van het Onze Lieve Vrouwe Gasthuis in Amsterdam Oost. Na het behalen van haar diploma als basisarts in 2016 is ze begin 2017 begonnen aan haar promotietraject onder begeleiding van prof. dr. J.T. Annema, dr. P.I. Bonta en dr. D.M. de Bruin. Per mei 2020 is ze in opleiding tot longarts in het AMC onder begeleiding van prof. dr. J.G. van den Aardweg.

PhD Portfolio

| PhD Training | Year | ECTS | |
|--------------------------------------------------------|-------------------------------|-----------|-----|
| General courses | | | |
| eBROK | 2017 | 1.0 | |
| World of Science | 2017 | 0.7 | |
| Endnote | 2017 | 0.1 | |
| Practical Biostatistics | 2018 | 1.1 | |
| Infectious Diseases | 2018 | 1.3 | |
| Advanced Topics in Biostatistics | 2019 | 2.1 | |
| Seminars, workshops and master classes | | | |
| NRS Young Investigators Meeting | 2017-2018 | 0.4 | |
| NRS National course on lung diseases and lung research | 2017 | 5.0 | |
| LUNG Amsterdam | 2017-2019 | 0.3 | |
| Symposium: doing a PhD without stress | 2017 | 0.1 | |
| Op de Hoogte van Astma symposium, Davos | 2018 | 1.0 | |
| ERS satellite symposium: focus on severe asthma | 2018 | 0.2 | |
| Hora Est minisymposium | 2018 | 0.1 | |
| Small airways symposium, UMCG | 2019 | 0.1 | |
| Symposium Update Regelgeving Klinisch Onderzoek | 2019 | 0.1 | |
| International conferences | | | |
| <i>Attended</i> | | | |
| European Respiratory Society (ERS) | 2017-2019 | 3.0 | |
| Nederlandse longdagen | 2018-2019 | 1.0 | |
| <i>Presentations</i> | | | |
| ERS | Thematic poster presentations | 2017-2019 | 1.5 |
| | Oral presentations | 2018-2019 | 2.0 |
| Longdagen | Oral presentations | 2018-2019 | 1.0 |
| Other | | | |
| Journal club respiratory medicine | 2017-2019 | 3.0 | |
| Research meeting respiratory medicine | 2017-2019 | 3.0 | |

Appendices

Teaching

Supervising

| | | |
|--------------------------------------------------|------|-----|
| Master thesis medical student: Mast cells and BT | 2019 | 1.0 |
|--------------------------------------------------|------|-----|

| | | |
|--------------------------------------------|------|-----|
| Master thesis medical student: HRCT and BT | 2019 | 1.0 |
|--------------------------------------------|------|-----|

Other

| | | |
|---------------------------------------|------|-----|
| Klinisch les verpleging F5 short stay | 2019 | 0.1 |
|---------------------------------------|------|-----|

| | | |
|----------------------------|------|-----|
| Onderwijs AIOS longziekten | 2019 | 0.1 |
|----------------------------|------|-----|

| | | |
|----------------------------------------------------------|-----------|-----|
| ERS Training programme endobronchial ultrasound – Part 2 | 2018-2019 | 2.0 |
|----------------------------------------------------------|-----------|-----|

Parameters of esteem

| | | |
|---------------------------------------------|------|--|
| ERS Interventional Pulmonology Travel Grant | 2018 | |
|---------------------------------------------|------|--|

| | | |
|---------------------------------|------|--|
| ERS Young Scientist sponsorship | 2018 | |
|---------------------------------|------|--|

| | | |
|-------------------------------------|------|--|
| “Stichting Astma Bestrijding” grant | 2018 | |
|-------------------------------------|------|--|

| | | |
|--------------|--|-------------|
| Total | | 31.8 |
|--------------|--|-------------|

List of Publications

1. d'Hooghe JNS, **Goorsenberg AWM**, de Bruin DM, Roelofs JJTH, Annema JT, Bonta PI. Identification and quantification of airway wall layers with optical coherence tomography: a histology based validation study. *PLoS One* 2017;12(10):e0184145
2. **Goorsenberg AWM**, d'Hooghe JNS, de Bruin DM, van den Berk IAH, Annema JT, Bonta PI. Bronchial Thermoplasty-Induced Acute Airway Effects Assessed with Optical Coherence Tomography in Severe Asthma. *Respiration* 2018;96(6):564-70
3. Feroldi F, Willemse J, Davidoiu V, Gräfe MGO, van Iperen DJ, **Goorsenberg AWM**, Annema JT, Daniels JMA, Bonta PI, de Boer JF. In vivo multifunctional optical coherence tomography at the periphery of the lungs. *Biomed Opt Express*. 2019;10(6):3070-3091. doi: 10.1364/BOE.10.003070.
4. d'Hooghe JNS, **Goorsenberg AWM**, Ten Hacken NHT, Weersink EJM, Roelofs JJTH, Mauad T, Shah PL, Annema JT, Bonta PI; TASMA research group. Airway smooth muscle reduction after Bronchial Thermoplasty correlates with FEV₁. *Clinical and Experimental Allergy* 2019;49(4):541-544.
5. **Goorsenberg AWM**, Kalverda K, Annema JT, Bonta PI. Advances in optical coherence tomography (OCT) and confocal laser endomicroscopy (CLE) in pulmonary diseases. *Respiration* 2020;99(3):190-205.
6. **Goorsenberg AWM**, d'Hooghe JNS, Slats AM, van den Aardweg JG, Annema JT, Bonta PI. Resistance of the respiratory system measured with forced oscillation technique (FOT) correlates with Bronchial Thermoplasty response. *Respiratory Research* 2020; 21(1):52.
7. Carpaij OA, **Goorsenberg AWM**, d'Hooghe JNS, de Bruin DM, van den Elzen RM, Nawijn MC, Annema JT, van den Berge M, Bonta PI, Burgess JK. Optical coherence tomography intensity correlates with extracellular matrix components in the airway wall. *Accepted for publication in American Journal of Respiratory and Critical Care Medicine* 2020
8. **Goorsenberg AWM**, d'Hooghe JNS, Srikanthan K, Ten Hacken NHT, Weersink EJM, Roelofs JJTH, Kemp SV, Bel EH, Shah PL, Annema JT, Bonta PI; TASMA research group. Bronchial Thermoplasty induced airway smooth muscle reduction and clinical response in severe asthma: the TASMA randomized trial. *Accepted for publication in American Journal of Respiratory and Critical Care Medicine* 2020

9. Ravi A, **Goorsenberg AWM**, Dijkhuis A, Dierdorp BS, Dekker T, Sabogal Piñero YS, Sterk PJ, Vaz FM, Annema JT, Bonta PI, Lutter R. Metabolic differences in bronchial epithelium in asthma patients and healthy individuals: impact of thermoplasty *Submitted for publication*

Contributing authors

Amsterdam University Medical Center, the Netherlands

Department of Respiratory Medicine

J.N.S. d'Hooghe (JNSdH)

E.J.M. Weersink (EJMW)

J.T. Annema (JTA)

P.I. Bonta (PIB)

E.H. Bel (EHB)

P.J. Sterk (PJS)

R. Lutter (RL)

J.G. van den Aardweg (JGvdA)

K. Kalverda (KK)

Department of Pathology

J.J.T.H. Roelofs (JJTHR)

Department of experimental immunology, Amsterdam Infection and Immunity Institute

A. Ravi (AR)

A. Dijkhuis (AD)

B.S. Dierdorp (BSD)

T. Dekker (TD)

Y.S. Sabogal Piñero (YSSP)

Department of Clinical Chemistry, Laboratory Genetic Metabolic Diseases

F.M. Vaz (FMV)

Department of Biomedical Engineering and Physics

D.M. de Bruin (DMdB)

R.M. van den Elzen (RMvdE)

Department of Radiology

I.A.H. van den Berk (IAHvdB)

University Medical Center Groningen, the Netherlands

Groningen Research Institute for Asthma and COPD (GRIAC)

N.H.T. ten Hacken (NHTtH)

O.A. Carpaij (OAC)

M.C. Nawijn (MCN)

M. van den Berge (MvdB)

J.K. Burgess (JKB)

University of São Paulo, School of Medicine, Brazil

Department of Pathology

T. Mauad (TM)

Royal Brompton Hospital and National Heart and Lung Institute, Imperial College, London, United Kingdom

Department of Respiratory Medicine

P.L. Shah (PLS)

K. Srikanthan (KS)

S.V. Kemp (SVK)

Leiden University Medical Center, the Netherlands

Department of Respiratory Medicine

A.M. Slats (AMS)

Authors' contributions per chapter

Chapter 2

Conception and design: NHTtH, PLS, JTA, PIB

Subject recruitment: AWMG, JNSdH, NHTtH, EJMw, PLS, JTA, PIB

Data collection: AWMG, JNSdH, JJTHR, NHTtH, PLS, JTA, PIB

Statistical analysis and interpretation of data: AWMG, JNSdH, NHTtH, TM, EJMw, PLS, JTA, PIB

Design of tables and figures: AWMG, JNSdH, PIB, JTA

Principle investigator and final responsibility: PIB, JTA, PLS, NHTtH

Writing original draft: JNSdH, AWMG

Review and editing: NHTtH, EJMw, JJTHR, TM, PLS, JTA, PIB

All authors approved the final version of the manuscript

Chapter 3

Conception and design: NHTtH, EHB, PLS, JTA, PIB

Subject recruitment: AWMG, JNSdH, EJMw, PIB, JTA, NHTtH, PLS

Data collection: AWMG, JNSdH, KS, SVK, JJTHR, NHTtH, PLS, JTA, PIB

Statistical analysis and interpretation of data: AWMG, JNSdH, KS, EJMw, SVK, NHTtH, EHB, PLS, JTA, PIB

Design of tables and figures: AWMG, PIB, JTA

Principle investigator and final responsibility: PIB, JTA, PLS, NHTtH

Writing original draft: AWMG

Review and editing: JNSdH, KS, NHTtH, EJMw, JJTHR, SVK, EHB, PLS, JTA, PIB

All authors approved the final version of the manuscript

Chapter 4

Conception and design: RL, PIB

Subject recruitment: PIB, JTA, NHTtH, RL

Data collection: AR, AWMG, AD, BSD, TD, YSSP, NHTtH, PIB, RL

Statistical analysis and interpretation of data: AR, AWMG, FMV, PIB, RL

Design of tables and figures: AR

Principle investigator and final responsibility: RL, PIB

Writing original draft: AR, AWMG

Review and editing: AD, BSD, TD, YSSP, PJS, FMV, NHTtH, JTA, PIB, RL

All authors approved the final version of the manuscript

Chapter 5

Conception and design: JTA, PIB

Subject recruitment: AWMG, JNSdH, JTA, PIB

Data collection: AWMG, JNSdH, JTA, PIB

Statistical analysis and interpretation of data: AWMG, PIB, AMS, JGvdA

Design of tables and figures: AWMG, PIB

Principle investigator and final responsibility: PIB, JTA

Writing original draft: AWMG

Review and editing: JNSdH, AMS, JGvdA, JTA, PIB

All authors approved the final version of the manuscript

Chapter 6

AWMG and KK were equally responsible for writing the first draft. PIB and JTA were responsible for reviewing the manuscript. All authors approved the final version of the manuscript.

Chapter 7

Conception and design: JTA, PIB

Subject recruitment: JNSdH, JTA, PIB

Data collection: JNSdH, JTA, PIB, AWMG, JJTH

Statistical analysis and interpretation of data: JNSdH, JTA, PIB, AWMG, DMdB

Design of tables and figures: JNSdH, AWMG

Principle investigator and final responsibility: JTA, PIB

Writing original draft: JNSdH, AWMG

Review and editing: JTA, PIB, DMdB, JJTH

All authors approved the final version of the manuscript

Chapter 8

Conception and design: JTA, PIB, JKB

Subject recruitment: JNSdH, JTA, PIB

Data collection: JNSdH, JJTH, JTA, PIB, AWMG, OAC, JKB, RvdE, DMdB

Statistical analysis and interpretation of data: AWMG, OAC, JKB, MvdB, PIB, DMdB, RvdE, MCN, JTA

Design of tables and figures: AWMG, OAC, JKB, PIB

Appendices

Principle investigator and final responsibility: JKB, PIB

Writing original draft: AWMG, OAC

Review and editing: JNSdH, DMdB, RMvdE, MCN, JTA, MvdB, PIB, JKB

All authors approved the final version of the manuscript

Chapter 9

Conception and design: PIB, JTA

Subject recruitment: AWMG, JNSdH, PIB, JTA

Data collection: AWMG, JNSdH, PIB, JTA

Statistical analysis and interpretation of data: AWMG, PIB, JTA, DMdB, IAHvdB

Design of tables and figures: AWMG, PIB, JTA

Principle investigator and final responsibility: PIB, JTA

Writing original draft: AWMG

Review and editing: PIB, JTA, JNSdH, DMdB, IAHvdB

All authors approved the final version of the manuscript

Dankwoord

Het meest gelezen maar misschien ook wel één van de moeilijkste onderdelen om te schrijven aangezien ik onmogelijk iedereen bij naam kan noemen die een aandeel heeft gehad in het tot stand komen van dit proefschrift. Veel mensen hebben een bijdrage geleverd, in de vorm van begeleiding en samenwerking of juist door voor de nodige ontspanning en afleiding te zorgen.

Ik wil hierbij dan ook iedereen ontzettend bedanken, met in het bijzonder:

Allereerst natuurlijk alle TASMA patiënten!

Mijn promotor Jouke Annema. Naast begeleiding en steun op wetenschappelijk gebied en mijn verdere loopbaan als longarts in opleiding, heb je mij altijd aangemoedigd om ook uitdagingen en plezier buiten het werk op te zoeken en te realiseren. Dit waardeer ik enorm en heeft er toe geleid dat ik met veel plezier terug kijk op mijn jaren als arts-onderzoeker.

Mijn co-promotores Peter Bonta en Martijn de Bruin. Peter, door de jaren heen hebben we heel wat brainstorm sessies en discussies gevoerd samen. Je kritische blik en gedrevenheid werkten vaak inspirerend en zorgden ervoor dat ik met hernieuwde energie verder kon werken aan een manuscript. Martijn, jij was mijn aanspreekpunt binnen de biomedical and engineering afdeling en ik heb je dan ook regelmatig opgezocht als ik ingewikkelde imaging analyses moest uitvoeren. Je was altijd bereid me hier bij te helpen. Heel erg bedankt allebei voor de vele uren die jullie in de begeleiding en in mij hebben gestoken om mij te laten groeien als wetenschapper.

De leden van mijn promotiecommissie

Mijn paranimfen Marije, Paula en Hanneke. Wat ontzettend fijn dat jullie naast mij staan op 26 november! We hebben zowel binnen de muren van het AMC als daarbuiten veel mooie herinneringen opgebouwd waarbij ik zowel met promotie als niet-promotie gerelateerde problemen altijd bij jullie terecht kon. Heel veel dank hiervoor.

Het TASMA team: Marianne van de Pol, Els Weersink, Liesbeth Bel, Peter Sterk, Christof Majoor (AMC); Nick ten Hacken, Jorine Hartman, Karin Klooster, Sonja Augustijn (UMCG); Pallav Shah, Samuel Kemp, Cielo Caneja, Karthi Srikanthan (Royal Brompton & Imperial College).

Sponsors van de TASMA studie: ZonMw, Longfonds en Boston Scientific.

Michael Tanck voor ondersteuning bij statistische analyses.

Imaging collega's van het UMCG: Orestes Carpaij, Janette Burgess, Maarten van den Berge en Martijn Nawijn.

Imaging collega's van de VU: Johannes de Boer, Margherita Vaselli en Fabio Feroldi.

Co auteurs: Inge van den Berk, Richard van den Elzen, Thais Mauad, Annelies Slats, Joost van den Aardweg. En niet te vergeten Kirsten Kalverda, zonder jou was het schrijven van een review een stuk minder leuk geweest!

Endoscopie afdeling: Henk Pelt, Agaath Hanrath - den Hollander, Marjon de Pater, Ann Duflou, John Stadwijk, Thomas Glawenda, Saskia van Nispen, Pascal Uiterwijk, Tecla Boonstra, Lydia Singels, Benedikt en Leo.

Longfunctie afdeling: Saeeda, Rachel, Maria, Erica, Tanja, Monique, Nurcan, Rika, Margôt, Lizzy, Jacqueline, Sabrina, Miranda, Martijn.

De experimentele immunologie: Rene Lutter, Barbara Dierdorp, Tamara Dekker, Annemiek Dijkhuis en Abilash Ravi.

Pathologie afdeling: Joris Roelofs, Onno de Boer, Theo Dirksen, Wim van Est en de rest van het team.

Collega's van F5-260: Julia en Lizzy, jullie zorgden ervoor dat ik me direct thuis voelde op de kamer, fijn dat we elkaar altijd konden helpen als er weer een onmogelijke scapie op het programma stond en wat ontzettend leuk dat we de komende jaren collega's zullen blijven, Job en Levi voor de dagelijkse koffiepauzes waarin ongegeneerd geklaagd mocht worden, Paul voor alle fiets momenten en verder Pieter-Paul, Katrien, Simone, Anirban, Rianne, Renate, Niloufar, Susanne, Anne, Elise, Zulfan, Olga, Mahmoud, Cristina, Dominic, Kornel, Yolanda, Tess en Pieta. Zonder jullie was onderzoek doen in ieder geval een stuk minder leuk geweest!

Stafleden van de longziekten met in het bijzonder Laurence Crombag, jij zorgde voor een ingang bij de longziekten in het AMC en zonder jou was dit proefschrift er dus misschien nooit van gekomen.

Jacquelien van der Vlies en Pearl Mau Asam

En verder natuurlijk:

De allerbeste huisgenootjes Stella, Nathalie en Ruby
Sarah en Florian

Sabrina voor een luisterend oor bij het kopieerapparaat
Marlot, Anne, Brechtje en de rest van Amitié

Mijn familie: mama, papa, Sander en Tessa. Olga en Peter.

Mijn lief, Olaf

